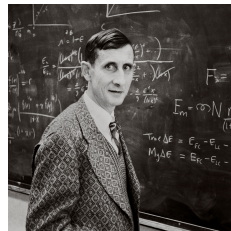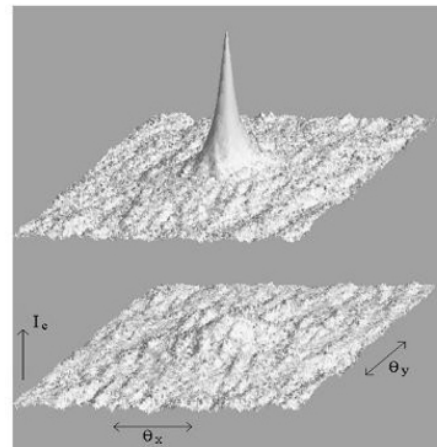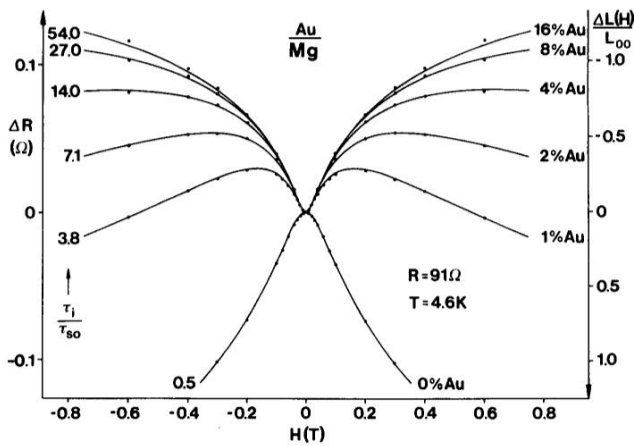# Christophe Texier

Laboratoire de Physique Théorique et Modèles Statistiques,
Université Paris-Saclay, Bâtiment Pascal n°530, F-91405 Orsay

Waves in disordered media and localisation phenomena

February 18, 2021

Figures :
Left : Weak localisation correction to resistance of thin metallic films (Mg dopped by Au). From Ref. [27].
Right : Speckle pattern for light scattered by a turbid granular medium. Time reversal symmetry is destroyed by using the Faraday effect. From Ref. [56].

Philip Warren Anderson (1923-2020)
Freeman John Dyson (1923-2020)
Ilya Mikhailovich Lifshitz (1917-1982)
Leonid Andreevich Pastur (1937-...)
David James Thouless (1934-2019)

Contents

Bibliography

Books

⬦ On probability and random processes (useful tools) : Gardiner [65], Risken [106] and van Kampen [132].

⬦ Localisation in 1D : J.-M. Luck [88].
More complete but less pedagogical : Lifshits, Gredeskul & Pastur [87].
Presentation of mathematical aspects : Bougerol & Lacroix [33, 35].

⬦ Random matrix approach of quantum transport : the very well writtten review of Beenakker [20] and the book of Mello & Kumar [95].

⬦ Introductory text for mesoscopic physics : Datta [45]

⬦ Advanced textbook (emphasize on weak disorder), both for photons and electrons : Akkermans & Montambaux [2, 3].

⬦ A pedagogical presentation of the field theoretical approach : the book of Altland & Simons [4]

⬦ Quantum Hall effect : two books [104, 75]

Review articles

- Introductory texts :

    ⋄ Altshuler and Lee [10] and Washburn and Webb [139].

    ⋄ Sanchez-Palencia and Lewenstein [107] (emphasize on cold atom physics).

- Experiment oriented :

    ⋄ The review on WL measurements in thin films of Bergmann [27].

    ⋄ A review article focused on conductance fluctuations and AB oscillations in normal metals : Washburn and Webb [138].

    ⋄ A review on quantum oscillations (AAS oscillations in metals and oscillations in superconductors) : Aronov and Sharvin [16].

- Theory oriented :

    ⋄ A pedagogical presentation on weak localisation using path integral : Chakravarty and Schmid [36].

    ⋄ A nice overview with emphasize on scaling theory : Kramer and MacKinnon [81].

    ⋄ Interaction effects in weakly disordered metals : Lee and Ramakrishnan [84] ; more difficult (but more detailed) is the review article by Altshuler and Aronov [6] (part of a book edited by Efreos and Shklovskii on interaction with disorder [54]).

    ⋄ A review (quite technical) on transmission correlations in optics : van Rossum and Nieuwenhuizen [133].

I Introduction : Disorder is everywhere

Aim :   Illustrate the importance of disorder in practical situations.
Introduce the notion of random potential (modelizing randomness).
Discuss : averaged quantities vs fluctuations.
Localisation : wave + disorder

I.A   Disorder in condensed matter

Real crystals (give illustrations)

- structural disorder

- substitutional disorder

I.B   Importance of disorder : how would be the world without disorder ?

1)   Free electrons in a metal

Imagine that disorder is absent, hence motion of electrons is *ballistic*, i.e. momentum is conserved $\vec{p}(t) \to \vec{p}$. Linear response gives the conductivity (response of current density to electric field)

$$\sigma(\omega) = \int_0^\infty \mathrm{d}t\, \mathrm{e}^{\mathrm{i}\omega t}\, \frac{\mathrm{i}ne^2}{\hbar}\langle[\, \underbrace{\hat{v}_x(t)}_{=\hat{p}_x/m}, \hat{x}]\rangle = \frac{1}{-\mathrm{i}\omega}\frac{ne^2}{m} \tag{I.1}$$

diverges as $\omega \to 0$!

Classical theory – Drude conductivity.—   Experiments show that the conductivity saturates at low frequency

$$\sigma(\omega) = \frac{ne^2}{m}\frac{1}{1/\tau - \mathrm{i}\omega} \xrightarrow[\omega \to 0]{} \sigma_{\mathrm{Drude}} = \frac{ne^2\tau}{m} \tag{I.2}$$

The transport scattering time encodes the effect of collisions which limits the ballistic propagation of electrons in the metal. These collisions can be of different nature : collisions with phonons (lattice vibrations), collision with impurities (lattice defects), spin scattering, etc. [1] The different rates characterizing these scattering processes are simply added (Matthiesen law) :

$$\frac{1}{\tau(T)} = \frac{1}{\tau_e} + \frac{1}{\tau_{\mathrm{e-ph}}(T)} + \cdots \tag{I.3}$$

Going to low temperature, degrees of freedom, like phonons, are frozen and the total rate (as the resistivity) saturates :
$$\lim_{T \to 0} 1/\tau(T) = 1/\tau_e \,. \tag{I.4}$$

In general, electron-phonon scattering provides the dominant scattering mechanism [17]. This leads to the following resistivity (Bloch-Grüneisen formula)

$$\rho(T) = \frac{1}{\sigma_0} + A\left(\frac{T}{T_D}\right)^5 \int_0^{T_D/2T} \mathrm{d}x\, \frac{x^5}{\sinh^2 x} \tag{I.5}$$

---

[1] Note that collisions among electrons themselves do not affect the conductivity because a collision between two electrons conserves the total current of electrons.

where T_D is the Debye temperature and $\sigma_0 = \frac{ne^2\tau_e}{m}$ is the residual conductivity). The power 5 comes from the temperature dependence of the electron-phonon scattering rate [17] $\tau_{e-ph}(T) \propto T^{-5}$. Note that electron-phonon scattering is strongly anisotropic, being the reason why transport time [2] deviates from the total scattering rate $\tau_{e-ph,\,tot}(T) \propto T^{-3}$ (involved for example in phase coherence properties).

Few order of magnitudes for Gold are given in the table.

Gold
$m_*/m_e = 1.1$
$n = \frac{k_F^3}{3\pi^2} = 55\,\text{nm}^{-3}$
$k_F^{-1} = 0.085\,\text{nm}$
$v_F = \frac{\hbar k_F}{m_*} = 1.25 \times 10^6\,\text{m/s}$
$\varepsilon_F = 5.5\,\text{eV}$ (*)
Work function $W = 5.1\,\text{eV}$
DoS $\nu_0 = 2_s \frac{m_* k_F}{2\pi^2\hbar^2} = 1.07 \times 10^{47}\,\text{J}^{-1}\text{m}^{-3} = 17\,\text{eV}^{-1}\text{nm}^{-3}$
Resistivity $\rho(T \to 0) = 1/\sigma_0 = 0.022 \times 10^{-8}\,\Omega.\text{m}$ [94]
$\ell_e = 4\,\mu\text{m}$ (in bulk) (**)
$\tau_e = 3.2\,\text{ps}$
$D = \frac{1}{3}v_F\ell_e = 1.7\,\text{m}^2/\text{s}$ (from $\sigma_0 = e^2\nu_0 D$)
Debye temperature $T_D = 170\,\text{K}$ [17]
melting point 1338 K and boiling point 3135 K [94]
phase coherence length $L_\varphi \sim 1\,\mu\text{m}$ at $T \sim 1\,\text{K}$

Table 1: *Few orders of magnitude for Gold.* (*) *Note that* $\frac{\hbar^2 k_F^2}{2m_*} = 4.9\ eV.$ (**) *In thin films the mean free path is strongly reduced : e.g. for a gold wire of thickness,* $50\,nm$ *it was observerd that* $\ell_e \simeq 22\,nm$ *[34].*

$\boxed{\textbf{Electronic transport is dominated by disorder at low temperature } (T \lesssim 1\,\text{K})}$

and by inelastic scattering processes at high temperature.

2)   Fermions in a periodic potential : Bloch oscillations

- semiconducting superlattices

- Experiments with cold atoms falling on a periodic potential $\Rightarrow$ oscillations !

I.C   The physics of the diffusion

Disorder leads to multiple scattering and **diffusion**.
Introduce few scales : τ_e, ℓ_e, $D = v_F\ell_e/d$,...
Einstein relation

$$\sigma = e^2\nu_0 D \tag{I.6}$$

where ν_0 is the density of states. Using that the electronic density is $n \propto k_F^d$, we have $\nu_0 = nd/(2\varepsilon_F)$.

Diffusion equation (free)

$$(\partial_t - D\Delta)\,\mathcal{P}_t(r|r') = \delta(t)\delta(r - r') \tag{I.7}$$

---

[2]Conductivity involves *transport* times.

Propagator of the diffusion

$$\mathcal{P}_t(r|r') = \frac{\theta_H(t)}{(4\pi Dt)^{d/2}} e^{-\frac{(r-r')^2}{4Dt}} \tag{I.8}$$

or its (spatial) Fourier transform

$$\widehat{P}(q;t) = \theta_H(t)\, e^{-Dt\,q^2} \tag{I.9}$$

or

$$\widetilde{P}(q;\omega) = \frac{1}{-i\omega + Dq^2} \tag{I.10}$$

I.D How to model disorder ? What is measured ? What should be studied ?

1) Electronic transport

Hamiltonian for one electron

$$H = \frac{\vec{p}^2}{2m_e} + V_{\text{crystal}}(\vec{r}) + \underbrace{V_{\text{disorder}}(\vec{r})}_{\text{fluctuates from sample to sample}} \tag{I.11}$$

Any observable depends on the disorder configuration

E.g. : conductance of a metallic wire $G[V_{\text{disorder}}]$

- In practice, we observe that in a long wire the conductance is not fluctuating from sample to sample! It is given by the Ohm's law $G = \sigma \frac{s}{L}$ (usual feature of statistical physics : fluctuations are washed out at macroscopic scale).

- Fluctuations may be observed by going to mesoscopic scale, $L \lesssim$ few μm and $T \lesssim$ few K

  Observe **reproducible** fluctuations (not experimental noise) as a function of an external parameter (here the magnetic field). These fluctuations are a signature of the presence of the disorder. Such a curve is called the **magnetofingerprint** of the mesoscopic sample.

Manifestation of (quantum) interferences
due to scattering of wave by disordered potential

2) Scattering of light by disorder

Speckle pattern, etc

3) Calculations

From the theoretical point of view : what can be computed ? We can only compute **averaged quantities**. Or study numerically some statistical properties of some observables.

I.E Outline of the course

Main purpose of the course : analyse the **interplay between wave character and disorder**. Where are we going ? Give an overview.

II Anderson localisation in one dimension

The main object of this course is the study of the wave dynamics (optical wave, electronic wave, etc) in a *disordered* medium. For concreteness we can think at an electronic wave in a crystalline structure. In practice, crystals are not perfect but subject to randomness, i.e. some atoms might be replaced by atoms of other nature (random alloy), or the structure of the crystal can present some defects (structural disorder) : cf. Fig. 1. We will first have to discuss how we can model the presence of the disorder, i.e. a **time independent potential** describing **sample to sample fluctuations** : ones says that the **disorder is quenched** in order to denote the absence of time dynamnics. This will be achieved by assuming that the (static) potential is *random in space*.

As a consequence of the presence of disorder, the **translational symmetry is broken** in a given sample (but restored after disorder averaging). Whereas eigenstates of a perfect crystal are extended Bloch waves forming energy bands (continuous spectrum), the presence of the disorder changes drastically the nature of the eigenstates, as we will see.
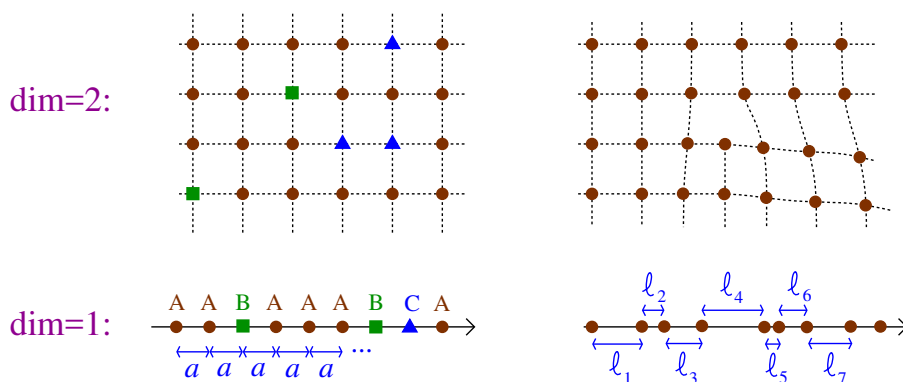
Figure 1: *Substitutional versus structural disorder. Below is the one-dimensional case.*

Aim : Although the 1D situation is somehow particular (dimension is crucial in localisation problems), it allows to solve many problems, sometimes exactly, thanks to some powerful nonperturbative methods. The aim of this chapter is to *demonstrate*, in the frame of several particular models, that the presence of disorder leads to the **localisation** of all one particle eigenstates, i.e. their exponential decay in space.

Reminder (some useful notions of probability) :

- Generating function, moments, cumulants

- Central limit theorem *versus* large deviations (for a simple and basic introduction, cf. appendix of chapter 2 of [127])

- Stochastic calculus (SDE and FPE) (cf. appendix)

I refer to the books of Gardiner [65] and van Kampen [132]. More advanced topics of probability theory can be found in the classical monograph of Feller [58].

II.A Models of disorder

In this section we discuss in details how can we model the disorder. We introduce several models that will be used in the following. Behind this discussion are the important questions :

- Is the precise nature of the model of importance ?
- What physical properties depend on the details of the model ? What properties are model independent, i.e. *universal* ?

The answers will be provided at the end of the chapter.

1) Discrete models

Anderson model (discrete Schrödinger equation).— As localisation theory has arised in the context of condensed matter physics [13], a popular and widely studied model is the tight binding model (Anderson model) describing an electron moving on a lattice of atoms, each characterised by a single orbital. In 1D, after projection on the orbitals $|n\rangle$ at position $x = na$, where a is the lattice spacing, the Schrödinger equation $H|\psi\rangle = \varepsilon|\psi\rangle$ takes the form :

$$-t_n^* \psi_{n+1} + V_n \psi_n - t_{n-1} \psi_{n-1} = \varepsilon \psi_n \,, \tag{II.1}$$

where $\psi_n = \langle n|\psi\rangle$ is the component of the wave function on the site n, $t_n \stackrel{\text{def}}{=} -\langle n+1|H|n\rangle$ describes the coupling between nearest neighbour atoms and $V_n \stackrel{\text{def}}{=} \langle n|H|n\rangle$ a potential. On the infinite line, one can always choose real hoppings (the phases can be removed by a gauge tranformation). This is however not possible if the line is closed (ring geometry).

At this level, two options are

- Consider the case of random potentials V_n ("diagonal disorder") describing a random alloy.

- Consider the case of random couplings t_n ("off-diagonal disorder") corresponding to the case of structural disorder.

In the following, we will focus on the first case for simplicity, and set the couplings to unity, $t = 1$.
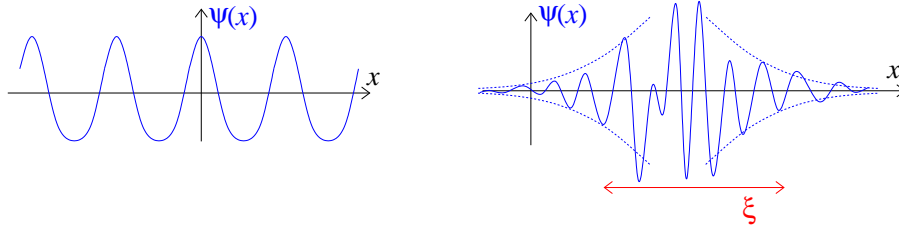
Figure 2: **Extended and localised states.** *Left : Typical shape of the extended states in a perfect 1D crystal. Right : In the presence of disorder, we will show that any amount of disorder make the eigenstates exponentially localized over a typical distance ξ, called the localisation length.*

Distribution of disordered potential V_n.– As mentioned, translation invariance is broken by the presence of disorder, i.e. for *one configuration* of the random potential. However, assuming homogeneity, translation invariance is restored after averaging over the disorder. As a consequence, a natural choice for the distribution of the set of potentials $\{V_n\}$ is to assume its independence with n :

$$P_n(V) = \text{Proba}[V_n = V] \stackrel{\text{transl. inv.}}{\longrightarrow} P(V) \tag{II.2}$$

We can give few examples of distributions :

1. The binary alloy : consider a lattice of atoms of type A. With probability p, one atom A is replaced by an atom B with an energy $V_n = W$, i.e. $P(V) = (1-p)\,\delta(V) + p\,\delta(V-W)$

2. A widely used distribution is the box distribution $P(V) = \frac{1}{W}\,\theta_{\mathrm{H}}(W/2 - |V|)$

3. The choice of a more regular distribution will lead to more regular results (for the spectral density, etc). Two convenient choices are : a Gaussian distribution $P(V) = \frac{1}{\sqrt{2\pi W^2}}\mathrm{e}^{-V^2/2W^2}$ or $P(V) = \frac{1}{2W}\mathrm{e}^{-|V|/W}$.

4. etc.

Correlations.– The statistical properties of the set of potentials $\{V_n\}$ is not only characterised by the marginal law $P(V)$, but should be fully characterized by a joint probability density $P(\cdots, V_1, V_2, \cdots)$. A partial information is the *correlation* between potentials, partly encoded in the correlation function $\langle V_n V_m\rangle = C(|n-m|)$. A **natural assumption** is that the correlations decay fast with the distance (exponentially fast). Studying the large scale properties, a simplification will be to assume that potentials are uncorrelated $\langle V_n V_m\rangle \propto \delta_{n,m}$.

Random spring chain.— Historically, the methods for disordered systems where first apply to a non quantum problem : the random spring chain. Consider atoms on a line and denote by u_n the displacement of the n-th atom. The Newton equations for the mode of frequency ω take the form

$$-m_n\omega^2\,u_n = k_n\,u_{n+1} - (k_n + k_{n-1})\,u_n + k_{n-1}\,u_{n-1} \tag{II.3}$$

where m_n is the mass of the n-th atom and k_n the spring constants between atom n and atom $n+1$. The equation is very similar to discrete Schrödinger equation (II.1). It describes a displacement wave in a disordered environment. The case of random masses (with fixed spring constant) was analyzed in Dyson's pioneering paper [51] (see the book of Lieb and Mattis [86] for an early review of the first works on random spring chains).

✍ *Exercice II.1 : Discuss the precise mapping between the Anderson model (II.1) and the spring chain (II.3) : establish the connection between (E, V_n, t_n) and (ω, m_n, k_n).*

2) Continuous models

Helmholtz equation with random dielectric constant.– In some cases, it can be more natural to consider a continuous model for the propagation of a wave. For example, the analysis of the propagation of an optical wave in a medium with fluctuating dielectric constant $\epsilon(\vec{r}) = \bar{\epsilon} + \delta\epsilon(\vec{r})$ leads to consider the Helmholtz equation

$$-\Delta E(\vec{r}) - k^2\,\frac{\delta\epsilon(\vec{r})}{\bar{\epsilon}}\,E(\vec{r}) = k^2\,E(\vec{r}) \tag{II.4}$$

describing the eigenmodes of the system (in the weak disorder regime, it is justified to decouple the polarisation effect and thus treat in a first step the electric field as a scalar field [2]).

Band edge : from Anderson model to the Schrödinger equation.— In a condensed matter physics context, lattice models are more natural, however their large scale properties can be more conveniently described by continuous models. For example, consider the 1D Anderson model

$$-t\,\psi_{n+1} + V_n\,\psi_n - t\,\psi_{n-1} = \varepsilon\,\psi_n\,. \tag{II.5}$$

In the absence of the random potential, the eigenstates are plane waves $\psi_n = \frac{1}{\sqrt{2\pi}} e^{ikn}$ of energy

$$\varepsilon_k = -2t \cos k \qquad \text{for } k \in [-\pi, \pi] \tag{II.6}$$

In the band edge, $|k| \ll 1$, the dispersion relation may be simplified as $\varepsilon_k \simeq -2t + t\, k^2$. This quadratic behaviour corresponds to a non relativistic particle of mass m with $\hbar^2/(2m) = ta^2$, where a is the lattice spacing. If we consider a potential with slow variations, $V_n = V(na)$ where $V(x)$ is smooth at the scale a, the low energy properties of the model (i.e. the continuum limit $a \to 0$) corresponds to the Schrödinger equation with a random potential

$$H = -\frac{\hbar^2}{2m} \frac{\mathrm{d}^2}{\mathrm{d}x^2} + V(x) \tag{II.7}$$

in the following we will set $\hbar^2/2m = 1$ (hence $[E] = L^{-2}$). This discussion holds if the disorder is weak $V_n \ll t$, so that it does only couple low energy states among themselves.

Band center : Dirac equation with random mass and random scalar field.– The Schrödinger equation with a random potential is not the only continuum limit of the lattice model. If, instead of studying the properties of the Anderson model at the band edge, one considers the low energy properties in the band center, the free spectrum $\varepsilon_k = -2t \cos k$ is linear $\varepsilon_k \simeq 2t(\pm k - \pi/2)$ for $k \sim \pm\pi/2$, hence the emerging theory is a relativistic wave equation. Wave vectors close to $+\pi/2$ are described by one field φ and wave vectors close to $-\pi/2$ by another field χ. If the random potential V_n presents a modulation on the scale of the lattice spacing, we write $V_n = A_0(na) + (-1)^n m(na)$, where $A_0(x)$ and $m(x)$ are two smooth functions. The function $A_0(x)$ is related to small transfer of wave vector, i.e. does not couple the two fields φ and χ. On the other hand, the modulated part corresponds to large transfers of wavevector $\delta k \sim \pm\pi$ and describes the coupling between the two fields. The natural wave equation modelizing this situation is therefore the Dirac equation with a random scalar potential and a random mass for the bi-spinor $\Psi = (\varphi, \chi)$

$$H_D \Psi(x) = \varepsilon\, \Psi(x) \qquad \text{for } H_D = -\mathrm{i} v_0\, \sigma_3\, \partial_x + \sigma_1\, m(x) + A_0(x)\,, \tag{II.8}$$

where σ_i's are Pauli matrices. The mapping is discussed in detail in the problem at the end of the chapter (and also in an appendix of [121] or in [105]).

Statistics of uncorrelated events - Poisson process.– In the calculation of the generating functional (II.18), we have taken the point of view that x_n's are independent random variables distributed with a uniform mean density ρ. I.e., when dropped on the interval $[0, L]$, their joint distribution is $P(x_1, \cdots, x_N) = \frac{1}{L^N}$.

Another point of view corresponds to order the random independent variable as $0 < x_1 < x_2 < \cdots < x_n < \cdots$. We now ask the question : what is the number $\mathcal{N}(x)$ of such impurities on the interval $[0, x]$? The random non decreasing process $\mathcal{N}(x) \in \mathbb{N}$ is called a "*Poisson process*". Its distribution function, $P_N(x) = \mathrm{Proba}\{\mathcal{N}(x) = N\}$, can be easily studied (be careful : N refers to the random variable whereas x is a parameter). We obtain

$$P_N(x) = \frac{(\rho x)^N}{N!} e^{-\rho x}\,, \tag{II.9}$$

which is proved in the exercice below.

✍ *Exercice II.2 Distribution of the Poisson process :* The occurence of "events" (impurity positions) are independent. On the infinitesimal interval of width $\mathrm{d}x$, the probability to find one impurity is $\rho \mathrm{d}x$.

a) Writing $P_0(x + \mathrm{d}x)$ in terms of $P_0(x)$, deduce a differential equation for $P_0(x)$ and solve it.

b) Proceeding in a similar way for $P_N(x)$, show that these probabilities solve the infinite set of coupled differential equations

$$\frac{\mathrm{d}}{\mathrm{d}x}P_N(x) = \rho\, P_{N-1}(x) - \rho\, P_N(x)\,. \tag{II.10}$$

c) These equations can be solved by the generating function technique. Introduce

$$G(s; x) \stackrel{\text{def}}{=} \left\langle s^{\mathcal{N}(x)} \right\rangle = \sum_{N=0}^{\infty} s^N\, P_N(x)\,, \tag{II.11}$$

where s is a complex number. Deduce a differential equation for $G(s;x)$. What is $G(s;0)$? Deduce $P_N(x)$.

d) Compute the mean $\langle \mathcal{N}(x) \rangle$ and the variance $\mathrm{Var}(\mathcal{N}(x))$.

Distribution of the random potential $V(x)$ $-$ Generating functionals.$-$ The notion of a "random function" leads to a small technical complication : the distribution of the potential must be encoded in a functional $\mathcal{D}V(x)\, P[V]$ and averaging involves functional integrals $\int \mathcal{D}V(x)\, P[V]\, (\cdots)$. This little difficulty can be circumvent by making use of the notion of generating functional. We define

$$G[b] \stackrel{\text{def}}{=} \overline{\mathrm{e}^{\int \mathrm{d}x\, V(x)\, b(x)}}\,, \tag{II.12}$$

where $\overline{\bullet}$ denotes averaging over $V(x)$, which is usually more easy to handle. The correlation functions can be deduced by functional derivation :

$$\overline{V(x_1)\cdots V(x_n)} = \left.\frac{\delta^n G[b]}{\delta b(x_1)\cdots \delta b(x_n)}\right|_{b=0} \tag{II.13}$$

It is usually more convenient to consider the *connected correlation functions* (cumulants)

$$\overline{V(x_1)\cdots V(x_n)}^c = \left.\frac{\delta^n W[b]}{\delta b(x_1)\cdots \delta b(x_n)}\right|_{b=0} \qquad \text{where } W[b] = \ln G[b] \tag{II.14}$$

In particular $\overline{V(x_1)\, V(x_2)}^c = \overline{V(x_1)\, V(x_2)} - \overline{V(x_1)} \times \overline{V(x_2)}$.

Two examples :

(i)   General Gaussian disorder

$$P[V] = \mathcal{N}\, \exp\left\{ -\frac{1}{2} \int \mathrm{d}x \mathrm{d}x'\, V(x) A(x, x') V(x') \right\} \tag{II.15}$$

where $\mathcal{N}$ is a normalisation. If we introduce the inverse of the integral kernel C, defined by $\int \mathrm{d}x'\, A(x, x'') C(x'', x') = \delta(x - x')$, we find the generating functional

$$G[b] = \exp\left\{ \frac{1}{2} \int \mathrm{d}x \mathrm{d}x'\, b(x) C(x, x') b(x') \right\}\,. \tag{II.16}$$

$\left.\frac{\delta^2 G[b]}{\delta b(x)\delta b(x')}\right|_{b=0} = C(x, x') = \overline{V(x)V(x')}$ is the two point correlation function.

Analogy : Gaussian measure in $\mathbb{R}^N$ If this seems too formal, think that it is just a generalisation of usual matrix manipulations (with discrete indices) to continuous indices. A general Gaussian measure would take the form $P(\cdots, V_x, \cdots) = \mathcal{N} \exp\{-\frac{1}{2}\sum_{x,x'} V_x A_{x,x'} V_{x'}\}$. The Generating function is then given by a simple Gaussian integration in $\mathbb{R}^N$: $G(\cdots, b_x, \cdots) = \overline{e^{\sum_x V_x b_x}} = \exp\{\frac{1}{2}\sum_{x,x'} b_x C_{x,x'} b_{x'}\}$. Functional derivation corresponds with partial derivative $\frac{\partial^2 G}{\partial b_x \partial b_{x'}}\big|_{b=0} = C_{x,x'} = (A^{-1})_{x,x'}$

Example 1 : the Gaussian measure with $A(x,x') = \frac{1}{\sigma}\delta(x-x')$ is the measure for the Gaussian white noise. Obviously $C(x,x') = \sigma\,\delta(x-x')$.

Example 2 : the Gaussian measure with $A(x,x') = \frac{1}{\sigma}\delta(x-x')\left[1 - \ell_c^2 \frac{d^2}{dx^2}\right]$ leads to correlations exponentially suppressed with the distance $C(x,x') = \frac{\sigma}{2\ell_c}e^{-|x-x'|/\ell_c}$.

The limit ℓ_c is the Gaussian white noise limit.

(ii) Random uncorrelated impurities. A natural model of disorder is the case of localised impurities at random positions x_n :

$$V(x) = \sum_n v_n\,\delta(x-x_n)\,. \tag{II.17}$$

A natural assumption is that the positions x_n's are independent random variables distributed with a uniform mean density ρ. Fixing the averaged density, the number N of independent impurities in a volume V is given by the Poisson distribution $P_N = \frac{(\rho V)^N}{N!}e^{-\rho V}$. The calculation of the generating functional follows straightforwardly :

$$G[b] = \left\langle \prod_{n=1}^N e^{v_n b(x_n)} \right\rangle_{N,\{x_n\},\{v_n\}} = \sum_{N=0}^\infty P_N \left(\int_V \frac{dx_n}{V}\overline{e^{v_n b(x_n)}}\right)^N \tag{II.18}$$

$$= \exp\left\{\rho \int dx \left(\overline{e^{v_n b(x)}} - 1\right)\right\} \tag{II.19}$$

where $\overline{\cdots}$ is the averaging over the random weights v_n. More conveniently

$$W[b] = \rho \int dx \left(\overline{e^{v_n b(x)}} - 1\right)\,. \tag{II.20}$$

Functional derivations lead straightforwardly to

$$\overline{V(x)} = \rho\,\langle v_i\rangle \tag{II.21}$$

$$\overline{V(x_1)\cdots V(x_n)}^c = \rho\,\overline{v_i^n}\,\delta(x_1-x_2)\cdots\delta(x_1-x_n) \tag{II.22}$$

(note that the *cumulants* of the potential are controlled by the *moments* of weights v_i's).

3) Averaging over the disorder : Quenched or annealed ?

Let us discuss an important point concerning the averaging over the disorder : what is the "good" quantity which should be averaged ?

Consider a system with configurations denoted by $\mathcal{C}$ within statistical physics, characterized by occupation probability $P(\mathcal{C})$ (this set of probabilities could as well be of quantum nature at $T=0$). For simplicity, consider the canonical distribution $P(\mathcal{C}) = 1/Z_V \exp\{-\beta V(\mathcal{C})\}$ where the partition function $Z_V = \sum_{\mathcal{C}} \exp\{-\beta V(\mathcal{C})\}$ *depends on the configuration V of the disorder,* as well as the thermodynamic properties encoded in the free energy $F_V = -(1/\beta)\ln Z_V$. The question is : what should be averaged ? the partition function Z_V or the free energy F_V ?

Quenched : In principle, thermodynamic observables (pressure p, magnetization M, ...) can be deduced from the free energy by simple derivation. For example the magnetization $\langle M_V \rangle = -\partial_B F_V$, where $\langle \bullet \rangle$ is the *thermal averaging*. Hence, in an experiment, what is measured (on a single sample) is linear in the free energy. Assuming the sample big enough and a finite correlation length, some spatial averaging is thus naturally performed and the free energy averaged over the disorder seems the relevant quantity : [3]

$$F_{\text{quenched}} \overset{\text{def}}{=} \overline{F_V} = -\frac{1}{\beta}\overline{\ln Z_V} \tag{II.23}$$

where $\overline{\bullet}$ denotes *disorder averaging* over V, with probability $w(V)$.

The knowledge of the quenched free energy provides the magnetization averaged over the disorder $\overline{\langle M \rangle} = -\partial_B \overline{F_V}$.

Note however that, although the free energy is self averaging, its derivatives may be not self averaging in the thermodynamic limit. Consider an observable X with fonjugated parameter ϕ (the magnetization and the magnetic field for instance). One expects that the free energy involves a characteristic scale $F_V(\phi) = f(\phi/\phi_c)$ this its derivative reads $\overline{X} = -f'(\phi/\phi_c)/\phi_c$. If ϕ_c is a microscopic scale, it may scale with the volume (like the mean level spacing) which makes $\overline{X}$ non self averaging.

Annealed : A different averaging procedure (over the disorder), could be to average the partition function

$$\overline{Z_V} = \overline{\sum_{\mathcal{C}} \exp\{-\beta V(\mathcal{C})\}} = \sum_V w(V) \sum_{\mathcal{C}} \exp\{-\beta V(\mathcal{C})\}$$

This expression reveals that both the configuration $\mathcal{C}$ and the disorder configuration V are treated on the same footing. Hence, this procedure corresponds to consider that disorder configuration changes during the time dynamics, in the same way as $\mathcal{C}$ (remember that, in statistical physics, statistical averaging replaces ergodic time dynamics). We introduce

$$F_{\text{annealed}} \overset{\text{def}}{=} -\frac{1}{\beta}\ln\left(\overline{Z_V}\right) \tag{II.24}$$

the annealed free energy.

We have the convexity inequality

$$\overline{\ln Z} \leqslant \ln\left(\overline{Z}\right) \quad \text{and} \quad F_{\text{quenched}} \geqslant F_{\text{annealed}} \tag{II.25}$$

In the following, we will consider the case of **quenched** disorder.

II.B Transfer matrix approach – The Furstenberg theorem

The concept of transfer matrix is a very important one in statistical physics [19]. We show in this section that the study of the models introduced previously within this formulation leads straightforwardly to the conclusion that the wave functions are exponentially localised, given an important theorem of the theory of random matrix products.

---

[3] Assuming short range interaction, one can show that **the free energy is self averaging** in the thermodynamic limit.

1) Furstenberg theorem

Preliminary : Consider some independent and identically distributed (i.i.d.) random variables x_n. What are the statistical properties of the product of these random variables $p_N = x_N \cdots x_2 x_1$? If $\overline{(\ln x_n)^2} < \infty$, the answer is given by the central limit theorem applied to the logarithm $\ln p_N = \sum_n \ln x_n$. In particular

$$\lim_{N \to \infty} \frac{\ln |p_N|}{N} = \overline{\ln x_n} \tag{II.26}$$

as the fluctuating part of $\ln |p_N|$ scales as $\sqrt{N}$ if $\overline{(\ln x_n)^2}$ is finite.

Central limit theorem for non commuting objects : The Furstenberg theorem is a generalisation of the trivial relation (II.26) to the highly non trivial situation where the random variables are *non commuting.*

Let us consider a sequence of i.i.d. random matrices M_n's, according to a suitable measure $\mu(\mathrm{d}M)$ defined over some group. Then we form the product of such matrices

$$\Pi_N = M_N \cdots M_2 M_1 \tag{II.27}$$

A natural question is : $\boxed{\text{given } \mu(\mathrm{d}M) \text{ what is the distribution of } \Pi_N \text{ ?}}$ The Furstenberg theorem (below) states that the matrix elements of the product Π_N typically grow **exponentially** with N as $N \to \infty$. Let us first give few precisions.

Example of measure $\mu(\mathrm{d}M)$ for the group $\mathrm{SL}(2,\mathbb{R})$: One considers a group of matrices labelled by some parameters (like angles for the rotation group). These parameters depend on the choice of the group representation. Consider for example $\mathrm{SL}(2,\mathbb{R})$, a three-parameter-group that will be important for the discussion.

Gauss decomposition : Matrices of $\mathrm{SL}(2,\mathbb{R})$ can be decomposed thanks to the well-known Gauss decomposition

$$M(a,b,c) = \begin{pmatrix} 1 & a \\ 0 & 1 \end{pmatrix} \begin{pmatrix} \mathrm{e}^b & 0 \\ 0 & \mathrm{e}^{-b} \end{pmatrix} \begin{pmatrix} 1 & 0 \\ c & 1 \end{pmatrix} \tag{II.28}$$

The measure $\mu(\mathrm{d}M)$ over $\mathrm{SL}(2,\mathbb{R})$ corresponds to some joint distribution $P(a,b,c)$.

Iwasawa decomposition : Another decomposition, that will be more useful below, is the Iwasawa decomposition, in terms of compact, Abelian and nilpotent subgroups :

$$\widetilde{M}(\theta,w,u) = \begin{pmatrix} \cos\theta & -\sin\theta \\ \sin\theta & \cos\theta \end{pmatrix} \begin{pmatrix} \mathrm{e}^w & 0 \\ 0 & \mathrm{e}^{-w} \end{pmatrix} \begin{pmatrix} 1 & u \\ 0 & 1 \end{pmatrix} \tag{II.29}$$

The measure $\mu(\mathrm{d}M)$ is then given by the joint distribution $\widetilde{P}(\theta,w,u)$.

Relating the two parametrisations $\widetilde{M}(\theta,w,u) = M(a,b,c)$, one can find in principle the relation between the two distribution $P(a,b,c)$ and $\widetilde{P}(\theta,w,u)$ characterizing the *same* measure $\mu(\mathrm{d}M)$.

Norm.– In order to measure the growth of the matrix elements, it is convenient to define the norm of the matrix. [4]

Several definitions are possible and the precise choice is not essential for the following.

Choice 1 : (for $m \times m$ matrices) :

$$||M|| \stackrel{\text{def}}{=} \text{Sup}\{||Mx|| \; ; \; x \in \mathbb{R}^m \; ; \; ||x|| = 1\} \tag{II.30}$$

where $||x||$ is the usual Euclidian norm in $\mathbb{R}^m$.

Choice 2 : (used by mathematicians in [33])

$$||M|| \stackrel{\text{def}}{=} \int_{||x||=1} \mathrm{d}^m x \, ||Mx|| \, . \tag{II.31}$$

Choice 3 : the Fröbenius norm

$$||M|| \stackrel{\text{def}}{=} \sqrt{\frac{1}{m} \text{Tr}\{M^\dagger M\}} \, . \tag{II.32}$$

For example for 2×2 real matrices

$$M = \begin{pmatrix} a & b \\ c & d \end{pmatrix} \quad \Rightarrow \quad ||M||^2 = \frac{1}{2}(a^2 + b^2 + c^2 + d^2) \tag{II.33}$$

For matrices of $\text{SL}(2, \mathbb{R})$, one can show that $||M|| \geqslant 1$.

Remark : this discussion of the matrix norm was just for the fun, as it will play no role in the following.

Furstenberg theorem (1963).– Assuming that $\overline{\ln^+ ||M_n||} < \infty$, where $\ln^+ x \stackrel{\text{def}}{=} \theta_{\text{H}}(x - 1) \ln x$, the Furstenberg theorem [62] states that

$$\boxed{\gamma \stackrel{\text{def}}{=} \lim_{N \to \infty} \frac{\ln ||\Pi_N||}{N} \geqslant 0} \tag{II.34}$$

Note that averaging is not needed, as in (II.26). γ is called the (largest) "Lyapunov exponent" of the random matrix product. It depends on the group and on the probability measure. Given this information, it is however difficult to compute it in general.

Central limit theorems for products of random matrices have been widely studied by mathematicians since the pioneering work of Bellman in 1954 [22]. Important developments are due to Furstenberg and Kesten [63, 62], Guivarc'h and Raugi [69], Le Page [83] and others [101]. Among the vast mathematical literature on this topic, one of the key problems is the derivation of sufficient conditions for the central limit theorem to hold. More information can be found in the monograph by Bougerol and Lacroix [33] or the recent one [23].

We now discuss how the Furstenberg theorem is related to the localisation problem.

---

[4]A norm $||x||$ is an application from a vectorial space $\mathscr{E}$ to the real with the following properties : (i) $\forall x \in \mathscr{E}$, $||x|| \in \mathbb{R}^+$. (ii) $||x|| = 0 \Leftrightarrow x = 0$, the null element of $\mathscr{E}$. (iii) $\forall \lambda \in \mathbb{C}$, $||\lambda \, x|| = |\lambda| \, ||x||$. (iv) $||x + y|| \leqslant ||x|| + ||y||$ (triangular inequality).
If $||x|| = 0$ does not imply $x = 0$, $|| \cdot ||$ is a semi-norm (example of semi-norm : for $||f|| = \int_{\mathbb{R}} \mathrm{d}x \, |f(x)|$, $||f|| = 0$ implies $f(x) = 0$ expect on a set of zero measure).

2)   A discrete model

The study of the tight binding equation (II.5) for $t = 1$ can be reformulated in terms of transfer matrices as follows

$$\begin{pmatrix} \psi_{n+1} \\ \psi_n \end{pmatrix} = \underbrace{\begin{pmatrix} V_n - \varepsilon & -1 \\ 1 & 0 \end{pmatrix}}_{=M_n \in \mathrm{SL}(2,\mathbb{R})} \begin{pmatrix} \psi_n \\ \psi_{n-1} \end{pmatrix} . \tag{II.35}$$

The behaviour of the wave function is controlled by those of the product of transfer matrices

$$\psi_n \sim ||\Pi_n|| \qquad \text{where } \Pi_n = M_n \cdots M_1 \tag{II.36}$$

The Furstenberg theorem immediatly tells us that, *given some initial values* (ψ_1, ψ_0), the wave function [5] grows exponentially

$$\ln |\psi_n| \underset{n \to \infty}{\sim} \gamma\, n \tag{II.37}$$

up to fluctuations of order $\sqrt{n}$, where γ is the Lyapunov exponent of the transfer matrices (the growth rate of the matrix product). The growth rate of the wave function furnishes a definition of the localisation length

$$\boxed{\xi \overset{\mathrm{def}}{=} 1/\gamma} \tag{II.38}$$

The identification of the inverse Lyapunov exponent and the localisation is at the heart of the connection between localisation and product of random matrices. This is related to the *Borland's conjecture* (cf. discussion below).

Weak disorder :   A lot of effort has been devoted to develop weak disorder expansion. For example, Derrida and Gardner have obtained several formulae were obtained for the Anderson model, depending on the energy [47]. (II.5) for $t = 1$ and set $\varepsilon = -2 \cos k$. Not too close to the band edges ($\varepsilon \simeq \pm 2$) nor to the band center [6] ($\varepsilon \simeq 0$), it was shown that the Lyapunov exponent is given by [47, 88]

$$\gamma \simeq \frac{\overline{V_n^2}}{8 \sin^2 k} = \frac{\overline{V_n^2}}{2(4 - \varepsilon^2)} . \tag{II.39}$$

✍ *Exercice II.3 Lyapunov exponent of the spring chain: (very easy) Consider the random spring chain model (II.3) for uniform spring constants $k_n = \kappa$ and random masses $m_n = m_0 + \delta m_n$, with $\delta m_n \ll m_0$ and $\overline{\delta m_n} = 0$. By mapping (II.3) onto the Anderson model (II.5), previous exercice, recover the formula of Ishii and Matsuda [93, 72] for the low frequency Lyapunov exponent of the spring chain*

$$\gamma(\omega) \simeq \frac{\overline{\delta m_n^2}\, \omega^2}{8 m_0 \kappa} \tag{II.40}$$

Justify the vanishing of $\gamma(\omega)$ for small frequency with a physical argument.

---

[5] We already stress that we consider here the solution of the *initial value problem*, and not the real normalised eigenstates solution of the *spectral problem*.

[6] Kappus and Wegner discovered in 1981 that the Lyapunov exponent at the band center presents an *anomaly* (i.e. its weak disorder expansion differs from the formula given here). Derrida and Gardner provided later a beautiful explanation. In the problem at the end of the chapter, I give a simple explanation within a continuum limit.

3) A continuous model : δ-impurities

Another interesting model is the delta impurity model (random Kronig-Penney model)

$$H = -\frac{\mathrm{d}^2}{\mathrm{d}x^2} + \sum_n v_n\,\delta(x - x_n) \tag{II.41}$$

We set $\hbar^2/(2m) = 1$ for convenience.
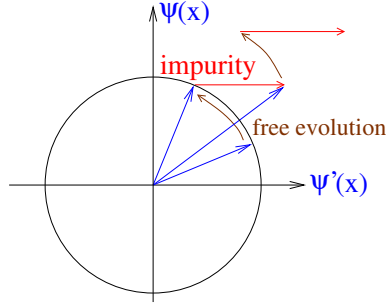
Figure 3: **Transformation of the vector** $(\psi', k\psi)$.

Let us gather the wave function and its derivative in a vector

$$\begin{pmatrix} \psi'(x) \\ k\,\psi(x) \end{pmatrix} \tag{II.42}$$

We may encode the evolution of the vector through the action of transfer matrices of two types (figure 3) :

- Between impurity n and $n + 1$, the evolution is free, hence

$$\begin{pmatrix} \psi'(x) \\ k\,\psi(x) \end{pmatrix} = k\,A_n \begin{pmatrix} \cos(kx + \varphi_n) \\ \sin(kx + \varphi_n) \end{pmatrix} \qquad \text{for } x_n < x < x_{n+1}\,, \tag{II.43}$$

  where A_n and φ_n are some amplitude and some phase, depending on each interval. This makes clear that the vectors at x_n^+ and x_{n+1}^- are related by a *rotation* of positive angle $\theta_n = k\ell_n$ where $\ell_n = x_{n+1} - x_n$.

- Evolution through the impurity n corresponds to $\psi'(x_n+) - \psi'(x_n-) = v_n\psi(x_n)$, with $\psi(x)$ continuous.

Therefore the evolution of the vector (II.42) involves a sequence of random matrices of the form

$$M_n = \begin{pmatrix} \cos\theta_n & -\sin\theta_n \\ \sin\theta_n & \cos\theta_n \end{pmatrix} \begin{pmatrix} 1 & u_n \\ 0 & 1 \end{pmatrix} \in \mathrm{SL}(2,\mathbb{R}) \tag{II.44}$$

with random positive angles $\theta_n = k\ell_n > 0$ and random coefficients $u_n = v_n/k$. We have

$$\begin{pmatrix} \psi'(x_{n+1}-) \\ k\,\psi(x_{n+1}-) \end{pmatrix} = \Pi_n \begin{pmatrix} \psi'(x_1-) \\ k\,\psi(x_1-) \end{pmatrix} \qquad \text{where } \Pi_n = M_n \cdots M_1\,, \tag{II.45}$$

20
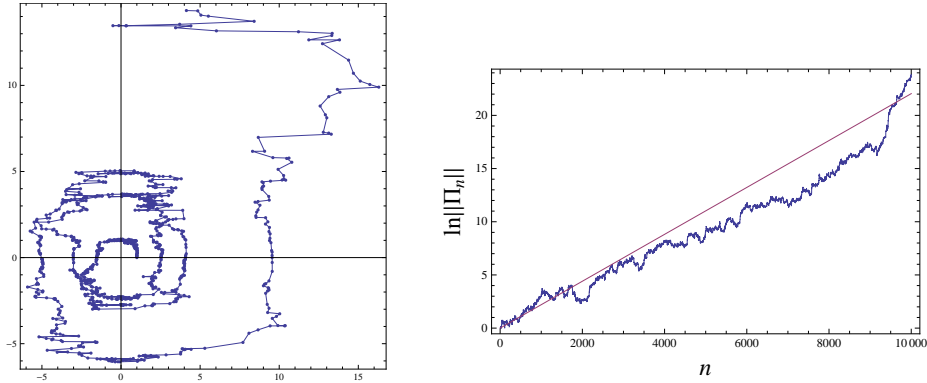
Figure 4: **Evolution of the random matrix product.** Left : *Motion of the vector under the action of the* 1000 *random matrices of the form* (II.44). *the angle are exponentially distributed with* $\bar{\theta} = 0.02$ *and the coefficients* u_n *under the symmetric PDF* $p(u) = \frac{1}{2a}e^{-|u|/a}$ *with* $a = 0.1$. Right : *Evolution of the modulus of the vector with n for two realisations of the disorder : slope indicates the Lyapunov exponent.*

Origin of the symplectic group $\mathrm{SL}(2,\mathbb{R}) \equiv \mathrm{Sp}(2,\mathbb{R})$ **:** Note that the fact that the matrix $M_n \in \mathrm{SL}(2,\mathbb{R})$ follows from the conservation of probability current : denoting $\Psi(x)$ the vector (II.42), the current density is expressed as

$$J_\psi = \mathrm{Im}[\psi^* \psi'] = -\frac{1}{2k}\Psi^\dagger \sigma_2 \Psi \, . \tag{II.46}$$

Hence current conservation between two points related by a transfer matrix M is ensured by the condition $M^\dagger \sigma_2 M = \sigma_2$. This implies that $M \in \mathrm{SL}(2,\mathbb{R})$, up to a global phase.

Impurities may form a lattice (fixed distances $\ell_n = 1/\rho$) or be randomly dropped; e.g. dropped independently and uniformly for a mean density ρ, i.e. $p(\ell) = \rho e^{-\rho\ell}$. Weights v_n may be random or not. The Furstenberg theorem again immediaty shows that the wave function envelope increases exponentially

$$\boxed{\lim_{x\to\infty} \frac{\ln|\psi(x)|}{x} = \gamma} \tag{II.47}$$

where γ coincides with the Lyapunov exponent of matrices (II.44) (up to a factor ρ coming from $n \sim \rho x$). This gives again a definition of the localisation length $\xi \overset{\text{def}}{=} 1/\gamma$ in this continuous model.

✍ *Exercice II.4 :* *The study of the perfect lattice of impurities is instructive. We consider transfer matrices* (II.44) *for* $\ell_n = a$ *and* $v_n = v$, $\forall n$.

a) Show that Bloch theorem implies that the transfer matrix M *has eigenvalue* e^{iK}.

b) Deduce the quantization equation and show that spectrum of eigenstates forms energy bands (hint : use a graphical resolution).

c) Wheck that the eigenvalues of M *can be written as* $e^{+\Omega}$ *and* $e^{-\Omega}$. *Show that for the perfect crystal we have either* $\Omega \in \mathbb{R}$ *or* $\Omega \in i\mathbb{R}$. *Deduce the expression of the Lyapunov expression and of the integrated density of states.*

Solution : exercice 6.10 of [118].
The exercice illustrates that for a non disordered problem, the Lyapunov vanishes on the spectrum, i.e. states are extended.

4) The Lyapunov exponent and the Borland conjecture

We have characterized above the localization properties through the Lyapunov exponent γ, which is defined as the growth rate of the wave function, (II.37) for discrete model or (II.47) for the continuous model. However, we have insisted on the fact that these definitions involve the solution of the initial value problem. Is it really what we are looking for ?

Spectral (Sturm-Liouville) problem : in principle, we should rather be interested in properties of the normalised wave functions, solutions of the spectral problem

$$-\varphi''(x) + V(x)\varphi(x) = E\,\varphi(x) \quad \text{with} \quad \begin{cases} \varphi(0) = 0 \\ \varphi(L) = 0 \end{cases} \tag{II.48}$$

where Dirichlet boundary conditions are here chosen.
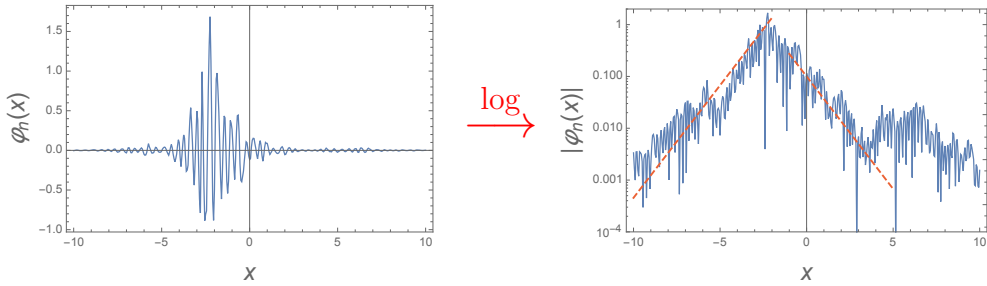
Figure 5: *An eigenstate obtained by exact diagonalisation.*

Eigenstates are localized at random places. Interestingly, when plot in semi-log scale, they present the same rate for exponential growth and exponential decay.

Initial value (Cauchy) problem : We have defined above the Lyapunov exponent as the growth rate

$$\gamma = \lim_{x \to \infty} \frac{\ln|\psi(x)|}{x} \tag{II.49}$$

of the solution of the initial value (Cauchy) problem

$$-\psi''(x) + V(x)\psi(x) = E\,\psi(x) \quad \text{with} \quad \begin{cases} \psi(0) = 0 \\ \psi'(0) = 1 \end{cases} \tag{II.50}$$

Such a solution exists $\forall E$ (while the solutions $\varphi(x)$ of the spectral problem exist only for a discrete set of energies).

The Borland conjecture : It is not completly obvious that $\xi \overset{\text{def}}{=} 1/\gamma$, a property of the initial value problem $\psi(x)$, is a good definition charaterizing the spreading of the wave function $\varphi(x)$, solution of the Sturm-Liouville problem. This assumption is known as the *"Borland conjecture"* [31]. It relies on the fact that $\varphi(x)$ is constructed by matching two solutions of two different initial value problem : one solution $\psi_+(x)$ satisfying $\psi_+(0) = 0$, growing exponentially from the left, and another one $\psi_-(x)$ satisfying $\psi_-(L) = 0$, growing exponentially from the right to the left. The two solutions are expected to present the same statistical properties, hence the definition. This assumes that the statistical properties of the envelopes of $\psi(x)$ and $\varphi(x)$ are the same, i.e. that *the matching procedure does not affect the statistical properties of the envelope.*

Is the Lyapunov exponent always a good measure of localisation ? Although the Borland conjecture is a reasonnable assumption for high energy wave functions rapidly oscillating, when oscillations and growth of the envelope decouple, it is more questionable for low energy states : see the discussion in the review article [42] and references therein ; a counter-example for which Borland's conjecture do not applied is discussed in [123] (also in [42]). We rediscuss this point below in § II.D

5) Preliminary conclusion

The use of the Furstenberg theorem has immediatly provided the nature of the eigenstates, shown to be *exponentially localised.* The argument is very **general** because any (linear) wave equation can be formulated with the help of transfer matrices (even in the multi-channel case ; strictly 1D is not a restriction). However it does not give the quantitative information about the localisation length. In general, given the measure $\mu(\mathrm{d}M)$ characterizing the random matrices, finding the Lyapunov exponent is a very hard task. From the point of view of the disordered model (II.5), the question would be : given the distribution $P(V)$ of the random potentials V_n, what is the Lyapunov exponent γ ? A review on how to answer to this precise question can be found in the first part of the book by Jean-Marc Luck [88].

We analyse below a continuous model where such an analysis will be facilitated.

II.C   Detailed study of a solvable continuous model

1) Definition of the model

Let us consider the Schrödinger Hamiltonian

$$H = -\frac{\mathrm{d}^2}{\mathrm{d}x^2} + V(x) \tag{II.51}$$

for the simplest model of random potential, namely the Gaussian white noise

$$P[V] \propto \exp\left\{-\frac{1}{2\sigma}\int \mathrm{d}x\, V(x)^2\right\} \qquad \Rightarrow \qquad \overline{V(x)V(x')} = \sigma\,\delta(x-x')\,. \tag{II.52}$$

✍ *Exercice II.5 Relation to other models :*
a) Relate σ to the strength of the disordered potentials of the lattice model $\langle V_n V_m\rangle = W^2\delta_{n,m}$.

b) Show that the model with the Gaussian white noise potential may be obtained by considering the high density limit ($\rho \to \infty$) with weak impurities ($v_n \to 0$) of the random impurity model introduced previously. What is the precise relation between the two models ? I.e. how can one relates σ to the parameters of the impurity model ?

Hint : *Find the proper non trivial limit of the characteristic functional (II.20).*

✍ *Exercice II.6 Dimensional analysis :*
a) Check that the dimension of disorder strength is

$$[\sigma] = L^{-3} \tag{II.53}$$

b) We consider the Lyapunov exponent $\gamma(E)$ (inverse localisation length) and the integrated density of states per unit length $N(E)$. Use dimensional analysis to express γ and N in terms of two scaling functions.

c) Deduce how the zero energy localisation length behaves with the disorder strength ? What is the amount of states that have migrated from $\mathbb{R}^+$ to $\mathbb{R}^-$?

2) Riccati analysis

We now show that the localisation properties and the spectral properties of the Schrödinger equation with a disordered potential can be obtained by studying a random process related to the solution of the Cauchy problem (the wavefunction), denoted $\psi(x)$ henceforth. The ideas will be applied to the case of the Gaussian white noise potential below. We introduce the Riccati variable

$$z(x) \stackrel{\text{def}}{=} \frac{\psi'(x)}{\psi(x)} \tag{II.54}$$

We will see that the study of this random process can be easily handled by standard techniques (Langevin and Fokker-Planck equations). From $-\psi'' + V\psi = E\psi$, we obtain that the Riccati variable obeys a first order non linear differential equation (use $\psi''/\psi = z' + z^2$)

$$\frac{\mathrm{d}}{\mathrm{d}x}z(x) = -E - z(x)^2 + V(x) = \mathcal{F}(z(x)) + V(x) \tag{II.55}$$

where we introduce the "force" $\mathcal{F}(z) = -E - z^2$ and the related "potential" :

$$\mathcal{U}(z) = -\int \mathrm{d}z\, \mathcal{F}(z) = Ez + \frac{1}{3}z^3 . \tag{II.56}$$

Equation (II.55) has the structure of the Langevin equation describing a fictitious Brownian particle of "position" $z(x)$ at "time" x, in the overdamped regime where the speed is proportional to the force.
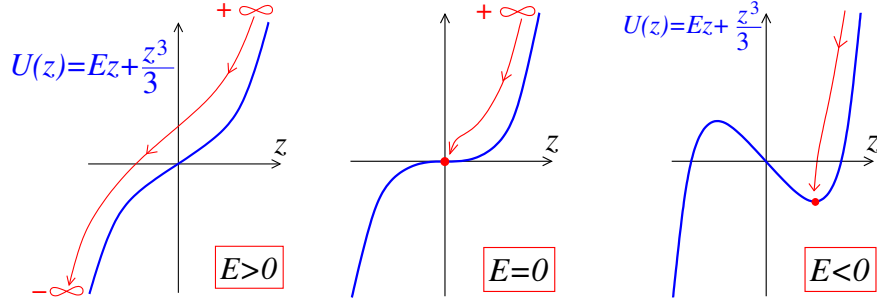
Figure 6: **Dynamics of the Riccati variable** *under the action of the deterministic force.*

The introduction of the Riccati variable will be very useful in order to analyze the dynamics of the process. We can already make the following observations :

- When $E > 0$, the "deterministic force" alone, i.e. the force $\mathcal{F}(z) = -E - z^2$ induces a flow of the process from $+\infty$ to $-\infty$. In the absence of the potential, the Riccati variable takes a finite "time" to cross $\mathbb{R}$. Let us start from $z(x_0) = +\infty$ (that corresponds to a node of the wave function, $\psi(x_0) = 0$). Then the next divergence (i.e. the next node of ψ) occurs after a "time" ℓ given by

$$\int_{x_0}^{x_0+\ell} \mathrm{d}x = -\int_{+\infty}^{-\infty} \frac{\mathrm{d}z}{E + z^2} \qquad \Rightarrow \qquad \ell = \frac{\pi}{\sqrt{E}} \tag{II.57}$$

  The distance between the nodes of the wave function is the inverse of the integrated density of states (IDoS) per unit length $N_0(E) = 1/\ell$. This is the result of a general theorem : the oscillation theorem (or Sturm-Liouville theorem, cf. 7).

  For $E < 0$, the potential traps the Riccati variable at $z_+ = \sqrt{-E}$.

24

- The random potential plays the role of a random (Langevin) force.

  For $E > 0$, it induces fluctuations of the time needed to go from $+\infty$ to $-\infty$, what is responsible for a deviation of the IDoS $N(E)$ from the free IDoS $N_0(E) = \frac{1}{\pi}\sqrt{E}$.

  For $E < 0$, a negative fluctuation of the potential may allow the process to escape the potential well and induces a finite flow of the Riccati.

Spectral properties (from the node counting method).— In the absence of the random potential $V(x)$, we have shown that the "time" needed by the process $z(x)$ to go from $+\infty$ to $-\infty$ coincides with the IDoS per unit length. This property remains true in the presence of the disordered potential, provided we consider the average time, i.e. $N(E) = 1/\bar{\ell}$.
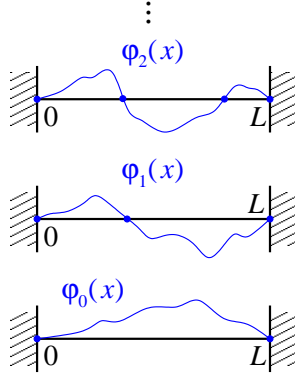
Figure 7: **Oscillation (Sturm-Liouville) theorem.** *In 1D, the number of nodes of the wavefunction coincides with the excitation degree n, i.e. the IDoS.*

This relation may be understood as follows : The density $1/\bar{\ell}$ is the average density of nodes of the wave function per unit length. From the oscillation (Sturm Liouville) theorem this coincides precisely with the IDoS per unit length. It will also be convenient for the following to notice that the density of the Riccati's infinitudes can be interpreted as the stationary probability current $-J$:

$$\boxed{N(E) = J = 1/\bar{\ell}} \tag{II.58}$$

J = number of infinitudes of the Riccati process per unit length ("time")= number of nodes of ψ per unit length= IDoS per unit length (oscillation theorem).

Another proof : Consider the IDoS $\mathcal{N}_L(E) = \sum_{k=1}^{\infty} \theta_H(E - E_k)$. For $E = E_N$, the Nth node coincides with the boundary, i.e. $L = \sum_{n=1}^{N} \ell_n$. Because the lengths are i.i.d. variables, we can write

$$L = \sum_{n=1}^{N} \ell_n \underset{L\to\infty}{\simeq} N\,\bar{\ell} = \mathcal{N}_L(E_N)\,\bar{\ell} \qquad \Rightarrow \qquad N(E) \overset{\text{def}}{=} \lim_{L\to\infty} \frac{\mathcal{N}_L(E)}{L} = 1/\bar{\ell}$$

QED.

Localisation length.— Our definition of the localisation length is the growth rate of the solution of the Cauchy (initial value) problem

$$\gamma = \lim_{x\to\infty} \frac{\ln|\psi(x)|}{x} = \lim_{x\to\infty} \int_0^x \frac{\mathrm{d}t}{x} z(t)\,. \tag{II.59}$$

25

Assuming some ergodic properties, we can express the Lyapunov exponent as an integral of the Riccati's stationary distribution $f(z)$ as

$$\boxed{\gamma = \fint dz\, z\, f(z)} \qquad \Rightarrow \qquad \xi \overset{\text{def}}{=} 1/\gamma \,. \tag{II.60}$$

We have introduced a principal part

$$\fint_{-\infty}^{+\infty} dx\, h(x) \overset{\text{def}}{=} \lim_{R \to +\infty} \int_{-R}^{+R} dx\, h(x) = \int_{-\infty}^{+\infty} dx\, \frac{h(x) + h(-x)}{2}$$

in order to account for the possible slow power law decay of the Riccati distributionn $f(z) \sim 1/z^2$.

Application to the model with Gaussian white noise disorder.— If the disordered potential is a Gaussian white noise, Eq. (II.52), then (II.55) is the usual Langevin equation with a force uncorrelated in "time" . Then we can directly relate this Langevin equation to a Fokker-Planck equation for the probability density of the Riccati variable $f(z;x) \overset{\text{def}}{=} \langle \delta(z - z(x)) \rangle$ (cf. appendix) :

$$\frac{\partial}{\partial x} f(z;x) = \left(\frac{\sigma}{2} \frac{\partial^2}{\partial z^2} - \frac{\partial}{\partial z} \mathcal{F}(z) \right) f(z;x) \,. \tag{II.61}$$

It can be conveniently recast under the form of a conservation equation

$$\frac{\partial}{\partial x} f(z;x) = -\frac{\partial}{\partial z} \mathcal{J}(z;x) \quad \text{where} \quad \mathcal{J}(z;x) = \left(\mathcal{F}(z) - \frac{\sigma}{2} \frac{\partial}{\partial z} \right) f(z;x) \tag{II.62}$$

is the probability current, given by the sum of a drift term and a diffusion current.

The Fokker-Planck involves the (forward) generator

$$\mathscr{G}^\dagger = \frac{\sigma}{2} \frac{d^2}{dz^2} - \frac{d}{dz} \mathcal{F}(z) \,, \tag{II.63}$$

adjoint of the generator of the diffusion $\mathscr{G} = \frac{\sigma}{2} \frac{d^2}{dz^2} + \mathcal{F}(z) \frac{d}{dz}$ (i.e. the backward generator). We prove in the exercice below that it has a *discrete spectrum of eigenvalues*. From this observation, we deduce that the distribution of the Riccati variable converges to a limit distribution on a finite length scale ℓ_c (the correlation length of the Riccati process)

$$f(z;x) \xrightarrow[x \to \infty]{} f(z) \,, \tag{II.64}$$

where $f(z)$ obeys

$$\boxed{\left(\frac{\sigma}{2} \frac{d}{dz} + E + z^2 \right) f(z) = N(E)} \tag{II.65}$$

where we have used that the steady current

$$\mathcal{J}(z;x) \xrightarrow[x \to \infty]{} -N \tag{II.66}$$

is the IDoS per unit length.

✍ *Exercice II.7 Spectrum of the generator : The aim of the exercice is to show that $f(z;x)$ reachs a limit distribution $f(z)$ over a characteristic scale ℓ_c (the correlation length). Assuming initial condition $z(0) = z_0$, we can write formally the propagator as* [7]

$$f(z;x) = \langle z | e^{x \mathscr{G}^\dagger} | z_0 \rangle = \sum_n \Phi_n^{\text{R}}(z) \, \Phi_n^{\text{L}}(z_0) \, e^{-x \mathscr{E}_n} \tag{II.67}$$

---

[7] **Propagator :** In order to introduce this concept in a more simple case, consider a Schrödinger operator H. the propagator is the evolution operator in imaginary time $K_t(x|x_0) = \theta_{\text{H}}(t) \langle x | e^{-tH} | x_0 \rangle$, Green's function of the time dependent Schrödinger equation $(\partial_t + H) K_t(x|x_0) = \delta(t)\, \delta(x - x_0)$.

in terms of left/right eigenvectors, $\mathscr{G}^\dagger \Phi_n^{\mathrm{R}}(z) = -\mathscr{E}_n \Phi_n^{\mathrm{R}}(z)$ and $\mathscr{G} \Phi_n^{\mathrm{L}}(z) = -\mathscr{E}_n \Phi_n^{\mathrm{L}}(z)$.

a) Consider the nonunitary transformation

$$\mathscr{H}_+ = e^{\frac{1}{\sigma}\mathcal{U}(z)}(-\mathscr{G}^\dagger)e^{-\frac{1}{\sigma}\mathcal{U}(z)} \tag{II.68}$$

This shows that $\mathscr{G}^\dagger$ and $\mathscr{H}_+$ are isospectral. [8] Chek that

$$\mathscr{H}_+ = -\frac{\sigma}{2}\frac{\mathrm{d}^2}{\mathrm{d}z^2} + \frac{[\mathcal{F}(z)]^2}{2\sigma} + \frac{\mathcal{F}'(z)}{2} = \frac{\sigma}{2}\left(\frac{\mathrm{d}}{\mathrm{d}z} + \frac{\mathcal{F}(z)}{\sigma}\right)\left(-\frac{\mathrm{d}}{\mathrm{d}z} + \frac{\mathcal{F}(z)}{\sigma}\right) \tag{II.69}$$

b) Analyse the shape of the effective potential for the Schrödinger operator $\mathscr{H}_+$ and deduce the nature of the spectrum of eigenvalues $\{\mathscr{E}_n\}$ (discrete/continuous).

The Hamiltonian (II.69) is called a *supersymmetric* operator in reference with the specific structure of the form $\mathscr{H}_+ = \frac{\sigma}{2}Q^\dagger Q$ (generalisation of the harmonic oscillator $a^\dagger a$) [77, 40].

✎ **Exercice II.8 Stationary solution :** a) Construct explicitly the solution of (II.65).

b) **Rice formula.**– Show that the asymptotic behaviour of the distribution is $f(z) \underset{z\to\pm\infty}{\simeq} N(E)/z^2$.

c) Show that the normalisation provides an integral representation of the IDoS (one of the two integrals can be done).

3) Localisation – Weak disorder expansion

It is possible to compute exactly the Lyapunov exponent (see exercice II.10 below), however we now only present a more simple perturbative analysis (in the disorder strength σ), valid in the high energy limit, $E \gg \sigma^{2/3}$. Let us assume that the stationary distribution and the IDoS have a perturbative expansion :

$$f(z) = f^{(0)}(z) + f^{(1)}(z) + \cdots \tag{II.70}$$

$$N = N^{(0)} + N^{(1)} + \cdots \tag{II.71}$$

Inject this form in (II.65) leads to

$$f^{(0)}(z) = \frac{N^{(0)}}{z^2 + k^2} \tag{II.72}$$

$$f^{(n)}(z) = \frac{N^{(n)}}{z^2 + k^2} - \frac{\sigma}{2(z^2 + k^2)}\frac{\mathrm{d}}{\mathrm{d}z}f^{(n-1)}(z) \tag{II.73}$$

where we have introduced $k = \sqrt{E}$. $f^{(0)}$ carries all the normalisation, hence we recover the well-known IDoS for the free case $N^{(0)} = \frac{\sqrt{E}}{\pi}$. At first order we must have $\int \mathrm{d}z\, f^{(1)}(z) = 0$, hence $N^{(1)} = 0$ and $f^{(1)}(z) = -\frac{\sigma}{2(z^2+k^2)}\frac{\mathrm{d}}{\mathrm{d}z}f^{(0)}(z)$, etc. Finally we get

$$f(z) = \frac{k/\pi}{z^2 + k^2} + \frac{\sigma k}{\pi}\frac{z}{(z^2 + k^2)^3} + \mathcal{O}(\sigma^2) \tag{II.74}$$

that can be introduced into (II.60) :

$$\gamma = 0 + \frac{\sigma k}{\pi}\int \mathrm{d}z\, \frac{z^2}{(z^2 + k^2)^3} + \mathcal{O}(\sigma^2) = \frac{\sigma}{8E} + \mathcal{O}(\sigma^2) \tag{II.75}$$

---

[8] The spectra of two operators differ by a zero mode (see Appendix D of Ref. [64] for a discussion of this subbtle point).

The important conclusion of this calculation is the fact the the *Lyapunov exponent is different from zero for any (positive) energy.* Therefore **all eigenstates get localised by the disorder**, how weak it is. The localisation length however increases with energy as

$$\boxed{\xi_E \underset{E \gg \sigma^{2/3}}{\simeq} \frac{8E}{\sigma}}$$

(II.76)

We may interpret this important result as follows :

- in the absence of disorder ($\sigma = 0$), the spectrum of eigenvalues is $\mathbb{R}_+$. Negative energies correspond to evanescent (non normalisable solutions) $\exp(\pm\sqrt{-E}\,x)$, hence the Lyapunov exponent is non zero outside of the spectrum, $\gamma = \sqrt{-E}$ for $E < 0$, and vanishes on the spectrum, $\gamma = 0$ for $E > 0$.

- In the presence of disorder ($\sigma \neq 0$), the Lyapunov exponent becomes non zero on the spectrum. Correlatively, the disorder drags some states in the negative part of the spectrum (figure 8).
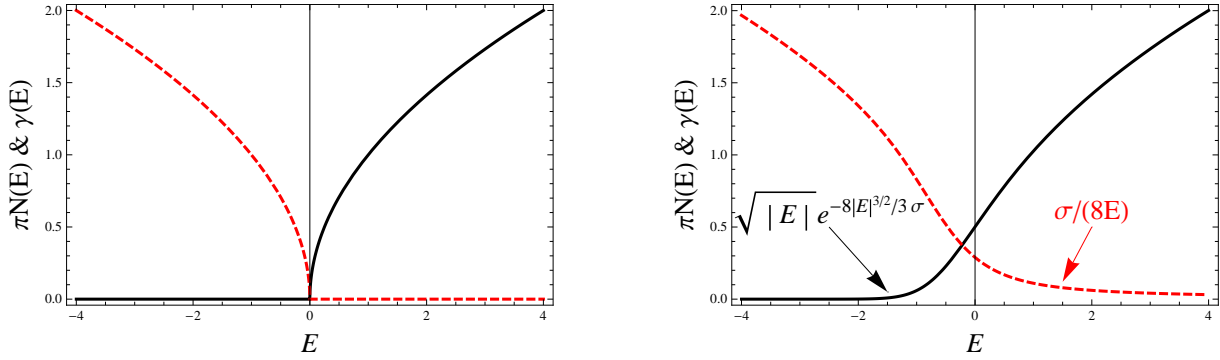
Figure 8: **Halperin model.**– *IDoS (black continuous line) and Lyapunov exponent (dashed red line) in the absence of disorder (left) and with Gaussian white noise potential (right). From Eq. (II.94)*

Generalisation : The perturbative formula for the Lyapunov exponent may be generalised to arbitrary random potentials with finite correlation function. It leads to [15, 87]

$$\gamma \simeq \frac{1}{8k^2} \int \mathrm{d}x \, \overline{V(x)V(0)}^c \cos(2kx) \qquad \text{as } E = k^2 \to \infty \,.$$

(II.77)

✎ ***Exercice II.9 :*** *In the experiment with cold atoms, the disordered potential is realised with a speckle pattern (Fig. 12). The potential felt by the atoms is proportional to the light intensity $V(x) \propto |\mathcal{E}(x)|^2$, where the electric field presents correlations $\langle \mathcal{E}(x)\mathcal{E}^*(x')\rangle^{(\text{speckle})} = I_0 \frac{\sin(|x-x'|/\ell_c)}{|x-x'|/\ell_c}$. What are the potential correlations ? Deduce the Lyapunov exponent from the perturbative formula (II.77). What can you expect when this expression vanishes ?*

See Ref. [89]

Remark : $V(x)$ **with infinite moments.**– The formula (II.77) emphasizes that the high energy behaviour of the localisation length $\xi_E \propto E$ is pretty universal for random potentials uncorrelated in space. This behaviour however obviously requires that the second moment of

the potential is finite, i.e. $\langle V(x)V(0)\rangle < \infty$. If this is not the case, large fluctuations of the random potential can induce unusual localisation properties, like a non linear dependence of the localisation length with E or the phenomenon of superlocalisation [28] (a clear discussion on sublocalisation and superlocalisation and references can be found in Ref. [30]).

4) Lifshitz tail

Another feature common to disordered systems is the existence of the low energy non analytic density of states (non analytic in the disorder strength σ). The fraction of states with energy $E < 0$ may be estimated by a simple dimensional analysis as

$$N(0) \sim \sigma^{1/3} \tag{II.78}$$

hence the DoS per unit length get finite at zero energy $\rho(0) \sim \sigma^{-1/3}$ (it diverges as disorder disappears, as it should). We may obtain the low energy behaviour of the IDoS by a very simple argument, remembering the interpretation of the IDoS as a current of the Riccati variable : for large $E = -k^2$, the potential $\mathcal{U}(z)$ developes a local minimum at $z = +k$, with a potential barrier $\Delta\mathcal{U} = \mathcal{U}(-k) - \mathcal{U}(k) = 4k^3/3$, that traps the process a very long time $\propto \exp\frac{2\Delta\mathcal{U}}{\sigma}$ (Arrhenius law). The current is expected to be diminished in inverse proportion, hence

$$N(E) \underset{E \to -\infty}{\sim} \exp\left[-\frac{8}{3\sigma}(-E)^{3/2}\right] . \tag{II.79}$$

This interpretation was first suggested by Jona-Lasinio [76].

Ordered spectral statistics and energy level correlations.–   It allows to obtain not only the average density of states per unit length, but although the order statistics of eigenvalue (distribution of ground state energy, first excited state, etc) [116]. I have shown in this paper that this ordered statistics problem for a priori *correlated* variables (the eigenvalues of a r andom operator) coincides with Gumbel laws describing *uncorrelated* random variables. This shows that in the strongly localised phase, eigenvalues behave as independent random variables [98].

5) Conclusion : universal *versus* non universal regimes

We have encountered two regimes :

- *Universal* results (high energy/weak disorder) do not depend on details of $P(V)$, but only on few properties, like $\langle V^2 \rangle$. **Anderson localisation** takes place in this regime : although the energy of the particle is much higher than the potential, $E \gg \sigma^{2/3}$, eigenstates are localised (particle would be free classically).

- *Non universal* results (low energy/strong disorder), such as Lifshitz tails, depend on the full distribution $P(V)$, as usual for *large deviations.* [9] In the low energy limit, localisation of eigenstates is somehow obvious and corresponds to trapping of the particle by deep potential wells (what would also occur classically).

---

[9]Cf. Refs. [41, 67] for reviews on low energy spectral singularities in 1D disordered systems.
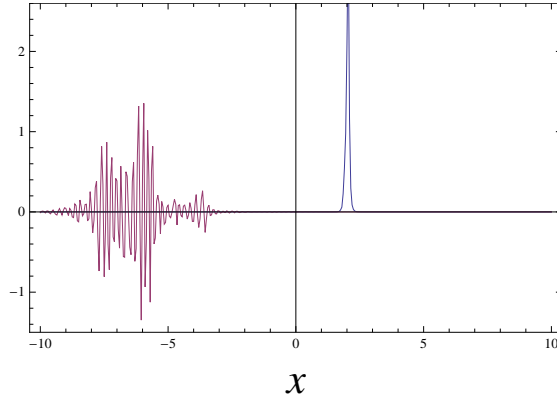
Figure 9: *The ground state and some high energy states of the Anderson model with Gaussian random potentials for $W/t = 0.79$.*

Final remark : Although we have developed the Riccati analysis in the frame of a continuous model, these ideas can be formulated in the context of the discrete Anderson model (II.81). In this case a natural definition for the Riccati variable is $R_n \stackrel{\text{def}}{=} \psi_{n+1}/\psi_n$ which obeys the recursion

$$R_n = V_n - \varepsilon - \frac{1}{R_{n-1}} \, . \tag{II.80}$$

A pedagogical description can be found in the book of J.-M. Luck [88].

6) Relation between spectral density & localisation : Thouless formula

We show that the IDoS and the Lyapunov exponent are related by analyticity.

An elementary derivation for the discrete Anderson model.— Let us consider the tight-binding Hamiltonian (for hopping $t = 1$)

$$-\psi_{n+1} + V_n \, \psi_n - \psi_{n-1} = \varepsilon \, \psi_n \tag{II.81}$$

on a finite interval $n \in \{1, \cdots, N\}$. We consider the initial boundary conditions $\psi_0 = 0$ (Dirichlet-like) and $\psi_1 = 1$. Wave function on the next sites can be computed from $\psi_{n+1} = (V_n - \varepsilon) \, \psi_n - \psi_{n-1}$. It will be useful to remark for the following that

$$\psi_{n+1} \simeq (-\varepsilon) \, \psi_n \qquad \text{for} \ \ \varepsilon \to \infty \tag{II.82}$$

The spectrum of the finite system is obtained by imposing a second boundary condition, say $\psi_{N+1} = 0$. This equation is nothing but the *quantification equation*, whose solutions are the eigenvalues $\{\varepsilon_\alpha\}_{\alpha=1,\cdots,N}$ of the Schrödinger Hamiltonian. We conclude that the solution ψ_n of the initial value problem $\psi_0 = 0$ & $\psi_1 = 1$ can be written as a function of the energy

$$\psi_{N+1} = \prod_{\alpha=1}^{N} (\varepsilon_\alpha - \varepsilon) \, , \tag{II.83}$$

where the prefactor has been fixed thanks to (II.82). Taking the logarithm of this equation, we obtain

$$\frac{1}{N} \ln |\psi_{N+1}| = \int \mathrm{d}\varepsilon' \, \rho(\varepsilon') \ln |\varepsilon' - \varepsilon| \tag{II.84}$$

30

where $\rho(\varepsilon) \stackrel{\text{def}}{=} \frac{1}{N} \sum_{\alpha=1}^{N} \delta(\varepsilon - \varepsilon_\alpha)$ is the density of states per site. Note that this equation is *general* and has not required any assumption on the potential. Now considering a disordered potential, the left hand side can be identitified with the Lyapunov exponent in the limit $N \to \infty$ when the spectrum becomes dense, thus

$$\boxed{\gamma(\varepsilon) = \int d\varepsilon' \, \rho(\varepsilon') \ln |\varepsilon' - \varepsilon|} \qquad \text{(for the Anderson model).} \qquad \text{(II.85)}$$

This formula is known as the Thouless formula [128].

Exactly the same idea can be performed for a continuous model by considering the wave function $\psi(x; E)$ solution of the initial value problem $\psi(0; E) = 0$ and $\psi'(0; E) = 1$. The quantification equation now reads $\psi(L; E) = 0$ providing the spectrum on a finite interval of length L with Dirichlet boundary conditions. A little technical difficulty however arises due to the fact that the spectrum is not bounded from above and involves an *infinite* number of eigenvalues. One can however show that the wavefunction is proportional to the *functional determinant* $2\psi(L; E) = \det(E + \partial_x^2 - V(x))$ (see [80] for a pedagogical introduction to functional determinants, or [71]).

Analytical properties for the continuous model.— The IDoS and the Lyapunov exponent are the real and imaginary part of a single analytic function defined in the upper complex plane. It follows that it is possible to write a Kramers-Kronig relation relating one to the other (the Thouless formula), as was well illustrated by the exercice below.

This might be understood in a simple way by considering the Fourier transform of the stationary distribution

$$\hat{f}_E(q) = \int dz \, e^{-iqz} \, f_E(z) \qquad \text{(II.86)}$$

For example, in the case of the Schrödinger equation with Gaussian white noise potential $V(x)$, it follows from (II.65) that $\hat{f}_E(q)$ obeys the differential equation

$$\left(-\frac{d^2}{dq^2} + E + \frac{i\sigma}{2} q \right) \hat{f}_E(q) = 2\pi \, N(E) \, \delta(q) \qquad \text{(II.87)}$$

For other models of random potential, we obtain a different differential equation. We can see that

$$\hat{f}_E'(0^+) = -\pi \, N(E) - i \, \gamma(E) \qquad \text{(II.88)}$$

thus the integrated density of states and the Lyapunov exponent are real and imaginary part of an *analytic* function of the energy *in the upper complex plane*, denoted as the characteristic function, or the complex Lyapunov exponent

$$\Omega(E) = \gamma(E) - i\pi \, N(E) \, . \qquad \text{(II.89)}$$

Kramers-Kronig relation can be obtained by performing some soustraction in order to deal with an asymptotically decaying function :

$$\widetilde{\Omega}(E) \stackrel{\text{def}}{=} \Omega(E) - \Omega_0(E) \qquad \text{where} \quad \Omega_0(E) = \sqrt{-E - i0^+} \qquad \text{(II.90)}$$

is the complex Lyapunov exponent in the free case. Considering the appropriate closed contour in the complex half plane gives :

$$\widetilde{\Omega}(E) = -i \fint_{\mathbb{R}} \frac{d\omega}{\pi} \frac{\widetilde{\Omega}(\omega)}{\omega - E} \qquad \text{(II.91)}$$

31

i.e., taking the real part

$$\gamma(E) - \gamma_0(E) = -\!\!\int dE' \, \frac{N(E') - N_0(E')}{E' - E} \, ,$$
(II.92)

where $\gamma_0(E) = \theta_H(-E)\sqrt{-E}$ and $\pi N_0(E) = \theta_H(E)\sqrt{E}$. We can rewrite the relation in terms of the density of states $\rho = N'$ as

$$\boxed{\gamma(E) - \gamma_0(E) = \int dE' \, \left[\rho(E') - \rho_0(E')\right] \ln|E' - E|}$$
(for the Schrödinger equation).
(II.93)

Up to the soustraction, required because the spectrum is unbounded from above, this is the same relation as (II.85). Analyticity shows that real and imaginary parts of $\Omega(E)$ are related through a Hilbert transform.

✍ **Exercice II.10 Halperin's result (1965) :** *In exercice II.8, we have obtained an integral representation of the IDoS, due to Frisch and Lloyd [60]. An integral representation of the Lyapunov exponent could be obtained similarly from the knowledge of the stationary distribution $f(z)$. In this exercice we show that γ and N can be expressed in terms of Airy functions. This result is due to Halperin [70].*
a) Fourier transform the differential equation (II.65) : $\hat{f}(q) = \int dz\, e^{-iqz} f(z)$.

b) Solve the differential equation for $\hat{f}(q)$ on $\mathbb{R}_+$ (find the solution decaying for $q \to +\infty$). Deduce that the complex Lyapunov exponent is

$$\Omega(E) = \gamma(E) - i\pi\, N(E) = \left(\frac{\sigma}{2}\right)^{1/3} \frac{\mathrm{Ai}'(\xi) - i\,\mathrm{Bi}'(\xi)}{\mathrm{Ai}(\xi) - i\,\mathrm{Bi}(\xi)} \quad \text{where } \xi = -\left(\frac{2}{\sigma}\right)^{2/3} E \, .$$
(II.94)

c) Recover the asymptotic behaviour for the Lyapunov exponent and the low energy density of states (use that the Wronskian of the two Airy functions is $W[\mathrm{Ai}, \mathrm{Bi}] = 1/\pi$).

Appendix :
Airy equation $f''(z) = z\,f(z)$ admits two independent real solutions Ai *and* Bi *with asymptotic behaviours* $\mathrm{Ai}(z) \simeq \frac{1}{\sqrt{\pi}\,(-z)^{1/4}} \cos\left[\frac{2}{3}(-z)^{3/2} - \frac{\pi}{4}\right]$ *and* $\mathrm{Bi}(z) \simeq \frac{-1}{\sqrt{\pi}\,(-z)^{1/4}} \sin\left[\frac{2}{3}(-z)^{3/2} - \frac{\pi}{4}\right]$ *for* $z \to -\infty$, *and* $\mathrm{Ai}(z) \simeq \frac{1}{2\sqrt{\pi}\,z^{1/4}} \exp\left[-\frac{2}{3}z^{3/2}\right]$ *and* $\mathrm{Bi}(z) \simeq \frac{1}{\sqrt{\pi}\,z^{1/4}} \exp\left[\frac{2}{3}z^{3/2}\right]$ *for* $z \to +\infty$.

II.D   Another localization criterion : boundary conditions sensitivity (Thouless)

We have mentioned above that, although it is not the generic case in 1D, the Lyapunov exponent may not provide a good measure of the localization properties. This occurs for example by considering the Dirac equation with random mass

$$\left(i\,\sigma_2\,\partial_x + \sigma_1\,m(x)\right)\Psi(x) = \varepsilon\,\Psi(x)$$
(II.95)

where $\Psi(x)$ is a two-component spinor. In this case, it is well known that for $\langle m(x)\rangle = 0$, the Lyapunov vanishes at low energy as $\gamma \sim 1/\ln(g/|\varepsilon|)$, where g is the disorder strength with $\overline{m(x)\,m(x')}^c = g\,\delta(x - x')$ (see [32] and the reviews [40, 42]). Hence, the Lyapunov exponent does not provide a good measure of the localization properties (see the discussions in [116, 123]).

Is is possible to use a different localization criterion, which has been introduced by Thouless, and corresponds to probe the boundary conditions sensitivity. It is frequently used in numerical simulations by imposing the quantization condition $\varphi(L) = \varphi(0)\,e^{i\phi}$ (this corresponds to consider

the problem on a ring of perimeter L, threaded by a magnetic flux). If states do not depend on the parameter ϕ (i.e. they do not feel the boundaries) they are localized. When ϕ-dependence manifests, this corresponds to the crossover $\xi \sim L$.

In analytical calculations, this is usually very difficult to implement, since this requires to study deviations from translation invariance (effect of the boundaries). However, for the Dirac equation with random mass, I have shown in [123] that the averaged density of states for the problem for a finite length L presents the low energy behaviour

$$\overline{\rho_L(\varepsilon)} = \rho_{\text{bulk}}(\varepsilon)\,\mathcal{D}(L/\xi_\varepsilon) \qquad \text{with } \xi_\varepsilon \sim \frac{1}{g}\,\ln^2(g/|\varepsilon|) \tag{II.96}$$

where the scaling function $\mathcal{D}(y)$ depends on the precise boundary conditions and presents the behaviour $\mathcal{D}(y) \simeq 1$ for $y \gg 1$. Its analytical expression was derived in [123] :

$$\mathcal{D}(y) = \frac{4}{\sqrt{\pi\,y^3}} \sum_{n=1}^{\infty} n^2\,e^{-n^2/y} \tag{II.97}$$

(here for Dirichlet boundary conditions). This analysis shows that the localization length scales as $\xi_\varepsilon \sim \frac{1}{g}\,\ln^2(g/|\varepsilon|)$ for $\varepsilon \ll g$, i.e. is much larger than the scale provided by the Lyapunov exponent $1/\gamma \sim \frac{1}{g}\ln(g/|\varepsilon|)$.
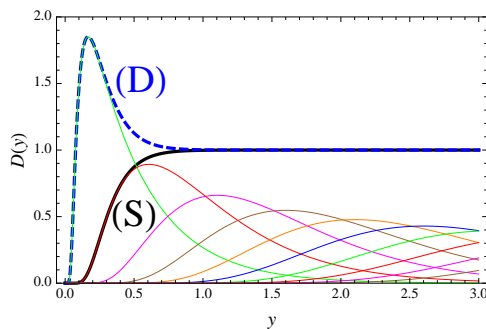
Figure 10: *Function $\mathcal{D}(y)$ (black curve with label "S"). From [123].*

II.E   Self-averaging and non self-averaging quantities – Conductance distribution

Importance of fluctuations.–   The wave function fluctuations can play an important role. We have seen above that $\ln|\psi(x)|$ is expected to have additive properties, hence to obey a generalised central limit theorem. Precisely, if one introduces a Wiener process [10] $W(x)$, we can write

$$\text{`` } \ln|\psi(x)| = \gamma_1\,x + \sqrt{\gamma_2}\,W(x) \text{ ''}. \tag{II.98}$$

The presence of the quotation marks is here to remind that this representation only holds over large scales $x \gg \ell_c$, where ℓ_c is the correlation length, and *neglect the rapid oscillations* of the wave function on short scale. [11] We have introduced

$$\gamma_1 \overset{\text{def}}{=} \lim_{x\to\infty} \frac{\overline{\ln|\psi(x)|}}{x} \qquad \text{and} \qquad \gamma_2 \overset{\text{def}}{=} \lim_{x\to\infty} \frac{\text{Var}\big(\ln|\psi(x)|\big)}{x} \tag{II.99}$$

---

[10] A Wiener process $W(x)$ is a normalised Brownian motion, i.e. a Gaussian process characterised by $\langle W(x)\rangle = 0$ and $\langle W(x)W(x')\rangle = \min(x,x')$.

[11] More rigorously we can follow the *phase formalism* : we perform the change of variable $(\psi,\psi') \to (\xi,\theta)$ according to $\psi = e^\xi \sin\theta$ and $\psi' = k e^\xi \cos\theta$. Considering the envelope $e^\xi = \sqrt{\psi^2 + (\psi'/k)^2}$ is a natural way to eliminate the oscillations. We write more corretly $\xi(x) = \gamma\,x + \sqrt{\gamma_2}\,W(x)$ (although this relation is only true over scale larger than the correlation length).

where γ_1 is a new notation for the Lyapunov exponent (denoted γ above). γ_2 has been studied in [105] for the model (II.51) (Fig. 11) and also for the Dirac equation with random mass.

The *relative* fluctuations of $\ln|\psi(x)|$ are negligible, however, when considering the wave function $\psi(x)$ itself, the fluctuations appear in the exponential and can therefore have a very strong effect on physical quantities, like the local DoS [11]. For example they dominate the moments of the wave function

$$\langle |\psi(x)|^q \rangle \simeq \exp\left\{ \left(q\gamma_1 + \frac{1}{2}q^2\gamma_2 + \cdots \right) x \right\} \tag{II.100}$$

where in principle the expansion in the exponential continues (the full expansion involves the *cumulants* γ_n of $\ln|\psi(x)|$).
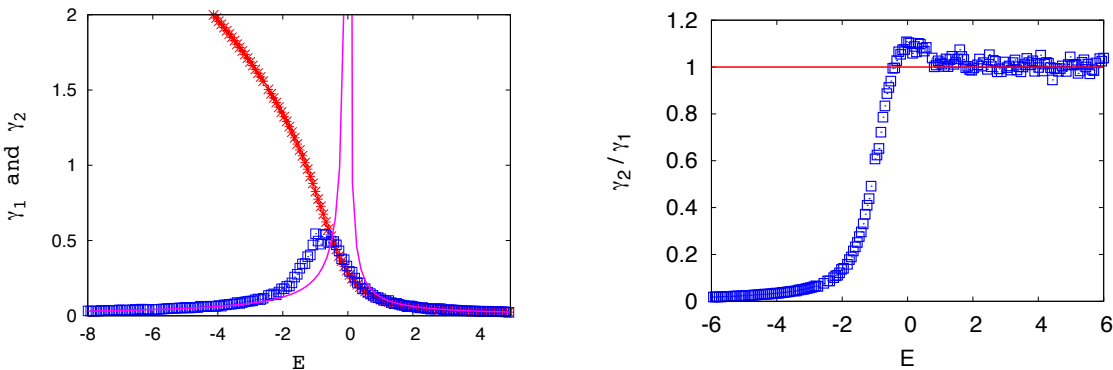
Figure 11: *The two cumulants of* $\gamma_1 = \lim_{x\to\infty}\frac{1}{x}\ln|\psi(x)|$ *(red cross) and* $\gamma_2 = \lim_{x\to\infty}\frac{1}{x}\mathrm{Var}\left(\ln|\psi(x)|\right)$ *(blue squares) for the model* $-\frac{\mathrm{d}^2}{\mathrm{d}x^2} + V(x)$ *as a function of the energy. Whereas* $\gamma_1 \simeq \gamma_2$ *for* $E \gg \sigma^{2/3}$, *they strongly deviates at low energy* $\gamma_1 \gg \gamma_2$ *for* $-E \gg \sigma^{2/3}$. *From [105].*

Single parameter scaling (SPS) hypothesis.– The analysis of the fluctuations have plaid a very important role in the theory of disordered systems since the early steps of the scaling theory. The most simple scaling hypothesis was assumed, i.e. a single parameter scaling theory [1, 14]. This was to assume that the *full distribution* of random quantities (like the conductance) is controlled by a single length scale, i.e. $\gamma_1 \simeq \gamma_2$ (note that this property is only asymptotically correct, for $E \to \infty$, see the recent discussion in [119, 120]).

It was later realised that such an assumption only holds in the weak disorder regime/high energy, whereas the study of the strong disorder/low energy regime requires a two parameter scaling theory [37] (i.e. average and fluctuations are controlled by two different scales $\gamma_1 > \gamma_2$).

Distribution of the conductance/transmission probability.– If we consider the solution of the initial value problem $\psi(x)$, say $\psi(0) = 1$ and $\psi'(0) = 0$ for example, we can express the dimensionless conductance (i.e. the transmission probability) of a long wire as

$$g \sim |\psi(L)|^{-2} \tag{II.101}$$

This relation is only true for long $L \gg \xi_E$. In principle the conductance involves a property of the eigenstates (the scattering state) that is constructed by satisfying some appropriate matching at the boundaries [15, 115], however over large scales, the wave function behaves exponentially

and loose the memory of its initial condition. We immediatly deduce that $\ln g$ is distributed according to a normal distribution :

$$P_L(\ln g) \simeq \frac{1}{\sqrt{8\pi\gamma_2 L}} \exp\left\{ -\frac{(\ln g + 2\gamma_1 L)^2}{8\gamma_2 L} \right\} , \tag{II.102}$$

which tells us that the distribution of the conductance is log-normal

$$Q_L(g) = \frac{1}{g} P_L(\ln g) \sim \frac{1}{g} \exp\left\{ -\frac{1}{8\gamma_2 L} \ln^2 g \right\} \quad \text{as } g \to \infty \tag{II.103}$$

i.e. with extremely long tail. Note that we are here characterizing the *typical fluctuations*. The distribution does not describe the large deviation for $g \to 0$, not the rare events corresponding to conducting disorder configurations (large g). The moments increase exponentially fast

$$\boxed{\langle g^n \rangle \simeq e^{2n(n\gamma_2 - \gamma_1)L}} \tag{II.104}$$

at large L ($\forall E$).

Moreover, assuming SPS, $\gamma_1 \simeq \gamma_2$, which occurs for energy$\gg$disorder [15, 115] (cf. Fig. 11), leads to

$$\langle g^n \rangle \simeq e^{2n(n-1)\gamma_1 L} , \tag{II.105}$$

with $\langle g \rangle \simeq 1$. In particular the relation $\langle g^n \rangle^{1/n} \simeq e^{2(n-1)\gamma_1 L}$ shows that the moment of order n characterises fluctuations exponentially larger than the moment of order $n - 1$.

Conclusion :

- g is not self averaging. Moments exponential in L are expected ; the n-th moment is typically $\sim e^{(\cdots)n^2 L}$.

- $\frac{1}{L} \ln g$ is self averaging.

Distribution of the LDoS.– Another case where the fluctuations play a crucial role is for the statistical properties of the local DoS. Cf. chapter 6 of [121]

Further reading : Recent developments on the study of fluctuations can be found in Refs. [119, 120].

II.F   Experiment with cold atoms

Anderson localisation is an interference effect, and thus requires coherence on a large scale.

In metals, Anderson localisation competes with interaction whose effect is twofold : first it breaks phase coherence in the weak disorder regime, second it can induce localisation (Mott transition) in the strong localisation regime.

In optics, Anderson localisation is difficult (but not impossible) to distinguish from absorption.

Recently, a beautiful observation of localisation of matter waves has been achieved in a cold atom experiment. An atomic gas is trapped by a harmonic well (figure 12.a). A disordered potential is superimposed, resulting from a speckle pattern (blue) together with a one-dimensional confinement (pink). At some initial time the harmonic well is released (figure 12.b) : a fraction of the gas remains localised by the disordered potential (green profile on figure b), exhibiting exponential tails. This experiment is therefore a rather direct observation of exponential localisation of wave functions, Fig. 12.d, (although what is observed is not a wave function but a density profile). The remarkable control on microscopic parameters in cold atom experiment allows for a quantitative analysis.
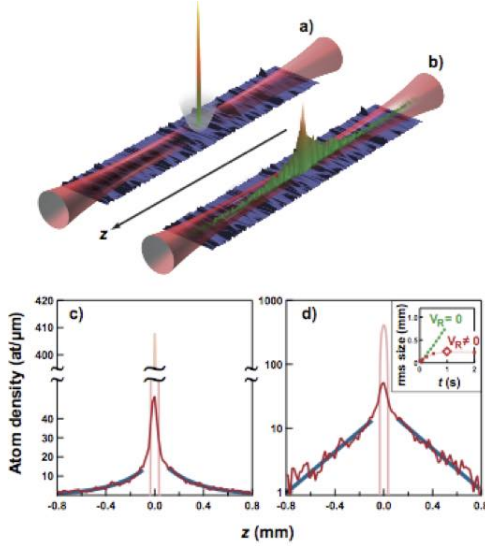
Figure 1. Observation of exponential localization. a) A small BEC (1.7 x 10⁴ atoms) is formed in a hybrid trap, which is the combination of a horizontal optical waveguide ensuring a strong transverse confinement, and a loose magnetic longitudinal trap. A weak disordered optical potential, transversely invariant over the atomic cloud, is superimposed (disorder amplitude V_R small compared to the chemical potential μ_{in} of the atoms in the initial BEC). b) When the longitudinal trap is switched off, the BEC starts expanding and then localises, as observed by direct imaging of the fluorescence of the atoms irradiated by a resonant probe. On a and b, false colour images and sketched profiles are for illustration purpose, they are not exactly on scale. c-d) Density profile of the localised BEC, 1s after release, in linear or semi-logarithmic coordinates. The inset of Fig d (rms width ot the profile vs time t, with or without disordered potential) shows that the stationary regime is reached after 0.5 s. The diamond at t=1s corresponds to the data shown in Fig c-d. Blue solid lines in Fig c are exponential fits to the wings, corresponding to the straight lines of Fig d. The narrow profile at the centre represents the trapped condensate before release (t=0).

Figure 12: *Strong localisation of cold atoms localised by the random potential resulting from a Speckle pattern. From Ref. [29].*

II.G   The quasi-1D situation (multichannel case)

In practice, the strictly one-dimensional description may not be relevant, in particular in the context of electronic transport. Most of the experiments on quantum wires deal with wires with a large number of **conducting channels** $N_c \gg 1$ (metallic wires are equivalent, for electronic waves, to optical waveguides for electromagnetic waves). Only few experimental setup correspond to the 1D situation : conducting carbon nanotubes are effectively 1D with 4 degenerate channels, the cleaved edge overgrowth technique also allows to realise 1D devices (spin degenerate) [46]. However, in these cases, the existence of interaction drastically affect the electronic properties and the 1D electron liquid cannot be described like a Fermi liquid.

Some of the ideas introduced for the strictly 1D case can be extended to the multichannel case : it is possible to develop a **transfer matrix** formalism, known as the DMPK formalism [48, 96, 49]. An excellent review article is the one written by Beenakker [20] (also see the book [95]). Assuming some maximal entropy principle (i.e. conducting channels are all mixed with equal probability after an elementary slice of disorder medium) it is possible to obtain a spectrum of Lyapunov exponents characterising the transfer matrix, which is linear in the index [20] :

$$\gamma_n \simeq \frac{1}{\alpha_d \ell_e} \frac{1 + \beta (n-1)}{2 + \beta (N_c - 1)} \qquad \text{for } n \in \{1, \cdots, N_c\} \tag{II.106}$$

where $\beta \in \{1, 2, 4\}$ is the Dyson index [12] and ℓ_e the elastic mean free path. $\alpha_d = V_d/V_{d-1}$ is a number of order 1 ($V_d = \pi^{d/2}/\Gamma(d/2 + 1)$ being the volume of the unit sphere). The smallest Lyapunov exponent is interpreted as the inverse localisation length, which thus scales as

$$\boxed{\xi \sim N_c \ell_e} \tag{II.107}$$

An interesting outcome of this analysis is the identification of a **new regime** that was not present in the strictly 1D situation. Considering a wire of finite length L with a large number of channels $N_c \gg 1$, there exists a room between the **localised regime** ($L \gg \xi \sim N_c \ell_e$) and

---

[12] In random matrix theory, Dyson index corresponds to the symmetry of the problem : $\beta = 1$ corresponds to a problem with TRS (time reversal symmetry). $\beta = 2$ in the presence of a strong magnetic field breaking TRS. $\beta = 4$ when the disorder breaks the spin rotational symmetry (with TRS).

the **ballistic regime** ($\ell_e \gg L$) for a new regime : the **diffusive regime** ($\ell_e \ll L \ll \xi$). This regime will be the main subject of investigation of the chapter IV.

II.H The scaling analysis (towards higher dimension)

Having introduced the concept of multichannel disordered wires, we can jump towards the more general situation and reallistic models describing higher dimensions. We consider a general model of multichannel wire in 2D or 3D with transverse dimension W. This means that the number of channels is $N_c \sim W^{d-1}$. This model can be a lattice model for example (isotropy is not assumed like in DMPK models discussed previously, which describe the 1D case). The (numerical) scaling analysis works as follows

- extract the "localization length" ξ_W for width W (ξ_W is the inverse of the smallest Lyapunov exponent)

- Extrapolate to get ξ_∞, which represent a characteristic length scale for the disorder

- Perform a scaling analysis
$$\xi_W/W = f(\xi_\infty/W) \tag{II.108}$$
where the function f reveals the nature of the phase (localized or metallic).

- **Localization criterion of the scaling approach** : study the growth/decay of the conductance $g(L)$ with L for a square sample $L = W$. If $g(L)$ grows with L, the sample is in the metallic phase and if $g(L)$ decays, the sample is in the insulating phase.

- The connection with the provious analysis is made by noticing that the log of the conductance of the multichannel wire is $\ln g(L) = -2L/\xi_W$.

- $f(x) \nearrow$ corresponds to the insulating phase

- $f(x) \searrow$ corresponds to the metallic phase

- In the metallic phase, ξ_∞ is a correlation length (by dimensional analysis, it is related to the conductivity in 3D as $\sigma \sim \frac{e^2}{\hbar}\xi_\infty$). In the localized phase, ξ_∞ is the loclisation length

The figure 13 shows the difference between 2D and 3D wires : the former are in a localised phase, while the latter can be either localized or metallic (existence of a localization transition).
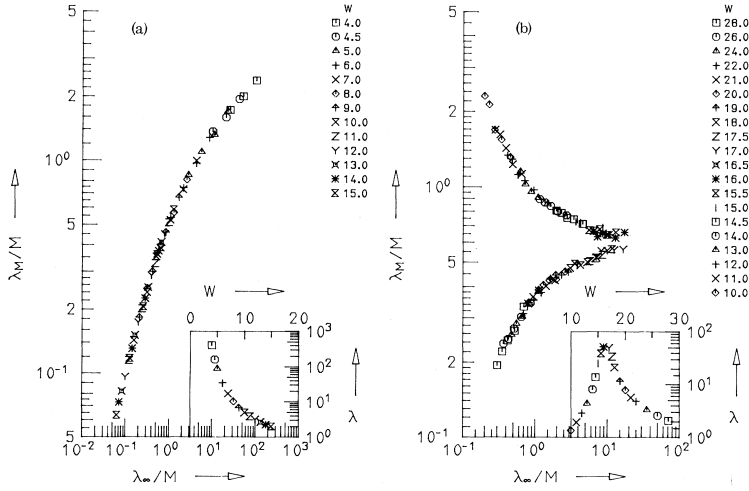
FIG. 1. Scaling function λ_M/M vs λ_∞/M for the localization length λ_M of a system of thickness M for (a) $d=2$ ($M \geqslant 4$) and (b) $d=3$ ($M \geqslant 3$). Insets show the scaling parameter λ_∞ as a function of the disorder W.

Figure 13: *The scaling function f of Eq.* (II.108) *in 2D (left) and 3D (right). In this latter case, the exsitence of two branches is related to the Anderson (localization) transition, which does not occur in 2D. From [90].*

Further reading

$\diamond$ The review by Ishii [72].

$\diamond$ Localisation and spectral properties of 1D disordered discrete models are described in the pedagogical book of J.-M. Luck [88].

$\diamond$ The book of Crisanti, Paladin and Vulpiani [43] provides a nice overview on random matrix products and the connection with Anderson localization.

$\diamond$ More diverse but less pedagogical reference is the book by Lifshits, Gredeskul & Pastur [87].

$\diamond$ The reader interested in mathematical aspects can have a look on Bougerol, Carmona & Lacroix' monographs [33, 35].

$\diamond$ A recent review on Lyapunov exponent for 1D localisation is [42].

$\diamond$ For the study of the multichannel disordered wires : the pedagogical review of Beenakker [20] or the more complete book of Mello & Kumar [95].

$\diamond$ A nice little review article on multichannel disordered wires in the presence of interaction is the (unpublished paper) [97].

$\diamond$ On the scaling approahc, see the nice review of Kramer and MacKinnon [81].

Appendix : Langevin equation and Fokker-Planck equation

a) Preliminary : Gaussian white noise and Wiener process

We introduce a normalised Gaussian white noise $\eta(t)$, distributed according to the measure

$$P[\eta] = \exp\left\{-\frac{1}{2}\int \mathrm{d}t\,\eta(t)^2\right\}\ , \tag{II.109}$$

i.e. such that $\langle\eta(t)\rangle = 0$ and $\langle\eta(t)\eta(t')\rangle = \delta(t-t')$. The solution of the differential equation

$$\frac{\mathrm{d}W(t)}{\mathrm{d}t} = \eta(t) \tag{II.110}$$

with initial condition $W(0) = 0$ is a Wiener process. It is obvious that $W(t) = \int_0^t \mathrm{d}t'\,\eta(t')$ is a Gaussian process, characterised by the correlation function

$$\langle W(t)\,W(t')\rangle = \min\left(t, t'\right)\ . \tag{II.111}$$

Rescaling the time : let us consider the mapping $t = f(u)$, where f is a function increasing monotenously. We have

$$\langle\eta(f(u))\,\eta(f(u'))\rangle = \frac{\delta(u-u')}{f'(u)} \tag{II.112}$$

what we rewrite under the form of an *"equality in law"*

$$\boxed{\eta(f(u)) \overset{\text{(law)}}{=} \frac{\eta(u)}{\sqrt{f'(u)}}} \tag{II.113}$$

meaning that the two sides of the equation have the same statistical properties (they are both Gaussian and have the same two point correlation function).

As a trivial example we choose $f(t) = \alpha\,t$, where α is a positive number

$$\eta(\alpha\,t) \overset{\text{(law)}}{=} \frac{1}{\sqrt{\alpha}}\,\eta(t) \qquad\Rightarrow\qquad W(\alpha\,t) \overset{\text{(law)}}{=} \sqrt{\alpha}\,W(t)\ , \tag{II.114}$$

which is the usual scaling property of the Brownian motion.

b) Stochastic differential equation and Fokker-Planck equation

We recall some basic tools for homogeneous random process (process with no jumps). Consider the stochastic differential equation (SDE) [13]

$$\frac{\mathrm{d}}{\mathrm{d}t}x(t) = \mathcal{F}(x(t)) + B(x(t))\,\eta(t)\ , \tag{II.115}$$

interpreted within the **Stratonovich** convention. $\mathcal{F}(x)$ is a force (drift) and $B(x) = \sqrt{2D(x)}$ describes an inhomogeneous diffusion constant. The SDE is related to the Fokker Planck equation

$$\frac{\partial}{\partial t}P(x;t) = \mathscr{G}^\dagger P(x;t) \quad\text{where }\ \mathscr{G} = \frac{1}{2}B(x)\partial_x B(x)\partial_x + \mathcal{F}(x)\partial_x \tag{II.116}$$

is the generator of the diffusion, i.e. the backward generator, adjoint of the forward generator $\mathscr{G}^\dagger = \frac{1}{2}\partial_x B(x)\partial_x B(x) - \partial_x\mathcal{F}(x)$. The Fokker-Planck equation may be written under the form of a conservation equation

$$\frac{\partial}{\partial t}P(x;t) = -\frac{\partial}{\partial x}J(x;t) \quad\text{where}\ \ J(x;t) = \left[\mathcal{F}(x) - \frac{1}{2}B(x)\partial_x B(x)\right]P(x;t) \tag{II.117}$$

---

[13] which Mathematicians prefer to write $\mathrm{d}x(t) = \mathcal{F}(x(t))\,\mathrm{d}t + B(x(t))\,\mathrm{d}W(t)$.

is the current density (in 1D, current density is a current).

Generalization to higher dimensions is rather natural ; it may be found in standard monographs like [65]. Consider the set of SDEs

$$\frac{\mathrm{d}}{\mathrm{d}t}x_i(t) = \mathcal{F}_i(\vec{x}(t)) + B_{ij}(\vec{x}(t))\,\eta_j(t) \tag{II.118}$$

with *implicit summation* over repeated indices. η_i's are identical and independent noises $\langle \eta_i(t)\eta_j(t')\rangle = \delta_{ij}\delta(t-t')$. The generator of the diffusion is now

$$\mathscr{G} = \frac{1}{2}B_{ik}\partial_i B_{jk}\partial_j + \mathcal{F}_i\partial_i \, , \tag{II.119}$$

where $\partial_i \equiv \partial/\partial x_i$.

c) The case of a constant diffusion constant

Let us focus on the simpler case where the diffusion constant is uniform in space : $B(x)^2 = 2D$. In 1D, the drift (the force) can always be written as the derivative of a potential : $\mathcal{F}(x) = -\mathcal{U}'(x)$. In this case it is useful to write

$$\mathscr{G}^\dagger = D\frac{\mathrm{d}^2}{\mathrm{d}x^2} + \frac{\mathrm{d}}{\mathrm{d}x}\mathcal{U}'(x) = D\frac{\mathrm{d}}{\mathrm{d}x}e^{-\frac{1}{D}\mathcal{U}(x)}\frac{\mathrm{d}}{\mathrm{d}x}e^{\frac{1}{D}\mathcal{U}(x)} \tag{II.120}$$

Stationary state.– This form of the generator immediatly allows to find the solution of $\mathscr{G}^\dagger P(x) = 0$, i.e. the stationary state. Three possibilities :

1. The solution
$$P_{\mathrm{eq}}(x) = C\,e^{-\frac{1}{D}\mathcal{U}(x)} \tag{II.121}$$
   is normalisatble. This describes an *equilibrium* state.

2. $P_{\mathrm{eq}}(x)$ is non normalisable, however the solution with finite current
$$P_J(x) = -\frac{J}{D}e^{-\frac{1}{D}\mathcal{U}(x)}\int^x \mathrm{d}x'\,e^{\frac{1}{D}\mathcal{U}(x')} \tag{II.122}$$
   is normalisable, now describing an out-of-equilibrium stationary state.

3. If none of the solutions is normalisable, the problem considered simply does not have a stationary state.

Examples :

1. *Ornstein-Uhlenbeck process.–* For $\mathcal{F}(x) = -2k\,x$, the equilibrium solution $P_{\mathrm{eq}}(x) = C\,e^{-\frac{k}{D}x^2}$ is normalisable.

2. For $\mathcal{F}(x) = F_0 - x^2$, the potential is unbounded from below $\mathcal{U}(x) = -F_0\,x + \frac{1}{3}x^3$, however the stationary distribution $P_J(x)$ is normalisable.

3. *Brownian motion.–* For $\mathcal{F}(x) = 0$, none of the two solutions $P_{\mathrm{eq}}(x)$ and $P_J(x)$ is normalisable and there exist no stationary state.

✍ **Exercice II.11 Mapping between the Wiener and Ornstein-Uhlenbeck processes :**
Consider a Wiener process, described by the SDE $\frac{d}{dt}x(t) = \eta(t)$, where $\eta(t)$ is a Gaussian white noise. Check that the transformation

$$\tau = \ln t \tag{II.123}$$

$$y(\tau) = \frac{x(t)}{\sqrt{t}} \tag{II.124}$$

maps the Wiener process onto the Ornstein-Ulhenbeck process

$$\frac{d}{d\tau}y(\tau) = -\frac{1}{2}y(\tau) + \eta(\tau)\,. \tag{II.125}$$

Problem : Weak disorder expansion in 1D lattice models and band center anomaly

Let us consider the 1D Anderson (tight binding) model

$$-t\,\psi_{n+1} + V_n\,\psi_n - t\,\psi_{n-1} = \varepsilon\,\psi_n \qquad (\text{II}.126)$$

where t is the coupling between nearest neighbouring sites and V_n a random potential.

In the absence of potential, eigenstates are plane waves $\psi_n = \mathrm{e}^{ikn}$ of energy $\varepsilon_k = -2t\,\cos k$, where the (dimensionless) wavevector belongs to the Brillouin zone $k \in [-\pi, \pi]$. Plane waves are characterised by the following density of states and Lyapunov exponent :

$$\rho_0(\varepsilon) = \frac{1}{\pi\sqrt{(2t)^2 - \varepsilon^2}} \quad \Rightarrow \quad N_0(\varepsilon) = \frac{1}{2} - \frac{1}{\pi}\arccos(\varepsilon/2t) \qquad (\text{II}.127)$$

$$\gamma_0(\varepsilon) = \operatorname{argcosh}|\varepsilon/2t| \qquad (\text{II}.128)$$

1/ Recover rapidly these properties. Check that $\gamma_0(\varepsilon)$ and $N_0(\varepsilon)$ are real and imaginary part of an analytic function of ε.

A natural question is the search for *weak disorder expansions* of the density of states and the Lyapunov exponent under the form of a weak disorder expansion (perturbative like). For uncorrelated site potentials, $\overline{V_n V_m} \propto \delta_{n,m}$, with finite moments, $\overline{V_n} = 0$, $\overline{V_n^2} < \infty$, etc, one finds [47, 88]

$$N(\varepsilon) = N_0(\varepsilon) - \frac{\overline{V_n^3}}{24\pi^3 t^3 \sin^3 k} + \mathcal{O}(V_n^5) \qquad (\text{II}.129)$$

$$\gamma(\varepsilon) = \frac{\overline{V_n^2}}{8t^2 \sin^2 k} + \mathcal{O}(V_n^4) \qquad (\text{II}.130)$$

where k parametrizes the energy $\varepsilon = -2t\,\cos k$.

2/ Plot the qualitative $\rho(\varepsilon)$ and $\gamma(\varepsilon)$ expected from these formulae (with the one corresponding to $V_n = 0$).

It was however observed, numerically by Czycholl, Kramer & MacKinnon [44], and by Kappus and Wegner [78], that these formulae fail to describe accuratly the band center properties ($\varepsilon \to 0$, i.e. $k \to \pi/2$). This is at first sight surprising : although it is clear that the expansion has some problem at the band egdes, $k \to 0$ ou π, where disorder is non perturbative, this seems not to be the case in the band center. Inspection of the full series however shows that it breaks down at the band center. It was shown by Derrida and Gardner [47] that the correct weak disorder expansion is

$$\gamma(\varepsilon) = \left(\frac{\Gamma(3/4)}{\Gamma(1/4)}\right)^2 \frac{\overline{V_n^2}}{t^2} + \mathcal{O}(\varepsilon) \qquad (\text{II}.131)$$

showing a small difference with the previous expansion, 0.125 vs 0.114... This phenomenon, denoted the "band center anomaly" (or "Kappus Wegner anomaly"), is a lattice effect due to commensurability. In order to clarify this, we now develop a continuous model. This is conveniently done by Fourier transforming the difference equation (II.126).

$$\tilde{\psi}(k) = \sum_n \psi_n\,\mathrm{e}^{-ikn} \qquad (\text{II}.132)$$

$$\psi_n = \int_{-\pi}^{+\pi} \frac{\mathrm{d}k}{2\pi}\,\tilde{\psi}(k)\,\mathrm{e}^{ikn} \qquad (\text{II}.133)$$

42

(we recall the Poisson formula $\sum_n e^{ikn} = 2\pi \sum_n \delta(k - 2\pi n)$).

3/ Rewrite the Schrödinger equation in Fourier space.

4/ We write $V_n = A_0(na) + (-1)^n m(na)$ where a is the lattice spacing ; $A_0(x)$ and $m(x)$ are two smooth functions. Discuss the qualitative structure of the Fourier transform $\tilde{V}(k)$. The low energy properties of the model involves the Fourier components of the wave function at $k \sim \pm\pi/2$. Argue that only the potential's Fourier components $|q| \ll 1$ and $|\pi \pm q| \ll 1$ are of importance in this case.

5/ For $|\kappa| \ll 1$, we introduce

$$\tilde{\psi}(\pi/2 + \kappa) = \tilde{\varphi}(\kappa) \tag{II.134}$$

$$\tilde{\psi}(-\pi/2 + \kappa) = \tilde{\chi}(\kappa) \tag{II.135}$$

Show that the $\tilde{\varphi}(\kappa)$ and $\tilde{\chi}(\kappa)$ obeys two coupled equations. Going back to real space, deduce that the low energy properties of the Anderson model are described by the Dirac equation

$$H_D \Psi(x) = \varepsilon \, \Psi(x) \qquad \text{for} \quad H_D = -i\sigma_3 \, v_0 \, \partial_x + \sigma_1 \, m(x) + A_0(x) \tag{II.136}$$

where $\Psi = (\varphi, \chi)$. At the light of this result, can you explain the breakdown of the weak disorder expansion at the band center ?

6/ The large scale (low energy) properties of the model are conveniently described by considering white noises :

$$\overline{A_0(x) \, A_0(x')}^c = g_0 \, \delta(x - x') \tag{II.137}$$

$$\overline{m(x) \, m(x')}^c = g_\pi \, \delta(x - x') \tag{II.138}$$

$$\tag{II.139}$$

The zero energy Lyapunov exponent has been computed exactly in this case [39, 105] and is given by elliptic integrals (now $v_0 = 1$)

$$\gamma(0) = g_\pi \left[\frac{1}{\xi^2} \left(\frac{\mathbf{E}(\xi)}{\mathbf{K}(\xi)} - 1 \right) + 1 \right] \quad \text{with} \quad \xi = \frac{1}{\sqrt{1 + g_0/g_\pi}} \tag{II.140}$$

What is the value of g_0/g_π describing the case originally studied of uncorrelated site potentials $\overline{V_n V_m} \propto \delta_{n,m}$? How can one make the small anomaly large ?

Appendix :   we recall few properties of the Elliptic integrals

$$\mathbf{K}(k) = \int_0^{\pi/2} \frac{dt}{\sqrt{1 - k^2 \sin^2 t}} \tag{II.141}$$

$$\mathbf{E}(k) = \int_0^{\pi/2} dt \, \sqrt{1 - k^2 \sin^2 t} \tag{II.142}$$

For $k \to 1^-$ we have (setting $k' = \sqrt{1 - k^2}$)

$$\mathbf{K}(k) = \ln(4/k') + \mathcal{O}(k'^2 \ln k') \tag{II.143}$$

$$\mathbf{E}(k) = 1 + \frac{1}{2} k'^2 \left[\ln(4/k') - 1/2 \right] + \mathcal{O}(k'^4 \ln(1/k')) \tag{II.144}$$

We give

$$2 \frac{\mathbf{E}(1/\sqrt{2})}{\mathbf{K}(1/\sqrt{2})} - 1 = \left(\frac{2\Gamma(3/4)}{\Gamma(1/4)} \right)^2 \tag{II.145}$$

43

TD 2 : Localisation for the random Kronig-Penney model – Concentration expansion and Lifshitz tail

The aim of the problem is to study a 1D disordered model introduced by Frisch and Lloyd in Ref. [60]. This model is a random version of the Kronig-Penney model

$$H = -\frac{d^2}{dx^2} + \sum_n v_n\,\delta(x - x_n)\,. \tag{II.146}$$

Impurity positions x_n's are distributed identically and independently for a uniform mean density ρ. We consider the case where the weights v_n's are also independent random variables. [14] We prove the Anderson localisation of eigenstates and analyse the low energy density of states.

1/ The positions are ordered as $x_0 = 0 < x_1 < x_2 < \cdots < x_n < \cdots$ Denoting by $\ell_n = x_{n+1} - x_n > 0$ the distance between consecutive impurities, recall the distribution of these lengths.

2/ Riccati.– We denote by $\psi(x;E)$ the solution of the initial value problem $H\psi(x;E) = E\,\psi(x;E)$ with $\psi(0;E) = 0$ and $\psi'(0;E) = 1$. Derive the stochastic differential equation controlling the evolution of the Riccati variable $z(x) \stackrel{\text{def}}{=} \psi'(x;E)/\psi(x;E)$.

3/ Describe the effect of the random potential on its dynamics (i.e. relate $z(x_n^+)$ to $z(x_n^-)$).

4/ We denote by $f(z;x) = \langle \delta(z - z(x)) \rangle$ the probability distribution of the random process. Show that the distribution of the Riccati variable obeys the integro-differential equation

$$\partial_x f(z;x) = \partial_z\left[(E + z^2)f(z;x)\right] + \rho\,\langle f(z-v;x) - f(z;x)\rangle_v \tag{II.147}$$

where $\langle\cdots\rangle_v$ denotes averaging over the random weights v_n's.

Hint : analyse the effects of the two terms of the SDE in order to relate $f(z; x + dx)$ to $f(z'; x)$.

5/ Probability current and stationary distribution.– Rewrite (II.147) under the form of a conservation equation $\partial_x f(z;x) = -\partial_z J(z;x)$, where $J(z;x)$ is the probability current density. We have seen that the disribution reaches a stationary distribution $f(z;x) \xrightarrow{x\to\infty} f(z)$ for a steady current $J(z;x) \xrightarrow{x\to\infty} -N$, related to the Integrated density of states per unit length of the disordered Hamiltonian. Show that the stationary distribution obeys the integral equation

$$N(E) = (E + z^2)f(z) - \rho\left\langle \int_{z-v}^z dz'\,f(z')\right\rangle_v\,. \tag{II.148}$$

What is the condition on the weights v_n for having a non vanishing density of states for $E < 0$?

6/ *High density limit.–* We consider the case $\langle v_n\rangle = 0$. Discuss the limit $\rho \to \infty$ and $v_n \to 0$ with $\sigma = \rho\langle v_n^2\rangle$ fixed (no calculation).

7/ *Small concentration expansion.–* We now discuss the opposite limit when $\rho \ll v_n$. We search for the solution of the integro-differential equation under the form of an expansion $f(z) =$

---

[14] Note that Frisch and Lloyd considered the case of random positions and fixed weights. The case of non random positions (on a lattice) and *fixed* weights was considered earlier by Schmidt in [109]. The case of random positions and random weights was also considered in several papers, e.g. by Nieuwenhuizen [99].

$f^{(0)}(z) + f^{(1)}(z) + f^{(2)}(z) + \cdots$ where $f^{(n)} = \mathcal{O}(\rho^n)$. Accordingly the density of states presents a similar expansion $N = N^{(0)} + N^{(1)} + \cdots$ We recall that the Lyapunov exponent is given by

$$\gamma = \fint_{\mathbb{R}} \mathrm{d}z\, z\, f(z) \qquad \text{where} \qquad \fint_{\mathbb{R}} \mathrm{d}z\, h(z) \overset{\text{def}}{=} \lim_{R \to +\infty} \int_{-R}^{+R} \mathrm{d}z\, h(z) = \int_{\mathbb{R}} \mathrm{d}z\, \frac{h(z) + h(-z)}{2}$$

$$(\text{II.149})$$

a) Compute $f^{(1)}$ and deduce that the Lyapunov exponent at lowest order in ρ is

$$\gamma = \frac{\rho}{2} \left\langle \ln \left[1 + \left(\frac{v_n}{2k} \right)^2 \right] \right\rangle_{v_n} + \mathcal{O}(\rho^2) \tag{II.150}$$

Hint : We give the integral

$$\int_{\mathbb{R}} \mathrm{d}t\, \frac{t}{t^2 + 1} \left(\arctan(t) - \arctan(t - x) \right) = \frac{\pi}{2} \ln \left(1 + (x/2)^2 \right) , \tag{II.151}$$

which could be computed by writing $\arctan(t) = \frac{1}{2i} \ln \left(\frac{i-t}{i+t} \right)$ and using the Residue's theorem.

b) Study the limiting cases, setting $E = k^2$:

(i) High energy limit $k \gg v_n,\, \rho$.

(ii) Intermediate energy range, $v_n \gg k \gg \rho$.

(iii) The concentration expansion breaks down at $k \sim \rho$. What is the estimate for the saturation value at $E = 0$?

8/ *Lifshits tail.–* For positive weights v_n, the sectrum is in $\mathbb{R}^+$. An approximation for the low energy IDoS can be obtained as follows. In the limit $v_n \to \infty$ the intervals between impurities are disconnected. We introduce the IDoS $\mathcal{N}(E; \ell) = \sum_{n=1}^{\infty} \theta_{\mathrm{H}}(E - (n\pi/\ell)^2)$ for the interval of length ℓ. Shows that the IDoS *per unit length* of the disordered Hamiltonian is given by $N(E) \simeq \rho \left\langle \mathcal{N}(E; \ell) \right\rangle_\ell$ for $\rho \to 0$. Deduce an explicit form for $N(E)$ and analyse the low energy behaviour $E \ll \rho^2$.

Further reading : This analysis was performed in our article with Tom Bienaimé, Ref. [28]. More information about the concentration expansion and be found in the book of Lishits, Gredeskul and Pastur [87].

TD 2 bis : Thouless relation

We demonstrate a relation between the Lyapunov exponent (i.e. the localisation) and the density of states. This relation relies on the existence of an analytic function encoding both informations.

A. Discrete tight binding model.– We study the Schödinger equation on a regular 1D lattice :

$$-\psi_{n+1} + V_n\,\psi_n - \psi_{n-1} = \varepsilon\,\psi_n \tag{II.152}$$

We first consider the problem on N sites $n \in \{1, \cdots, N\}$ and impose the boundary conditions $\psi_0 = \psi_{N+1} = 0$ (the quantification equation) resulting in the spectrum of N eigenvalues $\{\varepsilon_\alpha\}$.

1/ We denote by $\Psi_n(\varepsilon)$ the solution of the initial value problem Eq. (II.152) with $\Psi_0(\varepsilon) = 0$ and $\Psi_1(\varepsilon) = 1$. Argue that $\Psi_{N+1}(\varepsilon)$ is the polynomial of degree N

$$\Psi_{N+1}(\varepsilon) = \prod_{\alpha=1}^{N} (\varepsilon_\alpha - \varepsilon)\,. \tag{II.153}$$

2/ Thouless relation.– We define the density of states per site, which is a continuous function in the limit $N \to \infty$, and the Lyapunov exponent

$$\rho(\varepsilon) \overset{\text{def}}{=} \lim_{N\to\infty} \frac{1}{N} \sum_{\alpha=1}^{N} \delta(\varepsilon - \varepsilon_\alpha) \quad \text{and} \quad \gamma(\varepsilon) \overset{\text{def}}{=} \lim_{N\to\infty} \frac{\ln|\Psi_{N+1}(\varepsilon)|}{N}\,. \tag{II.154}$$

Deduce the relation

$$\boxed{\gamma(\varepsilon) = \int \mathrm{d}\varepsilon'\,\rho(\varepsilon')\,\ln|\varepsilon' - \varepsilon|} \tag{II.155}$$

3/ Complex Lyapunov exponent (characteristic function).– We consider the analytic function

$$\Omega(\varepsilon) \overset{\text{def}}{=} \lim_{N\to\infty} \frac{\ln\Psi_{N+1}(\varepsilon)}{N} \qquad \text{for } \varepsilon \in \mathbb{C}\,. \tag{II.156}$$

Discuss its analytic properties. Show that the Lyapunov exponent and the density of states are related to the real and imaginary parts of $\Omega(\varepsilon)$ on the real axis. What is the relation of this observation with the Thouless relation ?

Hint : we recall $\lim_{\eta\to 0^\pm} \ln(x + \mathrm{i}\eta) = \ln|x| \pm \mathrm{i}\pi\,\theta_{\mathrm{H}}(-x)$.

4/ As a first (trivial) application of the concept of complex Lyapunov exponent, we consider the free problem $(V_n = 0)$.

a) What is the spectrum of the Schrödinger equation (II.152) in this case ?

b) We consider an energy $\varepsilon = -2\cosh q < -2$. Find $\Psi_n(\varepsilon)$ and deduce $\Omega(\varepsilon)$.

c) By an analytic continuation, deduce the spectral density $\rho(\varepsilon)$. Plot on the same graph the Lyapunov exponent $\gamma(\varepsilon)$ and the spectral density $\rho(\varepsilon)$.

Hint :
$\mathrm{argcosh}(x) = \ln(x + \sqrt{x^2 - 1})$ for $x \in \mathbb{R}^+$ and $\arcsin(x) = -\mathrm{i}\,\ln(\mathrm{i}x + \sqrt{1 - x^2})$ for $x \in [-1, +1]$.

d) In the presence of a weak disordered potential, what behaviours do you expect for $\rho(\varepsilon)$ and $\gamma(\varepsilon)$?

B. Continuous model.– In this part we consider the continuous model

$$\left(-\frac{\mathrm{d}^2}{\mathrm{d}x^2} + V(x)\right)\varphi(x) = E\,\varphi(x) \tag{II.157}$$

where $V(x)$ is a Gaussian white noise of zero mean with $\langle V(x)V(x')\rangle = \sigma\,\delta(x-x')$. We denote by $\psi(x;E)$ the solution of the Cauchy problem satisfying $\psi(0;E)$ and $\psi'(0;E) = 1$, where $' \equiv \partial_x$. We will make use of the concept of complex Lyapunov exponent in order to get analytic expressions for the Lyapunov exponent and the spectral density.

Riccati analysis.– The Riccati variable $z(x;E) \stackrel{\text{def}}{=} \psi'(x;E)/\psi(x;E)$ obeys the Langevin equation $z' = -E - z^2 + V(x)$. The probability current of the Riccati variable through $\mathbb{R}$ coincides with the integrated density of states (IDoS) per unit length $N(E)$. It solves

$$\left(\frac{\sigma}{2}\frac{\mathrm{d}}{\mathrm{d}z} + E + z^2\right)f(z;) = N(E) \tag{II.158}$$

where $f(z;E)$ is the (normalised) probability density for the stationary process $z(x;E)$.

1/ Using only the definition of $z(x;E)$, show that its average $\langle z\rangle$ coincides with the Lyapunov exponent

$$\gamma(E) = \lim_{x\to\infty}\frac{\ln|\psi(x;E)|}{x}\,. \tag{II.159}$$

2/ We consider the Fourier transform of the distribution

$$\hat{f}(q;E) = \int \mathrm{d}z\,\mathrm{e}^{-\mathrm{i}qz}\,f(z;E) \tag{II.160}$$

Argue that $\mathrm{Im}[\hat{f}'(0^+;E)] = -\gamma(E)$. Fourier transforming Eq. (II.158), show that $\mathrm{Re}[\hat{f}'(0^+;E)] = -\mathrm{Re}[\hat{f}'(0^-;E)] = \pi\,N(E)$. Deduce the relation between $\hat{f}'(0^+;E)$ and the complex Lyapunov exponent

$$\Omega(E) = \gamma(E) - \mathrm{i}\pi\,N(E)\,. \tag{II.161}$$

3/ Justify that $\hat{f}(0;E) = 1$ and that $\hat{f}(q;E)$ decays at infinity. Show that the solution on $\mathbb{R}^{+*}$ vanishing at infinity is $\hat{f}(q;E) = C\left[\mathrm{Ai}(-E-\mathrm{i}q) - \mathrm{i}\,\mathrm{Bi}(-E-\mathrm{i}q)\right]$ (for $\sigma/2 = 1$).

4/ Recover the asymptotic behaviours for the Lyapunov exponent and the low energy density of states.

Appendix :

Airy equation $f''(z) = z\,f(z)$ admits two independent real solutions Ai and Bi with asymptotic behaviours $\mathrm{Ai}(z) \simeq \frac{1}{\sqrt{\pi}\,(-z)^{1/4}}\cos\left[\frac{2}{3}(-z)^{3/2} - \frac{\pi}{4}\right]$ and $\mathrm{Bi}(z) \simeq \frac{-1}{\sqrt{\pi}\,(-z)^{1/4}}\sin\left[\frac{2}{3}(-z)^{3/2} - \frac{\pi}{4}\right]$ for $z \to -\infty$, and $\mathrm{Ai}(z) \simeq \frac{1}{2\sqrt{\pi}\,z^{1/4}}\exp\left[-\frac{2}{3}z^{3/2}\right]$ and $\mathrm{Bi}(z) \simeq \frac{1}{2\sqrt{\pi}\,z^{1/4}}\exp\left[\frac{2}{3}z^{3/2}\right]$ for $z \to +\infty$. The Wronskian of the two Airy functions is $W[\mathrm{Ai},\mathrm{Bi}] = \mathrm{Ai}\,\mathrm{Bi}' - \mathrm{Ai}'\,\mathrm{Bi} = 1/\pi$.

Further reading : ● J.-M. Luck, *Systèmes désordonnés unidimensionnels*, coll. Aléa Saclay, (1992). ● The Thouless relation was introduced in : D. J. Thouless, A relation between the density of states and range of localization for one-dimensional random systems, J. Phys. C: Solid St. Phys. **5**, 77 (1972). ● Exact calculation of $N(E)$ for the continuous model has been performed in : B. I. Halperin, Green's Functions for a Particle in a One-Dimensional Random Potential, Phys. Rev. **139**(1A), A104–A117 (1965). ● The interest of the method we have exposed here is to relate the determination of the complex Lyapunov exponent to the resolution of a differential equation. This has been recently exploited for a more general class of models in : A. Grabsch, C. Texier and Y. Tourigny, One-dimensional disordered quantum mechanics and Sinai diffusion with random absorbers, J. Stat. Phys. **155**(2), 237–276 (2014).

TD 2 ter : 1D Anderson localisation – Conductance of a 1D wire (Landauer approach)

We analyse the problem of localisation of an electron in one dimension from the viewpoint of the electronic transport properties within the Landauer approach.

A. Landauer formula.– We consider the Schrödinger equation on $\mathbb{R}$ for a potential $V(x)$ defined on an interval $[x_L, x_R]$ (and zero outside the interval). The Landauer formula provides an expression of the **electric conductance** (inverse of the electric resistance) in terms of the scattering properties. In a first step we analyse the scattering problem in one dimension. For each energy E, the Schrödinger equation

$$-\frac{\hbar^2}{2m}\frac{\partial^2 \psi(x)}{\partial x^2} + V(x)\,\psi(x) = E\,\psi(x) \tag{II.162}$$

has two independent solutions. Several basis are possible. We choose the pair of eigenstates describing the particle incoming from the left or from the right. On $]-\infty, x_L] \cup [x_R, +\infty[$, the two eigenfunctions are superposition of plane waves :

$$\psi_{E,L}(x) = \frac{1}{\sqrt{h\,v_E}} \begin{cases} \mathrm{e}^{+\mathrm{i}k_E(x-x_L)} + r\,\mathrm{e}^{-\mathrm{i}k_E(x-x_L)} & \text{for } x < x_L \\ t\,\mathrm{e}^{+\mathrm{i}k_E(x-x_R)} & \text{for } x > x_R \end{cases} \tag{II.163}$$

and

$$\psi_{E,R}(x) = \frac{1}{\sqrt{h\,v_E}} \begin{cases} t'\,\mathrm{e}^{-\mathrm{i}k_E(x-x_L)} & \text{for } x < x_L \\ \mathrm{e}^{-\mathrm{i}k_E(x-x_R)} + r'\,\mathrm{e}^{+\mathrm{i}k_E(x-x_R)} & \text{for } x > x_R \end{cases} \tag{II.164}$$

where $E = \frac{1}{2}mv_E^2 = \frac{\hbar^2 k_E^2}{2m}$ and (r,t) and (r',t') are two sets of reflexion and transmission probability amplitudes.

1/ Normalisation.— For $V(x) = 0$, check that the normalisation factor ensures the orthonormalisation

$$\langle \psi_{E,\alpha} \,|\, \psi_{E',\beta} \rangle = \delta_{\alpha,\beta}\,\delta(E-E') \qquad \text{and} \qquad \sum_\alpha \int_0^\infty \mathrm{d}E \,|\psi_{E,\alpha}\rangle\langle\psi_{E,\alpha}| = 1 \tag{II.165}$$

with $\alpha,\ \beta \in \{L,\ R\}$ (for a proof for $V \neq 0$, cf. chapter 10 of [Texier, '15], footnote of pb. 10.1 p. 206).

2/ Probability currents.

a) If one considers a set of independent solutions ψ_1 and ψ_2 of (II.162), show that the Wronskian $\mathcal{W}[\psi_1, \psi_2] \stackrel{\text{def}}{=} \psi_1 \frac{\mathrm{d}\psi_2}{\mathrm{d}x} - \frac{\mathrm{d}\psi_1}{\mathrm{d}x}\psi_2$ is constant $\forall x$.

b) Applying this observation to (II.163,II.164), deduce $t = t'$.

c) Compute the probability currents $J_\alpha(E) \stackrel{\text{def}}{=} \frac{\hbar}{m}\,\mathrm{Im}\left[\psi_\alpha^*(x)\frac{\mathrm{d}\psi_\alpha(x)}{\mathrm{d}x}\right]$ with $\alpha \in \{L,\ R\}$ (argue that $J_\alpha(E)$ is constant).

3/ Electric current.— We now consider the situation where a voltage bias V is imposed on the wire. The Landauer's prescription corresponds to assume that the occupations of the eigenstates $\psi_{E,L}(x)$ and $\psi_{E,R}(x)$ are described by two different Fermi functions

$$f_{L,R}(E) = f(E - \mu_{L,R}) \qquad \text{where } f(E) = \frac{1}{\mathrm{e}^{\beta E} + 1}\,, \tag{II.166}$$

where μ_L and μ_R are the chemical potentials at $-\infty$ and $+\infty$, respectively. Deduce the expression of the electric current $I(V)$ in the wire, where $eV = \mu_L - \mu_R$.

4/ Landauer formula.— We consider the linear regime $V \to 0$. The current can then be written as $I(V) \simeq G V$ where G is the electric **conductance**.

a) In the zero temperature limit, show that

$$\boxed{G = \frac{2_s e^2}{h} \mathcal{T}(\varepsilon_F) \qquad \text{where } \mathcal{T}(\varepsilon_F) = |t|^2} \tag{II.167}$$

is the transmission probability at Fermi energy and 2_s the spin degeneracy. This remarkable formula (first written under this form by Fisher & Lee, Phys. Rev. B, 1981) establishes a connection between a property of the quantum scattering problem, the probability $\mathcal{T}$, and some measurable quantity.

b) In the absence of the potential, $\mathcal{T} = 1$ and the electric conductance is e^2/h per spin channel. The electric resistance of such a "perfect" 1D wire is given by the von Klitzing constant $R_K = h/(2_s e^2)$. Compute its numerical value. Could you propose an explanation for the origin of this resistance (difficult question) ?

c) Derive a formula for the conductance at finite temperature.

B. Application for the disordered 1D wire.— We now consider the situation where the potential $V(x)$ is a disordered potential, defined on the interval $[0, L]$ (and zero elsewhere).

1/ Localisation length.— In the lecture, we have defined the localisation length by studying the behaviour of the solution of the initial value (Cauchy) problem, i.e. the solution of (II.162) for $\psi_{\mathrm{Cauchy}}(0) = 0$ and $\psi'_{\mathrm{Cauchy}}(0) = 1$. Argue that, in the "large" L limit, the transmission probability is given by

$$g \equiv \mathcal{T} \sim |\psi_{\mathrm{Cauchy}}(L)|^{-2} \tag{II.168}$$

(from now on, we prefer to use the notation g for the "dimensionless conductance"). Propose a definition of the localisation length ξ_{loc} from the conductance.

2/ Distribution of the conductance.— In the lecture, the transfer matrix formulation has led to the conclusion that $\ln |\psi_{\mathrm{Cauchy}}(x)| = \int_0^x \mathrm{d}t\, z(t)$, where $z(x)$ is the Riccati variable, can be considered as a Brownian motion over large scale, [15] thus $\langle \ln |\psi_{\mathrm{Cauchy}}(x)| \rangle \simeq \gamma_1 x$ and $\mathrm{Var}\big(\ln |\psi_{\mathrm{Cauchy}}(x)| \big) \simeq \gamma_2 x$ for $x \gg \ell_c$; γ_1 is the Lyapunov exponent. Deduce the distribution of the dimensionless conductance. Derive its positive moments $\langle g^n \rangle$. Simplify the moments when "single parameter scaling" relation $\gamma_1 \simeq \gamma_2$ holds (at energy≫disorder). For a given sample, what is the self average quantity ?

C. β-function— We derive the central quantity the scaling approach of localisation. We still consider the situation where the random potential is defined on the interval $[0, L]$ and vanishes outside the interval.

1/ In order to deal with the conductance characterizing the scattering by the randomness, we substract the resistance in the presence and in the absence of the potential. Show that this gives a new formula for the conductance

$$\tilde{g} = \frac{\mathcal{T}}{1 - \mathcal{T}} \tag{II.169}$$

called the "four-terminal" conductance. What behaviour do you expect in the two limits of perfect and highly disordered wire (qualitatively).

---

[15]because $z(x)$ has a stationary distribution and is characterised by a finite correlation length ℓ_c.

2/ Assuming the form $\mathcal{T} \sim \exp[-2L/\xi_{\text{loc}}]$, deduce the β-function

$$\beta(\tilde{g}) \stackrel{\text{def}}{=} \frac{\mathrm{d}\ln\tilde{g}}{\mathrm{d}\ln L} \tag{II.170}$$

(show that it is a universal function of $\tilde{g}$ only). Plot neatly this function and interpret its limiting behaviours.

3/ The form $\mathcal{T} \sim \exp[-2L/\xi_{\text{loc}}]$ is in fact incorrect as it neglects the fluctuations ! At the light of the results of the part **B**, do you think that the argument of the β-function should be $\ln\langle\tilde{g}\rangle$ or $\langle\ln\tilde{g}\rangle$ in practice ?

Further reading :

• A general discussion of the scattering of a quantum particle in one-dimension can be found in the chapter 10 of :
[Texier, '15] Christophe Texier, *Mécanique quantique*, 2nd edition, Dunod, 2015.
and also in (oriented for random matrices) :
[Mello & Kumar, '04] P. A. Mello and N. Kumar, *Quantum transport in mesoscopic systems – Complexity and statistical fluctuations*, Oxford University Press, 2004.

• For the history of the Landauer formula, chapter 1 of :
[Texier, '10] Christophe Texier, *Désordre, localisation et interaction – Transport quantique dans les réseaux métalliques*, thèse d'habilitation à diriger des recherches de l'Université Paris-Sud, 2010. `http://tel.archives-ouvertes.fr/tel-01091550`

• About the distribution of the conductance, cf. chapter 6 of [Texier, '10] (for references and a simple discussion within the picture presented here).

• The function γ_2 characterising the fluctuations of $\ln|\psi_{\text{Cauchy}}(x)|$ has been recently studied for different models in :
Kabir Ramola & Christophe Texier, *Fluctuations of random matrix products and 1D Dirac equation with random mass*, J. Stat. Phys. **157**(3), 497–514 (2014). preprint cond-mat arXiv:1402.6943.

For a rigorous proof of Eq. (II.168) **:** cf. the (longer) online version of the exercices, at
`http://lptms.u-psud.fr/christophe_texier/enseignements/`
`enseignements-en-master/onde-en-milieu-desordonne/`

Appendix : Transfer matrices and a rigorous proof of Eq. (II.168)

We prove rigorously Eq. (II.168). Several methods are possible. Here we use the concept of transfer matrix : this will require a little bit more work however this is quite instructive.

We study the Schrödinger equation

$$-\psi''(x) + V(x)\psi(x) = k^2\psi(x) \tag{II.171}$$

where we have set $\hbar^2/(2m) = 1$ and $E = k^2$.

A. Cauchy problem and phase formalism

We consider first the solution of (II.171) for $x \in \mathbb{R}^+$. In order to extract the spectral and localisation informations from the initial value (Cauchy) problem, $\psi(0) = 0$ and $\psi'(0) = k$, we parametrize the solution as $\psi(x) = e^{\xi(x)}\sin\theta(x)$ and $\psi'(x) = ke^{\xi(x)}\cos\theta(x)$.

1/ Show that $\theta(x)$ and $\xi(x)$ obey the coupled first order differential equations

$$\begin{cases} \frac{d\theta(x)}{dx} &= k - \frac{V(x)}{k}\sin^2\theta \\ \frac{d\xi(x)}{dx} &= \frac{V(x)}{2k}\sin(2\theta) \end{cases} \tag{II.172}$$

What are the initial conditions for these two functions ?

2/ We assume $\langle V(x)\rangle = 0$, where $\langle\cdots\rangle$ denotes averaging over the disorder. In the high energy domain (energy≫disorder), it is possible to average over the fast variable (the phase θ) and obtain an equation for the envolpe $\exp\xi(x)$ of the wave function (the slow variable) only :

$$\frac{d\xi(x)}{dx} \simeq \gamma + \sqrt{\gamma}\,\eta(x) \tag{II.173}$$

where $\eta(x)$ is a normalised Gaussian white noise, $\langle\eta(x)\eta(x')\rangle = \delta(x - x')$, and γ the Lyapunov exponent [Antsygina *et al*, '81]

$$\gamma \simeq \frac{1}{8k^2}\int d(x - x')\,\langle V(x)V(x')\rangle \cos 2k(x - x')\,. \tag{II.174}$$

Deduce the statistical properties of $\xi(x)$.

B. Transfer matrices and the group $\mathrm{SU}(1,1)$

For an arbitrary potential (disordered or not), the evolution of the wave function can be conveniently studied thanks to transfer matrices. Several formulations are available, involving different groups of matrices, $\mathrm{SL}(2,\mathbb{R})$, $\mathrm{U}(1,1)$ or $\mathrm{SO}(2,1)$. The formulation most suitable to analyse the scattering problem is to gather the four reflection and transmission coefficients in the transfer matrix

$$T = \begin{pmatrix} 1/t^* & r'/t' \\ -r/t' & 1/t' \end{pmatrix} \quad \in\ \mathrm{U}(1,1) \tag{II.175}$$

characterizing the effect of the potential $V(x)$ in $[x_1, x_2]$. Precisely

$$\begin{pmatrix} C \\ D \end{pmatrix} = T\begin{pmatrix} A \\ B \end{pmatrix} \qquad \text{where } \psi(x) = \begin{cases} A\,e^{ik(x-x_1)} + B e^{-ik(x-x_1)} & \text{for } x < x_1 \\ C\,e^{ik(x-x_2)} + D e^{-ik(x-x_2)} & \text{for } x > x_2 \end{cases} \tag{II.176}$$

1/ Check the following properties :

- The two transfer matrices T_1 and T_2 describing two adjacent intervals obey the simple composition rule

$$T_{1\oplus2} = T_2 \, T_1 \, . \tag{II.177}$$

- $\det T = t/t'$ (note that $r'/t' = -(r/t)^*$ follows from unitarity of the evolution, i.e. current conservation).

- T conserves the norm $X^\dagger \sigma_z X = |x|^2 - |y|^2$ where $X^{\mathrm{T}} = (x, y)$.

2/ From the two last properties, we conclude that T is a parametrisation of the group $\mathrm{U}(1,1)$. How many independent parameters parametrize this group ? In the strictly 1D case, one has $t = t'$ and thus $T \in \mathrm{SU}(1,1)$.

3/ Polar representation.— We may write the transfer matrix under the form

$$T = \begin{pmatrix} \mathrm{e}^{\mathrm{i}(\alpha+\beta)/2} & 0 \\ 0 & \mathrm{e}^{-\mathrm{i}(\alpha+\beta)/2} \end{pmatrix} \begin{pmatrix} \cosh\xi & \sinh\xi \\ \sinh\xi & \cosh\xi \end{pmatrix} \begin{pmatrix} \mathrm{e}^{\mathrm{i}(\alpha-\beta)/2} & 0 \\ 0 & \mathrm{e}^{-\mathrm{i}(\alpha-\beta)/2} \end{pmatrix} \tag{II.178}$$

$$= \begin{pmatrix} \mathrm{e}^{\mathrm{i}\alpha}\cosh\xi & \mathrm{e}^{\mathrm{i}\beta}\sinh\xi \\ \mathrm{e}^{-\mathrm{i}\beta}\sinh\xi & \mathrm{e}^{-\mathrm{i}\alpha}\cosh\xi \end{pmatrix} \tag{II.179}$$

Check that the transmission and reflection amplitudes are related to the three parameters as

$$t = t' = \mathrm{e}^{\mathrm{i}\alpha} \frac{1}{\cosh\xi} \quad , \quad r = -\mathrm{e}^{\mathrm{i}(\alpha-\beta)}\tanh\xi \quad \text{and} \quad r' = \mathrm{e}^{\mathrm{i}(\alpha+\beta)}\tanh\xi \, . \tag{II.180}$$

C. Transfer matrix formulation of the scattering problem on $\mathbb{R}$

We derive a differential equation for the transfer matrix when the potential is defined on $[0, L]$ (and vanishes outside the interval). The starting point is to consider the left scattering state [we drop the normalisation factor of Eq. (II.163)]

$$\psi_{L,k}(x) = \begin{cases} \mathrm{e}^{\mathrm{i}kx} + r\,\mathrm{e}^{-\mathrm{i}kx} & \text{for } x < 0 \\ t\,\mathrm{e}^{\mathrm{i}k(x-L)} & \text{for } x > L \end{cases} \tag{II.181}$$

1/ Verify that it obeys the Lippmann-Schwinger integral equation

$$\psi_{L,k}(x) = \mathrm{e}^{+\mathrm{i}kx} + \int_0^L \mathrm{d}x'\, G^{\mathrm{R}}(x, x'; k^2)\, V(x')\, \psi_{L,k}(x') \quad \text{for } G^{\mathrm{R}}(x, x'; k^2) = \frac{1}{2\mathrm{i}k}\mathrm{e}^{\mathrm{i}k|x-x'|} \tag{II.182}$$

where

$$G^{\mathrm{R}}(x, x'; k^2) \stackrel{\text{def}}{=} \langle x | \frac{1}{k^2 - H_0 + \mathrm{i}0^+} | x' \rangle = \frac{1}{2\mathrm{i}k}\mathrm{e}^{\mathrm{i}k|x-x'|} \tag{II.183}$$

is the free retarded Green's function, $H_0 = -\partial_x^2$.

2/ Perturbation.— In the perturbative regime ($L \to 0$), check that

$$t \simeq \mathrm{e}^{\mathrm{i}kL}\left(1 + \frac{1}{2\mathrm{i}k}\int_0^L \mathrm{d}x'\, V(x')\right) \quad \text{and} \quad r \simeq \frac{1}{2\mathrm{i}k}\int_0^L \mathrm{d}x'\, V(x')\,\mathrm{e}^{2\mathrm{i}kx'} \tag{II.184}$$

Similarly, one could obtain the third coefficient

$$r' \simeq \frac{\mathrm{e}^{2\mathrm{i}kL}}{2\mathrm{i}k}\int_0^L \mathrm{d}x'\, V(x')\,\mathrm{e}^{-2\mathrm{i}kx'} \tag{II.185}$$

3/ Deduce that a tiny interval $L \to 0$ is characterized by the transfer matrix : [16]

$$T_{[0,L]} \simeq \mathbf{1}_2 + \begin{pmatrix} \mathrm{i}kL - \frac{\mathrm{i}LV(0)}{2k} & -\frac{\mathrm{i}LV(0)}{2k} \\ \frac{\mathrm{i}LV(0)}{2k} & -\mathrm{i}kL + \frac{\mathrm{i}LV(0)}{2k} \end{pmatrix} \tag{II.187}$$

where σ_i are the Pauli matrices.

4/ Deduce the evolution equation for the transfer matrix

$$T(x + \delta x) \simeq T_{[x,x+\delta x]} \times T(x) \tag{II.188}$$

Hence

$$\boxed{\frac{\mathrm{d}}{\mathrm{d}x} T(x) = \left[\frac{V(x)}{2k} \sigma_y + \mathrm{i} \left(k - \frac{V(x)}{2k} \right) \sigma_z \right] T(x)} \qquad \text{with initial condition } T(0) = \mathbf{1}_2 \, . \tag{II.189}$$

5/ Check that the three parameters of the polar representation obey the coupled differential equations :

$$\frac{\mathrm{d}\alpha}{\mathrm{d}x} = k - \frac{V(x)}{2k} \left(1 + \cos(\alpha + \beta) \tanh \xi \right) \tag{II.190}$$

$$\frac{\mathrm{d}\beta}{\mathrm{d}x} = k - \frac{V(x)}{2k} \left(1 + \frac{\cos(\alpha + \beta)}{\tanh \xi} \right) \tag{II.191}$$

$$\frac{\mathrm{d}\xi}{\mathrm{d}x} = -\frac{V(x)}{2k} \sin(\alpha + \beta) \tag{II.192}$$

D. Application for the random potential

Thus we can find two coupled equations for $\alpha + \beta$ and ξ (i.e. for the phase and modulus of the reflection coefficient alone). We define $\theta \stackrel{\text{def}}{=} \frac{\alpha + \beta + \pi}{2}$. We get the equations

$$\frac{\mathrm{d}\theta}{\mathrm{d}x} = k - \frac{V(x)}{2k} \left[1 - \frac{\cos(2\theta)}{\tanh(2\xi)} \right] \tag{II.193}$$

$$\frac{\mathrm{d}\xi}{\mathrm{d}x} = \frac{V(x)}{2k} \sin(2\theta) \tag{II.194}$$

(we do not consider the equation for $\alpha - \beta$). Conclude about Eq. (II.168).

Further reading :

• Green's function in quantum mechanics : appendix of chapter 10 of [Texier, '15].

• Transfer matrices (generalities) :
cf. chapters 5 and 10 of [Texier, '15], and in particular exercice 5.2.
[Mello & Kumar, '04] P. A. Mello and N. Kumar, *Quantum transport in mesoscopic systems – Complexity and statistical fluctuations*, Oxford University Press, 2004.
Connection to the group $SO(2,1)$:

---

[16] We recognize, as it should, the transfer matrix characterizing the potential $V(x) = v\,\delta(x)$:

$$\begin{pmatrix} 1 - \frac{\mathrm{i}v}{2k} & -\frac{\mathrm{i}v}{2k} \\ \frac{\mathrm{i}v}{2k} & 1 + \frac{\mathrm{i}v}{2k} \end{pmatrix} \tag{II.186}$$

A. Peres, *Transfer matrices for one-dimensional potentials*, J. Math. Phys. **24**(5), 1110–1119 (1983).

• Transfer matrices for the localisation problem, cf. the recent review article :
Alain Comtet, Christophe Texier & Yves Tourigny, *Lyapunov exponents, one-dimensional Anderson localisation and products of random matrices*, J. Phys. A: Math. Theor. **46**, 254003 (2013), Special issue "Lyapunov analysis: from dynamical systems theory to applications". preprint cond-mat arXiv:1207.0725.
    or
[Texier, '10] Christophe Texier, *Désordre, localisation et interaction – Transport quantique dans les réseaux métalliques*, thèse d'habilitation à diriger des recherches de l'Université Paris-Sud, 2010. `http://tel.archives-ouvertes.fr/tel-01091550`

• The phase formalism (§ **A**) has been introduced in :
[Antsygina *et al*, '81] T. N. Antsygina, L. A. Pastur, and V. A. Slyusarev, *Localization of states and kinetic properties of one-dimensional disordered systems*, Sov. J. Low Temp. Phys. **7**(1), 1–21 (1981).
I. M. Lifshits, S. A. Gredeskul and L. A. Pastur, *Introduction to the theory of disordered systems*, John Wiley & Sons (1988).
see also chapter 6 of [Texier, '10]

III Scaling theory : qualitative picture

Aim : The analysis of the 1D situation (chapter II) is interesting because it can be performed with the help of powerful (non perturbative) methods. The drawback is that we completely miss the rich phenomenology of Anderson localisation because **dimensionality plays a crucial role**.

We give a first presentation of the famous scaling theory developed by the "gang of four" [1] inspired by Thouless ideas [129, 14]. This will provide the useful concepts in order to have a **general view on localisation effects**.

III.A Several types of insulators

Several types of insulators in condensed matter :

- Band insulator (Fermi energy in a gap)

- Topological insulator (insulating phase in the presence of a topological constraint).
  An interesting aspect : existence of *edge states* between regions characterised by different topological properties.
  Example : quantum Hall state.

- Mott insulator : transport is forbidden due to a strong Coulomb interaction (example : a lattice with one electron per site and interaction $U \to \infty$)

- Anderson insulator : eigenstates becomes localised due to disorder.

III.B What is localisation ?

Anderson model

Let us introduce a model to which the people often refer. The Anderson model is a lattice model, i.e. $\vec{r} \in \mathbb{Z}^d$. The model is defined by the tight-binding Hamiltonian with nearest neighbour couplings

$$H_{\vec{r},\vec{r}'} = -t \sum_{\mu=1}^{d} \left(\delta_{\vec{r},\vec{r}'+\vec{e}_\mu} + \delta_{\vec{r},\vec{r}'-\vec{e}_\mu} \right) + \delta_{\vec{r},\vec{r}'} V_{\vec{r}} \tag{III.1}$$

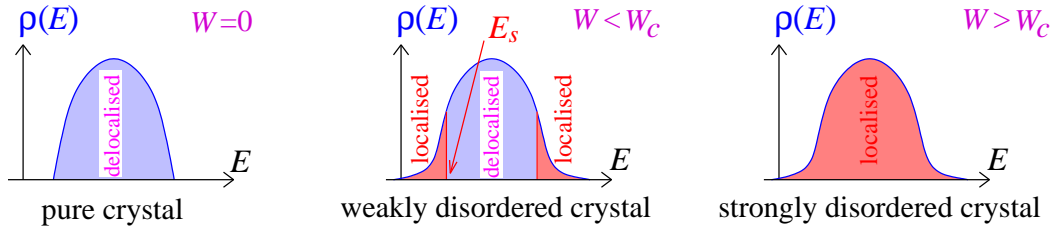The phase diagram given below is based on this model.

Figure 14: **Sketch of the DoS for the 3D Anderson model.** Left : In the absence of disorder. Center : *With "weak" disorder, i.e. below the threshold for complete localisation $W < W_c$. Existence of a mobility edge at E_S.* Right : *Above the threshold $W > W_c$ (for the cubic lattice $W_c = 16.3 \pm 0.5$ [81]).*

Transport properties

Vanishing of the diffusion constant $D = 0$

$$\lim_{t \to \infty} \frac{\langle \vec{r}(t)^2 \rangle}{t} = 0 \tag{III.2}$$

Inverse partition ratio

In a box of volume L^d, i.e. $\vec{r} \in \mathbb{Z}^d$ where $x_\mu \in \{1, \cdots, L\}$. Study the behaviour IPR

$$I(L) = \sum_{\vec{r} \in \text{box}} |\psi_{\vec{r}}|^4 \tag{III.3}$$

with L :

- Delocalised : $I(L) \sim L^{-d}$

- Localised : $I(L) \sim \xi^{-d} = L^0$

Criterion of the mathematicians

The definition of the mathematicians : absolute continuous spectrum (delocalised) *versus* pure point spectrum (localised).

Consider the problem in **infinite volume**, characterised by the local DoS

$$\rho(\vec{r}; \varepsilon) = \sum_n |\varphi_n(\vec{r})^2| \, \delta(\varepsilon - \varepsilon_n) \, . \tag{III.4}$$

The total density of states is a continuous function, weakly sensitive to the nature of the eigenstates (localised/delocalised), apart on the spectral boundaries.

We now integrate the LDoS in a finite volume v

$$\rho_v(\varepsilon) \stackrel{\text{def}}{=} \int_v \mathrm{d}^d \vec{r} \, \rho(\vec{r}; \varepsilon) \tag{III.5}$$

Two situations are encountered

1. The eigenstates are localised : $\rho_v(\varepsilon)$ only receives the contributions of the eigenstates localised in the volume v and therefore is a sum of few delta functions. The spectrum is said to be "*pure point*".

2. The eigenstates are delocalised : all eigenstates contribute to $\rho_v(\varepsilon)$, which is a continuous function of energy. The spectrum is said to be "*absolute continuous*".

The point of view of a mathematician on localisation : the course by Werner Kirsch [79]. Let's forget physics for the Anderson's paper 50th birthday !

III.C   Length scales

- λ : wavelength

- ℓ_{corr} : correlation length

- ℓ : mean free path

- ℓ^* : transport mean free path

- ξ_{loc} : localisation length

- L_φ : phase coherence length

- L : size of the system

$L \ll \ell$	ballistic
$\ell \ll L \ll \xi_{\text{loc}}$	diffusive
$\xi_{\text{loc}} \ll L \ll L_\varphi$	localised (by disorder)
$L_\varphi \ll L$	classical

Table 2: **Regimes**

Conductance

Conductance of a metallic box of section W^{d-1} and length L

$$G_{\text{Drude}} = \sigma \frac{W^{d-1}}{L} \tag{III.6}$$

Using Einstein's relation

$$\sigma = 2_s e^2 \rho_0 D \tag{III.7}$$

where 2_s is the spin degeneracy and ρ_0 the density of states per unit volume at Fermi energy per spin channel.

$\rho_0 \sim n/\varepsilon_F \sim \frac{m_* k_F^{d-2}}{\hbar^2}$, we obtain the **dimensionless conductance** :

$$g \overset{\text{def}}{=} \frac{G}{2_s e^2/h} \sim \frac{e^2 \frac{m_* k_F^{d-2}}{\hbar^2} \frac{v_F \ell_e}{d} }{e^2/\hbar} \frac{W^{d-1}}{L} \sim \frac{(k_F W)^{d-1} \ell_e}{L} \tag{III.8}$$

$N_c \sim (k_F W)^{d-1}$ is the number of conducting channels.

More precisely, electon density is

$$n = 2_s \frac{V_d k_F^d}{(2\pi)^d} = 2_s \frac{k_F^d}{(4\pi)^{d/2}\Gamma(\frac{d}{2}+1)} \; . \tag{III.9}$$

Thus $2\pi\hbar\rho_0 D = \frac{(4\pi)^{1-d/2}}{2\Gamma(\frac{d}{2}+1)} k_F^{d-1} \ell_e$ and

$$g = c_d \frac{(k_F W)^{d-1} \ell_e}{L} \qquad \text{where } c_d = \frac{(4\pi)^{1-d/2}}{2\Gamma(\frac{d}{2}+1)} = \begin{cases} 2 & \text{in } d=1 \\ 1/2 & \text{in } d=2 \\ 1/(3\pi) & \text{in } d=3 \end{cases} \tag{III.10}$$

Thouless energy

The dimensionless conductance can be expressed in terms of the Thouless energy :

$$g = h\rho_0 D \frac{W^{d-1}}{L} = \frac{hD}{L^2} \rho_0 \overbrace{\underbrace{W^{d-1} L}_{\text{Vol}}}^{\text{DoS}=1/\delta} \tag{III.11}$$

The dimensionless conductance is given by the ratio of two energies : the Thouless energy, related to the Thouless time $\tau_D = L^2/D$ required to explore the system, and the mean level spacing δ (inverse of the DoS) :

$$\boxed{g = 2\pi \frac{E_{\text{Thouless}}}{\delta} \qquad \text{where } E_{\text{Thouless}} \overset{\text{def}}{=} \frac{\hbar D}{L^2}} \tag{III.12}$$

Ioffe-Regel criterion

localisation threshold (for $d \geqslant 3$) :

$$k_F \ell_e \sim 1 \qquad \text{(III.13)}$$

III.D   Scaling theory of localisation

$\diamond$ Generalities on scaling theories.

$\diamond$ Explicit calculation for 1D and quasi-1D systems.

$\diamond$ Scaling theory in arbitrary dimension and possible existence of a metal-insulator transition (Thouless criterion).

$\diamond$ Experimental results in 3D on light, microwave, acoustic waves, electrons, cold atoms. Large fluctuations in the vicinity of the transition, multifractality of the wavefunctions.

$\diamond$ Specific case of dimension 2. Importance of the symmetry class.

$\diamond$ Scaling properties of the plateaux of the Integer Quantum Hall Effect (Chalker-Coddington model).
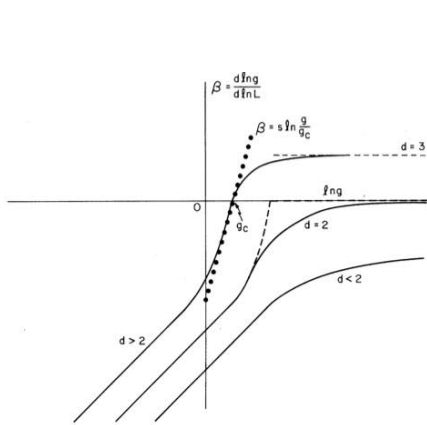

FIG. 1.   Plot of $\beta(g)$ vs $\ln g$ for $d > 2$, $d = 2$, $d < 2$. $g(L)$ is the normalized "local conductance." The approximation $\beta = s \ln(g/g_c)$ is shown for $g > 2$ as the solid-circled line; this unphysical behavior necessary for a conductance jump in $d = 2$ is shown dashed.
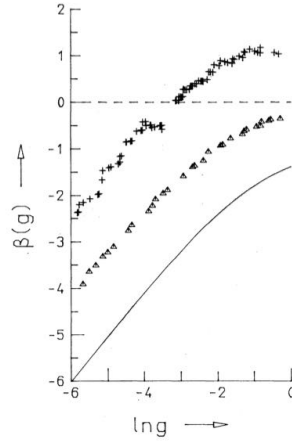
FIG. 2.   Scaling function $\beta(g)$ for the conductance g. Full line is for $d = 1$. Triangles and plusses are for $d = 2$ and $d = 3$, respectively, as calculated from the data in Fig. 1.

Figure 15: Gauche : *Allure schématique de la fonction $\beta(g)$ d'un conducteur désordonné en dimension d, proposée dans la Réf. [1] (pour une potentiel désordonné scalaire). La transition d'Anderson ne se produit qu'en dimension strictement supérieure à 2.* Droite : *Résultat obtenu numériquement dans la Réf. [90] pour les dimensions $d = 2 \, \& \, 3$ et $\beta(g) = -(1+g)\ln(1+1/g)$ pour $d = 1$ [14].*

Definition of the metallic and insulating phases within the scaling theory

In a gedanken experiment, study how the conductance of a cube of size L^d behaves with system size.

- $L \nearrow \Rightarrow \; g \nearrow$: metallic phase

- $L \nearrow \Rightarrow \; g \searrow$: insulating phase

This can be conveniently described by considering the function

$$\beta(g) \stackrel{\text{def}}{=} \frac{\mathrm{d}\ln g}{\mathrm{d}\ln L} \qquad \text{(III.14)}$$

58

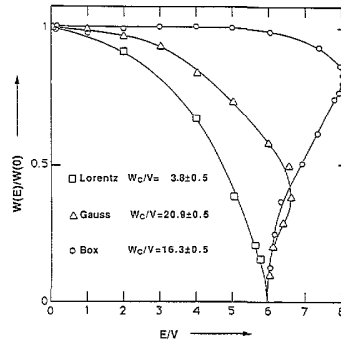The non trivial assumption is that it depends only on one parameter (here chosen to be the conductance).
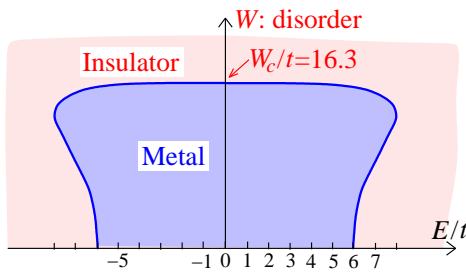
Figure 33. The phase diagram of localization, $W(E_C)$, for the Anderson model with box, Gaussian and Lorentzian distributions of site energies. Energy E is in units of V, the off-diagonal element of the Hamiltonian. $W(0) \equiv W_C$ are the critical disorders for the Anderson transition.

Figure 16: À gauche : *Diagramme de phases pour le modèle d'Anderson 3d sur réseau cubique avec énergies sur sites distribuées selon $p(\varepsilon) = \frac{1}{W}\theta(\frac{1}{2}W - |\varepsilon|)$ [en l'absence de désordre la bande d'états a pour largeur $12t$, où t est le terme de saut ($\varepsilon_{\vec{k}} = -2t\sum_{\mu}\cos k_{\mu}$)]. À droite : Diagrammes de phase obtenus numériquement pour les distributions $p(\varepsilon) = \frac{1}{W}\theta(\frac{1}{2}W - |\varepsilon|)$, gaussienne et lorentzienne ; figure tirée de [81].*

Conclusion of the chapter : Determination of the $\beta(g)$ function is extremely difficult task. A natural strategy is to consider (quantum) corrections to the classical (Drude) transport. This leads to the developement of the perturbative approach (chapter IV)...

TD 3 : Distribution of the transmission in 1D and the scaling approach

We consider the transmission through a one-dimensional disordered medium and derive the distribution of the tranmission probability.

Introduction : transfer matrix.– The solution of the Schrödinger equation can be conveniently analysed with a transfer matrix formalism. Transfer matrix relates left amplitudes to right amplitudes of the wave function

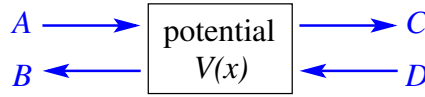$$\begin{pmatrix} C \\ D \end{pmatrix} = T \begin{pmatrix} A \\ B \end{pmatrix} \tag{III.15}$$

Figure 17: *The transfer matrix relates the left to right amplitudes. I.e. the wave function is $\psi(x) = A\,e^{ik(x-x_L)} + B\,e^{-ik(x-x_L)}$ at the left and $\psi(x) = C\,e^{ik(x-x_R)} + D\,e^{-ik(x-x_R)}$ at the right.*

The scattering on a potential is characterised by two sets of reflection/transmission amplitudes, (r,t) if a plane wave is sent from the left and (r',t') if it is sent from the right (cf. for instance exercice 5.2 of [118]) :

$$T = \begin{pmatrix} 1/t^* & r'/t' \\ -r/t' & 1/t' \end{pmatrix} \quad \in\ \mathrm{U}(1,1) \tag{III.16}$$

with $\det T = t/t'$ (note that $r'/t' = -(r/t)^*$ follows from unitarity). Moreover in 1D $t = t'$. The transfer matrix conserves the norm $X^\dagger \sigma_z X = |x|^2 - |y|^2$.

1/ Composition rule.– The first step is to determine the composition rule for the transmission amplitudes when combining two regions characterised by two transfer matrices $T = T_2 T_1$. Show that :

$$t_{1\oplus 2} = t_2 t_1 + t_2(r'_1 r_2)t_1 + \cdots = \frac{t_2 t_1}{1 - r'_1 r_2} \tag{III.17}$$

Evolution of the transmission.– We search the differential equation for the transmission probability $\tau(x)$ characterising transmission through an interval $[0,x]$ with disorder. We consider a small slice of disordered medium in $[x, x + \delta x]$, described by reflexion and transmission amplitudes t_2, r_2 and r'_2. We introduce the reflection probability $\rho = |r_2|^2 \ll 1$. If transmission through $[0,x]$ is encoded in the coefficients t_1, r_1 and r'_1, Eq. (III.17) gives

$$\tau(x + \delta x) = \frac{\tau(x)(1-\rho)}{|1 + e^{i\theta}\sqrt{1-\tau(x)}\sqrt{\rho}|^2} \tag{III.18}$$

where θ is the sum of the phases of the reflection coefficients. Expanding in powers of $\rho \ll 1$ we obtain

$$\delta\tau(x) = \tau(x+\delta x) - \tau(x) = -2\cos(\theta)\,\tau\sqrt{1-\tau}\sqrt{\rho} + \left[-\tau(2-\tau) + 4\,\tau(1-\tau)\cos^2(\theta)\right]\rho + \mathcal{O}(\rho^{3/2}) \tag{III.19}$$

Assumptions :

- $\langle \rho \rangle \simeq \delta x / \ell$, where ℓ is the scattering length (an effective parameter characterising the strength of the disorder).

- The phase θ is independent of $\tau(x)$, but also of ρ (of course the second assumption is not exact) and uniformly distributed.

2/ Express $\langle \delta \tau \rangle$ and $\langle \delta \tau^2 \rangle$ in terms of averages of functions of τ. Deduce that the transmission obeys the stochastic differential equation (SDE)

$$d\tau(x) = -\tau^2 \frac{dx}{\ell} + \sqrt{\frac{2}{\ell} \tau^2 (1 - \tau)} \, dW(x) \qquad \text{(Itô)} \qquad \text{(III.20)}$$

3/ Lyapunov exponent.– Using the Itô formula (cf. appendix), show that

$$-d \ln \tau(x) = \frac{dx}{\ell} - \sqrt{\frac{2}{\ell}(1 - \tau)} \, dW(x) \qquad \text{(Itô)} \qquad \text{(III.21)}$$

Deduce the relation between the effective parameter ℓ and the Lyapunov exponent γ.

4/ Distribution of the transmission probability.– We parametrise the transmission probability as $\tau(x) = 1/\cosh^2 u(x)$. Using that $\text{argcosh}\, y = \ln(y + \sqrt{y^2 - 1})$, show that

$$du(x) = \frac{\gamma}{\tanh 2u} \, dx - \sqrt{\gamma} \, dW(x) \qquad \text{(III.22)}$$

Considering the limit of large x, find the distribution of $u(x)$. Compare the mean value and the variance.

5/ The above calculation is adapted from the well-known article [14]. The *ad hoc* hypothesis made above is equivalent to the **Single Parameter Scaling** hypothesis of the gang of four [1]. In the article [105], we have compared (analytically and numerically) $\gamma_1 = \lim_{x \to \infty} \frac{1}{x} \overline{\ln |\psi(x)|}$ and $\gamma_2 = \lim_{x \to \infty} \frac{1}{x} \text{Var}(\ln |\psi(x)|)$ for the model

$$H = -\frac{d^2}{dx^2} + V(x) \qquad \text{where } \overline{V(x)V(x')} = \sigma \, \delta(x - x') . \qquad \text{(III.23)}$$
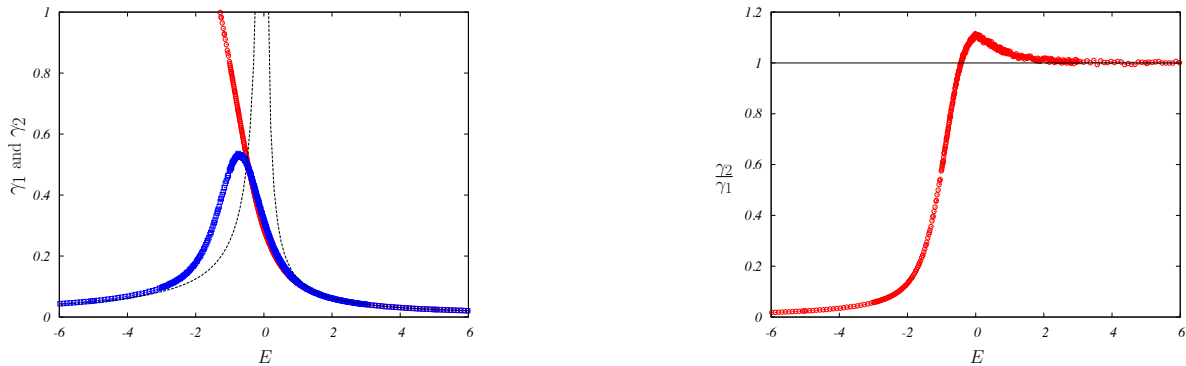
The result is plotted on the Figure 18.

Figure 18: *The two first cumulants of $\ln |\psi(x)|$ for $\sigma = 1$. From [105].*

Discuss the relation with the previous results.

Appendix : Itô calculus

We introduce a normalised Wiener process $W(t)$, i.e. $\langle W(t) \rangle = 0$ and $\langle W(t)W(t') \rangle = \min(t, t')$. Consider the stochastic differential equation (SDE)

$$\mathrm{d}x(t) = A(x(t))\,\mathrm{d}t + B(x(t))\,\mathrm{d}W(t) \qquad \text{(Itô)}$$

understood with the Itô convention, which refers to a prescription for the equal time correlations : $\langle f(x(t))\,\mathrm{d}W(t) \rangle = 0$. The usual rule for a change of variable is modified according to the Itô formula

$$\mathrm{d}\varphi(x(t)) = \left[A(x)\,\varphi'(x) + \frac{1}{2}B(x)^2\varphi''(x) \right]\,\mathrm{d}t + B(x)\,\varphi'(x)\,\mathrm{d}W(t) \qquad \text{(Itô)} \qquad \text{(III.24)}$$

(which follows from $\mathrm{d}W(t)^2 = \mathrm{d}t$, roughly speaking).

The related Fokker-Planck equation is

$$\partial_t P_t(x) = \frac{1}{2}\partial_x^2\big[B(x)^2 P_t(x)\big] - \partial_x\big[A(x)P_t(x)\big] \,.$$

The relation with the SDE in the Stratonovich convention

$$\mathrm{d}x(t) = \widetilde{A}(x(t))\,\mathrm{d}t + B(x(t))\,\mathrm{d}W(t) \qquad \text{(Stratonovich)} \,,$$

describing the *same process*, is $\widetilde{A}(x) = A(x) - (1/2)B(x)\,B'(x)$. We recall that the Stratonovich convention is obtained in particular when the Gaussian white noise $W'(t)$ is the singular limit of a regular noise. Then the process and the noise at equal time are correlated, $\langle f(x(t))\,\mathrm{d}W(t) \rangle \neq 0$. The Stratonovich convention allows to use usual rule for differential calculus, i.e. $\mathrm{d}\varphi(x(t)) = \varphi'(x(t))\,\mathrm{d}x(t)$.

For a pedagogical presentation of stochastic calculus, cf. the book of Gardiner [65].

☞ **If you want to learn more :**

The existence of a second length scale in the strong disorder regime has been nicely discussed by Cohen, Roth and Shapiro [37] (cf. this article for references). See also discussion and further references in the recent article [105].

IV Electronic transport in weakly disordered metals : perturbative (diagrammatic) approach

Aim : In most of real situations, the disorder is weak compared to the energy of the diffusing particle : this is true for the electron dynamics in a metal or the diffusion of the light in a turbid medium. The aim of the chapter is to give the tools for a *quantitative* analysis of a weakly disordered medium. Although the presentation will mostly concern electronic transport, the basic concepts can be easily adapted to consider any other types of waves.

IV.A Introduction : importance of the weak disorder regime

1) Multiple scattering – Weak disorder regime

The aim of the course is to discuss the interaction of a wave with a static disordered potential, i.e. the regime of multiple scattering.

The study of simple scattering (by a single scattering center) can be found in many textbooks : scattering of a wave of wavelength λ is described by a differential cross-section $\frac{d\sigma}{d\Omega}(\theta, \varphi)$ giving the probabilty for the incident particle to be scattered in the direction (θ, φ). The total cross-section $\sigma = \int d\Omega \frac{d\sigma}{d\Omega}$ measures the probability for the incident particle to interact with the scatterer.

In practice, a target is usually made of *many* equivalent scattering centers with whom the incident particle may interact. If the cross-section and/or the thickness of the sample is large enough, multiple scattering must be taken into account. The typical distance between two collisions by defects is the elastic **mean free path** ℓ_e (i.e. the incident particle interact with a scattering center with probability 1 on a distance $\gtrsim \ell_e$). Let us consider a diffusing medium with a density n_i of scattering centers. We expect simple behaviours with σ and n_i, precisely $\ell_e \propto 1/\sigma$ and $\ell_e \propto 1/n_i$, thus

$$\ell_e = 1/(n_i \sigma) \, . \tag{IV.1}$$

Multiple scattering is therefore characterised by two important length scales : the wave length λ (wave) and the m.f.p. ℓ_e (disorder). This allows to define the **weak disorder regime** as

$$\boxed{\lambda \ll \ell_e} \tag{IV.2}$$

In this case, it is possible to treat *each collision perturbatively* (in the strength of the disordered potential), however we will have to account for multiple scattering events which will make most results *non perturbative*. For example, the residual Drude conductivity (at $T \to 0$) $\sigma = \frac{ne^2 \tau_e}{m}$, is inversely proportional to the *rate* $\gamma_e = 1/\tau_e$ which is the perturbative quantity.

Example : disordered metals.– Let us consider Gold, a good metal : Fermi wavelength is $k_F^{-1} = 0.085$ nm, which is much smaller than the elastic mean free path, $\ell_e^{(\text{bulk})} \simeq 4 \, \mu$m in bulk, or $\ell_e^{(\text{film})} \simeq 20$ nm in thin metallic films (thickness $\lesssim 50$ nm).

2) Interference effects in multiple scattering

If a wave interacts with many scattering centers, we expect that an extremely complex interference pattern is produced. Let us examine the typical situations where this occurs.

First of all, interferences are not necessarily dominant in the situation where a wave diffuses in a turbid medium. For example, in a cloudy day, the light of the sun diffuses inside the clouds, what is the reason for the uniformly white sky. This is not an interference effect.

When discussing interference effects, it is always useful to come back to the simple Young double slit experiment. In this case, the two possible paths are each associated with an amplitude and the total intensity involves the sum of two amplitudes

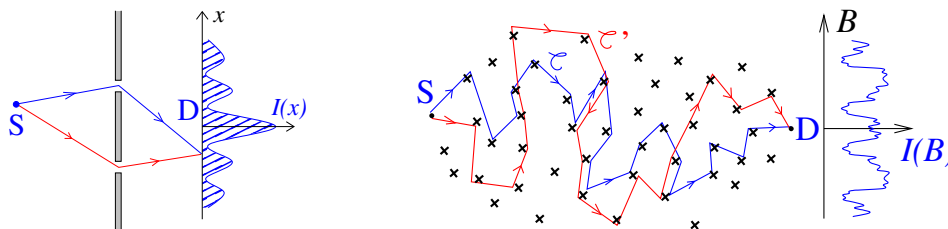$$I = |\mathcal{A}_1 + \mathcal{A}_2|^2 \; . \tag{IV.3}$$

Figure 19: **Interference : Two path interference (Young experiment)** *versus* **multiple path interference.**

In a disordered medium, the wave can be scattered by many centers, what defines an extremely large number of scattering paths

$$I = \left| \sum_{\mathcal{C}} \mathcal{A}_{\mathcal{C}} \right|^2 = \underbrace{\sum_{\mathcal{C}} |\mathcal{A}_{\mathcal{C}}|^2}_{\text{incoherent}} + \underbrace{\sum_{\mathcal{C} \neq \mathcal{C}'} \mathcal{A}_{\mathcal{C}} \mathcal{A}_{\mathcal{C}'}^*}_{\text{interferences}} \tag{IV.4}$$

We now discuss few situations where the interference term manifests itself.

Example 1 (light) : Speckle pattern (fluctuations).– If coherent light (from a laser) is sent on a disordered medium, the resulting interference pattern is extremely complicate, exhibiting intensity fluctuations of the same order than the mean intensity (right part of Fig. 20). The typical result of such an experiment is shown on Fig. 20 and is called a *speckle* pattern. In the Young experiment, the specific intensity profile is a signature of the double slit device. Similarly, the speckle pattern is the fingerprint of the disordered potential.
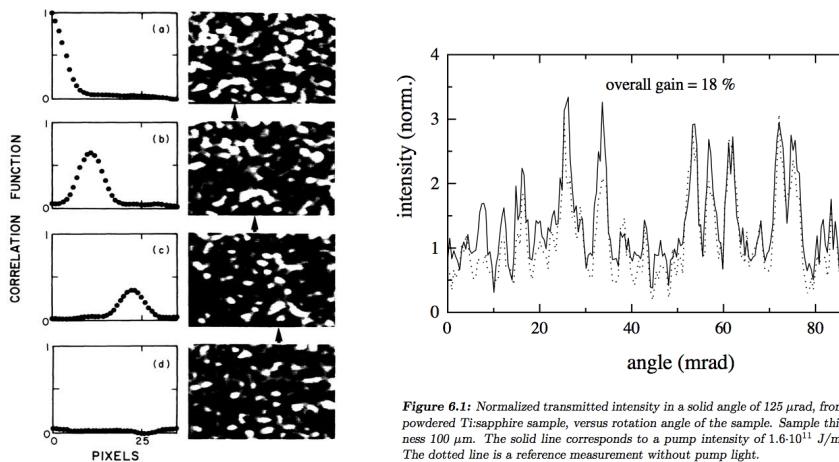
Figure 6.1: *Normalized transmitted intensity in a solid angle of 125 μrad, from a powdered Ti:sapphire sample, versus rotation angle of the sample. Sample thickness 100 μm. The solid line corresponds to a pump intensity of $1.6 \cdot 10^{11}$ J/m²s. The dotted line is a reference measurement without pump light.*

Figure 20: **Speckle patterns.** Left : *Interference pattern resulting from the scattering of a laser beam (633 nm) by a thin (370 μm) opal glass ; Estimated m.f.p. $\ell_e \sim 100$ μm. From Ref. [59].* Right : *Scattered light intensity (532 nm) by a powdered Ti:saphire sample. From Ref. [142].*

Example 2 (light) : Albedo (average).– The speckle pattern is a manifestation of (sample to sample) *fluctuations*. The complex structure of the interference pattern is due to the rapidly varying phase of the amplitudes $\mathcal{A}_{\mathcal{C}} \simeq |\mathcal{A}_{\mathcal{C}}|\mathrm{e}^{\mathrm{i}k\ell_{\mathcal{C}}}$ in Eq. (IV.4), where $\ell_{\mathcal{C}}$ is the length of the path $\mathcal{C}$. A naive guess could be that such interferences do not survive averaging. This is however not the case. If one considers the configuration represented in Fig. 21, the measurement of the scattered intensity in the direction θ shows some intensity profile almost flat, apart for an increase at back-scattering : $I(\theta) \simeq I_0 + I_{\mathrm{CBS}}(\theta)$ where $I_{\mathrm{CBS}}(\theta)$ is a very narrow function (we will show that the back-scattering cone has a typical width $\delta\theta \sim 1/(k\ell_e)$). The experimental data shows that the intensity is almost exactly doubled $I(\theta = 0) \simeq 2I_0$ (Fig. 21). This phenomenon is due to constructive **interference of reversed trajectories**, leading to an **increase of the back-scattering** (Fig. 22). Thus, this is an effect of *localisation*.
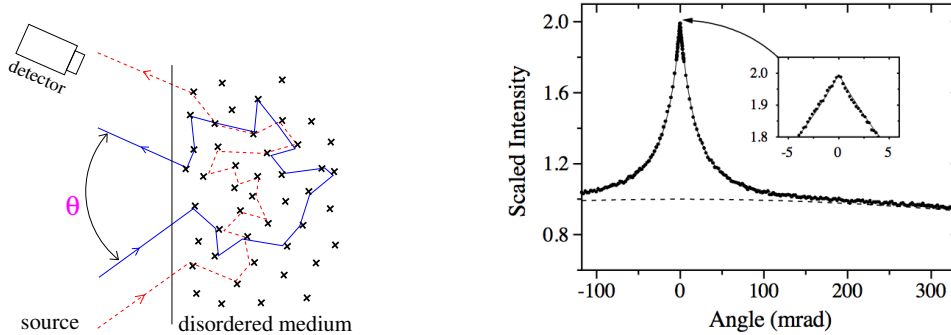

Figure 21: **Coherent back-scattering of light.** Left : *Principle of measurement.* Right : *Coherent back-scattering of light (wavelength* 514 nm*) by ZnO powder sample. Mean free path is* $\ell_e = 1.9\,\mu$m. *From Ref. [142]. The smooth background of the intensity profile originates from the diffusion of light in the disordered medium. The narrow peak,* $\delta\theta \sim 0.05$ rad*, is the CBS.*

This can be understood with the help of the qualitative representation (IV.4). Among all interference terms, one is related to the interference of the two paths corresponding to the reversed sequences of scattering events (path $\mathcal{C}$ and $\widetilde{\mathcal{C}}$). Exactly at back-scattering ($\theta = 0$), time reversed symmetry implies that $\mathcal{A}_{\mathcal{C}} = \mathcal{A}_{\widetilde{\mathcal{C}}}$, what explains the doubling of the intensity :

$$I(\theta = 0) = \sum_{\mathcal{C}} |\mathcal{A}_{\mathcal{C}}|^2 + \underbrace{\sum_{\mathcal{C}} \mathcal{A}_{\mathcal{C}}\mathcal{A}_{\widetilde{\mathcal{C}}}^*}_{\text{CBS } (\mathcal{C}'=\widetilde{\mathcal{C}})} + \underbrace{\sum_{\mathcal{C},\,\mathcal{C}'\neq\mathcal{C} \text{ and } \widetilde{\mathcal{C}}} \mathcal{A}_{\mathcal{C}}\mathcal{A}_{\mathcal{C}'}^*}_{\simeq 0} \simeq \mathbf{2}\sum_{\mathcal{C}} |\mathcal{A}_{\mathcal{C}}|^2 \ . \tag{IV.5}$$

Although the effect is not small exactly at back-scattering, it is globally a small effect : the contribution of interferences to the total scattered intensity $\int \mathrm{d}\theta\, I_{\mathrm{CBS}}(\theta) \sim I_0/k\ell_e$ is small.

Example 3 (electrons) : Weak localisation correction (average).– The increase of back-scattering due to interferences of reversed diffusive trajectories can also be demonstrated in electronic transport. Quantum transport in metallic films and wires was investigated systematically in several experiments (cf. [27] for films). In this case, the interference pattern must be revealed by tuning some external parameter, like the chemical potential or the magnetic field. The typical low temperature resistance of a long and narrow wire [17] as a function of the magnetic field presents the profile shown on Fig. 23, with a narrow peak around zero field. The experiment

---

[17] The effect is re-inforced in a narrow wire of sub-micron cross-section. The reason is related to the fact that localisation effects are stronger in low dimension. The precise criterion for the wire to be "narrow" will be made clear later.
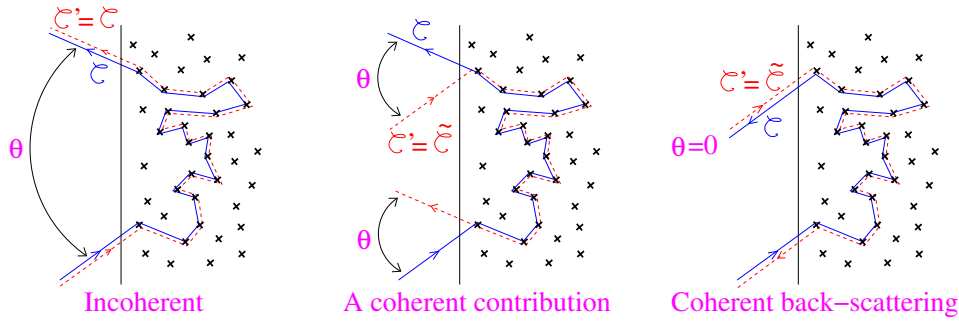
Figure 22: **Coherent back-scattering.** Left : *The classical term can be understood as the pairing of two equal trajectories $\mathcal{C}' = \mathcal{C}$. Center and Right : The contribution of reversed trajectories $\mathcal{C}' = \widetilde{\mathcal{C}}$ to the interference term.*

demonstrates a *decrease* of the resistance with the magnetic field, i.e. an opposite effect to the classical magneto-resistance (cf. problem page 98). For this reason, this phenomenon is called "anomalous magneto-resistance". It is equivalent (but not exactly similar) to the CBS cone in optical experiments. Being an increase of the electric resistance, this is also a manifestation of *localisation.*
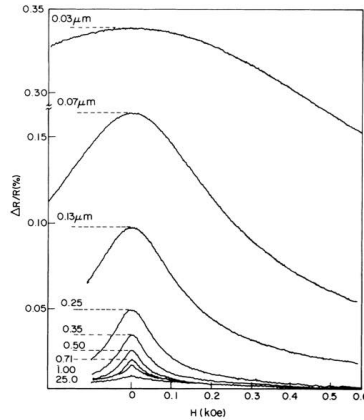
FIG. 1. Magnetoresistance data for L_i films varying in width, W, down to 0.03 ± 0.01 μm.

Figure 23: **Magneto-resistance $\Delta R(\mathcal{B})$ of thin metallic Lithium wires.** *Sample are made of 27 to 101 Lithium wires of length $L = 1$ mm in parallel. Depending on sample, width W varies between 1 μm to 0.03 μm, and thickness is ~ 25 nm. From Ref. [85].*

3)   Phase coherence

A crucial point of the above discussion is that all effects aforementioned are *interference effects*, requiring that the wave remains coherent in the diffusion process on the static potential. In practice the incoming wave may also interact with other degrees of freedom, what limits coherent properties. Two examples are

- In optical experiments : the motion of scatterers.

- In electronic transport : the electron-phonon interaction (lattice vibrations), or the electron-electron interaction.

66

Figure 24: **Decoherence.** *Decoherence may be viewed as contributions of random phases arising from the interaction with other degrees of freedom.*

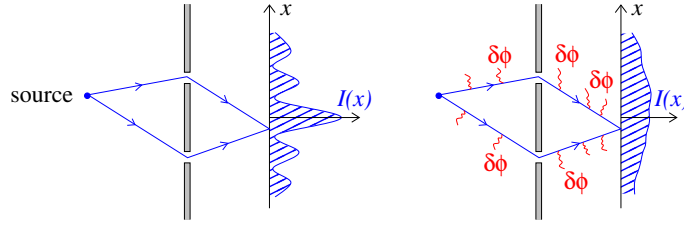In a metal, the increase of the temperature leads to the activation of all degrees of freedoms (thermal fluctuations above the Fermi sea, phonons, etc). Hence interferences of electronic waves progressively disappear, as illustrated by the experimental results shown on Fig. 25. The phase coherent electronic transport only manifests itself below few Kelvins.
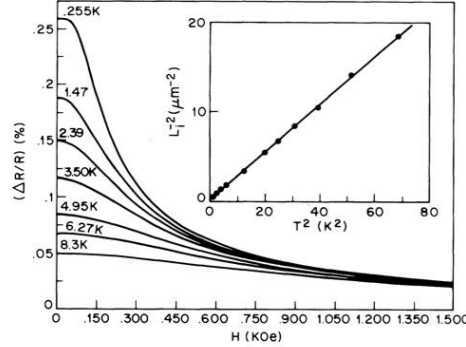

FIG. 3. Detailed fits of magnetoresistance data at various temperatures for $W = 0.074\,\mu$m. Except for the elimination of noise, the fitted curves are indistinguishable from the data. Inset: Values for the quantity $\tilde{L}_i(T)^{-2}$ as a function of T^2 for part of our temperature range.

Figure 25: **Magneto-resistance $\Delta R(\mathcal{B})$ of thin metallic Lithium wires.** *As temperature is increased, phase coherence is limited and magneto-resistance peak is suppressed. From Ref. [85].*

The efficiency of decoherence is characterised by the **phase coherence time τ_φ**. I.e. phase coherence is lost after a time $t \gtrsim \tau_\varphi$. This allows to define several regimes for coherent physics. In general the problem is controlled by three time scales : the elastic mean free time $\tau_e = \ell_e/v_F$, the phase coherent time τ_φ and the Thouless time τ_{Th}, which is the time needed to explore the full system.

- **Coherent ballistic regime.–** Coherent properties are maintained over distances such that the motion is ballistic

$$\min(\tau_\varphi, \tau_{\mathrm{Th}}) < \tau_e$$

  In this case $\tau_{\mathrm{Th}} = L/v_F$, where L is the system size, and $\tau_\varphi = L_\varphi/v_F$, where L_φ is the phase coherence length.

- **Coherent diffusive regime.–** The particle is scattered many times by the disorder before loosing its coherence :

$$\tau_e < \min(\tau_\varphi, \tau_{\mathrm{Th}})$$

  The relation between length and time is characteristic of diffusive motion : $\tau_{\mathrm{Th}} = L^2/D$ and $\tau_\varphi = L_\varphi^2/D$.

4)   Motivation : why coherent experiments are interesting ?

Looking at figures 21 and 23, one could legitimately ask the question : what is the interest for studying such tiny effects ? The CBS cone is extremely narrow. The weak localisation correction is less than $\Delta R/R \lesssim 1\,\%$.

The motivation for studying these small effects is both practical and fundamental. Being a manifestation of interference effects, the measurement of these quantities furnishes an experimental probe for coherent properties in diffusive systems. Moreover, the precise knowledge of how weak localisation depends on the phase coherence length L_φ provides its possible *definition*. Weak localisation measurement is a common tool in condensed matter experiments for probing the *fundamental question of phase coherent (quantum) properties of electrons*.

The precise question could be : how to extract the phase coherence length from the magneto-resistance curve ? The answer to this question obviously requires the knowledge of the $\mathcal{B}$-dependence and L_φ-dependence of the magneto-resistance :

$$\mathsf{Q} : \Delta R(\mathcal{B}, L_\varphi) =?$$

IV.B   Kubo-Greenwood formula for the electric conductivity

The remaining of the chapter will focus on electronic transport properties. We first recall some basic formulae for the electrical conductivity of a metal.

1)   Linear response

The starting point is the linear response theory (see for instance [117]). We recall the main result (cf. appendix A). If one considers a time dependent perturbation involving an observable A of the system :

$$\hat{H}(t) = \hat{H}_0 - f(t)\,\hat{A} \tag{IV.6}$$

The "response" of any other observable B

$$\langle \hat{B}(t)\rangle_f = \langle \hat{B}\rangle + \int \mathrm{d}t'\, \chi_{BA}(t-t')\, f(t') + \mathcal{O}(f^2) \tag{IV.7}$$

is controlled at lowest order in perturbation theory by an *equilibrium* correlation function

$$\chi_{BA}(t) = \frac{\mathrm{i}}{\hbar}\,\theta_{\mathrm{H}}(t)\langle [\hat{B}(t),\hat{A}]\rangle \tag{IV.8}$$

where $\langle\cdots\rangle$ is the quantum-statistical average related to H_0 and $\langle\cdots\rangle_f$ the one related to $H(t)$.

2)   Conductivity

The conductivity characterises the response of the current density to the electric field. In principle it probes local properties. However, usual transport experiments probe global properties of the system, and the measured quantity is usually the *conductance*. On the other hand, measurements of small contributions are facilitated by the introduction of a small modulation of the excitation, i.e. measuring a signal at small but finite frequency, what allows to distinguish more easily the signal from the noise (AC lock-in technique). For these reasons we have to consider the conductivity with the proper limits [18] $\lim_{\omega\to 0}\lim_{q\to 0}\sigma(q,\omega)$. We will thus consider a uniform perturbation, i.e. a time-dependent uniform electric field $\vec{\mathcal{E}}(t)$. Due to gauge invariance, we still have some freedom on the choice of the perturbation : we can consider a gauge $\phi_{\mathrm{ext}}(\vec{r},t) = -\vec{\mathcal{E}}(t)\cdot\vec{r}$ and $\vec{A}_{\mathrm{ext}} = 0$, or $\phi_{\mathrm{ext}} = 0$ et $\vec{A}_{\mathrm{ext}}(t) = -\int^t \mathrm{d}t'\,\vec{\mathcal{E}}(t')$. We prefer the

---

[18] Recall that these limits do not commute [117].

second choice, that will lead more directly to a representation of the conductivity in terms of a current-current correlator, close in spirit to the classical definition of the diffusion constant $D = \int_0^\infty \mathrm{d}t \, \langle v_x(t) v_x(0) \rangle$ (recall that the diffusion constant and the conductivity are related by Einstein relation $\sigma_0 = e^2 \nu_0 D$). We consider the single electron Hamiltonian

$$\hat{H}_{\mathrm{tot}}(t) = \frac{1}{2m} \left(\hat{\vec{p}} - e\vec{A}(\hat{\vec{r}}) - e\vec{A}_{\mathrm{ext}}(t) \right)^2 + U(\hat{\vec{r}}) = \underbrace{\frac{1}{2m}\hat{\vec{v}}^2 + U(\hat{\vec{r}})}_{\hat{H}} \underbrace{-e\vec{A}_{\mathrm{ext}}(t) \cdot \hat{\vec{v}}}_{\hat{H}_{\mathrm{pert}}(t)} + \cdots \quad \text{(IV.9)}$$

where $\vec{v} \overset{\text{def}}{=} (\vec{p} - e\vec{A})/m$ is the speed.

The spatially averaged current for one electron [19] is simply

$$\vec{j} = \frac{e}{\mathrm{Vol}} \vec{v} \,. \quad \text{(IV.10)}$$

In the presence of the external vector potential, the speed also receives the contribution of the external vector potential $\vec{v}_{\mathrm{tot}} = \frac{1}{m} \left(\vec{p} - e\vec{A} - e\vec{A}_{\mathrm{ext}} \right)$. Accordingly, the current of the electron gas is splitted in two terms

$$\langle j_i^{\mathrm{tot}}(t) \rangle_{\vec{A}_{\mathrm{ext}}} = \langle j_i(t) \rangle_{\vec{A}_{\mathrm{ext}}} - \frac{Ne^2}{\mathrm{Vol}} A_i^{\mathrm{ext}}(t) \,, \quad \text{(IV.11)}$$

where $N = \sum_\alpha f_\alpha$ is the number of electrons, expressed in terms of the Fermi function $f_\alpha \equiv f(\varepsilon_\alpha)$. The first term is given by the linear response theory

$$\langle j_i(t) \rangle_{\vec{A}_{\mathrm{ext}}} = \frac{e^2}{\mathrm{Vol}} \int \mathrm{d}t' \, K_{ij}(t - t') \, A_i^{\mathrm{exp}}(t') + \cdots \quad \text{(IV.12)}$$

and involves a velocity-velocity (i.e. current-current) correlator [20]

$$K_{ij}(t) = \mathrm{i}\theta(t) \langle [v_i(t), v_j] \rangle \quad \text{(IV.14)}$$

(we now set $\hbar = 1$). After Fourier transform, we express the current in terms of the electric field and obtain the conductivity

$$\widetilde{\sigma}_{ij}(\omega) = \frac{1}{\mathrm{i}\omega} \frac{e^2}{\mathrm{Vol}} \left(-\frac{N}{m}\delta_{ij} + \mathrm{i} \int_0^\infty \mathrm{d}t \, \mathrm{e}^{(\mathrm{i}\omega - 0^+)t} \, \langle [v_i(t), v_j] \rangle \right) = \frac{\mathrm{i}}{\omega} \frac{e^2}{\mathrm{Vol}} \left[\frac{N}{m}\delta_{ij} - \widetilde{K}_{ij}(\omega) \right] \quad \text{(IV.15)}$$

where we have introduced an infinitesimally small regulator 0^+. Using the spectral representation of the correlator

$$\widetilde{K}_{ij}(\omega) = -\sum_{\alpha,\beta} (f_\alpha - f_\beta) \frac{(v_i)_{\alpha\beta}(v_j)_{\beta\alpha}}{\omega + \varepsilon_\alpha - \varepsilon_\beta + \mathrm{i}0^+} \,, \quad \text{(IV.16)}$$

---

[19] In a one-particle picture, the current density operator is $\hat{\vec{j}}(\vec{r}) = e \left[\hat{n}(\vec{r}) \hat{\vec{v}} + \hat{\vec{v}} \hat{n}(\vec{r}) \right]$ where $\hat{n}(\vec{r}) = \delta(\vec{r} - \hat{\vec{r}}) = |\vec{r}\rangle\langle\vec{r}|$ is the density operator, $\hat{\vec{r}}$ the position operator and $\hat{\vec{v}}$ the speed operator.

[20] The discussion can be done at the one-particle level. The N-particle formula is then easy to get thanks to a simple summation. This relies on the following property : consider many body operators A and B sums of one body operators $A = \sum_{i=1}^N a^{(i)}$. Then, the grand canonical average of the commutator is

$$\langle [A, B] \rangle = \mathrm{Tr} \{ \rho [A, B] \} = \sum_n (P_n - P_m) A_{nm} B_{mn} = \sum_\alpha (f_\alpha - f_\beta) a_{\alpha\beta} b_{\beta\alpha} \quad \text{(IV.13)}$$

where the first sum is over many-body eigenstates and $P_n \propto \mathrm{e}^{-\beta(E_n - \mu N)}$ the grand canonical weight, while the second sum runs over one-body eigenstates, f_α being the Bose-Einstein or the Fermi-Dirac distribution (see lectures [117]).

where $(v_i)_{\alpha\beta} \overset{\text{def}}{=} \langle \varphi_\alpha | \hat{v}_i | \varphi_\beta \rangle$ is a one-particle matrix element, we deduce the real (dissipative) part of the conductivity. For simplicity we restrict ourselves to the longitudinal resistivity ($i = j$) :

$$\operatorname{Re}\widetilde{\sigma}_{xx}(\omega) = \frac{\pi e^2}{\text{Vol}} \sum_{\alpha,\beta} \frac{f(\varepsilon_\alpha) - f(\varepsilon_\alpha + \omega)}{\omega} |(v_x)_{\alpha\beta}|^2 \, \delta(\omega + \varepsilon_\alpha - \varepsilon_\beta) \qquad \text{(IV.17)}$$

Introducing $\int \mathrm{d}\varepsilon \, \delta(\varepsilon - \varepsilon_\alpha) = 1$ in the expression, we can rewrite this expression as a trace over the one-particle Hilbert space :

$$\boxed{\operatorname{Re}\widetilde{\sigma}_{xx}(\omega) = \frac{\pi e^2}{\text{Vol}} \int \mathrm{d}\varepsilon \frac{f(\varepsilon) - f(\varepsilon + \omega)}{\omega} \operatorname{Tr}\left\{ \hat{v}_x \, \delta(\varepsilon + \omega - \hat{H}) \, \hat{v}_x \, \delta(\varepsilon - \hat{H}) \right\}} \qquad \text{(IV.18)}$$

We can deduce the zero frequency conductivity $\sigma \overset{\text{def}}{=} \widetilde{\sigma}_{xx}(\omega = 0)$:

$$\sigma = \frac{\pi e^2}{\text{Vol}} \int \mathrm{d}\varepsilon \left(-\frac{\partial f}{\partial \varepsilon} \right) \operatorname{Tr}\left\{ \hat{v}_x \, \delta(\varepsilon - \hat{H}) \, \hat{v}_x \, \delta(\varepsilon - \hat{H}) \right\} \xrightarrow[T\to 0]{} \frac{\pi e^2}{\text{Vol}} \operatorname{Tr}\left\{ \hat{v}_x \, \delta(\varepsilon_F - \hat{H}) \, \hat{v}_x \, \delta(\varepsilon_F - \hat{H}) \right\} \qquad \text{(IV.19)}$$

Because the function $-\frac{\partial f}{\partial \varepsilon}$ is a narrow function of width $k_B T$ much small that the Fermi energy, this expression emphasises that only eigenstates in the close neighbourhood of the Fermi level, $|\varepsilon_\alpha - \varepsilon_F| \lesssim k_B T$, are involved in longitudinal transport properties. **Longitudinal conductivity is a Fermi surface property** (contrary to the transverse conductivity [113, 114]). Finally, let us remark that the Kubo-Greenwood formula, Eq. (IV.17) or Eq. (IV.18), presents the desired structure of a speed-speed correlator reminiscent of the diffusion constant.

Remark : More on the correlator K.– The relation between σ_{ij} and the correlator K_{ij} can be improved by making use of the f-sum rule.

✍ **Exercice IV.1 : f-sum rule.–** Show that $\frac{1}{2m} + \sum_\beta \frac{|(v_x)_{\alpha\beta}|^2}{\varepsilon_\alpha - \varepsilon_\beta} = 0$, where $(v_x)_{\alpha\beta} \overset{\text{def}}{=} \langle \alpha | v_x | \beta \rangle$. Deduce

$$\frac{1}{m} \sum_\alpha f_\alpha + \sum_{\alpha,\beta} (f_\alpha - f_\beta) \frac{|(v_x)_{\alpha\beta}|^2}{\varepsilon_\alpha - \varepsilon_\beta} = 0 \qquad \text{(IV.20)}$$

✍ **Exercice IV.2 :** *Using the spectral representation for $\widetilde{K}_{ij}(\omega)$, analyse $\widetilde{K}_{xx}(\omega = 0)$*

Hint : *note that when $\omega = 0$, the 0^+ becomes useless because the numerator vanishes when $\varepsilon_\alpha = \varepsilon_\beta$.* [21]

For free electrons, the matrix elements are : $\langle \vec{k} | \vec{v} | \vec{k}' \rangle = \frac{\vec{k}}{m} \delta_{\vec{k},\vec{k}'}$, where $|\vec{k}\rangle$ denotes a plane wave. Show that $\widetilde{K}_{xx}(\omega \neq 0) = 0$. Deduce the conductivity for free electrons.

The f-sum rule expresses conservation of particle number. We have shown that

$$\widetilde{\sigma}_{ij}(\omega) = \frac{\mathrm{i} e^2}{\text{Vol}} \frac{\delta_{ij}\,\widetilde{K}_{xx}(0) - \widetilde{K}_{ij}(\omega)}{\omega} \qquad \text{(IV.21)}$$

This structure may also be understood as a consequence of gauge invariance, which is not a surprise since Gauge invariance and charge conservation are closely related by Nœther theorem. The expression (IV.21) must be manipulated with caution. We have indeed seen that $\widetilde{K}_{xx}(\omega)$ is discontinuous at $\omega = 0$ for free electrons.

To close the remark, let us point out that, being the correlation function of the electron velocity, $\widetilde{K}_{xx}(\omega)$ can be related by the fluctuation-dissipation theorem to the power spectrum of the electron velocity [117], i.e. the diffusion constant $D = \int_0^\infty \mathrm{d}t \, \langle v_x(t) v_x(0) \rangle$. Therefore, we can extract from Eq. (IV.21) the **Einstein relation** between conductivity and diffusion constant.

---

[21] if $f(0) = 0$ and $|f'(0)| < \infty$ we have $\frac{f(x)}{x + \mathrm{i}0^+} = \frac{f(x)}{x}$ since $f(x)\delta(x) = 0$ and $\mathcal{P}\frac{f(x)}{x} = \frac{f(x)}{x}$.

3) Conductivity in terms of Green's function

A question of methodology is : how to analyse the Kubo-Greenwood formula (IV.17), in particular with the aim of building a pertubative expansion in the disordered potential ? It is obviously excluded, because far too complicated, to use the well-known perturbative formulae for the spectrum of the Hamiltonian $\{\varepsilon_\alpha, |\varphi_\alpha\rangle\}$; moreover the calculation requires the matrix elements $(v_x)_{\alpha\beta} = \langle \varphi_\alpha |v_x| \varphi_\beta \rangle$. It is therefore essential to introduce a compact object encoding all spectral information and allowing for a convenient and simple perturbative expansion. Such an object is the **Green's function**, i.e. matrix elements of the resolvent operator,

$$\mathcal{G}(\vec{r}, \vec{r}'; z) \stackrel{\text{def}}{=} \langle \vec{r}| \frac{1}{z - H} |\vec{r}'\rangle = \sum_\alpha \frac{\varphi_\alpha(\vec{r})\varphi_\alpha^*(\vec{r}')}{z - \varepsilon_\alpha} \ , \tag{IV.22}$$

whose poles are located on the eigenvalues of the Hamiltonian with residues related to the eigenfunctions. The calculations will involve the *retarded* and *advanced* Green's functions :

$$G^{\text{R,A}}(\vec{r}, \vec{r}'; E) \stackrel{\text{def}}{=} \mathcal{G}(\vec{r}, \vec{r}'; E \pm \text{i}0^+) \ , \tag{IV.23}$$

which can be related to the matrix elements appearing the Eq. (IV.18) by noticing that

$$\Delta G(\vec{r}, \vec{r}'; E) \stackrel{\text{def}}{=} G^{\text{R}}(\vec{r}, \vec{r}'; E) - G^{\text{A}}(\vec{r}, \vec{r}'; E) = -2\text{i}\pi \langle \vec{r}|\delta(E - H)|\vec{r}'\rangle \tag{IV.24}$$

$$= -2\text{i}\pi \sum_\alpha \varphi_\alpha(\vec{r})\, \varphi_\alpha^*(\vec{r}')\, \delta(E - \varepsilon_\alpha) \ . \tag{IV.25}$$

Let us point out that the diagonal matrix elements of this latter function is the local density of states

$$\rho(\vec{r}; E) = \frac{1}{-2\text{i}\pi} \Delta G(\vec{r}, \vec{r}; E) = \sum_\alpha |\varphi_\alpha(\vec{r})|^2\, \delta(E - \varepsilon_\alpha) \ . \tag{IV.26}$$

Its integral is the DoS $\rho(E) = \int \text{d}^d\vec{r}\, \rho(\vec{r}; E) = \sum_\alpha \delta(E - \varepsilon_\alpha)$.

Because the starting point of the perturbative expansion is the free particle problem, it will be quite natural to work in a momentum representation, i.e. in the basis of plane waves

$$\psi_{\vec{k}}(\vec{r}) = \langle \vec{r}| \vec{k} \rangle = \frac{1}{\sqrt{\text{Vol}}} e^{\text{i}\vec{k}\cdot\vec{r}} \tag{IV.27}$$

where we choose plane waves normalised in a box (i.e. with quantised wave vectors [22] $\langle \vec{k}|\vec{k}'\rangle = \delta_{\vec{k},\vec{k}'}$). Accordingly we introduce the Green's function in momentum space (keeping the same notation as in real space)

$$G^{\text{R,A}}(\vec{k}, \vec{k}'; E) \stackrel{\text{def}}{=} \langle \vec{k}| \frac{1}{E - H \pm \text{i}0^+} |\vec{k}'\rangle \ . \tag{IV.28}$$

Kubo-Greenwood formula (IV.18) now reads

$$\boxed{\operatorname{Re}\widetilde{\sigma}(\omega) = -\frac{2_s e^2}{4\pi m^2} \int \text{d}\varepsilon \frac{f(\varepsilon) - f(\varepsilon + \omega)}{\omega} \frac{1}{\text{Vol}} \sum_{\vec{k}, \vec{k}'} k_x\, k_x'\, \Delta G(\vec{k}, \vec{k}'; \varepsilon + \omega)\, \Delta G(\vec{k}', \vec{k}; \varepsilon)} \tag{IV.29}$$

where we have taken into account the spin degeneracy 2_s. It is useful to emphasize that the Fermi functions constraint the energy ε to be close to the Fermi energy ε_F.

---

[22] in a cubic box we have $\vec{k} = \frac{2\pi}{L}(n_x, n_y, n_z)$.

IV.C   Méthode des perturbations et choix d'un modèle de désordre

La méthode ? Maintenant que nous avons introduit le "bon" objet, reste à savoir comment le manipuler, *i.e.* comment effectuer la moyenne sur le désordre de produits de fonctions de Green, supposant donnée la distribution $\mathcal{D}\mathcal{V}\,P[\mathcal{V}]$ du désordre. La difficulté vient notamment de la présence du potentiel au dénominateur dans la fonction de Green $G(E) = \frac{1}{E-H}$. Deux méthodes utilisent un "truc" pour exponentier le dénominateur et faire apparaître la fonctionnelle caractéristique du potentiel : la *méthode des répliques* [73] et la *méthode supersymétrique* [141, 53]. La mise en œuvre de ces deux approches nécessite des techniques de théorie des champs assez sophistiquées dans lesquelles nous ne souhaitons pas entrer ici. Une présentation claire de l'utilisation de la méthode des répliques pour les systèmes désordonnés est proposée dans l'ouvrage de Altland et Simons [4].

The replica method relies on the following trick [52, 55]. Write :

$$\int \mathrm{d}^n \vec{\phi}\, \frac{\vec{\phi}^2}{n}\, \mathrm{e}^{-\frac{1}{2}A\vec{\phi}^2} = \frac{1}{A}\left(\frac{2\pi}{A}\right)^{n/2} \xrightarrow[n\to 0]{} \frac{1}{A}$$

where $\vec{\phi}$ is a n component "field" (the n replicas). The (difficult) computation of the average $\langle \frac{1}{A}\rangle$ is replaced by the (more easy) one of $\langle \mathrm{e}^{-kA}\rangle$. The cost to pay is to let the number of components n go continuously toward 0 ! This limit is not clearly defined in general, as it requires to make the continuation of a function over the integers to the reals, crossing our fingers ! Anyway, let us apply the trick to the average Green's function :

$$\overline{\langle x|(H-E)^{-1}|x'\rangle} = \lim_{n\to 0}\int \mathcal{D}\vec{\phi}\, \frac{\vec{\phi}(x)\cdot\vec{\phi}(x')}{n}\mathrm{e}^{-S} \quad \text{with } \mathrm{e}^{-S} = \overline{\exp -\frac{1}{2}\int \mathrm{d}x\left[(\partial_x\vec{\phi})^2 + (\mathcal{V}(x)-E)\vec{\phi}(x)^2\right]}$$

where $\vec{\phi}(x)$ is a n component field. Averaging over the Gaussian disorder, $\mathcal{D}\mathcal{V}\,P[\mathcal{V}] = \mathcal{D}\mathcal{V}\exp -\frac{1}{2w}\int \mathrm{d}x\,\mathcal{V}(x)^2$, provides the expression of the effective action $S = \int \mathrm{d}x L$. This action describes a theory with an interacting field $L = \frac{1}{2}(\partial_x\vec{\phi})^2 - \frac{E}{2}\vec{\phi}^2 - \frac{w}{8}\vec{\phi}^4$ (chapter 9 of volume 2 of Itzykson & Drouffe's monograph [73]). Using translation invariance of the problem, after disorder averaging, the calculation at coinciding points can be further simplified by writing

$$\overline{\langle x|(H-E)^{-1}|x\rangle} = \lim_{n\to 0}\frac{2}{n}\frac{\partial}{\partial E}\int \mathcal{D}\vec{\phi}\,\mathrm{e}^{-S}$$

from which the DoS can be extracted by considering the limit $E \to E + \mathrm{i}0^+$. More information can be found in the book [4].

The supersymmetric method also starts from a representation of the Green's function in terms of path integral, however it uses a different trick in order to eliminate the determinant related to the normalisation of the integral. Additionally to the integration with respect to the scalar "bosonic" complex field Φ_B, one introduce also a "fermionic" field Φ_F of Grassmanian nature (for the same action). The trick uses that the two normalisations are inverse : $\int \mathcal{D}\Phi_B\, \mathrm{e}^{-\frac{1}{2}\int \mathrm{d}x\left[|\nabla\Phi_B|^2+(\mathcal{V}(x)-E)|\Phi_B|^2\right]} \sim 1/\det(E+\Delta-\mathcal{V}(x))$ and $\int \mathcal{D}\Phi_F\, \mathrm{e}^{-\frac{1}{2}\int \mathrm{d}x\left[|\nabla\Phi_F|^2+(\mathcal{V}(x)-E)|\Phi_F|^2\right]} \sim \det(E+\Delta-\mathcal{V}(x))$. As a result, the Green's function can be represented as

$$\overline{\langle x|(H-E)^{-1}|x'\rangle} = \int \mathcal{D}\Phi_B\mathcal{D}\Phi_F\, \Phi_B(x)\Phi_B(x')^*\,\mathrm{e}^{-S[\Phi_B,\Phi_F]}$$

where the effective action S for the bosonic and fermionic fields, arise from disorder averaging of the original actions. More can be found in Efetov's book [53].

Si ces méthodes sophistiquées sont assez puissantes (elles permettent notamment de décrire la transition du régime de localisation faible vers le régime de localisation forte), elles se révèlent

cependant plutôt inadaptées pour étudier certains problèmes fondamentaux d'importance pratique comme la modélisation de la décohérence.

La troisième méthode, que nous suivrons, est l'approche perturbative où $G(E)$ est développé en puissances du potentiel désordonné, puis le développement moyenné. Les résultats que nous cherchons sont **non perturbatifs dans le désordre**. Cette approche n'est intéressante que si nous pouvons resommer les corrections perturbatives. [23] Le cas unidimensionnel permet une resommation complète des corrections perturbatives dans le cas où le potentiel est un bruit blanc [24, 25]. En vérité ces techniques assez lourdes ne sont pas indispensables et peuvent être évitées au profit de méthodes non perturbatives probabilistes plus élégantes [87, 88] (au moins à mon goût, par exemple *cf.* [38]). Dans les problèmes à plusieurs dimensions nous devrons nous contenter de resommations partielles qui ne seront valables que dans le domaine de *faible désordre*. Nous préciserons cette remarque par la suite.

1) Développements perturbatifs

L'intérêt d'avoir introduit la fonction de Green est que cet objet est le plus approprié pour développer une théorie de perturbation. Si l'on pose $G = \frac{1}{E-H}$ avec $H = H_0 + \mathcal{V}$ on a $G = G_0 + G_0 \mathcal{V} G_0 + G_0 \mathcal{V} G_0 \mathcal{V} G_0 + \cdots$ où $G_0 = \frac{1}{E-H_0}$. La fonction de Green libre est diagonale dans l'espace de Fourier (je laisserai dorénavant tomber les flèches des vecteurs pour alléger, sauf ambiguïté)

$$\langle\, k\,|\frac{1}{E-H_0}|\, k'\,\rangle = \delta_{k,k'} G_0(k) \quad \text{avec } G_0(k) = \frac{1}{E-\varepsilon_k} \tag{IV.30}$$

où $\varepsilon_k \stackrel{\text{def}}{=} \frac{k^2}{2m}$. (Tant que cela n'est pas nécessaire nous ne spécifions pas s'il s'agit de la fonction de Green avancée ou retardée). Pour aller plus loin il nous faut savoir comment modéliser les défauts (impuretés, défauts structurels) et le choix du modèle a-t-il une influence sur la physique ? En général la réponse est oui, évidemment, toutefois nous nous intéresserons à un régime de *faible désordre* et seul le second cumulant de $\mathcal{V}$ sera important. Pour cette raison nous pouvons nous limiter au choix d'une distribution gaussienne, entièrement caractérisée par la fonction de corrélation $\overline{\mathcal{V}(r)\mathcal{V}(r')}$. En pratique il est raisonnable de supposer que les corrélations du potentiel désordonné sont à courte portée, nous les prendrons de portée nulle pour simplifier. En conclusion, pour l'étude des propriétés de transport dans les métaux faiblement désordonnés il est suffisant de choisir le **modèle minimal** :

$$\mathcal{D}\mathcal{V}\, P[\mathcal{V}] = \mathcal{D}\mathcal{V} \exp\left[-\frac{1}{2w}\int \mathrm{d}r\, \mathcal{V}(r)^2\right]. \tag{IV.31}$$

Afin de dégager les règles permettant une construction systématique du développement perturbatif, analysons en détail les premiers termes correctifs du développement de la fonction de Green moyenne $\overline{G}$.

2) Vertex et règles de Feynman

Vertex pour le désordre.– Comme nous travaillons dans l'espace réciproque le calcul fera intervenir la moyenne des éléments de matrice de $\mathcal{V}$ (le vertex élémentaire décrivant l'interaction

---

[23] Si nous calculons la conductivité perturbativement dans l'intensité du désordre, contrôlé par le taux de collision $\gamma_e = 1/\tau_e$, nous obtenons une série $\sigma(\omega) = \frac{\mathrm{i}ne^2}{m\omega}\sum_{n=0}^{\infty}\left(\frac{\gamma_e}{\mathrm{i}\omega}\right)^n$. Après resommation, la limite de fréquence nulle conduit au résultat $\sigma(0) = \frac{ne^2}{m\gamma_e} = \frac{ne^2\tau_e}{m}$ (ce calcul sera effectué plus bas).

entre un électron et le potentiel désordonné pour le calcul de quantités moyennées) :

$$\overline{\langle k_g |\mathcal{V}| k_d \rangle \langle k'_g |\mathcal{V}| k'_d \rangle} = \int \frac{\mathrm{d}r}{\mathrm{Vol}} \mathrm{e}^{\mathrm{i}(k_d - k_g)\cdot r} \int \frac{\mathrm{d}r'}{\mathrm{Vol}} \mathrm{e}^{\mathrm{i}(k'_d - k'_g)\cdot r'} \, w \, \delta(r - r') \qquad \text{(IV.32)}$$

$$= \frac{w}{\mathrm{Vol}} \delta_{k_g + k'_g, k_d + k'_d} = \quad \raisebox{-1em}{} \qquad \text{(IV.33)}$$

où k_d et k'_d sont des impulsions entrantes et k_g et k'_g des impulsions sortantes. Cette expression, la TF de la fonction de corrélation $\overline{\mathcal{V}(r)\mathcal{V}(r')} = w \, \delta(r - r')$. On peut interpréter physiquement le corrélateur comme une *double interaction* avec *un défaut* localisé qui transfert une impulsion $k_g - k_d = k'_d - k'_g$ d'un point à un autre, i.e. d'une fonction de Green à une autre. [24]

Nous commençons par calculer le premier terme non nul en moyenne : $\overline{G_0 \mathcal{V} G_0 \mathcal{V} G_0}$. Le terme d'ordre 2 de $\overline{G(k, k')}$ s'écrit :

$$\overline{\langle k |G_0 \mathcal{V} G_0 \mathcal{V} G_0| k' \rangle} = G_0(k) \sum_{k''} \frac{w}{\mathrm{Vol}} \delta_{k,k'} G_0(k'') \, G_0(k') = \delta_{k,k'} G_0(k)^2 \frac{w}{\mathrm{Vol}} \sum_q G_0(q) \, . \quad \text{(IV.34)}$$

La présence du Kronecker assure la conservation de l'impulsion, ce qui découle de manière évidente de l'analyse du vertex, Éq. (IV.32). Cette propriété reste vraie à tous les ordres et on a donc $\overline{G(k, k')} \equiv \delta_{k,k'} \overline{G}(k)$, qui traduit le fait que *l'invariance par translation est restaurée après moyenne désordre*. Le premier terme du calcul perturbatif de la fonction de Green moyenne est finalement

$$\overline{\delta^2 G}(k) = G_0(k) \left[\frac{w}{\mathrm{Vol}} \sum_q G_0(q) \right] G_0(k) = \quad \raisebox{-1em}{} \qquad \text{(IV.35)}$$

La petite représentation graphique nous permet de déduire facilement les règles de Feynman permettant une construction systématique des diagrammes.

Règles de Feynman.− Les diagrammess sont construits en quatre étapes :

1. À l'ordre $2n$ des perturbations en $\mathcal{V}$, on dessine les $(2n - 1)!!$ diagrammes (pour le désordre gaussien) : une ligne continue représente une fonction de Green libre $G_0(k)$, une ligne pointillée une double interaction avec un défaut.

2. On associe des impulsions de façon à respecter la conservation de l'impulsion à chaque vertex.

---

[24] Si nous avions choisi un modèle plus général de désordre, le cumulant d'ordre p serait associé à p interactions avec un défaut. Pour clarifier cette remarque, considérons le modèle de potentiel désordonné $\mathcal{V}(r) = v_0 \sum_i \delta(r - r_i)$ où les positions sont distribuées selon la loi de Poisson (positions décorrélées pour une densité moyenne n_i). Le calcul du second moment $\overline{\mathcal{V}(r)\mathcal{V}(r')} = v_0^2 \sum_{i \neq j} \overline{\delta(r - r_i)\delta(r' - r_j)} + v_0^2 \delta(r - r') \sum_i \overline{\delta(r - r_i)} = (n_i v_0)^2 + n_i v_0^2 \delta(r - r')$ montre que le second cumulant s'interprète comme une double interaction avec une même impureté. Le cumulant $\overline{\mathcal{V}(r_1) \cdots \mathcal{V}(r_n)}^C = n_i v_0^n \delta(r_1 - r_2) \cdots \delta(r_1 - r_n)$ correspond à n interactions avec une impureté, ce que nous représentons comme :
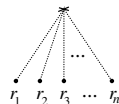
3. Chaque double interaction est associée à un poids $\dfrac{w}{\text{Vol}}$.

4. On somme sur toutes les impulsions libres selon $\sum\limits_{q}$.

Nous dessinons les trois diagrammes obtenus à l'ordre suivant :

$$\overline{\delta^4 G}(k) = \quad + \quad + \quad \tag{IV.36}$$

3) Diagrammes irréductibles et self énergie

Nous pouvons remarquer que le premier des diagrammes de (IV.36) correspond à une répétition du bloc de la première correction (IV.35), que nous notons :

$$\Sigma_2 = \quad = \frac{w}{\text{Vol}} \sum_q G_0(q) \tag{IV.37}$$

à chaque ordre, certaines des corrections contiendront également ce bloc et un des $(2n-1)!!$ termes sera n répétitions de ce bloc. Il y a un moyen très simple de resommer tous ces termes (c'est une série géométrique) :

$$\frac{1}{G_0(k)^{-1} - \Sigma_2} = \quad + \quad + \quad + \quad + \cdots \tag{IV.38}$$

Nous pouvons donc regrouper dans un objet que nous appelons la *self énergie* et notons $\Sigma(E)$, tous les blocs insécables par un seul "coup de ciseau" dans une ligne de fonction de Green (les diagrammes dit *irréductibles*). Outre que cette remarque permet de resommer une infinité de diagrammes sans effort, l'intérêt d'introduire cet objet est de conduire à une fonction de Green moyenne présentant une structure similaire à la fonction de Green libre :

$$\overline{G}(k) = \frac{1}{G_0(k)^{-1} - \Sigma(E)} = \frac{1}{E - \varepsilon_k - \Sigma(E)} \tag{IV.39}$$

pour le modèle avec potentiel nous corrélé spatialement, $\overline{\mathcal{V}(r)\mathcal{V}(r')} \propto \delta(r - r')$, il est clair que la self énergie est indépendante du vecteur d'onde. Le calcul du terme d'ordre n de $\Sigma(E)$ met en jeu bien moins de diagrammes que celui de $G(E)$. Considérer le développement perturbatif de $\Sigma(E)$ est une manière de prendre en compte des corrections d'ordre n de $G(E)$ se déduisant de manière évidente des ordres $n' < n$. Par exemple, à l'ordre w^2, Σ_4 sera donné par le diagramme de Σ_2 plus deux diagrammes d'ordre w^2 correspondant aux deux derniers termes de (IV.36) :

$$\Sigma_4 = \quad + \quad + \quad \tag{IV.40}$$

✍ ***Exercice IV.3*** : *Dessiner tous les diagrammes de Σ_6 (la self-énergie à l'ordre w^3). Comparer avec* $\overline{\delta^2 G}(k) + \overline{\delta^4 G}(k) + \overline{\delta^6 G}(k)$.

Dyson equation : The resummation of diagrams through the introduction of the self energy is particularly simple here because it is formulated in the basis that diagonalises the free Hamiltonian. In the more general case one should write a Dyson equation,

$$\boxed{\overline{G}(E) = G_0(E) + G_0(E)\Sigma(E)\overline{G}(E)} \tag{IV.41}$$

which takes the form of an integral equation in real space. For the model considered here, $\overline{\mathcal{V}(r)\mathcal{V}(r')} = w\,\delta(r-r')$, it takes a simpler form in momentum space $\overline{G}(k;E) = G_0(k;E) + G_0(k;E)\Sigma(E)\overline{G}(k;E)$.

   The Dyson equation allows for a reorganisation of the perturbation series for the averaged Green function. Instead of the series $\overline{G} = G_0 + G_0\overline{\mathcal{V}G_0\mathcal{V}}G_0 + \cdots$ in powers of w, we have now a perturbation series in terms of the numbers of irreducible diagrams :

$$\overline{G} = G_0 + \underbrace{G_0\,\Sigma\,G_0}_{\text{irreducible diag.}} + \overbrace{G_0\,\Sigma\,G_0\,\Sigma\,G_0}^{\text{reducible diag. made of 2 irred. diag.}} + \cdots$$

✎ **Exercice IV.4 :** *Let us consider the general case of a disordered potential with a **finite correlation length** :* $\overline{\mathcal{V}(r)\mathcal{V}(r')} = C(r-r')$ *where* $C(r)$ *decays on a microscopic scale* ℓ_{corr}. *If we introduce the Fourier transform* $\widetilde{C}(Q) = \int \mathrm{d}r\,C(r)\,\mathrm{e}^{-\mathrm{i}Q\cdot r}$, *show that the self energy now depends on the momentum as*

$$\Sigma_2(k;E) = \text{[diagram]} = \frac{w}{\mathrm{Vol}}\sum_q \widetilde{C}(k-q)\,G_0(q) \tag{IV.42}$$

where the argument of the correlation function is the transfered momentum $Q = k - q$.

   Les deux échelles du problème sont l'énergie de Fermi ε_F (rappelons-nous que la conductivité longitudinale fait intervenir les fonctions de Green à $E \simeq \varepsilon_F$) et le désordre w. La self énergie nous permet d'introduire une échelle plus pertinente que w :

$$\boxed{\frac{1}{2\tau_e} \overset{\text{def}}{=} -\operatorname{Im}\Sigma^{\mathrm{R}}(E)} \tag{IV.43}$$

où $\Sigma^{\mathrm{R}}(E)$ est la self énergie calculée avec des fonctions de Green retardées. La fonction de Green moyenne présente donc la structure

$$\boxed{\overline{G}^{\mathrm{R}}(k) = \frac{1}{E - \varepsilon_k + \frac{\mathrm{i}}{2\tau_e}}} \tag{IV.44}$$

La partie imaginaire est la plus importante car elle éloigne le pôle de la fonction de Green de l'axe réel, alors que la partie réelle de la self énergie peut en principe être absorbée dans une redéfinition de l'énergie. [25] La structure de la fonction de Green moyenne met en évidence le

---

[25] Nous jetons un voile pudique sur la partie réelle de la self énergie. A priori celle-ci est une fonction régulière de l'énergie et elle pourrait être éliminée par une reparamétrisation du spectre des énergies. En y regardant de plus près nous constatons que $\operatorname{Re}\Sigma$ diverge en dimension $d > 1$. Ce problème vient de la nature singulière des corrélations du potentiel en δ de Dirac. La même difficulté apparaît dans l'analyse de l'Hamiltonien $-\Delta + v\,\delta(r)$ en dimension $d > 1$. Une manière de donner un sens au problème a été proposée dans l'article [74]. Pour une présentation détaillée du problème : problème 10.3 de mon livre [118].

sens de τ_e, qui s'interprète comme la durée de vie de l'onde plane d'énergie $E \sim \varepsilon_F$, *i.e.* le temps pendant lequel la direction de l'impulsion est conservée (le module de l'impulsion est conservé au cours des processus de collision sur le désordre statique). Il s'agit donc du *temps de parcours moyen élastique*. On peut lui associer le libre parcours moyen élastique $\ell_e = v_F \tau_e$, où v_F est la vitesse de Fermi.

Dans le régime de faible désordre

$$\boxed{\varepsilon_F \tau_e \gg 1 \quad \text{ou} \quad k_F \ell_e \gg 1} \tag{IV.45}$$

l'énergie des électrons est bien supérieure au taux de probabilité pour quitter l'état quantique, i.e. la notion d'état libre (d'onde plane) reste pertinente pour des temps $t \lesssim \tau_e$. Dans ce cas l'approximation de Born $\Sigma(E) = \Sigma_2(E) + O(w^2)$ est justifiée. Fixant dorénavant $E = \varepsilon_F$, nous écrivons :

$$\frac{1}{2\tau_e} \simeq -\operatorname{Im}\Sigma_2^{\mathrm{R}}(\varepsilon_F) = -\frac{w}{\mathrm{Vol}}\sum_q \operatorname{Im}G_0^{\mathrm{R}}(q) = \pi\rho_0 w \quad \Rightarrow \quad \boxed{\frac{1}{\tau_e} = 2\pi\rho_0 w} \tag{IV.46}$$

où $\rho_0 = -\frac{1}{\pi}\operatorname{Im}G_0^{\mathrm{R}}(r,r)$ est la densité d'états au niveau de Fermi par unité de volume par canal de spin.

✍ **Exercice IV.5 :** *Montrer que, dans la limite de faible désordre, la fonction de Green dans l'espace réel présente la structure*

$$\overline{G}^{\mathrm{R}}(r,r') \simeq G_0^{\mathrm{R}}(r,r')\,\mathrm{e}^{-R/2\ell_e} \propto \frac{1}{R^{(d-1)/2}}\mathrm{e}^{\mathrm{i}k_F R - R/2\ell_e} \tag{IV.47}$$

où $R = \|r - r'\|$. (Le calcul est simple en $d = 1$ et $d = 3$; en $d = 2$ il n'est valable que pour $k_F R \gg 1$ et correspond au comportement asymptotique d'une fonction de Bessel).

IV.D La conductivité à l'approximation de Drude

Nous commençons par plusieurs remarques permettant de simplifier (IV.29).

(*i*) Dans la pratique les fréquences correspondant à une situation expérimentale sont toujours telles que $\omega \ll T$ (rappelons que $T = 1\,\mathrm{K}$ correspond à une énergie $86\,\mu\mathrm{eV}$ et à une fréquence $20.8\,\mathrm{GHz}$). Nous procédons à la substitution $\frac{f(\varepsilon) - f(\varepsilon + \omega)}{\omega} \to -\frac{\partial f}{\partial \varepsilon}$.

(*ii*) D'autre part l'élargissement thermique ne joue aucun rôle dans la calcul de la conductivité moyenne (ceci ne serait pas vrai si nous étudiions les fluctuations de la conductivité). Nous fixons $T = 0$.

(*iii*) Dans le produit $\Delta G\Delta G = (G^{\mathrm{R}} - G^{\mathrm{A}})(G^{\mathrm{R}} - G^{\mathrm{A}})$, on peut montrer que seuls les termes $G^{\mathrm{R}}G^{\mathrm{A}}$ et $G^{\mathrm{A}}G^{\mathrm{R}}$ apportent des contributions importantes, après moyenne. Finalement, notre point de départ est [26] :

$$\overline{\widetilde{\sigma}(\omega)} = \frac{2_s e^2}{2\pi m^2}\frac{1}{\mathrm{Vol}}\sum_{k,\,k'} k_x\,k'_x\,\overline{G^{\mathrm{R}}(k,k';\varepsilon_F + \omega)\,G^{\mathrm{A}}(k',k;\varepsilon_F)} \tag{IV.48}$$

La conductivité est donnée par un produit de fonctions de Green. La première chose la plus simple à faire consiste à négliger les corrélations entre les deux fonctions de Green : $\overline{G^{\mathrm{R}}G^{\mathrm{A}}} \simeq$

---

[26] Notons que ces trois hypothèses conduisent à $\overline{\operatorname{Re}\widetilde{\sigma}(\omega)} \propto \sum_{k,k'} k_x\,k'_x\,\operatorname{Re}[G^{\mathrm{R}}(k,k';\varepsilon_F + \omega)\,G^{\mathrm{A}}(k',k;\varepsilon_F)]$, ce qui est un petit peu plus faible que (IV.48), sauf dans le cas $\omega = 0$.
Dans la suite du chapitre, on pourra considérer que $\sigma \sim G^{\mathrm{R}}\,G^{\mathrm{A}}$ et oublier les termes $G^{\mathrm{R}}\,G^{\mathrm{R}}$ et $G^{\mathrm{A}}\,G^{\mathrm{A}}$. Notons toutefois que ceci n'est plus vrai lorsque l'on considère la correction venant des interactions électroniques (correction Altshuler-Aronov).

$\overline{G}^{\mathrm{R}}\overline{G}^{\mathrm{A}}$. En utilisant $\overline{G^{\mathrm{R}}(k,k')} = \delta_{k,k'}\overline{G}^{\mathrm{R}}(k)$, nous obtenons

$$\overline{\widetilde{\sigma}(\omega)}^{\mathrm{Drude}} = \frac{2_s e^2}{2\pi m^2}\frac{1}{\mathrm{Vol}}\sum_k k_x^2\, \overline{G}^{\mathrm{R}}(k;\varepsilon_F+\omega)\, \overline{G}^{\mathrm{A}}(k;\varepsilon_F) \tag{IV.49}$$

Le calcul de ce type de quantité est tout à fait standard et des expressions similaires apparaîtront par la suite. Nous remplaçons k_x^2 par k^2/d (isotropie de la relation de dispersion) puis k^2 par k_F^2 pour le sortir de la somme (ce qu'on peut justifier plus soigneusement en étudiant le calcul ci-dessous).

Calcul de $\sum_k \overline{G}^{\mathrm{R}}(k)\overline{G}^{\mathrm{A}}(k)$: Nous détaillons le calcul de la quantité

$$\frac{w}{\mathrm{Vol}}\sum_k \overline{G}^{\mathrm{R}}(k;\varepsilon_F+\omega)\, \overline{G}^{\mathrm{A}}(k;\varepsilon_F)\,. \tag{IV.50}$$

Le principe du calcul et les approximations s'appliqueront à d'autres quantités similaires.

Dans la limite de faible désordre $\varepsilon_F\tau_e \gg 1$, la somme est dominée par les énergies voisines de ε_F (rappelons que $\omega \ll \varepsilon_F$). Cette observation autorise deux approximations :

(i) On néglige la dépendance (lente) de la densité d'états en énergie $\frac{1}{\mathrm{Vol}}\sum_k = \int \frac{\mathrm{d}^d k}{(2\pi)^d} = \int_0^\infty \mathrm{d}\varepsilon_k\, \rho(\varepsilon_k) \longrightarrow \rho_0 \int_0^\infty \mathrm{d}\varepsilon_k$ où ρ_0 désigne la densité d'états au niveau de Fermi $\rho_0 = \rho(\varepsilon_F)$.
(ii) On étend l'intégrale sur l'énergie à tout $\mathbb{R}$, ce qui permet une utilisation directe du théorème des résidus.

On a donc

$$\frac{w}{\mathrm{Vol}}\sum_k \overline{G}^{\mathrm{R}}(k;\varepsilon_F+\omega)\, \overline{G}^{\mathrm{A}}(k;\varepsilon_F) \simeq w\rho_0 \int_{\mathbb{R}} \frac{\mathrm{d}\varepsilon_k}{\left(\varepsilon_F+\omega-\varepsilon_k+\frac{\mathrm{i}}{2\tau_e}\right)\left(\varepsilon_F-\varepsilon_k-\frac{\mathrm{i}}{2\tau_e}\right)}\,. \tag{IV.51}$$

On referme le contour d'intégration soit par le haut soit par le bas pour utiliser le théorème des résidus. On obtient :

$$w\rho_0\, \frac{2\mathrm{i}\pi}{\omega+\mathrm{i}/\tau_e}$$

i.e.

$$\frac{w}{\mathrm{Vol}}\sum_k \overline{G}^{\mathrm{R}}(k;\varepsilon_F+\omega)\, \overline{G}^{\mathrm{A}}(k;\varepsilon_F) = \frac{1}{1-\mathrm{i}\omega\tau_e} \tag{IV.52}$$

Remark on $\sum_k \varepsilon_k \overline{G}^{\mathrm{R}}(k)\overline{G}^{\mathrm{A}}(k)$: one might worry with the fact that the introduction of k^2 make the integral divergent. Indeed, a naive power counting gives

$$\frac{1}{\mathrm{Vol}}\sum_k \varepsilon_k \overline{G}^{\mathrm{R}}(k)\, \overline{G}^{\mathrm{A}}(k) \sim \int^\infty \mathrm{d}k\, k^{d-1}\, \frac{k^2}{k^4} = \infty \quad \text{for } d\geqslant 2\,! \tag{IV.53}$$

A more careful treatment is as follow (let us discuss the case $d=2$ with constant DoS for simplicity)

$$\frac{w}{\mathrm{Vol}}\sum_k \varepsilon_k \overline{G}^{\mathrm{R}}(k;\varepsilon_F+\omega)\, \overline{G}^{\mathrm{A}}(k;\varepsilon_F) = w\rho_0 \int_0^\Lambda \mathrm{d}\varepsilon\, \frac{\varepsilon}{(\varepsilon-\varepsilon_\omega)(\varepsilon-\varepsilon_0^*)} \tag{IV.54}$$

where $\varepsilon_\omega \overset{\text{def}}{=} \varepsilon_F+\omega+\mathrm{i}/(2\tau)$. I have introduced an upper cutoff Λ (remember that in a solid, there is always the natural cutoff provided by the lattice, $\Lambda \sim \hbar^2/(ma^2)$). Some simple algebra

gives

$$\frac{w\rho_0}{\varepsilon_\omega - \varepsilon_0^*} \int_0^\Lambda \mathrm{d}\varepsilon \left[\frac{\varepsilon}{\varepsilon - \varepsilon_\omega} - \frac{\varepsilon}{\varepsilon - \varepsilon_0^*} \right] = \frac{w\rho_0}{\varepsilon_\omega - \varepsilon_0^*} \int_0^\Lambda \mathrm{d}\varepsilon \left[\frac{\varepsilon_\omega}{\varepsilon - \varepsilon_\omega} - \frac{\varepsilon_0^*}{\varepsilon - \varepsilon_0^*} \right] \qquad \text{(IV.55)}$$

$$= \frac{w\rho_0}{\varepsilon_\omega - \varepsilon_0^*} \left(\varepsilon_\omega \left[\ln(\Lambda - \varepsilon_\omega) - \ln(-\varepsilon_\omega) \right] - \varepsilon_0^* \left[\ln(\Lambda - \varepsilon_0^*) - \ln(-\varepsilon_0^*) \right] \right) \qquad \text{(IV.56)}$$

Now we make use of the fact that $\Lambda \gg$ all other scales and we use that $\ln(\varepsilon_F + \omega) \simeq \ln(\varepsilon_F)$ since $\omega \ll \varepsilon_F$. The dominant contributions $\varepsilon_F \ln \Lambda$ cancel. Be careful with the branch cut of the logarithm. Finally, making use of $2\pi\rho_0 w\tau = 1$, we conclude that

$$\frac{w}{\text{Vol}} \sum_k \varepsilon_k \overline{G}^{\text{R}}(k; \varepsilon_F + \omega) \, \overline{G}^{\text{A}}(k; \varepsilon_F) = \frac{1}{1 - \mathrm{i}\omega\tau} \left[\varepsilon_F + \frac{1}{2}\omega - \frac{\mathrm{i}}{2\pi}(\omega + \mathrm{i}/\tau)\ln(\Lambda/\varepsilon_F) \right] \quad \text{(IV.57)}$$

The first term is the one given by the simple argument of the text ($\varepsilon_k \to \varepsilon_F$ in the integral). The ω should be neglected. The only contribution of the cutoff is the logarithmic term $\sim \frac{1}{\tau}\ln(\Lambda/\varepsilon_F) \ll \varepsilon_F$ in the weak disorder regime, when $\varepsilon_F\tau \ll 1$.

Conclusion : Finalement nous aboutissons à :

$$\overline{\widetilde{\sigma}(\omega)}^{\text{Drude}} = \frac{2_s e^2}{2\pi m^2} \frac{k_F^2}{d} 2\pi\rho_0\tau_e \frac{1}{1 - \mathrm{i}\omega\tau_e} = \frac{2_s e^2 \tau_e}{m} \frac{2\varepsilon_F\rho_0}{d} \frac{1}{1 - \mathrm{i}\omega\tau_e} \qquad \text{(IV.58)}$$

Nous reconnaissons la densité électronique, $n = 2_s \frac{2\varepsilon_F\rho_0}{d}$, et finalement

$$\boxed{\overline{\widetilde{\sigma}(\omega)}^{\text{Drude}} = \frac{\sigma_0}{1 - \mathrm{i}\omega\tau_e}} \quad \text{où} \quad \sigma_0 = \frac{n e^2 \tau_e}{m} \qquad \text{(IV.59)}$$

est la conductivité de Drude résiduelle (à $T \to 0$). Nous avons donc retrouvé le résultat du modèle semi-classique de Drude-Sommerfeld. Alors que la conductivité du système balistique présente une divergence à $\omega \to 0$, $\widetilde{\sigma}(\omega) \propto \mathrm{i}/\omega$, dont l'origine est le mouvement balistique des électrons, [27] les collisions sur les défauts sont responsables d'une conductivité finie à fréquence nulle.

Remarque : le résultat classique est non perturbatif.– Comme nous l'avions déjà noté dans l'introduction, la conductivité de Drude est non perturbative dans le désordre :

$$\sigma_0 \propto \tau_e \propto 1/w . \qquad \text{(IV.60)}$$

Partant d'un résultat divergent à basse fréquence en l'absence de désordre, $\widetilde{\sigma}(\omega) \propto \mathrm{i}/\omega$, il était clair que la coupure de la divergence pour $\omega \to 0$ ne pouvait venir d'un calcul perturbatif. [28]

✍ ***Exercice IV.6*** *: Montrer que la conductivité de Drude peut également se reécrire sous la forme $\sigma_0 = 2_s e^2 \rho_0 D$ (relation d'Einstein) où $D = \ell_e^2/(\tau_e d)$ est la constante de diffusion. On donne $k_F^{-1} = 0.85$ Å(or), quelle est la distance parcourue par un électron balistique en 1 s ? On donne $\ell_e^{\text{(bulk)}} \simeq 4\,\mu m$ et $\ell_e^{\text{(film)}} \simeq 20\,nm$. Calculer D. Quelle est la distance parcourue par un électron diffusif en 1 s ?*

Effet de la température : à $T \neq 0$, le résultat (IV.59) doit être convolué par la dérivée d'une fonction de Fermi $-\partial f/\partial\varepsilon$. Comme le résultat à $T = 0$K dépend faiblement de l'énergie (à travers n et τ_e), la convolution est sans effet. Toutefois la température n'est pas sans effet. En effet, nous venons de montrer que les collisions (élastiques) sur le désordre, induisent une conductivité finie. Si les électrons sont soumis à d'autres processus de collision [29] (électron-phonon,...) la self

---

[27] elle correspond à un comportement de la réponse impulsionnelle $\sigma(t) \propto \theta(t)$, traduisant l'apparition d'un courant constant (i.e. la conservation de l'impulsion des électrons) suite à une impulsion de champ électrique.

[28] Le calcul perturbatif pourrait néanmoins être mené à ω finie (c'est ce qui est fait dans [103]).

[29] autres que électron-électron qui conserve le courant total,

énergie de la fonction de Green reçoit les contributions des différentes perturbations : désordre, interaction électron-phonon, etc. Cela correspond à ajouter les *taux* de relaxation selon la loi de Matthiesen

$$\frac{1}{\tau(T)} = \frac{1}{\tau_e} + \frac{1}{\tau_{\text{e}-\text{ph}}(T)} + \cdots \tag{IV.61}$$

Le calcul de la conductivité conduit à $\sigma_{\text{Drude}} = \frac{ne^2\tau}{m}$.

Temps de vie et temps de transport.– Nous devons ici apporter une petite précision sur la nature du temps de relaxation intervenant dans la conductivité. Nous avons introduit le temps de vie des états électroniques comme : $1/\tau = -2\operatorname{Im}\Sigma^{\text{R}} = 2\pi\rho_0\langle C(\theta)\rangle_\theta$, où $C(\theta) \overset{\text{def}}{=} \int \mathrm{d}r\, e^{-i(k'-k)r}\overline{\mathcal{V}(r)\mathcal{V}(0)}$ où θ est l'angle entre les deux vecteurs k et k' sur la surface de Fermi, $||k|| = ||k'|| = k_F$ (à l'approximation de Born, $C(\theta)$ est proportionnelle à la section efficace de diffusion dans la direction θ). Le temps qui intervient dans la conductivité n'est en général pas ce temps mais le temps de relaxation de la vitesse [103, 2, 3] : $\sigma = \frac{ne^2\tau_{\text{tr}}}{m}$ (ceci est lié à la présence de $k_x k'_x$ dans les relations (IV.29,IV.48)) ; ce temps est appelé *temps de transport* $1/\tau_{\text{tr}} = 2\pi\rho_0\langle C(\theta)(1-\cos\theta)\rangle_\theta$. Dans le cas de la diffusion isotrope, $C(\theta) = w$ n'a pas de structure et les deux temps coïncident. Dans le cas de diffusion anisotrope (lorsque la fonction de corrélation de $\mathcal{V}$ présente une structure), les deux temps peuvent toutefois différer notablement $\tau_{\text{tr}} > \tau$. Cette discussion s'applique au cas de la diffusion électron-phonon (chap. 26 de [17]) : le temps de collision électron-phonon est $\tau_{\text{e}-\text{ph}} \propto T^{-3}$ mais la diffusion est fortement anisotrope à basse température ($\ll \omega_D$, la coupure de Debye) et le temps de transport correspondant est $\tau_{\text{e}-\text{ph, tr}} \propto T^{-5}$ ce qui conduit à la résistivité $\rho(T) = 1/\sigma(T) \simeq 1/\sigma_0 + C\,T^5$ pour $T \ll \omega_D$ (loi de Bloch-Grüneisen).

Drude conductance.– We can relate the Drude conductivity to the conductance $G = \sigma_0 s/L$ where s is the cross section of the wire and L its length. It will be useful to introduce the dimensionless conductance g defined by

$$G = \frac{2_s e^2}{h}\, g\,. \tag{IV.62}$$

We first consider the 1D case (long narrow wire) :

$$g_{\text{Drude}} = \frac{h}{2_s e^2}\frac{\sigma_0 s}{L} \sim \underbrace{\frac{\hbar k_F}{m}\tau_e}_{=\ell_e}\frac{k_F^{d-1}s}{L} \tag{IV.63}$$

where we have used $n \sim k_F^d$ where d is the real dimensionality of the system. We recognize $N_c \sim k_F^{d-1}s$, the number of conducting channels (i.e. number of open transverse modes of the wire with energy smaller than ε_F). Finally the dimensionless conductance can be written as the ratio of two lengths

$$g_{\text{Drude}} \sim \frac{N_c \ell_e}{L} \qquad \text{(quasi 1D)} \tag{IV.64}$$

The length at the numerator $\xi_{\text{loc}} \sim N_c \ell_e$ is the localisation length in weakly disordered wire [20]. So the validity of the treatment is $L \ll \xi_{\text{loc}}$ i.e.

$$\boxed{g_{\text{Drude}} \gg 1} \tag{IV.65}$$

The 2D case (plane in a 2DEG or thin metallic film) can be analysed by setting $s = bL$ in the previous expressions where b is the thickness (set $b = 1$ for the plane, in $d = 2$). We get

$$g_{\text{Drude}} \sim k_F \ell_e\, k_F^{d-2}b \qquad \text{(2D)} \tag{IV.66}$$

In $d = 2$ (in a DEG) the Drude dimensionless conductance is simply proportional to the large parameter $k_F \ell_e$: $g_{\text{Drude}}^{\text{plane}} \sim k_F \ell_e$.

IV.E   Corrélations entre fonctions de Green

Nous avons retrouvé le résultat semi-classique en négligeant les corrélations entre les fonctions de Green dans l'équation (IV.48), i.e. en écrivant $\overline{G^R G^A} \simeq \overline{G}^R \overline{G}^A$. Nous souhaitons maintenant étudier l'effet des corrélations entre fonctions de Green sur la conductivité moyenne. Il convient d'identifier quel type de corrections est dominant. À cette fin nous commençons par donner la représentation diagrammatique de (IV.48), que nous dessinons comme une bulle (figure 26) constituée par les deux fonctions de Green. Les lignes ondulées représentent les éléments de matrice de l'opérateur courant moyen, ek_x/m et ek'_x/m, et nous rappellent que la conductivité est une fonction de corrélation courant-courant.
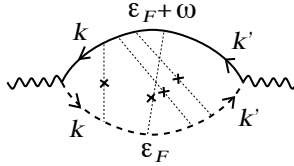
Figure 26: *Représentation diagrammatique d'une correction perturbative pour la conductivité moyenne donnée par l'équation (IV.48). Les lignes continues (tirés) représentent des fonctions de Green retardées $\overline{G}^R$ (avancées $\overline{G}^A$). Les lignes ondulées représentent l'opérateur de courant (ek_x/m et ek'_x/m). Les lignes pointillées reliant les lignes retardées et avancées correspondent à corréler les fonctions de Green G^R et G^A dans l'équation (IV.48).*

Dans le cas du terme de Drude les lignes de fonctions de Green sont les fonctions de Green moyennes $\overline{G}^R$ et $\overline{G}^A$. Les corrélations entre fonctions de Green sont représentées par des diagrammes dans lesquels les lignes de fonctions de Green retardée et avancée sont couplées par des lignes d'impureté (figure 26).

⚠ **Légère modification des règles de Feynman pour la conductivité** ⚠**.–** Dans les diagrammes, les lignes de fonctions de Green seront désormais des fonctions de Green *moyennes*, $\overline{G}^R$ et $\overline{G}^A$ (au lieu des fonctions de Green libres), ce qui est une manière de resommer une partie des diagrammes ne couplant pas les fonctions retardées et avancées.

Transport classique et localisation faible : présentation heuristique

Nous avons déjà noté au cours du calcul de la conductivité à l'approximation de Drude que les résultats intéressants sont *non perturbatifs* et correspondent à resommer certaines classes de diagrammes décrivant la physique de la diffusion. La question est donc d'identifier les classes de diagrammes qui apportent les corrections dominantes. Pour cela nous faisons une petite digression et donnons une image plus qualitative de l'étude du transport dans un métal diffusif. Lorsqu'on étudie la conductance d'un système relié à deux contacts, on peut montrer que la conductance est reliée à la probabilité de traverser le système. Cette probabilité s'exprime comme le module carré d'une somme d'amplitudes de probabilité :

$$G = \frac{2_s e^2}{h} g \sim \frac{2_s e^2}{h} \Big| \sum_{\mathcal{C}} \mathcal{A}_{\mathcal{C}} \Big|^2 \tag{IV.67}$$

où la somme porte sur tous les chemins $\mathcal{C}$ allant d'un contact à l'autre, pour un électron d'énergie ε_F. La conductance adimensionnée est notée g. Cette formulation des propriétés de transport

peut être rendue rigoureuse, c'est l'approche de Landauer-Büttiker. La relation avec la formule de Kubo se comprend en remarquant que l'amplitude $\mathcal{A}_\mathcal{C}$ est associée à la fonction de Green retardée, et l'amplitude conjuguée $\mathcal{A}_\mathcal{C}^*$ à la fonction de Green avancée (formule de Fisher & Lee $G^{\mathrm{R}}(\text{contact } 1 \leftarrow \text{contact } 2; \varepsilon_F) \sim \sum_\mathcal{C} \mathcal{A}_\mathcal{C}$) : cette expression de la conductance possède la structure $g \sim |G^{\mathrm{R}}(\text{contact } 1 \leftarrow \text{contact } 2; \varepsilon_F)|^2 \sim G^{\mathrm{R}} G^{\mathrm{A}}$.

Dans le cas d'un métal faiblement désordonné ($k_F \ell_e \gg 1$), la somme porte sur les chemins de collisions sur les impuretés. La phase d'une amplitude associée à un de ces chemins de collision est proportionnelle à la longueur $\ell_\mathcal{C}$ du chemin de diffusion : $\mathcal{A}_\mathcal{C} \propto \mathrm{e}^{\mathrm{i} k_F \ell_\mathcal{C}}$.

La conductance moyenne est donnée en moyennant l'expression :

$$\overline{g} \sim \underbrace{\overline{\sum_\mathcal{C} |\mathcal{A}_\mathcal{C}|^2}}_{\text{classique}} + \underbrace{\overline{\sum_{\mathcal{C} \neq \mathcal{C}'} \mathcal{A}_\mathcal{C} \mathcal{A}_{\mathcal{C}'}^*}}_{\text{quantique}} \tag{IV.68}$$

Le premier terme, la somme des probabilités, doit correspondre au terme classique (Drude). C'est le terme dominant car donné par une somme de termes positifs. En revanche le terme d'interférences (quantique) est une somme de termes portant des phases $\mathcal{A}_\mathcal{C} \mathcal{A}_{\mathcal{C}'}^* \propto \mathrm{e}^{\mathrm{i} k_F (\ell_\mathcal{C} - \ell_{\mathcal{C}'})}$. On comprend que ce type de contributions a d'autant plus de mal à survivre à la moyenne sur le désordre que la différence $\ell_\mathcal{C} - \ell_{\mathcal{C}'}$ est grande (le terme classique $|\mathcal{A}_\mathcal{C}|^2$ domine car les deux chemins correspondent à la même séquence de collisions (figure 27)). Une façon de minimiser la différence des longueurs est de considérer une séquence de collisions identiques au milieu de laquelle on introduit un **croisement**. [30] Cette construction fait apparaître une boucle à l'intérieur de laquelle une des trajectoires est renversée (figure 27). Ce terme décrit l'interférence entre deux trajectoires diffusives renversées : dans la boucle, les deux trajectoires subissent les collisions dans l'ordre inverse, ce qui correspond aux *diagrammes maximallement croisés* (figure 28) que nous analyserons. À cause du croisement les phases des deux amplitudes diffèrent légèrement et cette contribution est petite (une bonne introduction est donnée au chapitre 1 de [2, 3]).
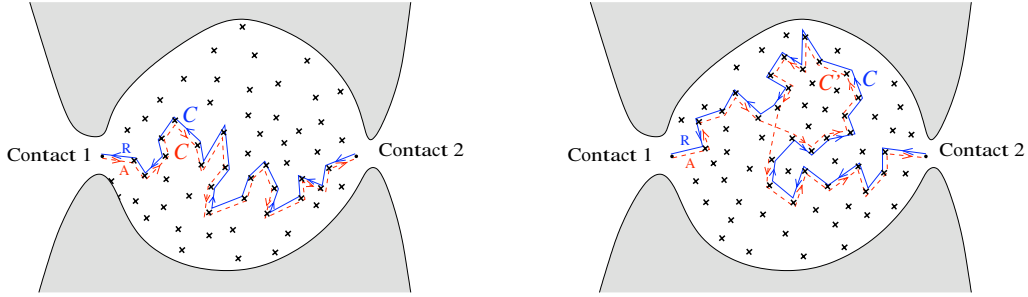

Figure 27: À gauche : *contribution au terme classique* $\sum_\mathcal{C} |\mathcal{A}_\mathcal{C}|^2$. À droite : *contribution au terme quantique* $\sum_{\mathcal{C} \neq \mathcal{C}'} \mathcal{A}_\mathcal{C} \mathcal{A}_{\mathcal{C}'}^*$ *qui minimise* $\ell_\mathcal{C} - \ell_{\mathcal{C}'}$. *La boucle décrit l'interférence quantique de trajectoires renversées.*
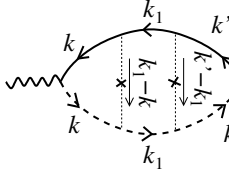
IV.F   Diagrammes en échelle – Diffuson (contribution non cohérente)

Nous venons de montrer par des arguments heuristiques que les séquences de collisions identiques jouent un rôle important. Si nous traduisons les diagrammes de la figure 27 pour des conductivité, le diagramme de gauche prend la forme des diagrammes en échelle ("ladder diagrams") :

$$\overline{\sigma(\omega)}^{\text{Diffuson}} = \text{} + \ldots \tag{IV.69}$$

---

[30] Rigoureusement, le croisement devrait être décrit par une *"boîte de Hikami"*.
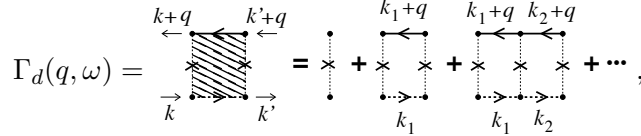
Chaque contribution peut être analysée facilement à l'aide des règles de Feynman énoncées plus haut. À ce stade il est instructif d'analyser précisément le second diagramme :

$$\sim \sum_{k,\,k'} k_x k'_x \overline{G}^{\mathrm{R}}(k)\,\overline{G}^{\mathrm{A}}(k)\,\frac{w}{\mathrm{Vol}}\underbrace{\sum_{k_1}\overline{G}^{\mathrm{R}}(k_1)\,\overline{G}^{\mathrm{A}}(k_1)}_{\Lambda(0,\omega)}\,\frac{w}{\mathrm{Vol}}\overline{G}^{\mathrm{R}}(k')\,\overline{G}^{\mathrm{A}}(k')$$

où les fonctions retardées sont prises à énergie $\varepsilon_F + \omega$ et les avancées à ε_F.

La série de diagrammes en échelles, i.e. le milieu de la bulle de conductivité (IV.69)

$$\Gamma_d(q,\omega) = \quad \text{(IV.70)}$$

est appelé le **Diffuson**. Une impulsion supplémentaire q a été introduite dans les fonctions de Green retardées, ce qui sera utile pour la suite. Il est facile de voir que Γ_d obéit à l'**équation de Bethe-Salpether**

$$\Gamma_d(q,\omega) = \frac{w}{\mathrm{Vol}} + \Lambda(q,\omega)\,\Gamma_d(q,\omega)\,, \qquad \text{(IV.71)}$$

où $\Lambda(q,\omega)$ est le bloc élémentaire

$$\Lambda(q,\omega) \overset{\mathrm{def}}{=} \frac{w}{\mathrm{Vol}}\sum_k \overline{G}^{\mathrm{R}}(k+q;\varepsilon_F+\omega)\,\overline{G}^{\mathrm{A}}(k;\varepsilon_F) = \qquad \text{(IV.72)}$$

Autrement dit, Γ_d correspond à une série géométrique que nous resommons :

$$\Gamma_d(q,\omega) = \frac{w}{\mathrm{Vol}}\,\frac{1}{1-\Lambda(q,\omega)} \qquad \text{(IV.73)}$$

✍ *Exercice IV.7 Calcul de* $\Lambda(q,\omega)$ *:* *Nous calculons* $\Lambda(q,\omega)$ *dans la limite* $q\to 0$ *et* $\omega\to 0$. *Vérifier que* $\overline{G}^{\mathrm{R}}(k+q;\varepsilon_F+\omega) = \overline{G}^{\mathrm{R}}(k) + (v_k\cdot q - \omega)[\overline{G}^{\mathrm{R}}(k)]^2 + (v_k\cdot q)^2[\overline{G}^{\mathrm{R}}(k)]^3 + \cdots$ *où toutes les fonctions de Green du membre de droite sont prises à énergie de Fermi ;* $v_k = k/m$ *(on admettra que le terme* $\varepsilon_q[\overline{G}^{\mathrm{R}}(k)]^2$ *d'ordre* q^2 *peut être négligé, ainsi que le terme* ω^2*). Comme nous l'avons signalé, les quantités* $\frac{w}{\mathrm{Vol}}\sum_k[\overline{G}^{\mathrm{R}}(k)]^n\,[\overline{G}^{\mathrm{A}}(k)]^m$ *se calculent aisément en faisant* $\frac{1}{\mathrm{Vol}}\sum_k \to \rho_0\int_{\mathbb{R}}\mathrm{d}\varepsilon_k$ *puis en utilisant le théorème des résidus.* [31] *En déduire que*

$$\Lambda(q,\omega) = 1 + \mathrm{i}\omega\tau_e - q^2\ell_e^2/d + \cdots \qquad \text{(IV.75)}$$

Ce résultat sera utilisé à plusieurs reprises.

Validité *de l'approximation :* $\boxed{\omega\tau_e \ll 1 \text{ et } q\ell_e \ll 1}$

---

[31] **Hikami boxes :** the diagram contains little "boxes" of short range nature with several Green's functions. They can be computed by using the following useful integrals

$$f_{n,m} \overset{\mathrm{def}}{=} \frac{w}{\mathrm{Vol}}\sum_k[\overline{G}^{\mathrm{R}}(k)]^n\,[\overline{G}^{\mathrm{A}}(k)]^m = \mathrm{i}^{-n+m}\,\frac{(n+m-2)!}{(n-1)!(m-1)!}\,\tau_e^{n+m-2}\,. \qquad \text{(IV.74)}$$

Approximation de la diffusIon – Pôle de diffusion.– D'après (IV.75), nous voyons que, dans la limite $\omega\tau_e \ll 1$ et $q\ell_e \ll 1$, le Diffuson coïncide avec la fonction de Green de l'équation de diffusion :

$$\Gamma_d(q,\omega) \simeq \frac{w}{\text{Vol}} \frac{1/\tau_e}{-\mathrm{i}\omega + Dq^2} \stackrel{\text{def}}{=} \frac{w}{\text{Vol}} \frac{1}{D\tau_e} \widetilde{P}_d(q,\omega) \tag{IV.76}$$

Nous comprenons qu'il n'est pas possible de tronquer la série perturbative (IV.70) à un ordre donné car la limite $q \to 0$ et $\omega \to 0$ nous conduit *au bord du domaine de convergence de la série* géométrique $\Gamma_d = \frac{w}{\text{Vol}} \sum_{n=0}^{\infty} \Lambda^n$.

Nous sommes en mesure de calculer la contribution des diagramnes en échelle à la conductivité

$$\overline{\sigma(\omega)}^{\text{Diffuson}} = \frac{2_s e^2}{2\pi m^2} \frac{1}{\text{Vol}} \sum_{k,k'} k_x\, k'_x\, |\overline{G}^{\mathrm{R}}(k)|^2\, \Gamma_d(0,\omega)\, |\overline{G}^{\mathrm{R}}(k')|^2 \tag{IV.77}$$

L'isotropie de la relation de dispersion conduit à $\frac{1}{\text{Vol}} \sum_k k_x\, |\overline{G}^{\mathrm{R}}(k)|^2 = 0$ et donc

$$\overline{\sigma(\omega)}^{\text{Diffuson}} = 0 \tag{IV.78}$$

Ce résultat s'interprète facilement : rappelons-nous que la conductivité est reliée à constante de diffusion, *i.e.* à la fonction de corrélation de la vitesse $\sigma \sim D = \int_0^{\infty} \mathrm{d}t\, \langle v_x(t)\, v_x \rangle$ (ce que nous rappelle la présence de $k_x k'_x$ dans (IV.48)). Le Diffuson (IV.70) décrit une séquence de collisions arbitrairement grande, après laquelle la mémoire de la direction initiale de la vitesse est perdue. [32]

Remarque : pôle de diffusion et conservation du courant.– Le comportement de Γ_d est la signature de la nature diffusive des trajectoires électroniques dans le métal (on pourrait s'en convaincre en calculant la fonction de réponse densité-densité du métal qui est reliée au Diffuson $\chi_0(q,\omega) \simeq -\rho_0 \frac{Dq^2}{-\mathrm{i}\omega + Dq^2}$ [6] ; cette remarque permet de relier le pôle de diffusion à la conservation du nombre de particules [134]).

✍ *Exercice IV.8 Conductivité non locale : Nous discutons l'importance de l'ordre des limites $\lim_{q \to 0}$ et $\lim_{\omega \to 0}$. Si le système est soumis à un champ inhomogène, la réponse sera caractérisée par une conductivité non locale $j_a(r,t) = \int \mathrm{d}t' \int \mathrm{d}r'\, \sigma_{ab}(r,t;r',t')\, \mathcal{E}_b(r',t')$. Nous considérons sa transformée de Fourier $\sigma(q,\omega)$. On admet que la conductivité moyenne à $q \neq 0$ est donnée par : $\overline{\sigma_{xx}(q,\omega)} = \frac{2_s e^2}{2\pi m^2} \frac{1}{\text{Vol}} \sum_{k,k'} k_x\, k'_x\, \overline{G^{\mathrm{R}}(k+q, k'+q; \varepsilon_F + \omega)\, G^{\mathrm{A}}(k',k;\varepsilon_F)}$. Montrer que la contribution des diagrammes en échelle (le Diffuson) est $\overline{\sigma_{xx}(q,0)}^{\text{Diffuson}} = -\sigma_0 \frac{q_x^2}{q^2}$ (qui diffère donc de $\overline{\sigma_{xx}(0,\omega)}^{\text{Diffuson}} = 0$).*
Indication : En utilisant les mêmes approximations que dans l'exercice IV.7, montrer que
$\frac{w}{\text{Vol}} \sum_k k_x \overline{G}^{\mathrm{R}}(k+q)\overline{G}^{\mathrm{A}}(k) \simeq -\mathrm{i}\frac{k_F \ell_e}{d} q_x$.

IV.G   Quantum (coherent) correction : weak localisation

The discussion of the introduction, § IV.A, has underlined the importance of interferences between *time reversed* diffusive electronic trajectories. Starting from the Landauer picture of quantum transport, we have reformulated more precisely this idea in § IV.E. This discussion has emphasized the role of maximally crossed diagrams : [33] interference of reversed diffusive trajectories corresponds to follow the same sequence of scattering events in reversed order (figure 28)

After twisting the diagram of the left part of Fig. 28, the structure of the central bloc is very similar to the one involved in the Diffuson (right part of Fig. 28), up to a change in the relative

---

[32] Notons que dans le cas où la diffusion est anisotrope, la contribution du Diffuson est non nulle. Elle fait
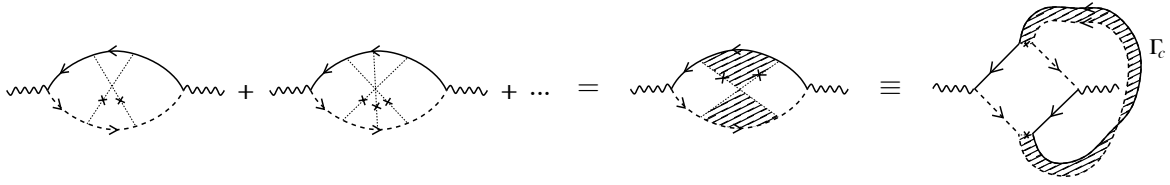
Figure 28: **Contribution of maximally crossed diagrams (Cooperon)** $\overline{\sigma(\omega)}^{\text{Cooperon}}$.

directions of the two Green's function lines. It is useful to study carefully the structure of the first diagram :

$$\sim \sum_{k,\,k'} k_x k'_x \overline{G}^{\text{R}}(k)\,\overline{G}^{\text{A}}(k)\,\frac{w}{\text{Vol}} \underbrace{\sum_{k_1} \overline{G}^{\text{R}}(k_1+k+k')\,\overline{G}^{\text{A}}(-k_1)}_{\Lambda(k+k',\omega)}\,\frac{w}{\text{Vol}}\overline{G}^{\text{R}}(k')\,\overline{G}^{\text{A}}(k')$$

where retarded and advanced lines carry energies $\varepsilon_F + \omega$ and ε_F, respectively. This analysis makes clear that the series of maximally crossed diagrams is also a geometric series involving the quantity $\Lambda(k+k',\omega)$ computed above :

$$\Gamma_c(Q = k+k',\omega) = \quad \text{(IV.79)}$$

(the single impurity line was already included in the Diffuson). As a consequence, the calculation is similar, and the resummation of the ladder diagrams is obtained by replacing the wave vector q in the Diffuson (IV.70) by $k+k'$. This new object is named the **Cooperon**. As for the Diffuson, the Cooperon presents a **diffusion pole** when $Q = k+k' \to 0$:

$$\Gamma_c(Q,\omega) = \frac{w}{\text{Vol}}\frac{\Lambda(Q,\omega)}{1-\Lambda(Q,\omega)} \stackrel{\text{def}}{=} \frac{w}{\text{Vol}}\frac{1}{D\tau_e}\,\widetilde{P}_c(Q,\omega) \simeq \frac{w}{\text{Vol}}\frac{1/\tau_e}{-\mathrm{i}\omega + DQ^2}\,. \quad \text{(IV.80)}$$

Introducing the Cooperon in (IV.48) we obtain the structure

$$\overline{\sigma(\omega)}^{\text{Cooperon}} = \frac{2_s e^2}{2\pi m^2}\frac{1}{\text{Vol}}\sum_{k,\,k'} k_x\,k'_x\,|\overline{G}^{\text{R}}(k)|^2\,\Gamma_c(k+k',\omega)\,|\overline{G}^{\text{R}}(k')|^2\,. \quad \text{(IV.81)}$$

Contrary to the Diffuson contribution, where the sequence of scattering events on the disorder decouples the incoming wavevector k' to the outgoing one k, now the diffusion pole of the Cooperon constraints the two wave vectors to be opposite. The diffusion approximation requires a small momentum $||Q|| \ll 1/\ell_e$; because the two momenta are on the Fermi surface $||k|| \simeq ||k'|| \simeq k_F \gg 1/\ell_e$, the sum over k and k' is dominated by $k+k' \simeq 0$:

$$\sum_{k,\,k'} k_x\,k'_x\,|\overline{G}^{\text{R}}(k)|^2\,\Gamma_c(k+k',\omega)\,|\overline{G}^{\text{R}}(k')|^2 \simeq -\frac{k_F^2}{d}\sum_{k}|\overline{G}^{\text{R}}(k)|^4\sum_{Q}\Gamma_c(Q,\omega) \quad \text{(IV.82)}$$

---

apparaître le temps de transport τ_{tr} lorsqu'elle est ajoutée à la contribution de Drude [2, 3].

[33] Much before the development of the theory of weakly disordered metals by Altshuler, Aronov, Khmelniskii, Lee, Stone, Anderson, etc in the early 1980', the importance of maximally crossed diagrams was recognised by Langer & Neal [82]

The fact that $\overline{\widetilde{\sigma}(\omega)}^{\text{Cooperon}}$ is dominated by the contribution of momenta such that $k \simeq -k'$ is a manifestation of the **enhancement of back-scattering** of electrons, due to interferences of reversed diffusive trajectories. This is the origin of the minus sign of the Cooperon's contribution to the conductivity, i.e. this is indeed a **localisation** effect.

✍ ***Exercice IV.9*** : *Check that* $f_{2,2} = \frac{w}{\text{Vol}} \sum_k |\overline{G}^{\text{R}}(k)|^4 = 2\tau_e^2$.

Using the result of exercice IV.9, and introducing the notation

$$\overline{\Delta\sigma}(\omega) \stackrel{\text{def}}{=} \overline{\widetilde{\sigma}(\omega)}^{\text{Cooperon}} \simeq \overline{\widetilde{\sigma}(\omega)} - \overline{\widetilde{\sigma}(\omega)}^{\text{Drude}} \tag{IV.83}$$

(the Cooperon contribution is the dominant correction to the classical result). We find

$$\boxed{\overline{\Delta\sigma}(\omega) = -\frac{2_s e^2}{\pi\hbar}\frac{1}{\text{Vol}}\sum_Q \widetilde{P}_c(Q,\omega)} \quad \text{where} \quad \widetilde{P}_c(Q,\omega) = \frac{1}{-\mathrm{i}\omega/D + Q^2} \tag{IV.84}$$

If we set the frequency to zero, the correction to the static conductivity seems at first sight to involve a divergent quantity : $\overline{\Delta\sigma}(\omega = 0) = -\frac{2_s e^2}{\pi\hbar}\frac{1}{\text{Vol}}\sum_Q Q^{-2}$. As usual, the occurence of a divergence hides interesting physical phenomenon : this physical (measurable) observable is controlled by the cutoffs. The large scale cutoff, which dominates in low dimensions ($d \leqslant 2$) is the interesting quantity.

Remark : Kubo *vs* Landauer and current conservation.– The comparison of the maximally crossed conductivity diagrams of Fig. 28 with the real space diagram of Fig. 27 leads to the question of the precise correspondence, since the latter diagrams present two additional Diffuson legs. The answer to this question lies in the connection between the Landauer picture (conductance) and the Kubo picture (local conductivity), with some interesting relation to the fundamental question of current conservation. This has been discussed in our paper [125] where the weak localisation correction to the *non local* conductivity was constructed (in real space).

1) Small scale cutoff

The derivation of (IV.84) has involved several approximations : first of all, assuming weak disorder $k_F\ell_e \gg 1$, we have argued that the quantum correction to the conductivity is dominated by the maximally crossed diagram (Ladder approximation). Then, the Diffuson and the Cooperon were computed in the diffusion approximation, i.e. for

$$||Q|| \ll 1/\ell_e . \tag{IV.85}$$

This provides a first **ultraviolet cutoff** in the calculation of (IV.84). There remains the problem of the infrared divergence $\overline{\Delta\sigma}(\omega = 0) = -\frac{2_s e^2}{\pi\hbar}\int^{1/\ell_e}\frac{\mathrm{d}^d Q}{(2\pi)^d}Q^{-2}$, in low dimension $d \leqslant 2$.

2) Large scale cutoff (1) : the system size

In a real situation, the transport is studied in finite size system. For example, if we consider a transport in the Ox direction through a rectangular piece of metal of size $L_x \times L_y \times L_z$ (Fig. 29), when solving the diffusion equation, we must account for the geometry of the system ; as a consequence the wavevectors are quantized. In order to account for the electric contacts (transport experiment), we use the following *phenomenological prescription* : we assume Dirichlet boundary condition in the Ox direction (absorbing boundary conditions for an electron touching one

contact) and Neumann boundary conditions in the two other directions (reflexion boundary conditions) :

$$Q = \left(\frac{\pi n_x}{L_x}, \frac{\pi n_y}{L_y}, \frac{\pi n_z}{L_z} \right) \quad \text{with} \quad n_x \in \mathbb{N}^*, \; n_y \in \mathbb{N}, \; n_z \in \mathbb{N} \tag{IV.86}$$
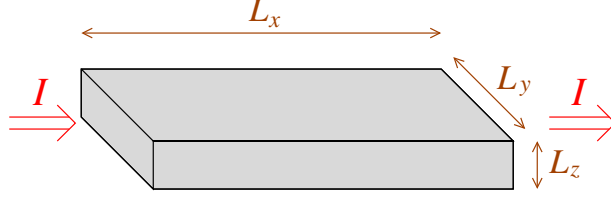

Figure 29: **A metallic wire.**

a) Wire (1D).– In the very asymmetric case $L_x \gg L_y, L_z$ (quasi-1D geometry) we can neglect the contributions of the transverse components of the wave vector :

$$\overline{\Delta\sigma}(\omega = 0) = -\frac{2_s e^2}{\pi\hbar} \frac{1}{L_x L_y L_z} \sum_{n_x=1}^{\infty} \frac{1}{(n_x\pi/L_x)^2} = -\frac{2_s e^2}{\pi\hbar} \frac{L_x}{L_y L_z} \frac{1}{6} . \tag{IV.87}$$

We prefer to translate the result in terms of the dimensionless conductance

$$g = \frac{\sigma}{2_s e^2/h} \frac{L_y L_z}{L_x} , \tag{IV.88}$$

from which we get the **universal** weak localisation correction

$$\boxed{\overline{\Delta g} = -\frac{1}{3}} \tag{IV.89}$$

independent on the material properties. This universal contribution to the *mean* conductance must be compared to the large classical Drude conductance $g_{\mathrm{D}} \sim N_c \ell_e/L \gg 1$ (where N_c is the number of conducting channels).

b) Plane (2D).– In the quasi 2D geometry $L = L_x = L_y \gg L_z$ (thin film), the details of the wave vector quantization are inessential and we can write

$$\overline{\Delta\sigma}(\omega = 0) = -\frac{2_s e^2}{\pi\hbar} \frac{1}{L_z} \int_{1/L < ||\vec{Q}|| < 1/\ell_e} \frac{\mathrm{d}^2\vec{Q}}{(2\pi)^2} \frac{1}{\vec{Q}^{\,2}} = -\frac{2_s e^2}{\pi\hbar} \frac{1}{L_z} \frac{1}{2\pi} \int_{1/L}^{1/\ell_e} \frac{\mathrm{d}Q}{Q} \tag{IV.90}$$

In the 2D case, the weak localisation is controlled both by the short scale cutoff, ℓ_e, and by the large scale cutoff, L. We get

$$\overline{\Delta\sigma}(\omega = 0) \simeq -\frac{2_s e^2}{\pi\hbar} \frac{1}{L_z} \frac{1}{2\pi} \ln(L/\ell_e) \tag{IV.91}$$

therefore

$$\boxed{\overline{\Delta g} \simeq -\frac{1}{\pi} \ln(L/\ell_e)} \tag{IV.92}$$

c) Bulk (3D).– In 3D, we consider a cubic box of size $L = L_x = L_y = L_z$

$$\overline{\Delta\sigma}(\omega = 0) = -\frac{2_s e^2}{\pi\hbar} \int_{1/L < ||\vec{Q}|| < 1/\ell_e} \frac{\mathrm{d}^3\vec{Q}}{(2\pi)^3} \frac{1}{\vec{Q}^{\,2}} = -\frac{2_s e^2}{\pi\hbar} \frac{1}{2\pi^2} \int_{1/L}^{1/\ell_e} \mathrm{d}Q = -\frac{2_s e^2}{h} \frac{1}{\pi^2} \left(\frac{1}{\ell_e} - \frac{1}{L}\right).$$
(IV.93)

Finally

$$\overline{\Delta g} \simeq -\frac{1}{\pi^2} \left(\frac{L}{\ell_e} - 1\right).$$
(IV.94)

Note that in this case, contrary to the 2D case, the prefactor depends on the detail of the regularization of the sum over Q.

3) Large scale cutoff (2) : the phase coherence length

Weak localisation correction arises from the (quantum) interferences of reversed trajectories, i.e. is a *coherent* phenomenon. The results obtained in the previous paragraph hence describe systems (of size L) fully coherent. In practice, phase coherence is *extremely fragile* and is only preserved over lengths smaller than the **phase coherence length L_φ**. This length is of fundamental importance since it set a frontier between the semi-classical transport regime, where quantum interferences are negligible, [34] and the quantum regime, where transport properties depend on the wave nature of the electrons.
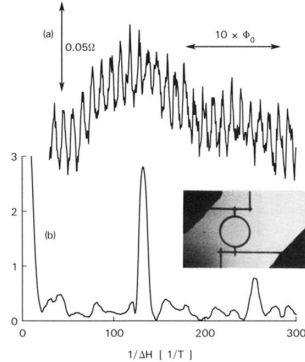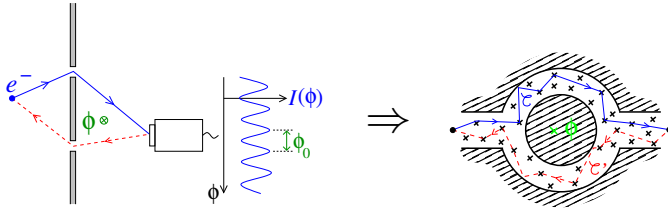
FIG. 1. (a) Magnetoresistance of the ring measured at $T = 0.01$ K. (b) Fourier power spectrum in arbitrary units containing peaks at h/e and $h/2e$. The inset is a photograph of the larger ring. The inside diameter of the loop is 784 nm, and the width of the wires is 41 nm.

Figure 30: **Aharonov-Bohm oscillations in a metallic ring.** *Aharonov-Bohm oscillations realises the Young experiment. Oscillating curve is the magnetoconductance.* From [140].

We can obtain a direct estimation of the phase coherence length with an experimental setup realizing the principle of the Young experiment : the Aharonov Bohm (AB) ring (Fig. 30). The geometry of the ring defines two paths and the interference fringes are revealed by changing the magnetic field. One observes regular oscillations of the conductance with a period in magnetic field corresponding to one quantum flux $\phi_0 = h/e$ in the ring. The amplitude of the AB oscillations can be studied as a function of the temperature (Fig. 31) : the experimental result (for a ring of perimeter $L \simeq 0.9\,\mu$m) shows that oscillations are only visible below few Kelvins. We can keep in mind the typical value for the phase coherence length

$$L_\varphi(T \sim 1\,\mathrm{K}) \sim 1\,\mu\mathrm{m}\,.$$

---

[34] Eventhough the effect of quantum interferences has disappeared above few Kelvins, the electronic transport is not really classical : up to high temperatures, the dynamics of the electron liquid in a metal is completely dominated by the Pauli principle (the Fermi-Dirac distribution).
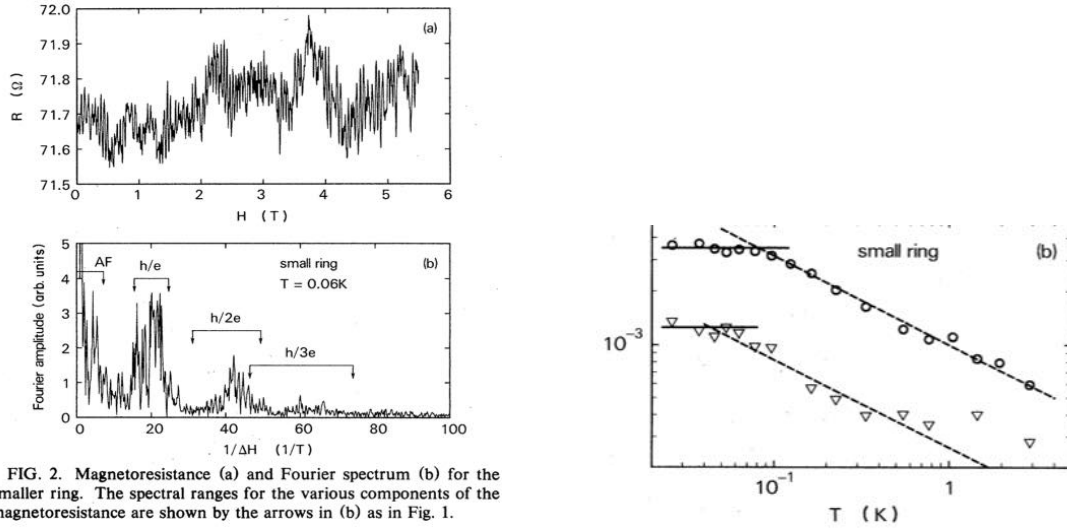
FIG. 2. Magnetoresistance (a) and Fourier spectrum (b) for the smaller ring. The spectral ranges for the various components of the magnetoresistance are shown by the arrows in (b) as in Fig. 1.

Figure 31: **Aharonov-Bohm amplitude.** *The study of AB amplitude as a function of temperature in a Gold ring (diameter 285 nm) with wire width 37 nm ; $R \simeq 76\,\Omega$. AB amplitude (right) is obtained by averaging over 45 h/e periods (i.e. $\mathcal{B} \in [-1.1\,\mathrm{T}, +1.1\,\mathrm{T}]$). From [137].*

As decoherence arises from interaction between a given electron (the interfering wave) and other degrees of freedom (phonons, other electrons, etc), it is rather complicate to modelize (see chapters IX and X). We will limit ourselves, in a first time, to introduce decoherence within a simple **phenomenological** description corresponding to the elimination of trajectories spreading over scale larger than the phase coherence length L_φ.

Remembering that $1/(-\mathrm{i}\omega + DQ^2)$ is a propagator, a natural way to introduce a cutoff is to shift the pole by a rate $1/\tau_\varphi$ (now setting $\omega = 0$), i.e. a "mass" term in the diffusion propagator :

$$\overline{\Delta\sigma} = -\frac{2_s e^2}{\pi\hbar} \frac{D}{\mathrm{Vol}} \sum_Q \frac{1}{DQ^2} \quad \longrightarrow \quad \overline{\Delta\sigma} = -\frac{2_s e^2}{\pi\hbar} \frac{D}{\mathrm{Vol}} \sum_Q \frac{1}{DQ^2 + 1/\tau_\varphi} \tag{IV.95}$$

where $L_\varphi^2 = D\tau_\varphi$.

We can shed light on this substituion by reformulating the calculation of the weak localisation correction in a time-space representation. The expression (IV.95) can be understood as a trace of the diffusion propagator integrated over all time scale

$$\overline{\Delta\sigma} = -\frac{2_s e^2}{\pi\hbar} D \int_0^\infty \mathrm{d}t \underbrace{\int \frac{\mathrm{d}r}{\mathrm{Vol}} \mathcal{P}_t(r|r)}_{\mathcal{P}_c(t) \overset{\mathrm{def}}{=}} \quad \text{where} \quad \mathcal{P}_t(r|r') = \langle r | \mathrm{e}^{tD\Delta} | r' \rangle \tag{IV.96}$$

solves $(\partial_t - D\Delta)\mathcal{P}_t(r|r') = \delta(t)\delta(r - r')$. The space averaged return probability $\mathcal{P}_c(t)$ counts the number of closed diffusive trajectories for a given time scale t. This representation makes clear how the large scales can be eliminated : we simply cut the integral at the time τ_φ, where $L_\varphi = \sqrt{D\tau_\varphi}$. The most natural way is to introduce an exponential in the time integration [35]

$$\overline{\Delta\sigma} = -\frac{2_s e^2}{\pi\hbar} D \int_0^\infty \mathrm{d}t \, \mathcal{P}_c(t) \, \mathrm{e}^{-t/\tau_\varphi} \tag{IV.97}$$

Meanwhile, we can also eliminate the shortest scale contributions ($< \ell_e$), where the diffusion

---

[35] This is justified within microscopic models of decoherence or dephasing. See chapter 6 and 7 of [3].

approximation ceases to be valid, by introducing another exponential :

$$\boxed{\overline{\Delta\sigma} = -\frac{2_se^2}{\pi\hbar}D\int_0^\infty \mathrm{d}t\, \mathcal{P}_c(t)\left(\mathrm{e}^{-t/\tau_\varphi} - \mathrm{e}^{-t/\tilde{\tau}_e}\right)}\qquad \text{with } \mathcal{P}_c(t) \stackrel{\text{def}}{=} \int \frac{\mathrm{d}r}{\text{Vol}}\,\mathcal{P}_t(r|r)\,, \qquad \text{(IV.98)}$$

where $\tilde{\tau}_e = \ell_e^2/D = \tau_e d$ (we have introduced this new scale to have an expression symmetric with $\tau_\varphi = L_\varphi^2/D$). This new representation (IV.98) will be very convenient for subsequent analysis.

Remark : Real space derivation : A direct real space derivation of the result (IV.98) is possible. It can be found in chapters 4 and 7 of the book [2, 3].

Simple applications.– As an application we immediatly obtain the weak localisation in the 1D and 2D case by using that the return probability is simply [36]

$$\mathcal{P}_c(t) = \frac{1}{(4\pi Dt)^{d/2}}\,. \qquad \text{(IV.99)}$$

Using the integral

$$\int_0^\infty \mathrm{d}t\,\frac{\mathrm{e}^{-at} - \mathrm{e}^{-bt}}{t^{d/2}} = \Gamma\left(1 - \frac{d}{2}\right)\left[a^{\frac{d}{2}-1} - b^{\frac{d}{2}-1}\right] \qquad \text{(IV.100)}$$

we deduce the weak localisation correction

$$\overline{\Delta\sigma} = -\frac{2_se^2}{h}\frac{2\,\Gamma\left(1-\frac{d}{2}\right)}{(4\pi)^{d/2}}\left(L_\varphi^{2-d} - \ell_e^{2-d}\right)\,. \qquad \text{(IV.101)}$$

a) The narrow wire

We first consider the case of a long (quasi-1D) wire :

$$\overline{\Delta\sigma} = -\frac{2_se^2}{h}\,(L_\varphi - \ell_e) \simeq -\frac{2_se^2}{h}\,L_\varphi \qquad \text{in } d=1 \qquad \text{(IV.102)}$$

i.e. the WL correction to the dimensionless conductance

$$\boxed{\overline{\Delta g} = -\frac{L_\varphi}{L}} \qquad \text{(IV.103)}$$

For $L\sim L_\varphi$ we recover the result of the coherent wire $\overline{\Delta g}\sim -1$, Eq. (IV.89).

b) The plane (or the thin film)

The 2D case can be simply studied by dimensional regularization $d = 2(1-\varepsilon)$ with $\varepsilon\to 0$. Remembering that $\Gamma(\varepsilon)\simeq 1/\varepsilon$, we find the logarithmic behaviour

$$\overline{\Delta\sigma} = -\frac{2_se^2}{h}\frac{1}{\pi}\ln(L_\varphi/\ell_e) \qquad \text{in } d=2 \qquad \text{(IV.104)}$$

i.e.

$$\boxed{\overline{\Delta g} = -\frac{1}{\pi}\ln(L_\varphi/\ell_e)} \qquad \text{(IV.105)}$$

We may again check that at the crossover $L\sim L_\varphi$ we recover the result of the coherent plane Eq. (IV.92). Contrary to the 1D case, controlled by the large scale cutoff only, both short scale and large scale cutoffs appear in the 2D result.

---

[36] We omit the section of the film for $d \leqslant 2$; in principle we should write $\mathcal{P}_c(t) = \frac{1}{(4\pi Dt)^{d/2}W^{3-d}}$ where W is the thickness of the film ($d = 2$) and W^2 the cross-section of the wire ($d = 1$).

c) The 3D bulk

Finally, we mention the result in 3D for the sake of completeness

$$\overline{\Delta\sigma} = -\frac{2_s e^2}{h}\frac{1}{2\pi}\left(\frac{1}{\ell_e} - \frac{1}{L_\varphi}\right) \qquad \text{in } d = 3 \qquad \text{(IV.106)}$$

However we recall that the typical order of magnitudes for the elastic mean free path in bulk makes the coherent properties unlikely to be in the diffusive regime (recall that in Gold $\ell_e^{(\text{bulk})} \simeq 4\,\mu$m most surely exceeds L_φ in usual situations). The related correction to the dimensionless conductance is (square box)

$$\overline{\Delta g} = -\frac{1}{2\pi}\left(\frac{L}{\ell_e} - \frac{L}{L_\varphi}\right)\;. \qquad \text{(IV.107)}$$

Note that the prefactor $1/(2\pi)$ differs from the one found above for the coherent wire, Eq. (IV.94), the reason being that we used different regularizations in the two cases (the prefactor depends on regularisation in $d = 3$ but not in $d \leqslant 2$).

4) A pratical question : How to identify the WL ?

In $d \leqslant 2$, the fact that (IV.84) exhibits an infrared (large scales) divergence has required a regularization of the sum, what makes the weak localisation $\overline{\Delta g}$ strongly dependent on L_φ (we mean that the dominant term of $\overline{\Delta g}$ depends on L_φ). The measurement of the WL provides therefore a direct information on the phase coherence length. On the other hand, in $d = 3$, only the subdominant term of the WL depends in L_φ ; the WL is therefore not a good tool to probe phase coherence in this case.

The WL is a very small correction to the classical conductance. The question is : **how can we identify the WL correction ($\lesssim 1\%$) on the top of a large conductance $G = G_{\text{Drude}} + \Delta G_{\text{quantum}}$?** Obviously, one should vary some parameter on which the WL depends.

Because decoherence is activated by increasing the temperature, a first natural suggestion would be to study the temperature-dependence of the conductance. This is however not a good idea for the reason that the WL is not the only temperature-dependent quantum correction to the conductivity. We will see (chapter X) that the conductivity receives another correction from the electronic interactions, named the Altshuler-Aronov (AA) correction. This has led to some confusion in the analysis of the first measurements of temperature-dependent quantum corrections to transport (like in Ref. [66]).

Another possibility is to vary the magnetic field, on which the WL depends, as we explain below, but not the AA correction ΔG_{ee}. In summary, the low field and low temperature conductance may be written as

$$G(\mathcal{B}, T) = G_{\text{Drude}} + \underbrace{\Delta G_{\text{WL}}(\mathcal{B}, L_\varphi(T))}_{\text{weak loc. corr.}} + \overbrace{\Delta G_{\text{ee}}(T)}^{\text{Altshuler-Aronov corr.}} \qquad \text{(IV.108)}$$

The understanding of the WL's magnetic-field dependence is thus a crucial issue in order to identify the WL correction and extract the phase coherence length. This has been used in many experiments in thin films [26] and narrow wires [108].

5) Magnetic field dependence – Path integral formulation

We have shown that the WL correction is related to the interference of time reversed trajectories, what we write schematically as

$$\overline{\Delta\sigma} \sim -\sum_\mathcal{C} \mathcal{A_C}\, \mathcal{A}_{\widetilde{\mathcal{C}}}^*\,, \qquad \text{(IV.109)}$$

where $\widetilde{\mathcal{C}}$ is the reversed trajectory. In the presence of a weak magnetic field (recall that usual magnetic field are not able to bend significantly the electronic trajectories on the scale ℓ_e), an amplitude receives an additional magnetic phase :

$$\mathcal{A}_{\mathcal{C}} = |\mathcal{A}_{\mathcal{C}}| \; e^{ik_F\ell_{\mathcal{C}}} \, e^{\frac{ie}{\hbar} \int_{\mathcal{C}} d\vec{r}\cdot\vec{A}} \, . \tag{IV.110}$$

The magnetic phase remains unchanged under the combination of complex conjugation and time reversal, therefore the pair of amplitudes carries *twice* the magnetic phase

$$\mathcal{A}_{\mathcal{C}} \, \mathcal{A}_{\widetilde{\mathcal{C}}}^* = \left| \mathcal{A}_{\mathcal{C}} \, \mathcal{A}_{\widetilde{\mathcal{C}}}^* \right| \, \exp\left\{ \frac{2ie}{\hbar} \oint_{\mathcal{C}} d\vec{r}\cdot \vec{A}(\vec{r}) \right\} \tag{IV.111}$$

This discussion, in the spirit of § IV.E, can be made precise by reformulating the analysis of the Cooperon in time representation, Eq. (IV.98), within the frame of path integration. The diffusion propagator has the path integral representation

$$\mathcal{P}_t(\vec{r}|\vec{r}') = \int_{\vec{r}(0)=\vec{r}'}^{\vec{r}(t)=\vec{r}} \mathcal{D}\vec{r}(\tau) \, e^{-\frac{1}{4D} \int_0^t d\tau \left(\frac{d\vec{r}(\tau)}{d\tau} \right)^2} \tag{IV.112}$$

where the integral corresponds to a summation over all diffusive paths $\vec{r}(\tau)$ going from $\vec{r}'$ to $\vec{r}$ with the **Wiener measure** $\mathcal{D}\vec{r}(\tau) \exp\left[-\frac{1}{4D} \int_0^t d\tau \left(\frac{d\vec{r}(\tau)}{d\tau} \right)^2 \right]$. The form of the measure ensures that paths, which are Brownian motions, are *continuous* (i.e. the discontinuous functions in the integral have zero weight) but is not differentiable. The path integral (IV.112) corresponds to a summation over all diffusing electronic trajectories for a given time scale, i.e. for loops with a given number of collisions [37] t/τ_e. In Eq. (IV.98), the remaining integral over time realises the summation over the trajectories length :

$$\sum_{\mathcal{C}} \mathcal{A}_{\mathcal{C}} \, \mathcal{A}_{\widetilde{\mathcal{C}}}^* \longrightarrow \int_{\tilde{\tau}_e}^{\infty} dt \int_{\vec{r}(0)=\vec{r}}^{\vec{r}(t)=\vec{r}} \mathcal{D}\vec{r}(\tau) \, e^{-\int_0^t d\tau \frac{1}{4D} \dot{\vec{r}}(\tau)^2} \tag{IV.113}$$

(the time integral is cut off at the time $\tilde{\tau}_e = \ell_e^2/D$ below which the diffusion approximation breaks down).

The path integral representation (IV.112) allows us to add in a natural way the contribution of the magnetic phase. We obtain the path integral representation of the Cooperon

$$\mathcal{P}_t(\vec{r}|\vec{r}) = \int_{\vec{r}(0)=\vec{r}}^{\vec{r}(t)=\vec{r}} \mathcal{D}r(\tau) \, e^{-\int_0^t d\tau \left[\frac{1}{4D} \dot{\vec{r}}(\tau)^2 + \frac{2ie}{\hbar} \vec{A}(\vec{r})\cdot\dot{\vec{r}}(\tau) \right]} \, . \tag{IV.114}$$

From this representation, we deduce that $\mathcal{P}_t(\vec{r}|\vec{r}')$ solves

$$\left[\frac{\partial}{\partial t} - D \left(\vec{\nabla} - \frac{2ie}{\hbar} \vec{A}(\vec{r}) \right)^2 \right] \mathcal{P}_t(\vec{r}|\vec{r}') = \delta(t)\,\delta(\vec{r} - \vec{r}') \tag{IV.115}$$

The presence of the charge $2e$ reminds us that the Cooperon is a two particle propagator in the *particle-particle channel*, which is the reason for the terminology "Cooperon".

---

[37] In a time t, an electron experiences t/τ_e collisions, i.e. the time t corresponds to trajectories of length $\ell_{\mathcal{C}} = \ell_e \, (t/\tau_e) = dDt/\ell_e$. The Brownian motion is the continuum limit of the random walk on defects, $\ell_e \to 0$; in this limit the length of the Brownian curve is infinite $\ell_{\mathcal{C}} \propto t/\ell_e \to \infty$.

Summary.– The weak localisation correction will be conveniently computed with the space-time representation (IV.98) with (IV.115). The time integral can be performed to obtain the useful representation

$$\boxed{\overline{\Delta\sigma} = -\frac{2_s e^2}{\pi\hbar} \int \frac{\mathrm{d}^d\vec{r}}{\mathrm{Vol}} P_c(\vec{r},\vec{r})} \tag{IV.116}$$

where the Cooperon is the Green's function of a diffusion-like operator

$$\boxed{P_c(\vec{r},\vec{r}\,') = \langle\vec{r}| \frac{1}{1/L_\varphi^2 - \left(\vec{\nabla} - \frac{2\mathrm{ie}}{\hbar}\vec{A}(\vec{r})\right)^2} |\vec{r}\,'\rangle} \tag{IV.117}$$

In pratice, this means that the Cooperon is given by solving the equation

$$\boxed{\left[\frac{1}{L_\varphi^2} - \left(\vec{\nabla} - \frac{2\mathrm{ie}}{\hbar}\vec{A}(\vec{r})\right)^2\right] P_c(\vec{r},\vec{r}\,') = \delta(\vec{r}-\vec{r}\,')} \tag{IV.118}$$

The connection between these representation and the time-space representation is obviously established through the transformation

$$P_c(\vec{r},\vec{r}\,') = \int_0^\infty \mathrm{d}t\, \mathrm{e}^{-t/\tau_\varphi}\, \mathcal{P}_t(\vec{r}|\vec{r}\,')\,.$$

Magneto-conductance in a narrow wire.– A precise study of the magneto-conductance of a narrow wire could be done : we only give here a first qualitative description of the magnetic-field dependence of the WL correction $\overline{\Delta g}(\mathcal{B})$.

We first notice that we expect a quadratic weak magnetic field dependence (this results from the fact that the WL involves a propagator at coinciding point, spatially integrated ; hence it must be a symmetric function of $\mathcal{B}$) :

$$\overline{\Delta g}(\mathcal{B}) \underset{\mathcal{B}\to 0}{\simeq} \overline{\Delta g}(0) + c\,\mathcal{B}^2 \tag{IV.119}$$

with $c > 0$ (this is the positive – anomalous – magneto-conductance, cf. TD 4).

The large field behaviour is obtained as follows : the presence of the $\mathcal{B}$ field adds the magnetic phase (IV.111) to the contributions of the reversed electronic trajectories. The presence of this phase is responsible for an **effective $\mathcal{B}$-dependent cutoff** since it eliminates all trajectories encircling a magnetic flux larger that the quantum flux $\phi_0 = h/e$. For a given time scale t, a diffusive trajectory typically spreads over a distance $L_t \sim \sqrt{Dt}$ along the wire. If the wire has a width W, the trajectory typical encloses a magnetic flux $\Phi \sim \mathcal{B}W L_t$. Contributions of the trajectories such that $\Phi \sim \mathcal{B}W L_t \gtrsim \phi_0$ are eliminated, what gives the cutoff

$$L_\mathcal{B} \sim \frac{\hbar}{e|\mathcal{B}|W} \qquad \text{(narrow wire)}\,. \tag{IV.120}$$

For $L_\mathcal{B} < L_\varphi$, the dominant cutoff is the magnetic field, hence we should perform the substitution $L_\varphi \to L_\mathcal{B}$ in Eq. (IV.103) :

$$\overline{\Delta g}(\mathcal{B}) \simeq -\frac{L_\mathcal{B}}{L} \propto -1/|\mathcal{B}| \tag{IV.121}$$

at large field. The crossover between the low field and the high field behaviour occurs when $L_\mathcal{B} \sim L_\varphi$, thus the WL curve has a typical width in magnetic field

$$\Delta\mathcal{B}_{\mathrm{wire}} = \frac{\phi_0}{W L_\varphi}\,, \tag{IV.122}$$

corresponding to one quantum flux $\phi_0 = h/e$ in the area $W L_\varphi$.

We will demonstrate later that the correct definition for the magnetic length of the narrow wire is $L_\mathcal{B} = \hbar/(\sqrt{3}|\mathcal{B}|W)$ and will obtain the precise crossover function interpolating between (IV.119) and (IV.121), perfectly describing the experimental results like the one of Fig. 23 or Fig. 32.
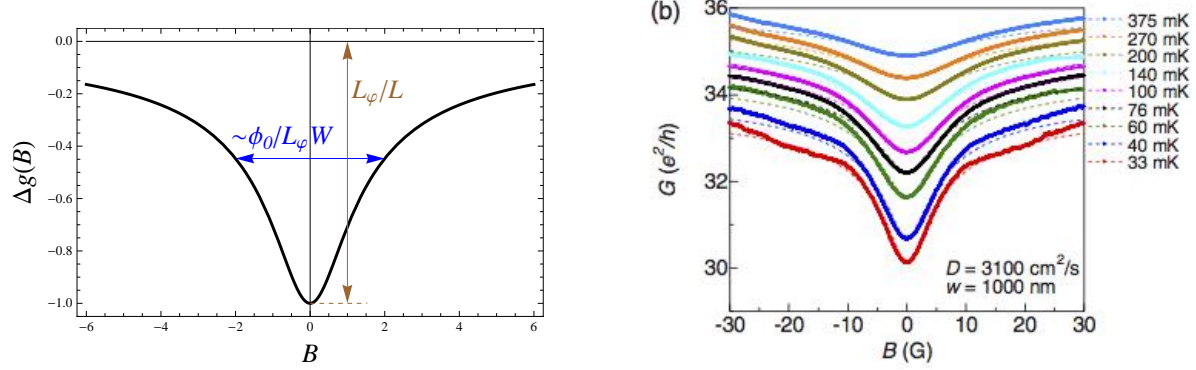

Figure 32: **Weak localisation correction of a long wire.** Left : *Theoretical result, Eq. (IV.152).* Right : *Experimental MC of a long wire ($L = 150$ μm) etched in a 2DEG ; width $W = 0.63$ μm (lithographic width $w_{\mathrm{litho}} = 1$ μm). From [100].*

Magneto-conductance in thin metallic film.– We can repeat the same exercice for a metallic film. The low field dependence is again expected to be quadratic, Eq. (IV.119). The high field dependence is obtained as follows : for a given time scale t, a diffusive trajectory typically spreads over a distance $L_t \sim \sqrt{Dt}$ in the plane, and typical encloses a magnetic flux $\Phi \sim \mathcal{B}L_t^2$. Longest trajectories, such as $\Phi \sim \mathcal{B}L_t^2 \gtrsim \phi_0$, do not contribute to the WL, what gives the cutoff

$$L_\mathcal{B} \sim \sqrt{\frac{\hbar}{e|\mathcal{B}|}} \qquad \text{(thin film)} . \tag{IV.123}$$

Replacing L_φ by $L_\mathcal{B}$ in Eq. (IV.105) gives the large field behaviour

$$\overline{\Delta g}(\mathcal{B}) \simeq -\frac{1}{\pi} \ln(L_\mathcal{B}/\ell_e) \simeq +\frac{1}{2\pi} \ln |\mathcal{B}| + \text{cste} . \tag{IV.124}$$

As a consequence, the crossover between the low field and high field behaviours occurs on a scale

$$\Delta \mathcal{B}_{\mathrm{plane}} = \frac{\phi_0}{L_\varphi^2} . \tag{IV.125}$$

The precise magneto-conductance curve will be derived in the exercices (TD5, p. 101).

IV.H Scaling approach and localisation (from the metallic phase)

1) The β-function

The starting point of the scaling approach is the *gedanken experiment* where one analyses the conductance of a cubic box of size L^d connected at two opoosite sides, as a function of the size. The Drude conductance was analysed in the introductory chapter

$$g_\mathrm{D} = c_d \frac{(k_F W)^{d-1}\ell_e}{L} \qquad \text{where } c_d = \frac{(4\pi)^{1-d/2}}{2\,\Gamma(\frac{d}{2}+1)} = \begin{cases} 2 & \text{in } d = 1 \\ 1/2 & \text{in } d = 2 \\ 1/(3\pi) & \text{in } d = 3 \end{cases} \tag{IV.126}$$

94

The WL correction for a coherent piece of metal is (see above)

$$
\overline{\Delta g} = \begin{cases} -\frac{1}{3} & \text{in } d=1 \\ -\frac{1}{\pi}\ln(L/\ell_e) & \text{in } d=2 \\ -\frac{1}{2\pi}\left(\frac{L}{\ell_e}-1\right) & \text{in } d=3 \end{cases}
\tag{IV.127}
$$

(note that, in $d=3$, the subdominant term $+1/2\pi$ is important : it will provide the asymptotic of the β-function). As noticed, being a *negative* correction to the conductance, the WL is a precursor of the localisation effect. We can now analyse the asymptotic behaviour of the scaling approach's β-function (i.e. from the conducting phase). We compute the β-function

$$
\beta(g) = \frac{\mathrm{d}\overline{\ln g}}{\mathrm{d}\ln L} \; .
\tag{IV.128}
$$

Note that in numerical calculations, scaling analysis is performed on the Lyapunov exponent, i.e. consider $\overline{\ln g}$ [81]. In the conducting limit, we can write $\overline{\ln g} \simeq \ln(g_\mathrm{D}) + \frac{\overline{\Delta g}}{g_\mathrm{D}}$. We deduce the expression of the β-function in the metallic limit $g \to \infty$

$$
\boxed{\beta(g) \underset{g\to\infty}{\simeq} d-2-\frac{a_d}{g}} \qquad \text{where } a_d = \begin{cases} \frac{1}{3} & \text{in } d=1 \text{ (multichannel)} \\ \frac{1}{\pi} & \text{in } d=2 \\ \frac{1}{2\pi} & \text{in } d=3 \end{cases}
\tag{IV.129}
$$

which suggests a monotonous behaviour, which is confirmed by numerical calculations (see Fig. 15) [81].

2) Localisation length in 1D and 2D

The weak localisation phenomenon is a precursor of the strong localisation, as suggested by the behaviour of the β-function. Since g_D and $\overline{\Delta g}$ have opposite signs, we can expect that the localisation length corresponds to the length at which the two quantities become comparable (although this is in principle out of the range of validity of the calculation of the WL) :

$$
g_\mathrm{D} \sim |\overline{\Delta g}| \quad \text{for } L \sim \xi_{\mathrm{loc}} \; .
\tag{IV.130}
$$

Narrow wire.– The general expression of the Drude conductance in a wire is $g_\mathrm{D} = k_F W \ell_e/2L = \alpha_d N_c \ell_e/L$ where $\alpha_d = V_d/V_{d-1}$ (where V_d is the volume of the unit sphere) and N_c the number of conducting channels : $N_c = k_F W/\pi$ in $d=2$, i.e. for a wire of width W etched in a two dimensional electron gas (2DEG). And $N_c = (k_F W)^2/4\pi$ in $d=3$, i.e. in a thin and narrow metallic wire of section W^2.

This leads to

$$
\boxed{\xi_{\mathrm{loc}}^{(\mathrm{1D})} \sim N_c \ell_e}
\tag{IV.131}
$$

This expression of the localisation length has been confirmed by other approaches, like the random matrix approach of Dorokhov-Mello-Pereyra-Kumar (see the review by Beenakker [20]).

Planes and thin films.– In $d=2$, i.e. in a 2DEG, we have $g_\mathrm{D} = k_F \ell_e/2$ and $\Delta g = -\frac{1}{\pi}\ln(L/\ell_e)$, therefore $g_\mathrm{D} \sim |\overline{\Delta g}|$ gives the localisation length

$$
\boxed{\xi_{\mathrm{loc}}^{(\mathrm{2D})} \sim \ell_e\, \mathrm{e}^{\frac{\pi}{2}k_F \ell_e}}
\tag{IV.132}
$$

is very large.

In $d=3$, i.e. in a thin film of thickness W, we have $g_\mathrm{D} = k_F^2 W \ell_e/3\pi$, therefore we obtain

$$
\xi_{\mathrm{loc}}^{(\mathrm{2D})} \sim \ell_e\, \mathrm{e}^{\frac{1}{3}k_F^2 W \ell_e} \; .
\tag{IV.133}
$$

IV.I   Conclusion : a probe for quantum coherence

The main interest in WL analysis is to provide a practical probe of phase coherence properties. Moreover, the analysis of $\overline{\Delta\sigma}(\mathcal{B}, L_\varphi)$ defines [38] the phase coherence length L_φ. We can show that this method is effective in practical situation : in typical WL measurements, the value of L_φ can be obtained from the fit of the magneto-conductance curve at different temperatures, what provides the temperature dependence of the phase coherent length. The typical temperature dependence (for a narrow wire) is shown on Fig. 33. The analysis of the temperature dependence provides information on the microscopic mechanisms responsible for the decoherence. For example, the behaviour $\tau_\varphi \propto T^{-3}$ above $T = 1\ K$ is attributed to elctron-phonon interaction. Below $T = 1\ K$, the dominant decoherence mechanism is provided by electronic interacions, characterised by the behaviour $\tau_\varphi \propto T^{-2/3}$ in 1D.
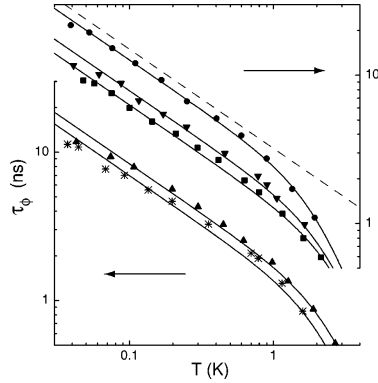
FIG. 4. Phase coherence time vs temperature in samples Ag(6N)a (■), Ag(6N)b (▼), Ag(6N)c (●), Ag(6N)d (▲), and Au(6N) (*), all made of 6N sources. Continuous lines are fits of the data to Eq. (4). For clarity, the graph has been split in two part, shifted vertically one with respect to the other. The quantitative prediction of Eq. (3) for electron–electron interactions in sample Ag(6N)c is shown as a dashed line.

Figure 33: **Phase coherence length of narrow silver wires as a fonction of temperature.** *length ranging from* 135 *to* 400 *μm, thickness from* 35 *to* 55 nm *and with from* 65 *to* 105 nm. *From [102].*

In this chapter L_φ was introduced as a cutoff put by hand. It will be the purpose of the chapter IX to discuss the origin of this length scale on more microscopic grounds. In chapter X we will analyse more deeply the particular role of electronic interaction.

---

[38]Each phase coherent physical property, like AB amplitude, persistent current, etc, does the same job. It is not obvious that they all give the same length scale.

Exercices

✎ *Exercice IV.10 :* **Magnétoconductance classique et magnétoconductance anormale (d'un fil).**– *On rappelle que la conductivité de Drude varie à "bas" champ comme $\Delta\sigma_{\text{class}}(B)/\sigma_0 \simeq -(B\mu)^2$ où $\mu = \frac{e\tau_e}{m}$ est la mobilité. On considère de l'argent avec $\ell_e = 30\,nm$ (on rappelle que $k_F^{-1} = 0.83\,\text{Å}$). Vérifier que $\Delta\sigma_{\text{class}}(B)/\sigma_0 \simeq -10^{-5}B^2$ (B en Tesla).*

On considère un fil d'argent de section $S = W \times a = 60$ nm×50 nm soumis à un champ magnétique perpendiculaire. Calculer la longueur L_B pour $B = 1$ T. Vérifier que la localisation faible décroît comme $\overline{\Delta\sigma}/\sigma_0 \simeq -10^{-5}/B$ (B en Tesla).
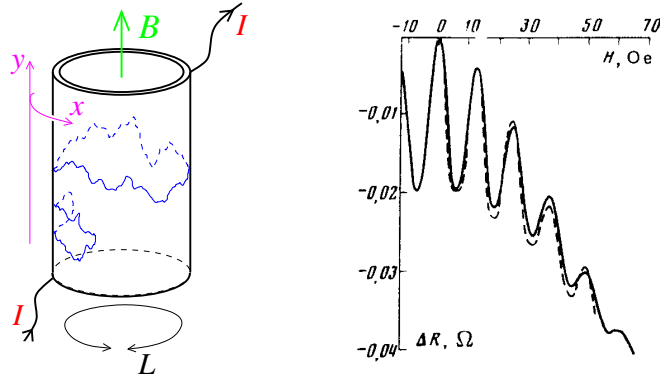
Figure 34: *Magnetoresistance of a hollow metallic cylinder in Oersted (1 Oersted= 1 Gauss= 10^{-4} Tesla). From [9].*

✎ *Exercice IV.11 :*

1/ Ballistic ring – Aharonov-Bohm oscillations.– *We consider a metallic ring of micrometric dimension such that the transport can be considered fully coherent (at low temperature). Discuss how the conductance depends on a magnetic field.*

2/ Diffusive ring – Altshuler-Aronov-Sharvin oscillations.– *Same question for a ring made of weakly disordered metal, in the diffusive regime [base your analysis on Eq. (IV.111)]. The first experiment was performed in a famous experiment by Sharvin and Sharvin [111, 9]. What is the diameter of the cylinder ?*

Further reading : *review by Aronov and Sharvin [16] and also the one by Washburn and Webb [138].*

✎ *Exercice IV.12 Complex geometry – Altshuler-Aronov-Spivak oscillations :* De-tailed study

- *Weak localisation correction in a metallic ring.*

- *Hollow cylinder.*

Theory by [8] ; experiment [111, 9]

97

TD 4 : Classical and anomalous magneto-conductance

4.1 Anomalous (positive) magneto-conductance

1/ Classical magneto-conductivity.– We first analyse transport coefficients in the presence of a magnetic field within the semi-classical Drude-Sommerfeld theory of electronic transport.

a) Show that the conductivity tensor in the presence of an external magnetic field is

$$\sigma_{xx} = \sigma_0 \frac{1}{1 + (\omega_c \tau)^2} \tag{IV.134}$$

$$\sigma_{xy} = \sigma_0 \frac{\omega_c \tau}{1 + (\omega_c \tau)^2} \tag{IV.135}$$

where $\omega_c = \frac{e\mathcal{B}}{m_*}$ is the cyclotron pulsation and $\sigma_0 = \frac{ne^2\tau}{m_*}$ the Drude conductivity. Deduce the resistivity tensor $\rho = \sigma^{-1}$.

b) Justify physically the decrease of $\sigma_{xx}(\mathcal{B})$ as $\mathcal{B}$ increases.

c) At low temperature, the relaxation time saturates at the elastic mean free time $\tau \to \tau_e$. What is the typical scale of magnetic field needed to decrease significantly $\sigma_{xx}(\mathcal{B})$? We give the inverse of the Fermi wavevector $k_F^{-1} = 0.85$ Å and the elastic mean free path $\ell_e = 4\,\mu$m in gold (bulk).

d) In thin metallic films with thickness $50\,$nm, the elastic mean free path is reduced by two order of magnitudes ! In thin silver wires, one measures $\ell_e \simeq 20\,$nm. How large must be the magnetic field to bend significantly the electronic trajectories between collisions on impurities ?

2/ Coherent enhancement of back-scattering.– In a weakly disordered metal, interferences of time reversed electronic trajectories enhance the back-scattering of electrons, and therefore diminishes the conductivity. In the absence of a magnetic field, the phase of probability amplitude is an orbital phase proportional to the length of the diffusive trajectory $\mathcal{A}_\mathcal{C} = |\mathcal{A}_\mathcal{C}|e^{ik_F\ell_\mathcal{C}}$:

$$\overline{\Delta\sigma}(\mathcal{B}=0) \sim -\sum_\mathcal{C} \mathcal{A}_\mathcal{C}\mathcal{A}_{\widetilde{\mathcal{C}}}^* = -\sum_\mathcal{C} |\mathcal{A}_\mathcal{C}|^2 < 0 \tag{IV.136}$$

where the sum runs over all closed diffusive trajectories.
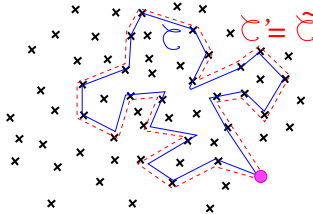
Figure 35: *Interference of reversed electronic trajectories $\mathcal{C}$ and $\widetilde{\mathcal{C}}$ increases back-scattering (weak localisation).*

a) If a weak magnetic field is applied, what is the magnetic field dependence of the probability amplitudes $\mathcal{A}_\mathcal{C}$?

b) How the right hand side of Eq. (IV.136) is modified ?

c) We consider a thin metallic film, i.e. *diffusive* electronic motion is *effectively two-dimensional.*

Argue that the presence of the perpendicular magnetic flux introduces a cutoff in the summation over electronic trajectories (IV.136).

d) **Anomalous magneto-conductivity.**– Deduce the qualitative behaviour of $\overline{\Delta\sigma}(\mathcal{B})$ and discuss the experimental result (Fig. 36).
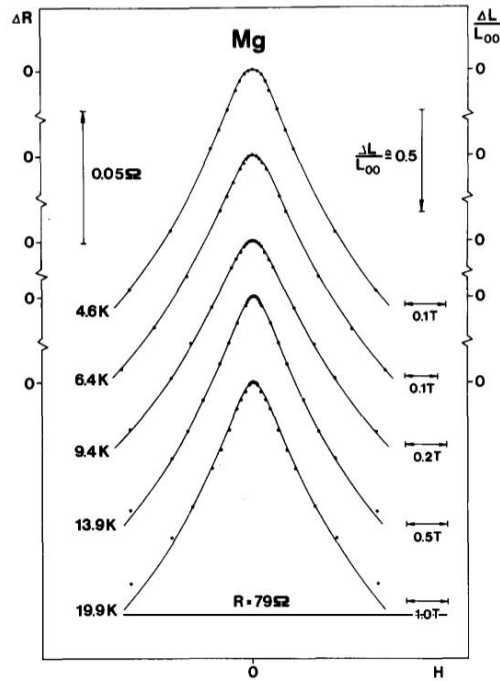

Figure 36: **Anomalous magneto-resistance of a thin Magnesium film ($^{24}_{12}$Mg).** *From Ref. [27].*

4.2 Green's function and self energy

1) Propagator and Green's functions

We introduce the propagator

$$K(\vec{r}, t | \vec{r}', 0) = -\mathrm{i}\, \theta_{\mathrm{H}}(t)\, \langle \vec{r} | \mathrm{e}^{-\mathrm{i}\hat{H}t} | \vec{r}' \rangle \qquad \text{(IV.137)}$$

where H is the Hamiltonian operator.

a) Check that $K(\vec{r}, t | \vec{r}', 0)$ is the Green's function of the time dependent Schrödinger equation.

b) Compute the Fourier transform $G^{\mathrm{R}}(\vec{r}, \vec{r}'; E) = \int_{-\infty}^{+\infty} \mathrm{d}t\, \mathrm{e}^{\mathrm{i}Et}\, K(\vec{r}, t | \vec{r}', 0)$. Check that this is the Green's function of the stationary Schrödinger equation.

2) Green's functions in momentum space and average Green's function

1/ Free Green's function.– The free Green's function in momentum space is

$$\mathcal{G}_0^{\mathrm{R}}(\vec{k}, \vec{k}') = \langle \vec{k} | \frac{1}{E_F - H_0 + \mathrm{i}0^+} | \vec{k}' \rangle \equiv \delta_{\vec{k}, \vec{k}'} G_0^{\mathrm{R}}(\vec{k}) \qquad \text{(IV.138)}$$

where $|k\rangle$ is a plane wave, eigenvector of $H_0 = -\frac{1}{2m}\Delta$ (the dependence in Fermi energy is implicit). Compute explicitly $G_0^{\mathrm{R}}(\vec{r}, \vec{r}')$ in dimension $d = 1$ and $d = 3$.

Hint : in $d = 1$, compute $G_0(x, x')$ for a negative energy $E = -\frac{k^2}{2m}$ and perform some analytic continuation.
In $d = 3$, show that $G_0^{(3D)}(\vec{r}, \vec{r}')$ can be related to a derivative of $G_0^{(1D)}(x, x')$ (after integrations over angles).

2/ Average Green's function in the presence of a weak disorder.– Assuming that the self energy is purely imaginary $\Sigma^{\mathrm{R}} = -\mathrm{i}/2\tau_e$, compute explicitly $\overline{G}^{\mathrm{R}}(\vec{r}, \vec{r}')$ for $d = 1, 3$.

Hint : express $\sqrt{2m(E_F + \mathrm{i}/2\tau_e)}$ in terms of k_F and ℓ_e.

Remark : cf. Appendix of chapter 10 of the book [118].

3) Self energy : stacking

1/ Recall the expression of the self energy at lowest order in the disorder, in terms of the free Green's function. Express its imaginary part.

2/ We now consider a particular class of diagrams :

$$\Sigma_{\text{stack}}^{\mathrm{R}} = \quad = \quad + \quad + \quad + \cdots \qquad \text{(IV.139)}$$

Deduce an equation for $\Sigma_{\text{stack}}^{\mathrm{R}}$ and solve it. Analyse the weak disorder limit $\epsilon_F \gg 1/\tau_e$.

TD 5 : Magneto-conductance of thin metallic films

The fit of the anomalous magneto-conductance of 2D electron gas (or metallic films) and wires is a powerful tool which has been extensively used in order to extract the phase coherence length L_φ of metallic devices at low T ($\lesssim$ few K). The fit of $\overline{\Delta\sigma}(\mathcal{B}, L_\varphi)$ is performed at several temperatures what allows to extract the temperature dependence $L_\varphi(T)$ and identify the microscopic mechanisms responsible for dephasing and/or decoherence.
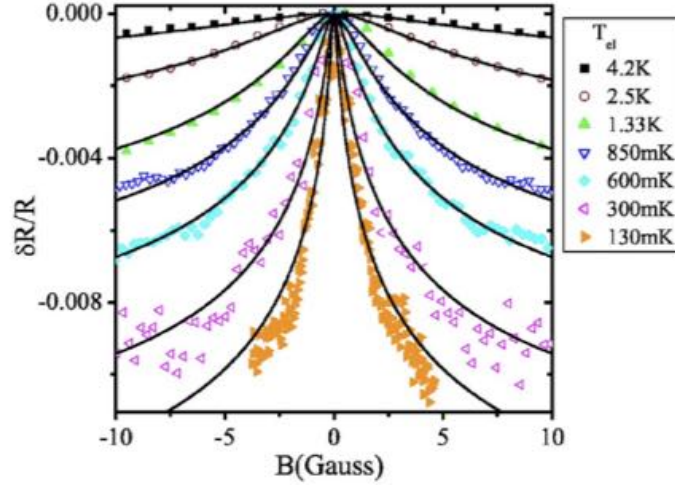
Figure 37: *Magnetoresistance curves for a 2DEG as a function of the magnetic field in Gauss (1 Gauss= 10^{-4} Tesla). From Ref. [57].*

We consider a two dimensional electron gas (2DEG) submitted to a perpendicular magnetic field $\mathcal{B}$. In this case it will be convenient to write the Cooperon as an integral of the propagator in time

$$\overline{\Delta\sigma} = -\frac{2_s e^2 D}{\pi\hbar} \int_0^\infty \mathrm{d}t\, \mathcal{P}_t(\vec{r}|\vec{r}) \left(\mathrm{e}^{-t/\tau_\varphi} - \mathrm{e}^{-t/\tilde{\tau}_e} \right) \tag{IV.140}$$

where the second exponential cut off the contribution of small times, that are not described by the diffusion approximation : $\tau_\varphi = L_\varphi^2/D$ and $\tilde{\tau}_e = \ell_e^2/D$. The factor 2_s is the spin degeneracy. The time propagator of the diffusion

$$\mathcal{P}_t(\vec{r}|\vec{r}') = \theta_{\mathrm{H}}(t) \, \langle \vec{r} | \mathrm{e}^{Dt\left(\vec{\nabla} - \frac{2\mathrm{i}e}{\hbar}\vec{A}\right)^2} | \vec{r}' \rangle \tag{IV.141}$$

solves the diffusion-like equation

$$\left[\partial_t - D \left(\vec{\nabla} - \mathrm{i}\frac{2e}{\hbar}\,\vec{A} \right)^2 \right] \mathcal{P}_t(\vec{r}|\vec{r}') = \delta(t)\delta(\vec{r} - \vec{r}') \tag{IV.142}$$

1/ Using the mapping onto the Landau problem, compute $\mathcal{P}_t(\vec{r}|\vec{r})$ in the plane.

Hint : We recall that the spectrum of eigenvalues of the 2D Hamiltonian $H_{\mathrm{Landau}} = -\frac{\hbar^2}{2m}(\vec{\nabla} - \frac{\mathrm{i}}{\hbar}e\vec{A})^2$ for a homogeneous magnetic field is the Landau spectrum $\varepsilon_n = \hbar\omega_c(n + 1/2)$ for $n \in \mathbb{N}$,

where $\omega_c = eB/m$ and where each Landau level has a degeneracy proportional to the surface of the plane $d_{\mathrm{LL}} = \frac{e\mathcal{B}\mathrm{Surf}}{h}$. The partition function of the Landau problem $Z_{\mathrm{Landau}} = \int \mathrm{d}\vec{r}\,\langle \vec{r}|\mathrm{e}^{-\frac{t}{\hbar}H_{\mathrm{Landau}}}|\vec{r}\rangle$ can be easily calculated.

2/ *a*) Using the integral given in the appendix, deduce that

$$\boxed{\overline{\Delta\sigma}(\mathcal{B}) = \frac{2_s e^2}{h}\frac{1}{2\pi}\left[\psi\left(\frac{1}{2} + \frac{L_{\mathcal{B}}^2}{L_\varphi^2}\right) - \psi\left(\frac{1}{2} + \frac{L_{\mathcal{B}}^2}{\ell_e^2}\right)\right]} \tag{IV.143}$$

where $L_{\mathcal{B}}$ will be related to the magnetic field.

b) What is the magnetic field corresponding to $L_{\mathcal{B}} = 1\,\mu\mathrm{m}$? And $L_{\mathcal{B}} = 20\,\mathrm{nm}$? Looking at the range of magnetic field on the experimental curve, argue that it is justified to simplify the result as

$$\overline{\Delta\sigma}(\mathcal{B}) = \frac{2_s e^2}{h}\frac{1}{2\pi}\left[\psi\left(\frac{1}{2} + \frac{L_{\mathcal{B}}^2}{L_\varphi^2}\right) - \ln\left(\frac{L_{\mathcal{B}}^2}{\ell_e^2}\right)\right] \tag{IV.144}$$

c) Analyse the zero field value $\overline{\Delta\sigma}(0)$. Discuss the limiting behaviours of $\overline{\Delta\sigma}(\mathcal{B}) - \overline{\Delta\sigma}(0)$.

3/ Discuss the experimental data of Fig. 37.

Appendix :

We give the integral (formula 3.541 of Gradshteyn & Ryzhik, Ref. [68])

$$\int_0^\infty \mathrm{d}x\,\frac{\mathrm{e}^{-ax} - \mathrm{e}^{-bx}}{\sinh \lambda x} = \frac{1}{\lambda}\left[\psi\left(\frac{1}{2} + \frac{b}{2\lambda}\right) - \psi\left(\frac{1}{2} + \frac{a}{2\lambda}\right)\right]\,, \tag{IV.145}$$

where $\psi(z) = \frac{\mathrm{d}}{\mathrm{d}z}\ln\Gamma(z)$ is the digamma function. We deduce the functional relation $\psi(z+1) = \psi(z) + \frac{1}{z}$. We give two values $\psi(1) = -\mathbf{C} \simeq -0.577215$ (Euler-Mascheroni constant) and $\psi(1/2) = -\mathbf{C} - 2\ln 2$, and the limiting behaviour

$$\psi(x + 1/2) \underset{x\to\infty}{=} \ln x + \frac{1}{24x^2} + \mathcal{O}(x^{-3}) \tag{IV.146}$$

5.2 Magneto-conductance in narrow wires

The aim of the exercice is to analyse the magneto-conductance of a long wire of section W submitted to a perpendicular *homogeneous* magnetic field. For simplicity we consider the two-dimensional situation of a wire etched in a two-dimensional electron gas (2DEG). We recall that the weak localisation correction to the conductivity is given by

$$\overline{\Delta\sigma} = -\frac{2_s e^2}{\pi\hbar}\, P_c(\vec{r},\vec{r}) \quad \text{with} \quad \left[\gamma - \left(\vec{\nabla} - \mathrm{i}\frac{2e}{\hbar}\,\vec{A}\right)^2\right] P_c(\vec{r},\vec{r}') = \delta(\vec{r}-\vec{r}')\,, \qquad \text{(IV.147)}$$

where $\gamma = 1/L_\varphi^2$.

We consider the geometry of a infinitly long quasi-1D wire, i.e. $x \in \mathbb{R}$ and $y \in [0,W]$.

1/ Relate the conductivity σ of the wire to the conductance $G = I/V$.

We choose the Landau gauge such that A_x is an **antisymmetric** function of the transverse coordinate. If $y \in [0,W]$ we choose $A_x(W-y) = -A_x(y)$, i.e.

$$A_x(y) = (W/2 - y)\,\mathcal{B} \quad \text{and} \quad A_y = 0\,. \qquad \text{(IV.148)}$$

We assume that the confinement imposes Neumann boundary conditions

$$\partial_y P_c(\vec{r},\vec{r}')\big|_{y=0\ \&\ W} = 0\,. \qquad \text{(IV.149)}$$

2/ Zero field.– The aim is to construct the spectrum of the Laplace operator $\Delta = \partial_x^2 + \partial_y^2$ in the wire.

a) Use the separability of the problem to find the spectrum of eigenvectors and eigenvalues of the Laplace operator in the infinitly long wire of width W.

b) **Green's function.**– Justify the following representation

$$P_c(\vec{r},\vec{r}') = \sum_{n=0}^{\infty} \chi_n(y)\, \underbrace{\langle x|\frac{1}{\gamma + \varepsilon_n - \partial_x^2}|x'\rangle}_{P_c(x,x')\ \text{for}\ \gamma\to\gamma+\varepsilon_n}\, \chi_n(y') \qquad \text{(IV.150)}$$

The functions $\chi_n(y)$ satisfy the differential equation $-\partial_y^2 \chi_n(y) = \varepsilon_n\, \chi_n(y)$ on $[0,W]$ with appropriate boundary conditions.

Under what condition on W and L_φ can the Cooperon be approximated by the 1D Cooperon $P_c(x,x') = \langle x|(\gamma - \partial_x^2)^{-1}|x'\rangle$?

3/ Weak magnetic field.– In the diffusion approximation, the Cooperon can be interpreted as the Green's function of the operator $-(\nabla - \frac{\mathrm{i}}{\hbar}2eA)^2$, Eq. (IV.147). We recall that this treatment of the magnetic field in the diffusion approximation supposes that $\ell_e \ll R_c$, where $R_c = v_F/\omega_c$ is the cyclotron radius of electrons with energy ε_F ($\omega_c = e\mathcal{B}/m_*$ is the cyclotron pulsation). Our aim is to compute the Cooperon in the weak magnetic field limit.

a) Projecting the differential equation (IV.147) (i.e. $\int_0^W \frac{\mathrm{d}y}{W} \times \cdots$), show that the effect of the magnetic field can be absorbed by a transformation of the phase coherence length in the one-dimensional cooperon

$$\frac{1}{L_\varphi^2} \longrightarrow \frac{1}{L_\varphi^{\text{eff}}(\mathcal{B})^2} \overset{\text{def}}{=} \frac{1}{L_\varphi^2} + \frac{1}{L_\mathcal{B}^2} \quad \text{where} \quad \frac{1}{L_\mathcal{B}^2} = \frac{4e^2}{\hbar^2}\int_0^W \frac{\mathrm{d}y}{W} A_x(y)^2\,. \qquad \text{(IV.151)}$$

b) Deduce explicitly $L_\mathcal{B}$ and discuss the range of validity of this approximation, i.e. what is the

condition on $\mathcal{B}$, W and L_φ ?

c) We recall the expression of the 1D Cooperon $P_c(x,x) = \langle x | \frac{1}{1/L_\varphi^2 - \partial_x^2} | x \rangle = L_\varphi/2$. Deduce the expression of the magneto-conductivity $\overline{\Delta\sigma}(\mathcal{B})$ of the infinitely long wire and show that the WL correction to the dimensionless conductance can be written as

$$\boxed{\overline{\Delta g}(\mathcal{B}) = \frac{\overline{\Delta g}(0)}{\sqrt{1 + (\mathcal{B}/\mathcal{B}_\varphi)^2}}} \tag{IV.152}$$

Give the expression of the scale $\mathcal{B}_\varphi$ and interpret physically this expression.

d) Discuss the experimental data of Fig. 38 at the light of this calculation. In particular, how can one interpret the evolution of the curve when the sample is cooled down ?
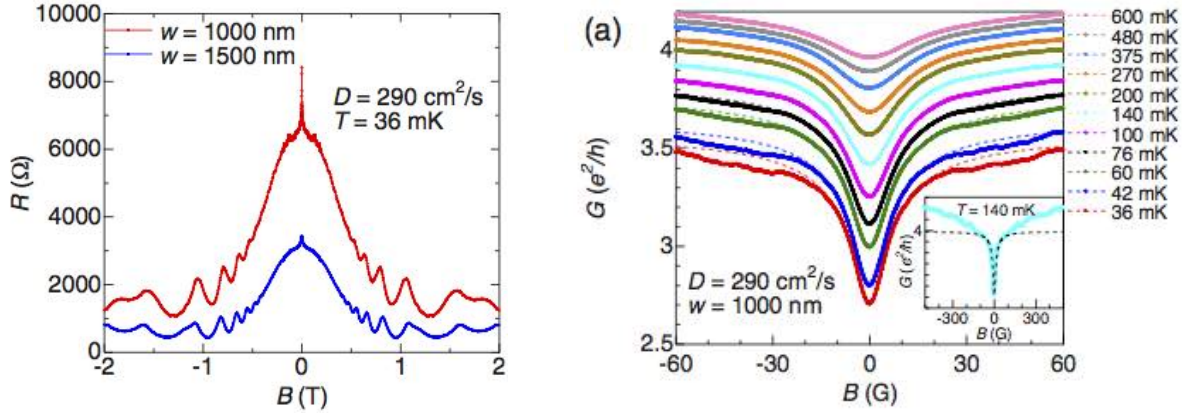
Figure 38: *Magnetoconductance curves for a long wire etched in a 2DEG as a function of the magnetic field in Gauss (1 Gauss= 10^{-4} Tesla). Length of the wire is $L = 150\,\mu$m, lithographic width $W_{\mathrm{litho}} = 1\,\mu$m and effective width $W = 630\,$nm. Electronic density is $n_e = 1.5 \times 10^{15}\,\mathrm{m}^{-2}$. Left : Resistance over a large window in $\mathcal{B}$ field, $[-2\,\mathrm{T}, +2\,\mathrm{T}]$. Right : Conductance over small window around zero field, $[-6\,\mathrm{mT}, +6\,\mathrm{mT}]$. From Niimi et al. Phys. Rev. B **81**, 245306 (2010) [100].*

e) In the "high field" regime, $L_\mathcal{B} < W$, what expression do you expect for the MC ?

Remarks :
• This analysis was performed in a well-known paper : by Altshuler and Aronov, Sov. Phys. JETP (1981) (Ref. [5]).

• **Semi-ballistic regime.**– Many experiments are performed on long wires etched in a two-dimensional electron gas (2DEG) at the interface of two semiconductors (GaAs/GaAl$_{1-x}$As$_x$). In this case the elastic mean free path $\ell_e^{(\mathrm{2D})}$ of the original 2DEG is usually larger than the section of the wire. The effective elastic mean free path in the wire is also larger than the section $\ell_e^{(\mathrm{1D})} > W$. The dephasing by the magnetic field involves different length scale due the phenomenon of flux cancellation. This has been described by semiclassical methods by Dugaev and Khmelnitskii [50] and Beenakker and van Houten, Phys. Rev. B (1988) (Ref. [21]).

TD 6 : Spin-orbit scattering and weak *anti*-localisation in metallic films

The magneto-resistance of films made of usual metals is not well described by the simple theory presented in the previous exercice session, i.e. by equation

$$\overline{\Delta\sigma}(\mathcal{B}) = \frac{2_s e^2}{h} \frac{1}{2\pi} \left[\psi\left(\frac{1}{2} + \frac{L_\mathcal{B}^2}{L_\varphi^2}\right) - \psi\left(\frac{1}{2} + \frac{L_\mathcal{B}^2}{\ell_e^2}\right) \right] \tag{IV.153}$$

The reason for this is that electronic spin degree of freedom cannot be ignored.

• First, the presence of spin-orbit coupling

$$H_{\mathrm{SO}} \sim -\frac{1}{m^2 c^2} (\vec{p} \times \vec{\nabla} V) \cdot \vec{S} \tag{IV.154}$$

is responsible for an additional phase originating from the rotation of the electronic spin, while the electron is scattered on the disordered potential V. Spin-orbit coupling is weak in light metals, like Lithium of Magnesium, but strong in heavy metals like Silver or Gold.

• Second, the presence of residual magnetic impurities is another source of electronic spin rotation :
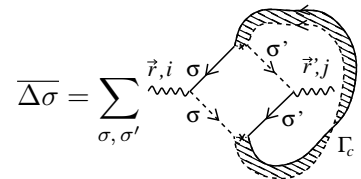
$$H_{\mathrm{mag}} = -\vec{S} \cdot \sum_i J_i \, \vec{s}_i \, \delta(\vec{r} - \vec{r}_i) \tag{IV.155}$$

where $\vec{r}_i$ are the positions of the magnetic impurities and $\vec{s}_i$ their spins (considered frozen).

The starting point of the study of quantum transport is the Kubo-Greenwood formula

$$\overline{\widetilde{\sigma}(\omega)} = \frac{e^2}{2\pi m^2} \frac{1}{\mathrm{Vol}} \sum_{k,\,k',\,\sigma,\,\sigma'} k_x \, k'_x \, \overline{G^{\mathrm{R}}_{\sigma,\sigma'}(k,k';\varepsilon_F + \omega) \, G^{\mathrm{A}}_{\sigma',\sigma}(k',k;\varepsilon_F)} \,, \tag{IV.156}$$

where the Green's function carry spin indices. Using that the average Green's function is diagonal in spin indices, we finally obtain the expression of the weak localisation correction

$$\overline{\Delta\sigma} = \sum_{\sigma,\sigma'} \quad \text{} \quad = -\frac{e^2}{\pi} \sum_{\sigma,\sigma'} P^{(c)}_{\sigma\sigma',\sigma'\sigma}(\vec{r},\vec{r}) \tag{IV.157}$$

where the Cooperon now propagates a pair of spins (Fig. 39).
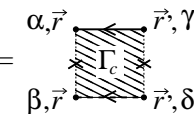
$$\Gamma^{(c)}_{\alpha\beta,\gamma\delta}(\vec{r},\vec{r}') = \quad \text{}$$

Figure 39: *In the presence of spin flip and spin-orbit scattering, the Cooperon depends on four spin indices.*
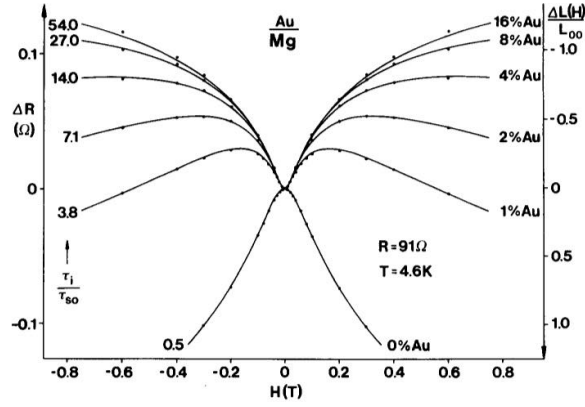
Figure 40: *Magneto-resistance curves for metallic films made of an alloy of Magnesium and Gold for difference concentration of gold. From Ref. [27].*

1/ Argue that the Cooperon $\Gamma^{(c)}_{\alpha\beta,\gamma\delta}(\vec{r},\vec{r}') = \frac{w}{D\tau_e} P^{(c)}_{\alpha\beta,\gamma\delta}(\vec{r},\vec{r}')$ can be written as the sum of two separate contributions associated with singlet and triplet channels.

2/ The efficiency of spin-orbit coupling and scattering by magnetic impurities are controlled by two lengths L_{so} and L_{m}. Introducing the projector in the singlet space, $(\Pi_0)_{\alpha\beta,\gamma\delta} = \frac{1}{2}(\delta_{\alpha\gamma}\,\delta_{\beta\delta} - \delta_{\alpha\delta}\,\delta_{\beta\gamma})$, we can write the Cooperon (in the space of the two spins) under the form

$$P^{(c)}(\vec{r},\vec{r}') = P_c(\vec{r},\vec{r}';1/L_S^2)\,\Pi_0 + P_c(\vec{r},\vec{r}';1/L_T^2)\,(1-\Pi_0)\,, \qquad \text{(IV.158)}$$

where $P_c(\vec{r},\vec{r}';\gamma) = \langle\vec{r}|\frac{1}{\gamma-\Delta}|\vec{r}'\rangle$ is the Cooperon in the absence of spin scattering. The two lengths L_S and L_T combine the effect of spin-orbit and magnetic impurities :

$$\frac{1}{L_S^2} = \frac{2}{L_m^2} \qquad \text{and} \qquad \frac{1}{L_T^2} = \frac{2}{3L_m^2} + \frac{4}{3L_{\text{so}}^2}\,. \qquad \text{(IV.159)}$$

Explain why $L_S > L_T$.

3/ Discuss the effect of time reversal in the singlet and triplet channel. Write $\overline{\Delta\sigma}$ in terms of $P_c(\vec{r},\vec{r}';1/L_{S,T}^2)$.

Hint : examine the spin structure in the diagram in Eq. (IV.157).

4/ Using the formula (IV.153) for the magneto-conductance of a thin film, deduce the expression of the weak localisation in the presence of spin-orbit and spin flip scattering. Explains (at least qualitatively) the experimental data of Fig. 40.

Further reading : A review article on weak localisation in thin metallic films is the famous article by Bergmann (1984) (Ref. [27]). A more intuitive description can be found in the review article of Chakravarty and Schmid (1986) (Ref. [36]).

V   Conductance fluctuations/correlations

An important aspect on which we have been elusive up to now is the question of how **disorder average** is realize. As we have pointed out, the theoretical tools can only provide information on *averaged* quantities, like the mean conductivity $\bar{\sigma}$. On the other hand, most of the experiments are performed on a *given sample*. Two questions immediatly arise : first, how can we understand that the weak localisation (an averaged quantity) describes so well the magnetoconductance of a given sample, as it was illustrated by showing several experimental data ? Second, can we characterize the *sample to sample* fluctuations (or correlations) of the conductance ?

V.A   Disorder averaging in large samples : heuristic analysis

We can answer to the first question by a simple qualitative argument. If a system is much larger than L_φ, electronic wave in different parts separated by L_φ do not interfere. When the system is splitted in pieces of size L_φ, they can therefore be considered as statistically *independent*. As an illustration, we consider a long wire of size $L \gg L_\varphi$. We recall that the *resistance* has additive properties : we introduce r_i, the resistance of a coherent piece, of size L_φ. The different pieces being incoherent, the classical law of addition of resistances holds

$$R \simeq \sum_{i=1}^{\mathcal{N}} r_i \qquad \text{where } \mathcal{N} = L/L_\varphi \, . \tag{V.1}$$

Weak localisation in a long wire.–   The resistance of each coherent part can be written as $r_i = r_i^{\text{cl}} + \Delta r_i$ where r_i^{cl} is the classical resistance and Δr_i the quantum correction. The quantum correction to the total resistance $\Delta R = R - R^{\text{cl}}$ can be related to the conductance correction

$$\underbrace{\Delta G}_{\text{one sample}} = -\frac{\Delta R}{R^2} = -\frac{\sum_i \Delta r_i}{\left(\sum_i r_i^{\text{cl}}\right)^2} \simeq -\frac{\mathcal{N} \, \overline{\Delta r}}{\left(\mathcal{N} \, r^{\text{cl}}\right)^2} = \frac{1}{\mathcal{N}} \, \overline{\Delta G_\varphi} \tag{V.2}$$

where we have introduced the weak localisation correction for the coherent piece $\overline{\Delta G_\varphi} = -\overline{\Delta r}/(r^{\text{cl}})^2$. We have shown above that $\overline{\Delta G_\varphi} = \frac{2_s e^2}{h} \overline{\Delta g_\varphi} \sim -e^2/h$. We have thus recovered the behaviour of the weak localisation correction

$$\underbrace{\Delta g}_{\text{one sample}} \sim -\frac{1}{\mathcal{N}} \overline{\Delta g_\varphi} \sim -\frac{L_\varphi}{L} \tag{V.3}$$

and shown how the measurement on a given sample, $\Delta g = g - g^{\text{cl}}$, can coincide with the averaged quantity, $\overline{\Delta g} \simeq -L_\varphi/L$.

Conductance fluctuations in a long wire.–   We can develope a similar argument in order to analyse the conductance fluctuations. We introduce the (sample to sample) fluctuation $\delta r_i = r_i - \overline{r_i}$ for the coherent piece of metal :

$$\overline{\delta G^2} \simeq \frac{\sum_{i,j} \overline{\delta r_i \delta r_j}}{\left(\sum_i r_i\right)^4} \simeq \frac{\mathcal{N} \, \overline{\delta r^2}}{\left(\mathcal{N} \, \overline{r}\right)^4} = \frac{1}{\mathcal{N}^3} \, \overline{\delta G_\varphi^2} \tag{V.4}$$

where $\overline{\delta G_\varphi^2}$ is the conductance fluctuation for a coherent metal. We deduce that the conductance fluctuations of the long wire behaves as

$$\overline{\delta g^2} \simeq \left(\frac{L_\varphi}{L}\right)^3 \overline{\delta g_\varphi^2} \, . \tag{V.5}$$

Naively, as we have seen that the quantum correction such as the weak localisation is $\Delta g_\varphi \sim 1$, we could expect that the fluctuations are also $\delta g_\varphi \sim 1$. However we rather have $\delta g_\varphi \lesssim 1$ due to the effect of thermal fluctuations which has not yet been discussed.

Effect of thermal fluctuations.— The conductance fluctuations of the coherent piece of metal $\overline{\delta g_\varphi^2}$ is controlled by two lengths : the phase coherence length L_φ and also the *thermal length*

$$L_T \overset{\text{def}}{=} \sqrt{\hbar D/k_B T} \, . \tag{V.6}$$

This second length scale has its origin in *thermal fluctuations*. We recall that the conductivity at finite temperature is a convolution of the zero temperature conductivity $\tilde{\sigma}(\varepsilon_F)$:

$$\sigma = \int \mathrm{d}\varepsilon \left(-\frac{\partial f}{\partial \varepsilon} \right) \tilde{\sigma}(\varepsilon) \, . \tag{V.7}$$

The average conductivity has no structure in energy, therefore the thermal smearing has no effect on averaged transport properties. On the other hand, the conductivity fluctuations $\overline{\delta \sigma^2}$ involves correlations at different energies :

$$\overline{\delta \sigma^2} = \int \mathrm{d}\varepsilon \mathrm{d}\varepsilon' \left(-\frac{\partial f}{\partial \varepsilon} \right) \left(-\frac{\partial f}{\partial \varepsilon'} \right) \overline{\delta\tilde{\sigma}(\varepsilon)\delta\tilde{\sigma}(\varepsilon')} = \int \mathrm{d}\omega \, \delta_T(\omega) \, \overline{\delta\tilde{\sigma}(\varepsilon_F)\delta\tilde{\sigma}(\varepsilon_F + \omega)} \tag{V.8}$$

where $\delta_T(\omega)$ is the convolution of the two derivatives of Fermi function, and therefore a narrow function of width $\sim T$. Correlations in energy decay over a characteristic energy scale which is the Thouless energy

$$E_{\text{Th}} = \frac{\hbar D}{L^2} \tag{V.9}$$

(we will prove this below by a detailed analysis of the correlator). Roughly, this can be understood from the structure of the diffusion propagator (diffusons and cooperons)

$$\langle r| \frac{1}{1/L_\varphi^2 - \mathrm{i}\omega/D - \Delta} |r'\rangle \tag{V.10}$$

involved in the conductance correlation : the denominator shows that we have to compare three scales :

(*i*)   the phase coherence length L_φ,

(*ii*)   the thermal length $\sqrt{D/T} = L_T$ (since $\omega \lesssim T$, we have $\sqrt{D/\omega} \gtrsim L_T$, hence the cutoff),

(*iii*)   the size L associated with the Laplacian (with eigenvalues $\sim 1/L^2$).

This has some consequence on the temperature dependence of the fluctuations $\overline{\delta \sigma^2}$ as the two Fermi functions constraint the two energies to be close, $|\varepsilon - \varepsilon'| \lesssim T$.

   In a coherent system ($L_\varphi > L$) and for $T \lesssim E_{\text{Th}}$, the conductance fluctuations are of order $\overline{\delta g^2} \sim 1$. On the other hand, when temperature is larger than the correlation energy, $T \gtrsim E_{\text{Th}}$, i.e. $L_T \lesssim L$, different energy shells of width E_{Th} can be considered as independent and the conductance fluctuations are reduced by a factor $\overline{\delta g^2} \sim E_{\text{Th}}/T = (L_T/L)^2$. This will be demonstrated by a precise calculation in the exercice.

   We can repeat the argument in the regime $L_\varphi < L$. If $L_T \gg L_\varphi$, the thermal smearing is negligible, hence $\overline{\delta g_\varphi^2} \sim 1$, however in the limit $L_T \ll L_\varphi$, it leads to a reduction of the fluctuations, by a factor $(L_T/L_\varphi)^2$. In conclusion, the conductance fluctuations of the long wire are

$$\overline{\delta g^2} \sim \begin{cases} (L_\varphi/L)^3 & \text{for } L_\varphi \ll L_T \ll L \\ L_T^2 L_\varphi/L^3 & \text{for } L_T \ll L_\varphi \ll L \end{cases} \tag{V.11}$$

The precise behaviours are obtained in the exercice (TD7).

Conclusion : this behaviour shows that the fluctuations are much smaller than the average

$$\delta g \sim \left(\frac{L_\varphi}{L}\right)^{3/2} \ll |\overline{\Delta g}| \sim \frac{L_\varphi}{L} \tag{V.12}$$

which explains which the weak localisation correction observed in *a single sample* of size $L \gg L_\varphi$, is very well described by the theoretical expression for the *averaged* correction to the conductance.

V.B Few experiments

1) Skocpol et al. (1986) :

Magneto-conductance measurements in coherent wires have been realised by Skocpol *et al* [112]. The conductance $g(B)$ of a given sample is shown on figure 41 for different gate voltages. It exhibits fluctuations of order $g \sim 1$ (i.e. $G \sim e^2/h$). The complicate erratic structure, perfectly reproducible (as soon as the disorder configuration is stable), represents the interference pattern characteristic of the disorder configuration : it is called the "**magneto-fingerprint**" of the sample.
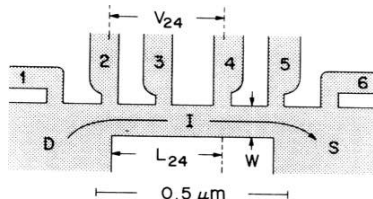
FIG. 1. Typical geometry of a MOSFET inversion layer with six voltage probes.
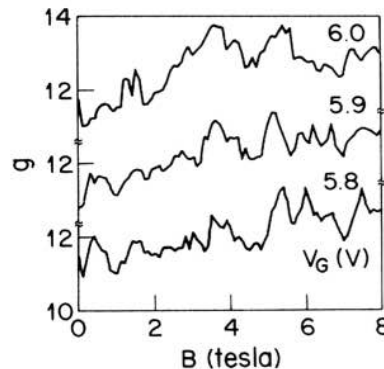
Figure 41: *Magneto-conductance of a short (coherent) wire in a 2DEG for different gate voltage. From [112].*

2) Mailly and Sanquer (1992) :

A remarkable experience was realised by Mailly and Sanquer [91] (Fig. 42) who were able to produce a set of 46 magneto-conductance (MC) curves associated with *different disorder configurations*. After having recorded a magneto-conductance curve, they changed the disorder configuration by heating the sample and injecting a high current pulse. The 46 MC curves are plotted on the figure. Then they perform some statistical analysis of the data by extracting the mean conductance and the variance.

The mean conductance $\overline{g(B)}$ shows a dip around zero field over a scale $B_c \sim 200$ Gauss, which we can identify with the weak localisation correction, which is expected to be present at zero field and vanish at high field. The form

$$\overline{\Delta g}(\mathcal{B}) = -\frac{L_\varphi}{L}\left(1 + \frac{1}{3}\left(\frac{e\mathcal{B}WL_\varphi}{\hbar}\right)^2\right)^{-1/2} \tag{V.13}$$
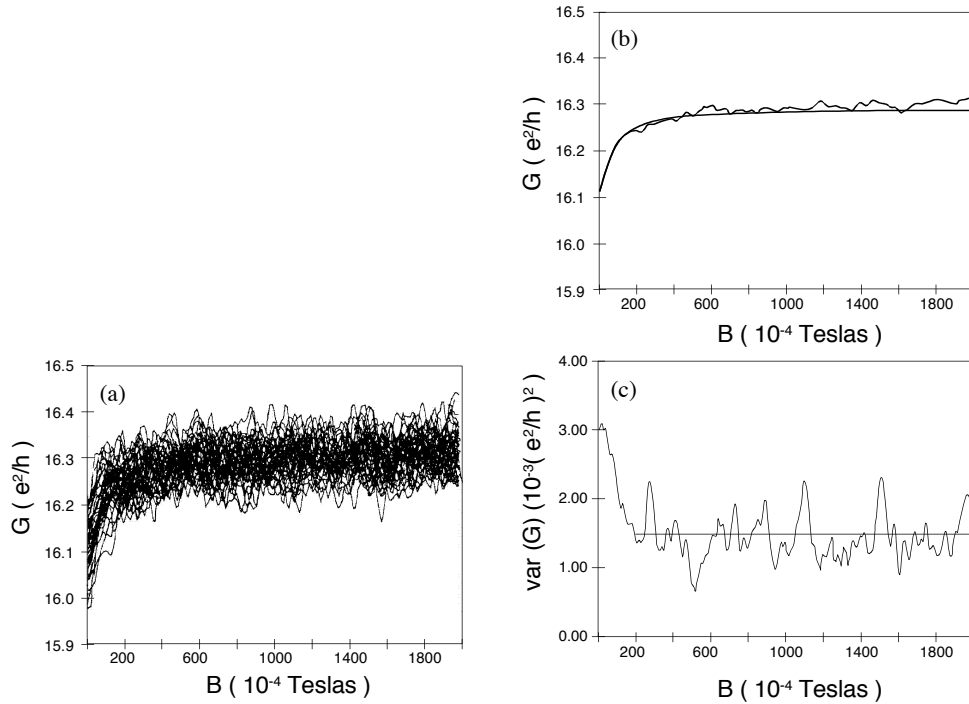
Figure 42: Left : *UCF : 46 MC curves obtained with a short (coherent) wire etched in a 2DEG* $(T = 45 \, \text{mK})$. *The different curves are obtained by modifying the disorder configuration.* Right : *Averaging the MC leads to the weak localisation. Figures of Ref. [91].*

has been obtained (see exercices, TD5), where W is the width of the wire.

Remarkably, the variance drops by a factor 2 over the same correlation field. We will explain precisely this behaviour in the exercice.

3) Correlation function :

Not only the variance of the conductance was extracted from experimental data but also the correlations $C(\Delta B) = \overline{G(B_0)G(B_0 + \Delta B)}$ (Fig. 43) : the correlation function was obtained from a given MC curve by sweeping the magnetic field B_0. The authors have assumed the equivalence of the two correlation functions $\int_{B_1}^{B_2} \frac{\mathrm{d}B_0}{B_2 - B_1} G(B_0)G(B_0 + \Delta B)$ and $C(\Delta B)$ (the "ergodic hypothesis").
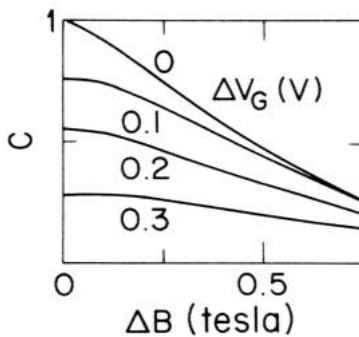
Figure 43: *Correlations* $\overline{G(B_0)G(B_0 + \Delta B)}$ *from the MC of a short wire in a 2DEG.* From [112].

110

V.C Conductivity correlations/fluctuations

In the spirit of what was done for the weak localisation, the identification of the diagrams providing the conductivity fluctuations requires to correlate two conductivity "bubbles", by connecting them with impurities lines. We have already discussed the importance of ladder diagrams. The game is then to couple the two bubbles with diffuson(s) and cooperon(s).

1) Identification of the four contributions (diagrams)

The first idea could be to introduce a single diffuson (or cooperon) to couple the two bubble (Fig. 44), however a precise calculation (which we do not perform here) shows that it is negligible.
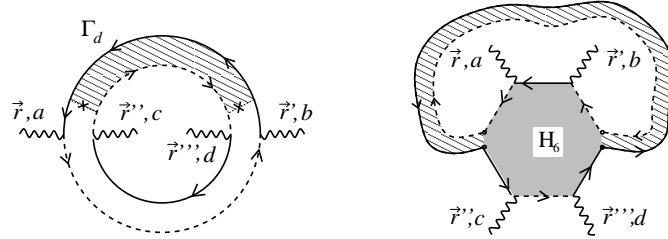
Figure 44: *A diagram that correlates the two conductivity bubbles with one diffuson only. The diagram of the right is a different representation that shows more clearly the short range nature of the contribution.*

Next we look at diagrams involving either two diffusons or two cooperons (one diffuson and one cooperon produces a more complicated diagram giving a negligible contribution again). We obtain the four diagrams in Fig. 45 (in fact sixt diagram if we account for the fact that diagrams equivalent to (c) and (d) can be obtained by exchanging R and A Green's function lines).
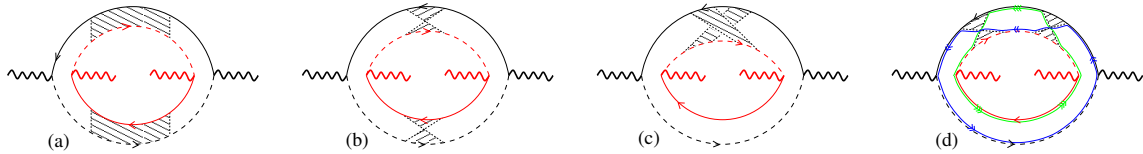
Figure 45: *Correlations of the two conductivity bubble with pairs of diffusons or cooperons.*

It is convenient to deform the diagrams of Fig. 45 and redraw them as follows

$$\mathcal{C}_{\mathrm{SR1}} = \qquad\qquad\qquad\qquad\qquad\qquad\qquad\qquad\qquad\qquad\qquad \tag{V.14}$$

$$\mathcal{C}_{\mathrm{SR2}} = \qquad\qquad\qquad\qquad\qquad\qquad\qquad\qquad\qquad\qquad\qquad \tag{V.15}$$

$$\mathcal{C}_{\mathrm{SR3}} = \qquad\qquad\qquad\qquad\qquad + \quad (\mathrm{R} \leftrightarrow \mathrm{A}) \tag{V.16}$$

$$\mathcal{C}_{\mathrm{SR4}} = \qquad\qquad\qquad\qquad\qquad + \quad (\mathrm{R} \leftrightarrow \mathrm{A}) \ , \tag{V.17}$$

which makes more clear the short range objects, small "*Hikami boxes*", and long range ones, diffusons and cooperon (remember that a line is an average Green's function line decaying as $\exp[-||r - r'||/(2\ell_e)]$ while a diffuson or a cooperon involves an arbitrary long sequence of scattering events, only limited by the phase coherence length). The second term in (V.16) and (V.17) correspond to exchange retarded Green's function and advanced one. The two first diagrams involves the same objects as the calculation of the weak localisation correction performes above : a small box (called a "Hikami box"), appearing twice (instead of once for the WL) on which are plugged two diffusons. We obtain the expressions :

$$\mathcal{C}_{\mathrm{SR1}} = 4 \left(\frac{2_s e^2}{h}\right)^2 \delta_{ac}\delta_{bd} \int \frac{\mathrm{d}^d \vec{r}\, \mathrm{d}^d \vec{r}'}{\mathrm{Vol}^2} \int \mathrm{d}\omega\, \delta_T(\omega) \left|P_d(\vec{r}, \vec{r}'; \omega)\right|^2 \tag{V.18}$$

$$\mathcal{C}_{\mathrm{SR2}} = 4 \left(\frac{2_s e^2}{h}\right)^2 \delta_{ad}\delta_{bc} \int \frac{\mathrm{d}^d \vec{r}\, \mathrm{d}^d \vec{r}'}{\mathrm{Vol}^2} \int \mathrm{d}\omega\, \delta_T(\omega) \left|P_c(\vec{r}, \vec{r}'; \omega)\right|^2 \tag{V.19}$$

$$\mathcal{C}_{\mathrm{SR3}} = 2 \left(\frac{2_s e^2}{h}\right)^2 \delta_{ab}\delta_{cd} \int \frac{\mathrm{d}^d \vec{r}\, \mathrm{d}^d \vec{r}''}{\mathrm{Vol}^2} \int \mathrm{d}\omega\, \delta_T(\omega)\, \mathrm{Re}\left[P_d(\vec{r}, \vec{r}''; \omega)\, P_d(\vec{r}'', \vec{r}; \omega)\right] \tag{V.20}$$

$$\mathcal{C}_{\mathrm{SR4}} = 2 \left(\frac{2_s e^2}{h}\right)^2 \delta_{ab}\delta_{cd} \int \frac{\mathrm{d}^d \vec{r}\, \mathrm{d}^d \vec{r}''}{\mathrm{Vol}^2} \int \mathrm{d}\omega\, \delta_T(\omega)\, \mathrm{Re}\left[P_c(\vec{r}, \vec{r}''; \omega)\, P_c(\vec{r}'', \vec{r}; \omega)\right] \ . \tag{V.21}$$

The thermal function is normalised, given by

$$\delta_T(\omega) = \frac{1}{2T}\, h\left(\frac{\omega}{2T}\right) \quad \text{with } h(x) = \frac{x \coth x - 1}{\sinh^2 x} \tag{V.22}$$

(see for example Appendix B of [124]). The precise shape of the function will play no role. It will be sufficient to use that $\int \mathrm{d}\omega\, \delta_T(\omega) = 1$ and $\delta_T(0) = 1/(6T)$.

The specific correlations of the indices follow from the fact that an Hikami box with indices a and b produces δ_{ab}. The correlation function is finally

$$\langle \delta\sigma_{ab}\, \delta\sigma_{cd}\rangle = \mathcal{C}_{\text{SR1}} + \mathcal{C}_{\text{SR2}} + \mathcal{C}_{\text{SR3}} + \mathcal{C}_{\text{SR4}}\,. \tag{V.23}$$

We can already provide some physiscal interpretation by inspection of the correlation of indices. Remember the Einstein relation $\sigma_{ab} = 2_s e^2 \rho\, D_{ab}$ relating the conductivity tensor to the density of states per spin channel ρ and the diffusion tensor D_{ab} (for isotropic material, $D_{ab} = D\,\delta_{ab}$). Einstein relation Since only the diffusion tensor carries inidces, one expect the structure

$$\langle \delta\sigma_{ab}\, \delta\sigma_{cd}\rangle = (2_s e^2)^2 \left[\rho^2 \left\langle \delta D_{ab}\, \delta D_{cd}\right\rangle + \left\langle \delta\rho^2\right\rangle D^2\, \delta_{ab}\delta_{cd}\right] \tag{V.24}$$

where we have assumed absence of correlations between ρ and D_{ab}. Comparison with the above expression shows that the two diagrams (V.14,V.15) can be interpreted as correlations of the diffusion constant, as they present non trivial correlations of indices, while the four diagrams (V.16,V.17) are related to density of states fluctuations, with trivial correlations of indices. This is corroborated by comparing to the density of state fluctuation diagrams (see Ref. [12], or Refs. [126, 124] for a more recent presentation).

We will see in the exercice how these contributions can be computed in a rather simple way (for a narrow wire).

2)   Effect of magnetic field

We have explained above, studying the weak localisation correction, how the introduction of the magnetic field affect the diffuson and the cooperon. Here, the novelty is that when considering the correlation function

$$\langle \delta\sigma_{ab}(\mathcal{B})\, \delta\sigma_{cd}(\mathcal{B}')\rangle$$

the Green's function lines associated with the two conductivity bubbles carry different magnetic phases associated with $\mathcal{B}$ or $\mathcal{B}'$. The diffuson involves lines in opposite directions, see (IV.70), while the cooperon involves lines going in the same direction, see (IV.79). Hence the diffusons and cooperons involved in (V.18,V.19,V.20,V.21) are

$$P_d(\vec{r},\vec{r}') = \langle\vec{r}\,|\frac{1}{1/L_\varphi^2 - \left(\vec{\nabla} - \frac{2\mathrm{ie}}{\hbar}\vec{A}_-\right)^2}|\,\vec{r}'\,\rangle \tag{V.25}$$

$$P_c(\vec{r},\vec{r}') = \langle\vec{r}\,|\frac{1}{1/L_\varphi^2 - \left(\vec{\nabla} - \frac{2\mathrm{ie}}{\hbar}\vec{A}_+\right)^2}|\,\vec{r}'\,\rangle \tag{V.26}$$

where

$$\vec{A}_\pm = \frac{\vec{A} \pm \vec{A}'}{2}\,. \tag{V.27}$$

For $\vec{A} = \vec{A}'$, the diffuson is independent of the magnetic field and we recover (IV.117), as it should.

Remark :   contrary to the diffuson involved in the calculation of $\bar{\sigma}$, which characterizes incoherent (classical) transport, the diffuson involved in the conductivity correlations originates from interference effects. This is why the cutoff of the phase coherence length is present in both the diffuson and the cooperon, which play purely symmetric roles here.

A simple consequence : We have noticed the symmetry between diffuson and cooperon diagrams, i.e. that diagrams (1) and (2) are symmetric under $P_d \leftrightarrow P_c$ and the same for diagrams (3) and (4). When $\mathcal{B} = \mathcal{B}'$, only the cooperon depends on the magnetic field, which provides another cutoff. Hence at strong field, cooperon contributions vanish while only diffuson contributions survive. This simple remark explain the observation made on the experimental data of Mailly and Sanquer :

$$\overline{\delta G(\mathcal{B})^2} \simeq \frac{1}{2}\overline{\delta G(0)^2} \qquad \text{for strong } \mathcal{B} \tag{V.28}$$

see Fig. 42.

3) Conductance correlations in the wire

In the exercice (TD7 below) we compute the correlation of the dimensionless conductance. We distinguish two regimes :

Thermal smearing negligible $(L_T \gg \min(L, L_\varphi))$: In this case we obtain

$$\overline{\delta g^2} = \frac{2}{15} \qquad \text{for } L_\varphi = \infty \tag{V.29}$$

$$\simeq 3\left(\frac{L_\varphi}{L}\right)^3 \qquad \text{for } L_\varphi \ll L \tag{V.30}$$

The second behaviour is in agreement with the behaviour discussed in the introduction of the chapter.

The correlator can also be obtained easily, by substitution of $1/L_\varphi^2 \to 1/L_\varphi^2 + 1/L_{(\mathcal{B}\mp\mathcal{B}')/2}^2$. In the limit $L_\varphi \ll L$, we get

$$\overline{\delta g(\mathcal{B})\delta g(\mathcal{B}')} \simeq \frac{3}{2}\left(\frac{L_\varphi}{L}\right)^3 \left\{ \left(1 + \frac{[e(\mathcal{B}-\mathcal{B}')WL_\varphi]^2}{12\hbar^2}\right)^{-3/2} + \left(1 + \frac{[e(\mathcal{B}+\mathcal{B}')WL_\varphi]^2}{12\hbar^2}\right)^{-3/2} \right\} \tag{V.31}$$

where the two terms corresponds to diffuson and cooperon contributions, respectively (W is the width of the wire). This suggests correlations decaying (at high field) as $\overline{\delta g(\mathcal{B})\delta g(\mathcal{B}')} \sim |\mathcal{B}-\mathcal{B}'|^{-3}$.

Thermal smearing dominant $(L_T \ll \min(L, L_\varphi))$: At "high" temperature, the effect of thermal fluctuations become important. Remember that this corresponds to averaging over independent shell of energy width $E_{\text{Thouless}} = D/L^2$. As we show in the exercice, this leads to the behaviour

$$\overline{\delta g^2} \simeq \frac{2\pi}{3}\frac{L_T^2 L_\varphi}{L^3} \tag{V.32}$$

when $L_T \ll L_\varphi \ll L$.

The correlations are obtained by the same substitution as for the first regime, leading to :

$$\overline{\delta g(\mathcal{B})\delta g(\mathcal{B}')} \simeq \frac{\pi}{3}\frac{L_T^2 L_\varphi}{L^3} \left\{ \left(1 + \frac{[e(\mathcal{B}-\mathcal{B}')WL_\varphi]^2}{12\hbar^2}\right)^{-1/2} + \left(1 + \frac{[e(\mathcal{B}+\mathcal{B}')WL_\varphi]^2}{12\hbar^2}\right)^{-1/2} \right\} \tag{V.33}$$

i.e. decay of correlations $\overline{\delta g(\mathcal{B})\delta g(\mathcal{B}')} \sim |\mathcal{B}-\mathcal{B}'|^{-1}$.

Remark : In pratice, at low temperature $(T \lesssim 1\,\text{K})$ the decoherence is dominated by electron-electron interaction (unless the presence of magnetic impurities). In this case, the phase coherence length satisfies the condition $L_T \ll L_\varphi$ (see Appendix B of chapter 5 of [121]).

V.D   AB versus AAS oscillations

Conductance fluctuations can also be revealed by studying magnetoconductance oscillations in devices with loops (ring, array of rings of large networks). The mangnetoconductance presents an erratic behaviour, with however regular periodic oscillations corresponding to a period $\phi_0 = h/e \simeq 41 \, \mathrm{Gauss}.\mu\mathrm{m}^2$ as a function of the flux through the ring. These are the **Aharonov-Bohm oscillations** (Fig. 30 and Fig. 46 below).[39]

Interestingly, the Aharonov-Bohm ϕ_0-periodic oscillations are clearly visible at strong field (right part of the left figure of Fig. 46). Around zero field, the oscillations are rather $\phi_0/2$-periodic : see the left part of the left figure of Fig. 46. Furthermore the $\phi_0/2$-periodic oscillations are more regular for $N = 30$ rings (below) than for $N = 1$ ring (top). This indicates that $\phi_0/2$-periodic oscillations are a consequence of *disorder averaging*.

Remember that the contribution of quantum interferences surviving disorder averaging are the interference of reversed trajectories. Such interference terms accumulate twice the magnetic phase $4\pi\phi/\phi_0$, hence the period $\phi_0/2$. These $\phi_0/2$-periodic oscillations are denoted the **Al'tshuler-Aronov-Spivak oscillations** [8]. Note that the phenomenon is the same as AB oscillations. As a matter of fact, AAS oscillations are part of the contributions of the second harmonic to the AB oscillations.

The Fig. 46 compare the oscillations around zero field, and in a window at strong magnetic field :

- Around zero field (left parts of the four figures) : $h/2e$ oscillations dominate. These are AAS oscillations of the averaged conductance.

- At large field (right parts of the four figures), h/e oscillations dominate. These are AB oscillations (fluctuations).
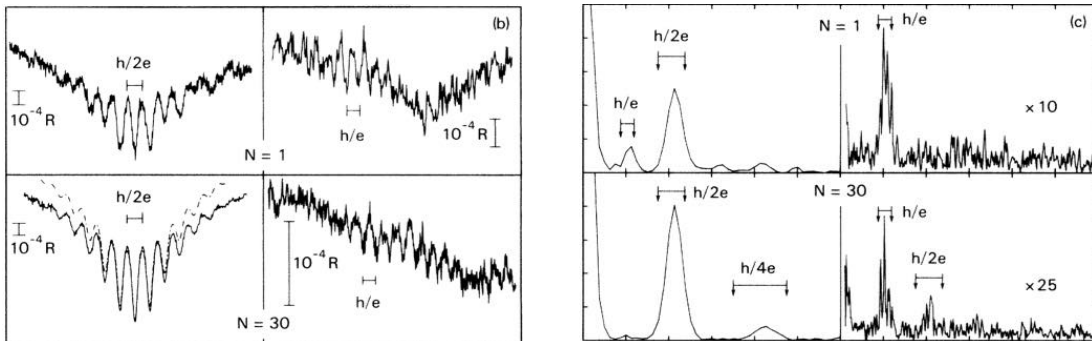

Figure 46: *Magneto-conductance of a single ring (top) and a series of* 30 *rings (bottom). The right part of the figure show the Fourier spectra: in a window centered on zero field (left) and in a window at high field (right). From [131].*

The amplitude of the AB and AAS oscillations have been studied in a series of rings (Fig. 47). Amplitude of AB oscillations decay with the number of rings, which is expected as AB oscillations corresponds to the conductance fluctuations. On the other hand, the AAS oscillation amplitude remains finite, in the same way as the weak localisation correction.

---

[39] In the ring, the electron can follow two trajectories, one in each arm, associated with two magnetic phases χ_1 and χ_2 such that $\chi_1 - \chi_2 = e\phi/\hbar$, where ϕ is the magnetic flux through the loop. Interference gives rise to the behaviour $G(\phi) \sim |e^{i\chi_1} + e^{i\chi_2}|^2 = \mathrm{cste} + \cos(2\pi\phi/\phi_0)$. Thus the conductance oscillates with a period $\phi_0 = h/e$. In the metallic ring, one should in principle account for the multiple scattering in each arm, which makes the conductance a non purely harmonic function.
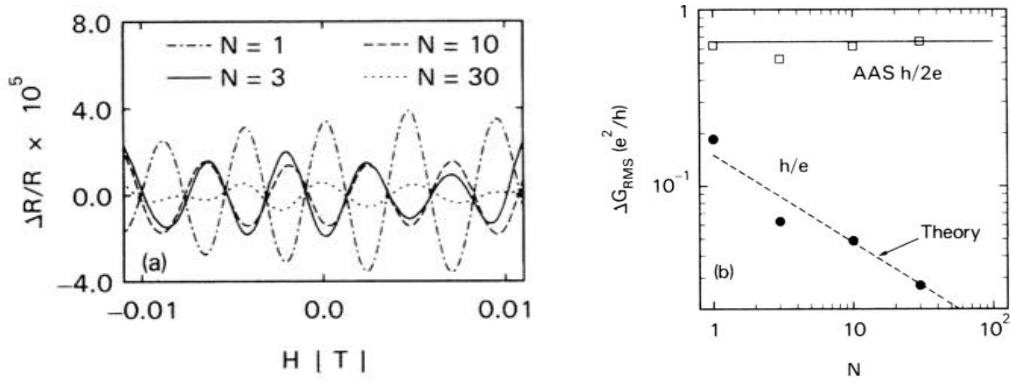
Figure 47: *AB and AAS amplitudes as a function of the number of rings. From [131].*

This has been further studied more recently in large networks of squares (Fig. 48). The sample are large networks with $N = N_x \times N_y$ loops. The size is changed keeping the same aspect ratio N_x/N_y fixed.
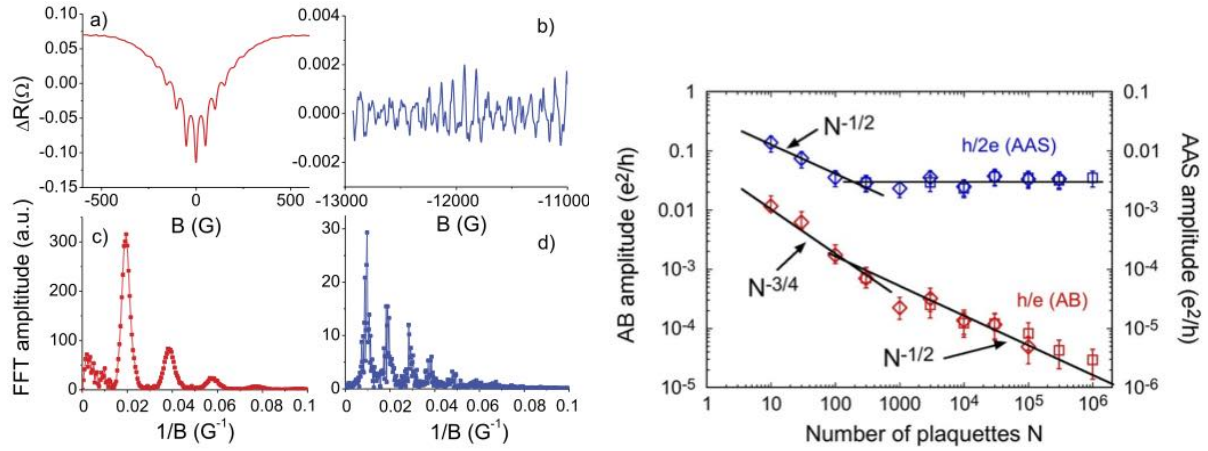

Figure 48: *AB and AAS amplitudes as a function of the number of plaquettes in large arrays. From [110].*

TD 7 : Conductance fluctuations and correlations in narrow wires

The purpose of the exercice is to analyse precisely the correlation function $\overline{\delta g(\mathcal{B})\delta g(\mathcal{B}')}$ for the dimensionless conductance of a narrow wire of length L and width W.
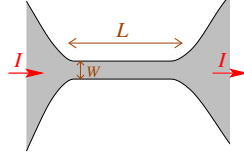
Figure 49: *Transport through a metallic wire of length L and width W.*

VI.E   Preliminary : weak localisation correction and role of boundaries

We recall that the weak localisation correction to the dimensionless conductance of a narrow wire ($W \ll L$) is given by

$$\overline{\Delta g} = -\frac{2}{L^2} \int_0^L \mathrm{d}x\, P_c(x,x) \tag{VI.34}$$

where the Cooperon solves $\left[\gamma - \partial_x^2\right] P_c(x,x') = \delta(x-x')$ where $\gamma = 1/L_\varphi^2$ encodes dephasing. We account for the connections at the two boundaries by imposing some Dirichlet boundary conditions $P_c(x,x')\big|_{x=0,L} = 0$.

1/ Show that the weak localisation correction can be expressed in terms of the spectrum of eigenvalues $\{\lambda_n\}$ of the Laplace operator in the wire (i.e. $-\partial_x^2\phi_n(x) = \lambda_n\phi_n(x)$ for $\phi_n(0) = \phi_n(L) = 0$).

2/ Write the weak localisation as $\overline{\Delta g} = -(2/L)\,\mathcal{G}(\gamma)$, where $\mathcal{G}(\gamma)$ is the spatial averaged Cooperon. Give $\mathcal{G}(\gamma)$ and analyse the limiting behaviours $L \gg L_\varphi$ and $L \ll L_\varphi$.

VI.F   Fluctuations and correlations

The correlation function for the narrow wire can be expressed as

$$\overline{\delta g(\mathcal{B})\delta g(\mathcal{B}')} = \frac{4}{L^2} \int \mathrm{d}\omega\, \delta_T(\omega) \int_0^L \frac{\mathrm{d}x\mathrm{d}x'}{L^2} \left[\left|P_d(x,x';\omega)\right|^2 + \frac{1}{2}\,\mathrm{Re}\left\{P_d(x,x';\omega)^2\right\} + (\, P_d \longrightarrow P_c\,) \right] \tag{VI.35}$$

where $\delta_T(\omega)$ is a normalised function of width T such that $\delta_T(0) = 1/(6T)$. The diffuson and cooperon solve

$$\left[-\mathrm{i}\omega/D + \gamma_{d,c} - \partial_x^2\right] P_{d,c}(x,x';\omega) = \delta(x-x')\,, \tag{VI.36}$$

where the expressions of the dephasing rates differ for diffuson and cooperon in the presence of a magnetic field :

$$\gamma_d = \frac{1}{L_\varphi^2} + \frac{1}{L_{\frac{\mathcal{B}-\mathcal{B}'}{2}}^2} \quad \text{and} \quad \gamma_c = \frac{1}{L_\varphi^2} + \frac{1}{L_{\frac{\mathcal{B}+\mathcal{B}'}{2}}^2} \quad \text{where} \quad L_\mathcal{B} = \sqrt{3}\,\frac{\hbar}{e|\mathcal{B}|W}\,. \tag{VI.37}$$

1/ Compare the fluctuations at zero field $\mathcal{B} = \mathcal{B}' = 0$ to the one at large field (no calculation).

2/ Show that the two diffuson contributions can be written in terms of the spectrum $\{\lambda_n\}$ under the form

$$\overline{\delta g(\mathcal{B})\delta g(\mathcal{B}')}^{(\text{diffuson})} = \frac{4}{L^3} \int d\omega \, \delta_T(\omega) \, \mathcal{F}(\gamma_\omega) \tag{VI.38}$$

where $\gamma_\omega = \gamma_d - i\omega/D$. Express the function $\mathcal{F}(\gamma_\omega)$ as a series.

3/ With the help of the representation obtained in the previous question, show that the expression of the correlator involves a new cutoff at the length given by the **thermal length** $L_T \overset{\text{def}}{=} \sqrt{D/T}$. Identify a "low temperature" regime and a "high temperature" regime by comparing the three lengths L_T, L_φ and L.

a) "Low" temperature regime ($L_T = \infty$)

In this case we simplify the calculation by performing the substitution $\delta_T(\omega) \to \delta(\omega)$ which allows for a straightforward integration over frequency.

1/ Show that the correlator $\overline{\delta g(\mathcal{B})\delta g(\mathcal{B}')}^{(\text{diffuson})}$ can be *formally* related to the weak localisation (i.e. that the two functions $\mathcal{F}(\gamma)$ and $\mathcal{G}(\gamma)$ are related).

2/ Analyse the limiting behaviours for $L \gg L_\varphi$ and $L \ll L_\varphi$. Recall the physical origin of the decay of $\overline{\delta g^2}$ with L/L_φ when $L \gg L_\varphi$.

3/ Adding the cooperon contribution, analyse the structure of the correlator as a function of the magnetic fields in the limit $L_\varphi \ll L$.

b) "High" temperature regime (small L_T)

1/ In the "high temperature" regime, justify the substitution $\delta_T(\omega) \to \delta_T(0)$ (the value $\delta_T(0)$ was given above). Deduce that the correlator $\overline{\delta g(\mathcal{B})\delta g(\mathcal{B}')}^{(\text{diffuson})}$ is simply related to the WL, i.e. expressed in terms of $\mathcal{G}(\gamma)$.

2/ Analyse the limiting behaviours for $L \gg L_\varphi$ and $L \ll L_\varphi$.

3/ Analyse the magnetic field dependence of the full correlator (diffuson and cooperon) when $L_\varphi \ll L$.

c) Experiment

The weak localisation correction $\overline{\Delta g(\mathcal{B})}$ and the conductance fluctuations $\overline{\delta g(\mathcal{B})^2}$ have been measured in a short wire etched in a 2DEG with a direct averaging procedure (Fig. 50). Discuss the experimental data at the light of your calculations.

Appendix

$$\sum_{n=1}^{\infty} \frac{1}{(n\pi)^2 + y^2} = \frac{1}{2y}\left(\coth y - \frac{1}{y}\right).$$

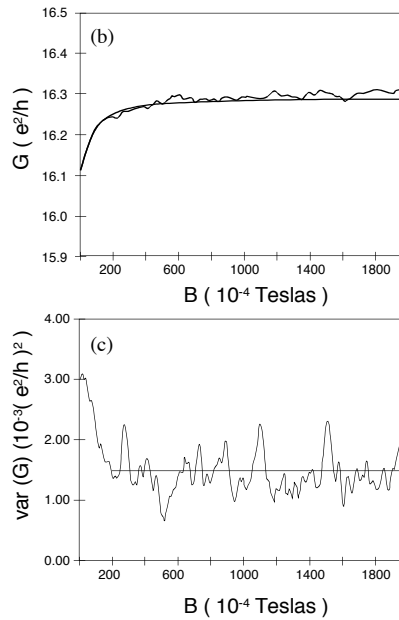$$\coth x = \frac{1}{x} + \frac{1}{3}x - \frac{1}{45}x^3 + \frac{2}{945}x^5 + \mathcal{O}(x^7).$$

Figure 50: *WL and CF of a short wire ($L \simeq 10\ \mu$m) etched in a 2DEG at $T = 45$ mK. Curves from Ref. [91].*

Further reading :

• The effect of boundary conditions in wires has been studied in the paper of Al'tshuler, Aronov and Zyuzin B. L. Al'tshuler, A. G. Aronov and A. Yu. Zyuzin, *Size effects in disordered conductors*, Sov. Phys. JETP **59**, 415 (1984).

• A measurement of conductance fluctuations with direct averaging over disorder configurations has been performed by Dominique Mailly and Marc Sanquer, *Sensitivity of quantum conductance fluctuations and $1/f$ noise to time reversal symmetry*, J. Phys. I France **2**, 357 (1992).

• For a recent theoretical paper (with a short review) : Christophe Texier & Gilles Montambaux, *Four-terminal resistances in mesoscopic networks of metallic wires: Weak localisation and correlations*, Physica E **75**, 33–46 (2016), special issue "*Frontiers in quantum electronic transport – in memory of Markus Büttiker*", available as preprint cond-mat arXiv:1506.08224.

7/ Correction de localisation faible du fil.– On rappelle que $\langle \Delta \sigma \rangle = -\frac{e^2}{\pi L} \int_0^L \mathrm{d}x \, P_c(x,x)$.

a) **Fil connecté cohérent.**– Construire la solution de l'équation $-\frac{\mathrm{d}^2}{\mathrm{d}x^2} P_c(x,x') = \delta(x-x')$ qui s'annule aux bords : $P_c(0,x') = P_c(L,x') = 0$. En déduire la correction à la conductance $\langle \Delta g \rangle$.

b) **Fil infini.**– Dans la limite $L \to \infty$ on utilise l'invariance par translation pour simplifier le calcul. Construire la solution invariante par translation de $(\frac{1}{L_\varphi^2} - \frac{\mathrm{d}^2}{\mathrm{d}x^2}) P_c(x,x') = \delta(x-x')$. En déduire $\langle \Delta g \rangle$.

9/ Déterminant spectral.– Lorsqu'il est légitime de considérer une conductivité *locale*, une manière très efficace de calculer différentes quantités est de considérer le déterminant spectral $S(\gamma) = \det(\gamma - \Delta)$. Pour des réseaux de fils, on rappelle que

$$S(\gamma) = \prod_{(\alpha\beta)} \frac{\sinh \sqrt{\gamma} l_{\alpha\beta}}{\sqrt{\gamma}} \, \det \mathcal{M} \qquad \text{(VI.39)}$$

où le produit porte sur tous les fils du réseau. La matrice $\mathcal{M}$ contient toute l'information sur le réseau. Cette matrice est de dimension $V \times V$ où V est le nombre de vertex. La matrice de conectivité est notée $a_{\alpha\beta}$ (on a $a_{\alpha\beta} = 1$ si $(\alpha\beta)$ est un fil et $a_{\alpha\beta} = 0$ sinon). $l_{\alpha\beta}$ désigne la longueur du fil $(\alpha\beta)$ et $\theta_{\alpha\beta}$ le flux magnétique.

$$\mathcal{M}_{\alpha\beta} = \delta_{\alpha\beta} \left(\lambda_\alpha + \sqrt{\gamma} \sum_\mu a_{\alpha\mu} \coth(\sqrt{\gamma} l_{\alpha\mu}) \right) - a_{\alpha\beta} \frac{\sqrt{\gamma} \, \mathrm{e}^{-\mathrm{i}\theta_{\alpha\beta}}}{\sinh(\sqrt{\gamma} l_{\alpha\beta})} \qquad \text{(VI.40)}$$

La présence de la matrice de connectivité dans $\sum_\mu a_{\alpha\mu} \cdots$ contraint la somme à porter sur les vertex voisins de α. Si le vertex α est connecté à un réservoir $\lambda_\alpha = \infty$, sinon $\lambda_\alpha = 0$.

a) Donner l'expression de $\mathcal{M}$ pour un fil isolé de longueur L. Calculer $S(\gamma)$.

b) Même question pour un fil connecté. On rappelle que

$$\langle \Delta \sigma \rangle = -\frac{e^2}{\pi} \frac{1}{\mathrm{Vol}} \frac{\partial}{\partial \gamma} \ln S(\gamma) \qquad \text{with } \gamma = 1/L_\varphi^2 \qquad \text{(VI.41)}$$

En déduire $\langle \Delta g \rangle$. Étudier les limites $L_\varphi \ll L$ et $L_\varphi \gg L$.

c) Montrer que pour un anneau isolé de périmètre L

$$S(\gamma) = 2(\cosh \sqrt{\gamma} L - \cos \theta) \qquad \text{(VI.42)}$$

où $\theta = 4\pi\phi/\phi_0$ est le flux réduit. Retrouver le résultat de Al'tshuler, Aronov & Sharvin (Sov. Phys. JETP, 1981). Déduire les harmoniques de la magnétoconductivité.

10/ Nonlocalité du cooperon.– On s'intéresse au réseau représenté sur la figure 51.

a) Que vaut la conductance classique g_{cl} ? On introduit la longueur $\mathcal{L}$ définie par $g_{\mathrm{cl}} = \alpha_d N_c \ell_e / \mathcal{L}$.

b) On rappelle que la correction de localisation faible est donnée en intégrant le cooperon dans le réseau, tout en pondérant l'intégrale le long d'un fil i par un poids $\partial \mathcal{L}/\partial l_i$:

$$\langle \Delta g \rangle = -\frac{2}{\mathcal{L}^2} \sum_i \frac{\partial \mathcal{L}}{\partial l_i} \int_{\mathrm{wire}\ i} \mathrm{d}x \, P_c(x,x) \qquad \text{(VI.43)}$$

Calculer les poids des fils a, b, c et d.

c) Le cooperon est solution de l'équation

$$\left[\frac{1}{L_\varphi^2} - \left(\frac{\mathrm{d}}{\mathrm{d}x} - 2\mathrm{i}eA\right)^2\right] P_c(x, x') = \delta(x - x') \tag{VI.44}$$

Rappeler le comportement de $P_c(x, x')$ pour $|x - x'| \gg L_\varphi$.

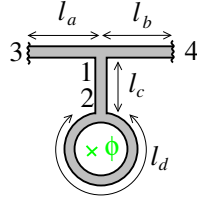d) Déduire le comportement des harmoniques de magnétoconductance en fonction de l_c et l_d.

Figure 51: Les lignes ondulées représentent les contacts aux réservoirs.

11/ Chaîne d'anneaux.– On considère la chaîne de N_r anneaux représentée sur la figure 52.

a) Que vaut la conductance classique g_{cl} de la chaîne ?
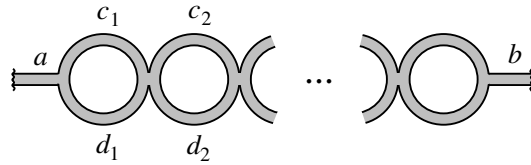
Figure 52: Chaîne d'anneaux

b) Déduire les poids des différents fils.

c) Montrer que dans la limite d'un grand nombre d'anneaux **symétriques** ($l_c = l_d = L/2$), $\langle \Delta g \rangle$ peut s'exprimer comme une intégrale uniforme du cooperon dans le réseau.

d) En négligeant les effets de bord, exprimer $\langle \Delta g \rangle$ en fonction du déterminant spectral.

e) Calculer le déterminant spectral d'une chaîne infinie d'anneaux. Pour cela on vérifie que la matrice $\mathcal{M}$ a une structure tridiagonale

$$\mathcal{M} = \begin{pmatrix} \ddots & -B & 0 & \\ -B & A & -B & 0 \\ 0 & -B & A & \ddots \\ & 0 & \ddots & \ddots \end{pmatrix} \tag{VI.45}$$

Calculer $\det \mathcal{M}$ (en admettant des conditions aux limites périodiques). Exprimer A et B en fonction de L, $\gamma = 1/L_\varphi^2$ et du flux réduit $\theta = 4\pi\phi/\phi_0$. Déduire $\langle \Delta g \rangle$.

f) Analyser la première harmonique AAS dans la limite $L_\varphi \ll L$. comparer avec le résultat de l'exercice 9.c.

12/ Correction Al'tshuler-Aronov à la densité d'états du fil infini.– On rappelle que la correction Al'tshuler-Aronov est donnée par :

$$\delta\rho(\varepsilon) = -\frac{\lambda_\rho}{2\pi} \int_0^\infty \mathrm{d}t \, \frac{\pi T t}{\sinh \pi T t} \, \mathcal{P}(t) \cos \varepsilon t \tag{VI.46}$$

où $\mathcal{P}(t) = \frac{1}{\mathrm{Vol}} \sum_n \mathrm{e}^{-E_n t}$. Les E_n sont les valeurs propres de l'équation de diffusion $-\Delta \psi_n = E_n \psi_n$.

a) Rappeler l'expression de $\mathcal{P}(t)$ pour le fil infini.

b) Calculer (VI.46) dans les limites $T \ll \varepsilon$ et $T \gg \varepsilon$.

13/ Longueur de Nyquist.– La longueur de Nyquist donne l'échelle de longueur sur laquelle l'interaction électron-électron détruit la cohérence de phase.

a) Montrer que la longueur de Nyquist

$$L_N = \left(\frac{\sigma_0 S D}{e^2 T} \right)^{1/3} \tag{VI.47}$$

peut s'écrire $L_N = \left(\frac{\alpha_d}{\pi} N_c \ell_e L_T^2 \right)^{1/3}$ où $L_T = \sqrt{D/T}$ est la longueur thermique, N_c le nombre de canaux et $\alpha_d = V_d / V_{d-1}$ où V_d est le volume de la sphère unité en dimension d.

b) *Application numérique.*
Calculer L_N pour l'échantillon Ag(6N)c de l'article : F. Pierre *et al*, Phys. Rev. B **68**, 085413 (2003). On donne : la longueur $L = 400 \, \mu\mathrm{m}$, la largeur $W = 105 \, \mathrm{nm}$, l'épaisseur : $t = 55 \, \mathrm{nm}$, la constante de diffusion $D = 185 \, \mathrm{cm}^2/\mathrm{s}$, et le vecteur de Fermi de l'argent : $k_F^{-1} = 0.85 \, \text{Å}$.

14/ Fluctuations de conductance.– On rappelle que les fluctuations de conductivité *locale* pour $L_\varphi \ll L_T$ s'expriment en fonction du déterminant spectral comme :

$$\langle \delta\sigma^2 \rangle = -6 \left(\frac{e^2}{h} \right)^2 \frac{1}{\mathrm{Vol}^2} \left[\frac{\partial^2}{\partial \gamma_d^2} \ln S(\gamma_d) + \frac{\partial^2}{\partial \gamma_c^2} \ln S(\gamma_c) \right] \tag{VI.48}$$

où $\gamma_d = 1/L_\varphi^2$ et $\gamma_c = 1/L_\varphi^2 + 1/L_\mathcal{B}^2$ avec $1/L_\mathcal{B} = \frac{e\mathcal{B}W}{\sqrt{3}\,\hbar}$.

a) À l'aide du calcul de l'exercice 9.b donner l'expression de $\langle \delta g^2 \rangle$ pour un fil connecté de longueur L. Étudier les limites $L_\varphi \ll L$ et $L_\varphi \gg L$.

b) Dans la limite $L_T \ll L_\varphi$ on montre en revanche que

$$\langle \delta\sigma^2 \rangle = \frac{2\pi}{3} \left(\frac{e^2}{h} \right)^2 \frac{L_T^2}{\mathrm{Vol}^2} \left[\frac{\partial}{\partial \gamma_d} \ln S(\gamma_d) + \frac{\partial}{\partial \gamma_c} \ln S(\gamma_c) \right] \tag{VI.49}$$

Exprimer $\langle \delta g^2 \rangle$ pour le fil connecté puis étudier les limites $L_\varphi \ll L$ et $L_\varphi \gg L$.

15/ Oscillations AB dans un anneau isolé.– Pour l'étude des corrélations paramétriques $\langle \delta\sigma(\mathcal{B}) \, \delta\sigma(\mathcal{B}') \rangle$ on utilise (VI.48,VI.49) où les contributions du diffuson et du cooperon sont calculées pour des champs magnétiques $(\mathcal{B} \mp \mathcal{B}')/2$. On négligera l'effet de pénétration du champ magnétique dans les fils pour simplifier.

a) Rappeler $\frac{\partial}{\partial \gamma} \ln S(\gamma)$ pour un anneau isolé. En déduire l'expression des corrélations paramétriques dans les limites $L_T \ll L_\varphi$ et $L_T \gg L_\varphi$.

b) Déduire l'amplitude des oscillations AB dans la limite $L_\varphi \ll L$.

16/ Oscillations AB dans la chaîne d'anneaux symétriques.– À l'aide des résultats de l'exercice 11, donner l'expression de l'amplitude des oscillations AB dans la limite $L_T \ll L_\varphi \ll L$.

$\boxed{\text{Annexe}}$

Règles de Feynman.– Pour le désordre gaussien défini par l'équation (**??**). Dans l'espace réciproque :

1. dessiner le diagramme, associer à chaque ligne une impulsion compatible avec la conservation des moments aux intersections.

2. chaque ligne est associée à une fonction de Green $G_0^{\mathrm{R}}(k)$ (ou $\overline{G}^{\mathrm{R}}(k)$).

3. une ligne d'impureté (double interaction avec le désordre) est associée à un facteur w/Vol.

4. on somme sur toutes les impulsions $\sum_k \equiv \int \frac{\mathrm{d}^d k}{(2\pi)^d}$.

Quelques intégrales.

$$\int_0^{2\pi} \frac{\mathrm{d}\theta}{2\pi} \frac{\sinh a}{\cosh a + \cos\theta} \, \mathrm{e}^{\mathrm{i}n\theta} \;=\; \mathrm{e}^{-|n|a} \tag{VI.50}$$

$$\int_0^\infty \mathrm{d}x \, x^{\mu-1} \cos ax \;=\; \frac{\Gamma(\mu)}{a^\mu} \cos\frac{\pi\mu}{2} \qquad 0 < \mathrm{Re}\,\mu < 1 \tag{VI.51}$$

$$\int_0^\infty \mathrm{d}x \, \frac{x^{\mu-1}}{\sinh ax} \;=\; \frac{2^\mu - 1}{2^{\mu-1}a^\mu} \, \Gamma(\mu)\,\zeta(\mu) \qquad \mathrm{Re}\,\mu > 1 \tag{VI.52}$$

$$\tag{VI.53}$$

VII   Coherent back-scattering

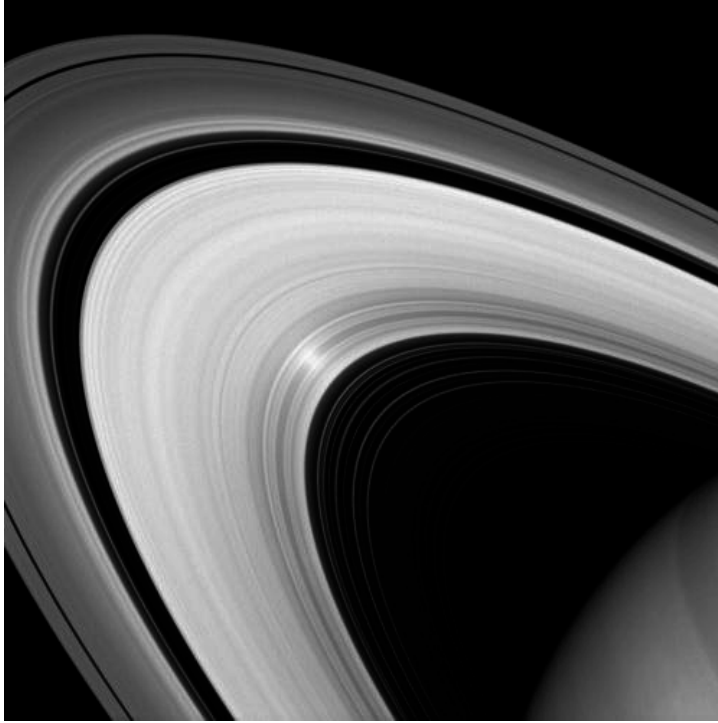

Figure 53: *Image of Saturn rings. The white spot is partly explained as a CBS (and partly by a shadow effect).* From `http://saturn.jpl.nasa.gov/`

VIII Toward strong disorder – Self consistent theory of localisation

Aim : After diagrammatic approach : come back on scaling theory and develope a quantitative analysis. I.e. use the weak localisation as a precursor of the strong localisation.

VIII.A Self-consistent theory of localization

A "mean field" like scaling theory of localization.
Ioffe-Regel criterion in 3D and the difficulty to observe the Anderson transition.

VIII.B Importance of symmetry properties

(Graphene may be discussed here).

VIII.C Transport by thermal hopping

transport between localised states (impurity states in a semiconductor)

$$\sigma(T) \sim \exp -(T_0/T)^{\alpha} \tag{VIII.1}$$

competition between thermal activation and

- tunneling (VRH)

- Coulomb interaction (Efros-Schklovskii)

IX Dephasing and decoherence

Aim : In chapter IV, we have seen that calculations require to introduce a large scale cutoff, denoted L_φ, that was put by hand. It is the purpose of the chapter to justify the introduction of cutoffs more rigorously.

More important : this chapter also emphasizes on the practical interest for studying such small corrections ($\lesssim \%1$) to transport coefficient for metals. Being a coherent property, the weak localisation may be used as a probe for quantum interference effects.

$\diamond$ Coupling with the environment and the induced dephasing.

$\diamond$ Microscopic processes leading to decoherence in solid state physics (phonons, magnetic impurities, electron-electron interaction...).

$\diamond$ Bloch oscillations and the restoration of classical transport in the presence of decoherence.

$\diamond$ Effect of decoherence on weak localization. Discussion of positive magneto-resistance in the presence of spin-orbit interaction.

$\diamond$ Effect of decoherence on CBS.

$\diamond$ Diffusive wave spectroscopy as a diagnostic tool in turbid media.

X   Interaction effects

X.A   Quantum (Altshuler-Aronov) correction to transport

- Useful practically : a local thermometer. Important for phase coherence measurement.
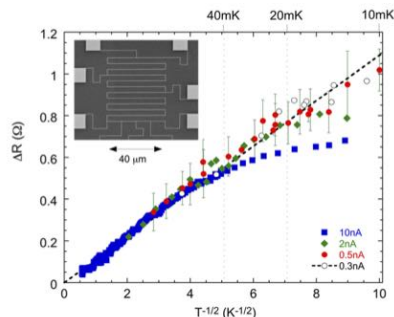
FIG. 2 (color online). Resistance variation of sample Au1 plotted as a function of $1/\sqrt{T}$ for different bias currents. The dotted line corresponds to the theoretical expectation for the resistance correction. The inset shows a scanning electron microscope photograph of the gold wire.

Figure 54: *Altshuler-Aronov correction to the conductivity of a long wire $\Delta\sigma_{\text{ee}} \propto -1/\sqrt{T}$. The deviation of the experimental data from the straight line for the largest current indicates a temperature larger than the fridge temperature, due to Joule heating ; from [18].*

- Importance for the scaling theory : In the presence of strong spin-orbit ("heavy" metals), there is no transition due to interaction.
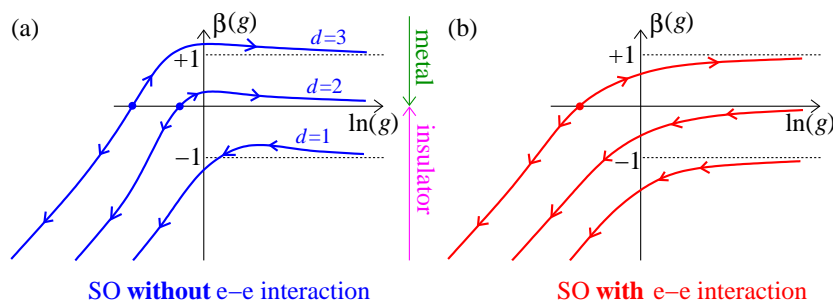
Figure 55: *Allure de la fonction $\beta(g) = \frac{\mathrm{d}\ln g}{\mathrm{d}\ln L}$ en présence de forte diffusion spin-orbite ; (a) sans prendre en compte les interactions électroniques ; (b) en les prenant en compte.*

X.B   Decoherence by electronic interactions

- Important : dominates at low T.

- Build a microscopic theory.

  Path integral $\rightarrow$ influence functional approach

  Extract typical length scales :
  $L_\varphi^{\text{ee}} \sim L_N \sim (L_T^2 \xi)^{1/3} \sim T^{-1/3}$ in 1D
  $L_N \sim T^{-1/2}$ in 2D The problem : short scale *versus* long scale cutoff

- Show recent experiments :
  F. Pierre, H. Pothier, N. Birge (2003)
  Saminadayar & Bäuerle, (2009) ; Niimi et al (2011)

X.C   More advanced topics (???)

⋄ Disordered superconductivity

⋄ Mean field approximation for condensed bosons, Gross-Pitaevskii equation. Effect of weak disorder, localization of Bogolyubov excitations in the presence of disorder. Interpretation of experimental results on cold atoms in terms of a classical fluid+percolation.

⋄ Beyond mean field : Mott insulator, MI/superfluid transition, Bose glass

⋄ Breaking of superfluidity by disorder. Recent experiments by Esslinger

TD 8 : Decoherence by electronic interactions – Influence functional approach

We have seen, within the diagrammatic approach, that the weak localisation (WL) correction to the conductivity $\overline{\Delta\sigma}$ involves a two particle propagator (in the particle-particle channel). In low dimensions ($d \leqslant 2$) and at low temperature ($T \lesssim 1$ K), the **dominant decoherence mechanism is the electronic interaction**. As we have seen, the interesting dependence of the WL in the phase coherence length L_φ arises from *large scale (infrared) cutoff*. The treatment of electronic interactions within diagrammatic technics is well formulated in the Fourier space, where small scale-high energy (ultraviolet) cutoff emerges naturally (due to the presence of Fermi distributions), but makes difficult a proper description of large scale cutoff : perturbation theory in Fourier space presents infrared divergences cut off usually by hand (see Fukuyama & Abrahams [61] ; the review by Chakravarty & Schmid [36]).

An alternative approach, pioneered by Al'tshuler, Aronov and Khmel'nitzkiĭ in 1982, was to follow an influence functional approach formulated in real space with path integral.

Let us first recall the expression of the WL seen in the lecture :

$$\overline{\Delta\sigma} = -\frac{2_s e^2}{\pi\hbar} D \int_0^\infty \mathrm{d}t\, \mathrm{e}^{-\Gamma_\varphi t} \overbrace{\int_{\vec{r}(0)=\vec{r}}^{\vec{r}(t)=\vec{r}} \mathcal{D}\vec{r}(\tau)\, \mathrm{e}^{-\int_0^t \mathrm{d}\tau\, \frac{1}{4D}\dot{\vec{r}}(\tau)^2}}^{\mathcal{P}_t(\vec{r}|\vec{r})} , \qquad (\mathrm{X}.1)$$

where the decoherence (cut off of large length scale $L \gtrsim L_\varphi = \sqrt{D/\Gamma_\varphi}$) was introduced by hand through an exponential damping with the rate Γ_φ. Our purpose is now to provide a microscopic theory justifying such a cutoff arising from electronic interactions.

Altshuler, Aronov and Khmelniskii have proposed to model interaction of a given electron with the surrounding electrons as the interaction with a fluctuating potential $V(\vec{r},t)$ (the vector potential was rather considered in the originial paper). Each contribution in (X.1) should be thus weighted by $\mathrm{e}^{\mathrm{i}\Phi_V}$, where

$$\Phi_V[\vec{r}(\tau)] = \frac{1}{\hbar} \int_0^t \mathrm{d}\tau \left[V(\vec{r}(\tau),\tau) - V(\vec{r}(\tau), t-\tau) \right] \qquad (\mathrm{X}.2)$$

is the phase peaked up by the two reversed electronic trajectories in the fluctuating field.

1/ Fluctuation-dissipation theorem.– The electric potential fluctuations are characterised by FDT (written in the classical regime $\hbar\omega \ll k_B T$)

$$\langle V(\vec{r},t)V(\vec{r}',t)\rangle_V \simeq \frac{2e^2 k_B T}{\sigma_0}\, \delta(t-t')\, P_d(\vec{r},\vec{r}') \qquad (\mathrm{X}.3)$$

where the Diffuson solves $-\Delta P_d(\vec{r},\vec{r}') = \delta(\vec{r}-\vec{r}')$. The Drude conductivity is $\sigma_0 = 2_s e^2 \rho_0 D$ where ρ_0 is the DoS per spin channel. Using the Gaussian nature of the fluctuations, perform averaging over potential fluctuations in $\langle \mathrm{e}^{\mathrm{i}\Phi_V} \rangle_V$. Show that the result can be interpreted in terms of a **trajectory dependent decoherent rate**

$$\overline{\Delta\sigma} = -\frac{2_s e^2}{\pi\hbar} D \int_0^\infty \mathrm{d}t \int_{\vec{r}(0)=\vec{r}}^{\vec{r}(t)=\vec{r}} \mathcal{D}\vec{r}(\tau)\, \mathrm{e}^{-\int_0^t \mathrm{d}\tau\, \frac{1}{4D}\dot{\vec{r}}(\tau)^2} \mathrm{e}^{-\Gamma_{\mathrm{ee}}[\vec{r}(\tau)]\, t} . \qquad (\mathrm{X}.4)$$

2/ Decoherence in a long wire.– In a long and narrow wire, justify the following expression of the diffuson :

$$P_d(\vec{r}, \vec{r}') \simeq -\frac{1}{2s}|x - x'| \tag{X.5}$$

where x measures the distance along the wire and s is the cross-section of the wire. Rescaling the variables in the path integral in order to deal with dimensionless coordinate and time, deduce the characteristic time scale and length scale controlling the decoherence in this case. Analyze the temperature dependence. Interpret physically the dependence of the phase coherent time with s and the diffusion constant D (remember FDT). Compare with experimental data.

Indication : The change of variable

$$\begin{cases} x = \lambda y \\ t = \eta \tau \end{cases} \tag{X.6}$$

is implemented in the path integral with the help of [40]

$$\int_{x(0)=0}^{x(t=\eta\tau)=\lambda y} \mathcal{D}x \, e^{-\int_0^t dt' \, (\dot{x}^2 + V(x))} = \frac{1}{\lambda} \int_{y(0)=0}^{y(\tau)=y} \mathcal{D}y \, e^{-\int_0^\tau d\tau' \, [\frac{\lambda^2}{\eta}\dot{y}^2 + \eta V(\lambda y)]}, \tag{X.8}$$

which can be interpreted as "$\mathcal{D}x = \frac{1}{\lambda}\mathcal{D}y$".
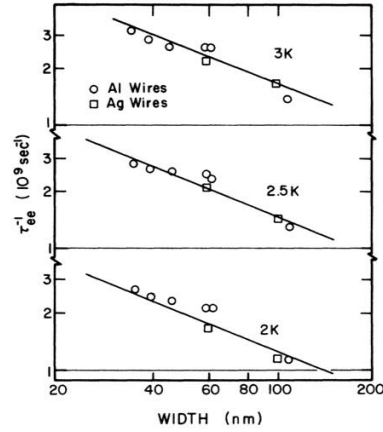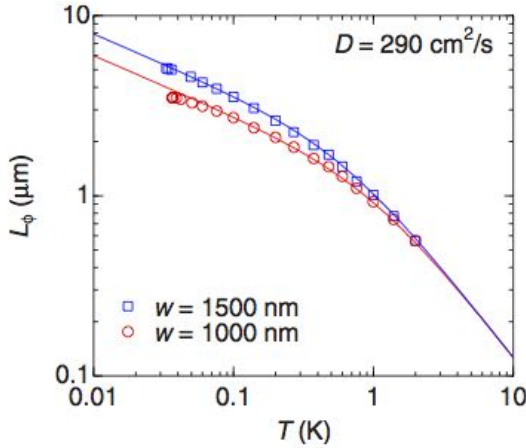
FIG. 3. Electron-electron contribution to $\tau_\phi^{-1} = $ [(total phase-breaking rate) − (electron-phonon rate = $A_{ep}T^3$)] as a function of wire width. The solid lines give the theoretical prediction of Eq. (1). The data are normalized to the $R_\square$ and D of samples Al2, according to Eq. (1).

Figure 56: **Left :** Phase coherence length at low T in wire etched in 2DEG ; from Ref. [100]. **Right :** The phase coherence time in Al and Ag wires as a function of the width ; from [143].

3/ Decoherence in confined geometry.– In a confined geometry, we may simply use the estimate $P_d(\vec{r}, \vec{r}') \sim \frac{1}{s}L$, where L is the size of the wire. Deduce the new temperature dependence of the phase coherence length.

In a recent experiment, the phase coherence lengths obtained in two different devices were compared : from the magneto-conductance of a long wire and the one from the analysis of the Aharonov-Bohm oscillations in a mesoscopic ring of perimeter $L \simeq 14\,\mu$m. Discuss the result (Fig. 57).

---

[40] Proof relies on the fact that

$$K_t(x|0) = \theta_{\mathrm{H}}(t) \int_{x(0)=0}^{x(t)=x} \mathcal{D}x \, e^{-\int_0^t dt' \, (\frac{1}{4}\dot{x}^2 + V(x))} \quad \text{solves} \quad \left(\frac{\partial}{\partial t} - \frac{\partial^2}{\partial x^2} + V(x)\right) K_t(x|0) = \delta(x)\,\delta(t). \tag{X.7}$$

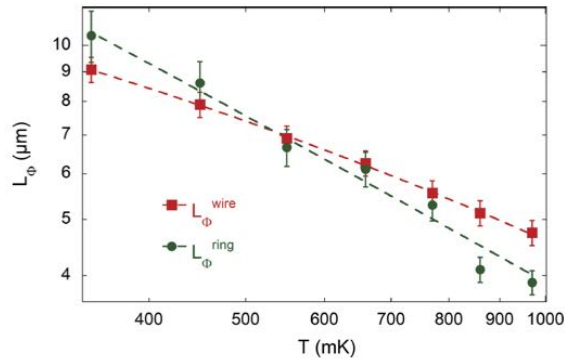FIG. 3. (Color online) Phase coherence lengths obtained in a wire, L_Φ^{wire}, and in a ring, L_Φ^{ring}, as a function of temperature. The dashed lines show the theoretical fit obtained with Eq. (2).

Figure 57: From Ref. [34].

The two-dimensional case : The study of the two-dimensional case along the same lines is more complicated because both large scale cutoff (well acounted for by the influence functional discussed above) and short scale cutoff (more naturally introduced in conventional perturbation theory in Fourier space) matter. The appropriate formulation within influence functional was finally achieved by Jan von Delft and collaborators [92, 136] (see also the review [135]. A more simple discussion was provided in Ref. [130].

Further reading :
• The famous paper : B. L. Altshuler, A. G. Aronov and D. E. Khmelnitsky [7].
• The pedagogical review : S. Chakravarty and A. Schmid [36].
• The present text is inspired by our article [122].

A Linear response theory

This is a piece of my lecture notes [117].

Consider the time dependent Hamiltonian

$$\hat{H}(t) = \hat{H}_0 - f(t)\,\hat{A} \tag{A.1}$$

where the time dependent perturbation is controlled by the force $f(t)$, coupled to the observable A. The question is to determine the quantum/statistical average of another observable B, under the form of an expansion in powers of the force

$$\langle \hat{B}(t) \rangle_f = \langle \hat{B} \rangle + \int \mathrm{d}t'\, \chi_{BA}(t - t')\, f(t') + \mathcal{O}(f^2)\,. \tag{A.2}$$

The question is now to determine the expression of the response function $\chi_{BA}(t)$, which can be done by using perturbation theory. We derive the formula (IV.8).

Density matrix.– Nous allons maintenant déterminer l'évolution de la moyenne de l'observable $\langle B(t) \rangle_f = \mathrm{Tr}\{\rho(t)B\}$ où la matrice densité encode l'information statistique et la dynamique, i.e. obéit à l'équation de von Neunmann (ou Liouville)

$$\frac{\mathrm{d}}{\mathrm{d}t}\rho(t) = \frac{\mathrm{i}}{\hbar}\left[\rho(t)\,,\,H(t)\right] \quad \text{avec } H(t) = H_0 + H_{\mathrm{pert}}(t) \tag{A.3}$$

pour $H_{\mathrm{pert}}(t) = -f(t)A$.

Représentation d'interaction.– Lorsqu'on développe une théorie de perturbation pour un problème dépendant du temps, il est naturel de commencer par "extraire" l'évolution libre en introduisant

$$\tilde{\rho}(t) \overset{\text{def}}{=} \mathrm{e}^{\mathrm{i}H_0 t/\hbar}\,\rho(t)\,\mathrm{e}^{-\mathrm{i}H_0 t/\hbar} \tag{A.4}$$

Ce faisant on reporte une partie de l'interaction sur les opérateurs (l'évolution libre) alors que les fonctions d'onde, ou plutôt la matrice densité, caractérise l'effet de la perturbation sur l'évolution. Ce point de vue intermédiaire entre les points de vue de Schrödinger (toute l'évolution est dans $\rho(t)$) et de Heisenberg (toute l'évolution est dans les observables) est appelée la *représentation d'interaction* :

$$\langle B(t) \rangle_f = \overbrace{\mathrm{Tr}\{\rho(t)\,B\}}^{\text{représ. de Schröd.}} = \overbrace{\mathrm{Tr}\{\tilde{\rho}(t)\,B(t)\}}^{\text{représ. d'inter.}} \quad \text{avec } B(t) = \mathrm{e}^{\mathrm{i}H_0 t/\hbar}\,B\,\mathrm{e}^{-\mathrm{i}H_0 t/\hbar}\,. \tag{A.5}$$

Nous obtenons facilement l'équation différentielle satisfaite par la matrice densité transformée :

$$\frac{\mathrm{d}}{\mathrm{d}t}\tilde{\rho}(t) = \frac{\mathrm{i}}{\hbar}\left[\tilde{\rho}(t)\,,\,H_I(t)\right] \tag{A.6}$$

où

$$H_I(t) \overset{\text{def}}{=} \mathrm{e}^{\mathrm{i}H_0 t/\hbar}H_{\mathrm{pert}}(t)\mathrm{e}^{-\mathrm{i}H_0 t/\hbar} = -f(t)A(t) \tag{A.7}$$

désigne la perturbation en représentation dîte "*d'interaction*".

Analyse perturbative.– L'équation (A.6) est maintenant parfaitement adaptée à la recherche de la solution sous la forme d'un développement en puissances de la perturbation $\rho(t) = \rho^{(0)}(t) + \rho^{(1)}(t) + \rho^{(2)}(t) + \cdots$ où $\rho^{(n)}(t) = O(f^n)$. Nous déduisons immédiatement la récurrence

$$\frac{\mathrm{d}}{\mathrm{d}t}\tilde{\rho}^{(n)}(t) = \frac{\mathrm{i}}{\hbar}\left[\tilde{\rho}^{(n-1)}(t),\, H_I(t)\right] \tag{A.8}$$

que nous résolvons en supposant que le système est initialement à l'équilibre thermodynamique : $\rho(-\infty) = \rho_0$ (c'est le cas si $f(-\infty) = 0$). Les conditions aux limites sont donc : $\rho^{(n)}(-\infty) = \rho_0\,\delta_{n,0}$, ce qui conduit à

$$\tilde{\rho}^{(n)}(t) = -\frac{\mathrm{i}}{\hbar}\int_{-\infty}^{t}\mathrm{d}t'\,f(t')\left[\tilde{\rho}^{(n-1)}(t'),\, A(t')\right] . \tag{A.9}$$

Finalement, si l'on se limite au premier ordre, nous obtenons

$$\tilde{\rho}(t) = \rho_0 - \frac{\mathrm{i}}{\hbar}\int_{-\infty}^{t}\mathrm{d}t'\,f(t')\left[\rho_0, A(t')\right] + O(f^2)\,, \tag{A.10}$$

qui permet de calculer $\langle B(t)\rangle_f = \mathrm{Tr}\left\{\tilde{\rho}(t)B(t)\right\}$. En remarquant que $\mathrm{Tr}\left\{[A,B]C\right\} = \mathrm{Tr}\left\{A[B,C]\right\}$, on aboutit au résultat

$$\boxed{\underbrace{\chi_{BA}(t)}_{\text{réponse}} = \frac{\mathrm{i}}{\hbar}\,\overbrace{\theta(t)}^{\text{causalité}}\,\underbrace{\langle[B(t),A]\rangle}_{\text{corrélation à l'équil.}}} = 2\mathrm{i}\theta(t)\,\xi_{BA}(t) = \theta(t)\,\beta\,K_{B\dot{A}}(t) \tag{A.11}$$

Nous venons donc d'identifier laquelle des fonctions de corrélation est reliée à la fonction de réponse. Insistons : cette fonction de réponse *dynamique*, coïncidant avec une fonction de corrélation *d'équilibre*, caractérise la façon dont le système réagit lorsqu'il est soumis à une perturbation extérieure, *i.e.* lorsqu'il est mis dans une situation *(faiblement) hors équilibre.*

References

[1] E. Abrahams, P. W. Anderson, D. C. Licciardello and T. V. Ramakrishnan, Scaling theory of localization: absence of quantum diffusion in two dimensions, Phys. Rev. Lett. **42**(10), 673 (1979).

[2] É. Akkermans and G. Montambaux, *Physique mésoscopique des électrons et des photons*, EDP Sciences, CNRS éditions (2004).

[3] E. Akkermans and G. Montambaux, *Mesoscopic physics of electrons and photons*, Cambridge University Press, Cambridge, UK (2007).

[4] A. Altland and B. Simons, *Condensed matter field theory*, Cambridge University Press (2006).

[5] B. L. Al'tshuler and A. G. Aronov, Magnetoresistance of thin films and of wires in a longitudinal magnetic field, JETP Lett. **33**(10), 499–501 (1981).

[6] B. L. Altshuler and A. G. Aronov, Electron-electron interaction in disordered conductors, in *Electron-electron interactions in disordered systems*, edited by A. L. Efros and M. Pollak, pp. 1–153, North-Holland, Amsterdam (1985).

[7] B. L. Altshuler, A. G. Aronov and D. E. Khmelnitsky, Effects of electron-electron collisions with small energy transfers on quantum localisation, J. Phys. C: Solid St. Phys. **15**, 7367 (1982).

[8] B. L. Al'tshuler, A. G. Aronov and B. Z. Spivak, The Aaronov-Bohm effect in disordered conductors, JETP Lett. **33**(2), 94 (1981).

[9] B. L. Al'tshuler, A. G. Aronov, B. Z. Spivak, D. Yu. Sharvin and Yu. V. Sharvin, Observation of the Aaronov-Bohm effect in hollow metal cylinders, JETP Lett. **35**(11), 588 (1982).

[10] B. L. Al'tshuler and P. A. Lee, Disordered Electronic Systems, Physics Today **41**, 36 (december 1988).

[11] B. L. Altshuler and V. N. Prigodin, Distribution of local density of states and NMR line shape in a one-dimensional disordered conductor, Sov. Phys. JETP **68**(1), 198–209 (1989).

[12] B. L. Al'tshuler and B. I. Shklovskiĭ, Repulsion of energy levels and conductivity of small metal samples, Sov. Phys. JETP **64**(1), 127–135 (1986).

[13] P. W. Anderson, Absence of diffusion in certain random lattices, Phys. Rev. **109**(5), 1492–1505 (1958).

[14] P. W. Anderson, D. J. Thouless, E. Abrahams and D. S. Fisher, New method for a scaling theory of localization, Phys. Rev. B **22**(8), 3519–3526 (1980).

[15] T. N. Antsygina, L. A. Pastur and V. A. Slyusarev, Localization of states and kinetic properties of one-dimensional disordered systems, Sov. J. Low Temp. Phys. **7**(1), 1–21 (1981).

[16] A. G. Aronov and Yu. V. Sharvin, Magnetic flux effects in disordered conductors, Rev. Mod. Phys. **59**(3), 755–779 (1987).

[17] N. W. Ashcroft and N. D. Mermin, *Solid State Physics*, Saunders College (1976).

[18] C. Bäuerle, F. Mallet, F. Schopfer, D. Mailly, G. Eska and L. Saminadayar, Experimental Test of the Numerical Renormalization Group Theory for Inelastic Scattering from Magnetic Impurities, Phys. Rev. Lett. **95**, 266805 (2005).

[19] R. J. Baxter, *Exactly Solved Models in Statistical Mechanics*, Academic Press, London (1982).

[20] C. W. J. Beenakker, Random-matrix theory of quantum transport, Rev. Mod. Phys. **69**(3), 731–808 (1997).

[21] C. W. J. Beenakker and H. Van Houten, Boundary scattering and weak localization of electrons in a magnetic field, Phys. Rev. B **38**(5), 3232 (1988).

[22] R. Bellman, Limit theorems for non-commutative operations. I., Duke Math. J. **21**(3), 491–500 (1954).

[23] Y. Benoist and J.-F. Quint, Random walks on reductive groups, volume 62 of *A series of modern surveys in Mathematics*, Springer (2016).

[24] V. L. Berezinskiĭ, Kinetics of a quantum particle in a one-dimensional random potential, Sov. Phys. JETP **38**(3), 620–627 (1974), [Zh. Eksp. Teor. Fiz. **65**, 1251 (1973)].

[25] V. L. Berezinskiĭ and L. P. Gor'kov, On the theory of electrons localized in the field of defects, Sov. Phys. JETP **50**(6), 1209 (1979).

[26] G. Bergmann, Consistent temperature and field dependence in weak localization, Phys. Rev. B **28**(2), 515 (1983).

[27] G. Bergmann, Weak localization in thin films, Phys. Rep. **107**(1), 1–58 (1984).

[28] T. Bienaimé and C. Texier, Localization for one-dimensional random potentials with large fluctuations, J. Phys. A: Math. Theor. **41**, 475001 (2008).

[29] J. Billy, V. Josse, Z. Zuo, A. Bernard, B. Hambrecht, P. Lugan, D. Clément, L. Sanchez-Palencia, P. Bouyer and A. Aspect, Direct observation of Anderson localization of matter-waves in a controlled disorder, Nature **453**, 891 (2008).

[30] D. Boosé and J.-M. Luck, Statistics of quantum transmission in one dimension with broad disorder, J. Phys. A: Math. Theor. **40**, 14045–14067 (2007).

[31] R. E. Borland, The nature of the electronic states in disordered one-dimensional systems, Proc. R. Soc. (London) **A274**, 529–545 (1963).

[32] J.-P. Bouchaud, A. Comtet, A. Georges and P. Le Doussal, Classical diffusion of a particle in a one-dimensional random force field, Ann. Phys. (N.Y.) **201**, 285–341 (1990).

[33] P. Bougerol and J. Lacroix, *Products of Random Matrices with Applications to Schrödinger Operators*, Birkhaüser, Basel (1985).

[34] T. Capron, C. Texier, G. Montambaux, D. Mailly, A. D. Wieck and L. Saminadayar, Ergodic versus diffusive decoherence in mesoscopic devices, Phys. Rev. B **87**, 041307 (2013).

[35] R. Carmona and J. Lacroix, *Spectral Theory of Random Schrödinger Operators*, Birkhaüser, Boston (1990).

[36] S. Chakravarty and A. Schmid, Weak localization: the quasiclassical theory of electrons in a random potential, Phys. Rep. **140**(4), 193–236 (1986).

[37] A. Cohen, Y. Roth and B. Shapiro, Universal distributions and scaling in disordered systems, Phys. Rev. B **38**(17), 12125–12132 (1988).

[38] A. Comtet, J. Desbois and C. Texier, Functionals of the Brownian motion, localization and metric graphs, J. Phys. A: Math. Gen. **38**, R341–R383 (2005).

[39] A. Comtet, J.-M. Luck, C. Texier and Y. Tourigny, The Lyapunov exponent of products of random 2×2 matrices close to the identity, J. Stat. Phys. **150**(1), 13–65 (2013).

[40] A. Comtet and C. Texier, One-dimensional disordered supersymmetric quantum mechanics: a brief survey, in *Supersymmetry and Integrable Models*, edited by H. Aratyn, T. D. Imbo, W.-Y. Keung and U. Sukhatme, Lecture Notes in Physics, Vol. **502** (available as arXiv:cond-mat/97 07 313), pp. 313–328. Springer (1998).

[41] A. Comtet, C. Texier and Y. Tourigny, Supersymmetric quantum mechanics with Lévy disorder in one dimension, J. Stat. Phys. **145**(5), 1291–1323 (2011).

[42] A. Comtet, C. Texier and Y. Tourigny, Lyapunov exponents, one-dimensional Anderson localisation and products of random matrices, J. Phys. A: Math. Theor. **46**, 254003 (2013), Special issue "Lyapunov analysis: from dynamical systems theory to applications".

[43] A. Crisanti, G. Paladin and A. Vulpiani, *Products of random matrices in statistical physics*, Springer-Verlag (1993), Springer Series in Solid-State Sciences vol. **104**.

[44] G. Czycholl, B. Kramer and A. MacKinnon, Conductivity and Localization of Electron States in One Dimensional Disordered Systems: Further Numerical Results, Z. Phys. B **43**, 5–11 (1981).

[45] S. Datta, *Electronic transport in mesoscopic systems*, Cambridge University Press, Cambridge, UK (1995).

[46] R. de Picciotto, H. L. Stormer, A. Yacoby, L. N. Pfeiffer, K. W. Baldwin and K. W. West, 2D-1D Coupling in Cleaved Edge Overgrowth, Phys. Rev. Lett. **85**(8), 1730 (2000).

[47] B. Derrida and E. J. Gardner, Lyapounov exponent of the one dimensional Anderson model: weak disorder expansions, J. Physique **45**(8), 1283–1295 (1984).

[48] O. N. Dorokhov, Transmission coefficient and the localization length of an electron in N bound disordered chains, JETP Lett. **36**(7), 318–321 (1982).

[49] O. N. Dorokhov, Solvable model of multichannel localization, Phys. Rev. B **37**(18), 10526–10541 (1988).

[50] V. K. Dugaev and D. E. Khmel'nitzkiĭ, Magnetoresistance of metal films with low impurity concentrations in parallel magnetic field, Sov. Phys. JETP **59**(5), 1038–1041 (1984).

[51] F. J. Dyson, The dynamics of a disordered linear chain, Phys. Rev. **92**(6), 1331–1338 (1953).

[52] S. F. Edwards and P. W. Anderson, Theory of spin glasses, J. Phys. F: Metal Phys. **5**(5), 965–974 (1975).

[53] K. Efetov, *Supersymmetry in disorder and chaos*, Cambridge University Press (1997).

[54] A. L. Efros and M. Pollak (editors), *Electron-electron interactions in disordered systems*, North-Holland (1985).

[55] V. J. Emery, Critical properties of many-component systems, Phys. Rev. B **11**(1), 239–247 (1975).

[56] F. A. Erbacher, R. Lenke and G. Maret, Multiple Light Scattering in Magneto-optically Active Media, Europhys. Lett. **21**(5), 551 (1993).

[57] M. Eshkol, E. Eisenberg, M. Karpovski and A. Palevski, Dephasing time in a two-dimensional electron Fermi liquid, Phys. Rev. B **73**(11), 115318 (2006).

[58] W. Feller, *An Introduction to Probability Theory and its Applications*, Wiley, New York (1971).

[59] I. Freund, M. Rosenbluh and S. Feng, Memory Effects in Propagation of Optical Waves through Disordered Media, Phys. Rev. Lett. **61**, 2328–2331 (Nov 1988).

[60] H. L. Frisch and S. P. Lloyd, Electron levels in a one-dimensional random lattice, Phys. Rev. **120**(4), 1175–1189 (1960).

[61] H. Fukuyama and E. Abrahams, Inelastic scattering time in two-dimensional disordered metals, Phys. Rev. B **27**(10), 5976–5980 (1983).

[62] H. Furstenberg, Noncommuting random products, Trans. Amer. Math. Soc. **108**, 377–428 (1963).

[63] H. Furstenberg and H. Kesten, Products of random matrices, Ann. Math. Statist. **31**(2), 457–469 (1960).

[64] Y. V. Fyodorov, P. Le Doussal, A. Rosso and C. Texier, Exponential number of equilibria and depinning threshold for a directed polymer in a random potential, Ann. Phys. **397**, 1–64 (2018).

[65] C. W. Gardiner, *Handbook of stochastic methods for physics, chemistry and the natural sciences*, Springer (1989).

[66] N. Giordano, W. Gilson and D. E. Prober, Experimental study of Anderson localization in thin wires, Phys. Rev. Lett. **43**(10), 725 (1979).

[67] A. Grabsch, C. Texier and Y. Tourigny, One-dimensional disordered quantum mechanics and Sinai diffusion with random absorbers, J. Stat. Phys. **155**(2), 237–276 (2014).

[68] I. S. Gradshteyn and I. M. Ryzhik, *Table of integrals, series and products*, Academic Press, fifth edition (1994).

[69] Y. Guivarc'h and A. Raugi, Frontière de Furstenberg, propriétés de contraction et théorèmes de convergence, Z. Wahrscheinlichkeitstheorie verw. Gebiete **69**(2), 187–242 (1985).

[70] B. I. Halperin, Green's Functions for a Particle in a One-Dimensional Random Potential, Phys. Rev. **139**(1A), A104–A117 (1965).

[71] J. M. Harrison, K. Kirsten and C. Texier, Spectral determinants and Zeta functions of Schrödinger operators on metric graphs, J. Phys. A: Math. Theor. **45**, 125206 (2012).

[72] K. Ishii, Localization of eigenstates and transport phenomena in the one dimensional disordered system, Prog. Theor. Phys. (Suppl.) **53**, 77–138 (1973).

[73] C. Itzykson and J.-M. Drouffe, *Théorie statistique des champs*, Interéditions–CNRS, Paris (1989), Tomes 1 et 2.

[74] R. Jackiw, δ-function potentials in two- and three-dimensional quantum mechanics, in *M. A. B. Bég memorial volume*, edited by A. Ali and P. Hoodbhoy, p. 1, World Scientific, Singapore (1991).

[75] M. Janßen, O. Viehweger, U. Fastenrath and J. Hajdu, *Introduction to the theory of the integer quantum Hall effect*, VCH, Weinheim (1994).

[76] G. Jona-Lasinio, Qualitative theory of stochastic differential equations and quantum mechanics of disordered systems, Helv. Phys. Act. **56**, 61 (1983).

[77] G. Junker, *Supersymmetric methods in quantum and statistical physics*, Springer (1996).

[78] M. Kappus and F. Wegner, Anomaly in the band centre of the one-dimensional Anderson model, Z. Phys. B **45**(1), 15–21 (1981).

[79] W. Kirsch, An invitation to Random Schrödinger operators (2007), extended version of the course given at the Summer School organised by Frédéric Klopp, États de la recherche: opérateurs de Schrödinger aléatoires, 2002, preprint arXiv:0709.3707.

[80] K. Kirsten and P. Loya, Computation of determinants using contour integrals, Am. J. Phys. **76**, 60–64 (2008).

[81] B. Kramer and A. MacKinnon, Localization: theory and experiment, Rep. Prog. Phys. **56**(12), 1469–1564 (1993).

[82] J. S. Langer and T. Neal, Breakdown of the concentration expansion for the impurity resistivity of metals, Phys. Rev. Lett. **16**(22), 984 (1966).

[83] E. Le Page, *Théorèmes limites pour les produits de matrices aléatoires*, pp. 258–303, Lecture notes in Math. n°928, Springer Verlag (1983).

[84] P. A. Lee and T. V. Ramakrishnan, Disordered electronic systems, Rev. Mod. Phys. **57**(2), 287–337 (1985).

[85] J. C. Licini, G. J. Dolan and D. J. Bishop, Weakly Localized Behavior in Quasi-One-Dimensional Li Films, Phys. Rev. Lett. **54**(14), 1585 (1985).

[86] E. H. Lieb and D. C. Mattis, *Mathematical Physics in one dimension – Exactly solvable models of interacting particles*, Academic Press, New York and London (1966), collection "*Perspective in Physics*".

[87] I. M. Lifshits, S. A. Gredeskul and L. A. Pastur, *Introduction to the theory of disordered systems*, John Wiley & Sons (1988).

[88] J.-M. Luck, *Systèmes désordonnés unidimensionnels*, CEA, collection Aléa Saclay, Saclay (1992).

[89] P. Lugan, A. Aspect, L. Sanchez-Palencia, D. Delande, B. Grémaud, C. A. Müller and C. Miniatura, One-dimensional Anderson localization in certain correlated random potentials, Phys. Rev. A **80**, 023605 (2009).

[90] A. MacKinnon and B. Kramer, One-Parameter Scaling of Localization Length and Conductance in Disordered Systems, Phys. Rev. Lett. **47**(21), 1546–1549 (1981).

[91] D. Mailly and M. Sanquer, Sensitivity of quantum conductance fluctuations and $1/f$ noise to time reversal symmetry, J. Phys. I France **2**, 357–364 (1992).

[92] F. Marquardt, J. von Delft, R. A. Smith and V. Ambegaokar, Decoherence in weak localization. I. Pauli principle in influence functional, Phys. Rev. B **76**, 195331 (2007).

[93] H. Matsuda and K. Ishii, Localization of Normal Modes and Energy Transport in the Disordered Harmonic Chain, Prog. Theor. Phys. Suppl. **45**, 56–86 (1970).

[94] R. A. Matula, Electrical resistivity of Copper, Gold, Palladium and Silver, J. Phys. Chem. Ref. Data **8**(4), 1147–1298 (1979).

[95] P. A. Mello and N. Kumar, *Quantum transport in mesoscopic systems – Complexity and statistical fluctuations*, Oxford University Press (2004).

[96] P. A. Mello, P. Pereyra and N. Kumar, Macroscopic approach to multichannel disordered conductors, Ann. Phys. (N.Y.) **181**, 290–317 (1988).

[97] T. Micklitz, A. Altland and J. S. Meyer, Low-energy theory of disordered interacting quantum wires, preprint pp. cond–mat arXiv:0805.3677 (2008).

[98] S. A. Molčanov, The local structure of the spectrum of the one-dimensional Schrödinger operator, Commun. Math. Phys. **78**(3), 429–446 (1981).

[99] T. M. Nieuwenhuizen, Exact electronic spectra and inverse localization lengths in one-dimensional random systems, Physica A **120**, 468–514 (1983).

[100] Y. Niimi, Y. Baines, T. Capron, D. Mailly, F.-Y. Lo, A. D. Wieck, T. Meunier, L. Saminadayar and C. Bäuerle, Quantum coherence at low temperatures in mesoscopic systems: Effect of disorder, Phys. Rev. B **81**, 245306 (2010).

[101] A. J. O'Connor, A central limit theorem for the disordered harmonic chain, Commun. Math. Phys. **45**(1), 63–77 (1975).

[102] F. Pierre, A. B. Gougam, A. Anthore, H. Pothier, D. Esteve and N. O. Birge, Dephasing of electrons in mesoscopic metal wires, Phys. Rev. B **68**, 085413 (2003).

[103] N. Pottier, *Mécanique statistique hors d'équilibre : processus irréversibles linéaires*, EDP Sciences – CNRS Éditions (2007), version publiée d'un cours du DEA de physique des solides, disponible sur le site du CCSD http://cel.archives-ouvertes.fr/, référence cel–00092930.

[104] R. Prange and S. Girvin (editors), *The quantum Hall effect*, Springer-Verlag, New York (1990).

[105] K. Ramola and C. Texier, Fluctuations of random matrix products and 1D Dirac equation with random mass, J. Stat. Phys. **157**(3), 497–514 (2014).

[106] H. Risken, *The Fokker-Planck Equation: Methods of Solution and Applications*, Springer, Berlin (1989).

[107] L. Sanchez-Palencia and M. Lewenstein, Disordered quantum gases under control, Nature Phys. **6**(2), 87–95 (2010).

[108] P. Santhanam, S. Wind and D. E. Prober, One-dimensional electron localization and superconducting fluctuations in narrow aluminium wires, Phys. Rev. Lett. **53**(12), 1179 (1984).

[109] H. Schmidt, Disordered one-dimensional crystals, Phys. Rev. **105**(2), 425–441 (1957).

[110] F. Schopfer, F. Mallet, D. Mailly, C. Texier, G. Montambaux, C. Bäuerle and L. Saminadayar, Dimensional crossover in quantum networks: from mesoscopic to macroscopic physics, Phys. Rev. Lett. **98**, 026807 (2007).

[111] D. Yu. Sharvin and Yu. V. Sharvin, Magnetic-flux quantization in a cylindrical film of a normal metal, JETP Lett. **34**(5), 272 (1981).

[112] W. J. Skocpol, P. M. Mankiewich, R. E. Howard, L. D. Jackel, D. M. Tennant and A. D. Stone, Universal Conductance Fluctuations in Silicon Inversion-Layer Nanostructures, Phys. Rev. Lett. **56**(26), 2865 (1986).

[113] P. Středa, Theory of quantised Hall conductivity in two dimensions, J. Phys. C: Solid St. Phys. **15**, L717 (1982).

[114] P. Středa and L. Smrčka, Transport coefficient in strong magnetic fields, J. Phys. C: Solid St. Phys. **16**, L895 (1983).

[115] C. Texier, *Quelques aspects du transport quantique dans les systèmes désordonnés de basse dimension*, Ph.D. thesis, Université Paris 6 (1999), `http://lptms.u-psud.fr/christophe_texier/` or , `http://tel.archives-ouvertes.fr/tel-01088853`.

[116] C. Texier, Individual energy level distributions for one-dimensional diagonal and off-diagonal disorder, J. Phys. A: Math. Gen. **33**, 6095–6128 (2000).

[117] C. Texier, *Physique statistique (faiblement) hors équilibre : formalisme de la réponse linéaire. Application à l'étude de la dissipation quantique et du transport électronique* (2013), notes de cours du DEA de physique quantique, École Normale Supérieure, disponible à l'adresse `http://www.lptms.u-psud.fr/christophe_texier/`.

[118] C. Texier, *Mécanique quantique*, Dunod, Paris, second edition (2015).

[119] C. Texier, Fluctuations of the product of random matrices and generalized Lyapunov exponent, J. Stat. Phys. **181**(3), 990–1051 (2020).

[120] C. Texier, Generalized Lyapunov exponent of random matrices and universality classes for SPS in 1D Anderson localisation, Europhys. Lett. **131**, 17002 (2020).

[121] C. Texier, *Désordre, localisation et interaction – Transport quantique dans les réseaux métalliques* (Habilitation à Diriger des Recherches, Université Paris-Sud, 2010), `http://tel.archives-ouvertes.fr/tel-01091550`.

[122] C. Texier, P. Delplace and G. Montambaux, Quantum oscillations and decoherence due to electron-electron interaction in networks and hollow cylinders, Phys. Rev. B **80**, 205413 (2009).

[123] C. Texier and C. Hagendorf, The effect of boundaries on the spectrum of a one-dimensional random mass Dirac Hamiltonian, J. Phys. A: Math. Theor. **43**, 025002 (2010).

[124] C. Texier and J. Mitscherling, Nonlinear conductance in weakly disordered mesoscopic wires: Interaction and magnetic field asymmetry, Phys. Rev. B **97**, 075306 (2018).

[125] C. Texier and G. Montambaux, Weak localization in multiterminal networks of diffusive wires, Phys. Rev. Lett. **92**, 186801 (2004).

[126] C. Texier and G. Montambaux, Four-terminal resistances in mesoscopic networks of metallic wires : Weak localisation and correlations, Physica E **75**, 33–46 (2016), Frontiers in quantum electronic transport - In memory of Markus Büttiker ; also Physica E **82**, 272–285 (2016).

[127] C. Texier and G. Roux, *Physique statistique : des processus élémentaires aux phénomènes collectifs*, Dunod, Paris (2017).

[128] D. J. Thouless, A relation between the density of states and range of localization for one-dimensional random systems, J. Phys. C: Solid St. Phys. **5**, 77 (1972).

[129] D. J. Thouless, Electrons in disordered systems and the theory of localization, Phys. Rep. **13**(3), 93–142 (1974).

[130] M. Treiber, C. Texier, O. M. Yevtushenko, J. von Delft and I. V. Lerner, Thermal noise and dephasing due to electron interactions in non-trivial geometries, Phys. Rev. B **84**, 054204 (2011).

[131] C. P. Umbach, C. van Haesendonck, R. B. Laibowitz, S. Washburn and R. A. Webb, Direct observation of Ensemble Averaging of the Aharonov-Bohm Effect in Normal Metal Loops, Phys. Rev. Lett. **56**(4), 386 (1986).

[132] N. G. van Kampen, *Stochastic processes in physics and chemistry*, North-Holland, Amsterdam (1992).

[133] M. C. W. van Rossum and T. M. Nieuwenhuizen, Multiple scattering of classical waves: microscopy, mesoscopy, and diffusion, Rev. Mod. Phys. **71**, 313 (1999).

[134] D. Vollhardt and P. Wölfle, Diagrammatic, self-consistent treatment of the Anderson localization problem in $d \leqslant 2$ dimensions, Phys. Rev. B **22**(10), 4666 (1980).

[135] J. von Delft, Influence Functional for Decoherence of Interacting Electrons in Disordered Conductors, Int. J. Mod. Phys. B **22**, 727 (2008), preprint cond-mat/05 10 563.

[136] J. von Delft, F. Marquardt, R. A. Smith and V. Ambegaokar, Decoherence in weak localization. II. Bethe-Salpeter calculation of the cooperon, Phys. Rev. B **76**, 195332 (2007).

[137] S. Washburn, C. P. Umbach, R. B. Laibowitz and R. A. Webb, Temperature dependence of the normal-metal Aharonov-Bohm effect, Phys. Rev. B **32**(7), 4789 (1985).

[138] S. Washburn and R. A. Webb, Aharonov-Bohm effect in normal metal. Quantum coherence and transport, Adv. Phys. **35**(4), 375–422 (1986).

[139] R. A. Webb and S. Washburn, Quantum interference fluctuations in disordered metals, Physics Today pp. 46–53 (December 1988).

[140] R. A. Webb, S. Washburn, C. P. Umbach and R. B. Laibowitz, Observation of h/e Aharonov-Bohm Oscillations in Normal-Metal Rings, Phys. Rev. Lett. **54**(25), 2696 (1985).

[141] F. Wegner, The mobility edge problem: continuous symmetry and a conjecture, Z. Phys. B **35**(3), 207 (1979).

[142] D. S. Wiersma, *Light in strongly scattering and amplifying random media*, Ph.D. thesis, Universiteit van Amsterdam (1995).

[143] S. Wind, M. J. Rooks, V. Chandrasekhar and D. E. Prober, One-Dimensional Electron-Electron Scattering with Small Energy Transfers, Phys. Rev. Lett. **57**(5), 633 (1986).

Index